

©Copyright 2016

Nathaniel Phillips-Sylvain

A Theoretical and Synthetic Investigation  
of New Donors for Organic Electro-Optic Chromophores:  
Understanding the Effects of Structure and Substituents on Donor  
Strength

Nathaniel Phillips-Sylvain

A dissertation  
submitted in partial fulfillment of the  
requirements for the degree of

Doctor of Philosophy

University of Washington

2016

Reading Committee:

Larry Dalton, Chair

Phil Reid

Bruce Robinson

Program Authorized to Offer Degree:  
Department of Chemistry

University of Washington

## Abstract

A Theoretical and Synthetic Investigation  
of New Donors for Organic Electro-Optic Chromophores:  
Understanding the Effects of Structure and Substituents on Donor Strength

Nathaniel Phillips-Sylvain

Chair of the Supervisory Committee:  
Professor Emeritus Larry Dalton  
Department of Chemistry

Understanding of the intricate connection between shape, structure and property has allowed many challenges facing the adoption of organic chromophores for electro-optic (EO) applications to be overcome. Still, there is much to be learned about designing donors that localize electron density in the ground state, but not in the electronically polarized state to allow for enhanced charge transfer, and thus, large first-order molecular hyperpolarizability ( $\beta$ ). To address this, density functional theory has been used to evaluate a large number of potential donors based on alkyl, aryl, saturated and unsaturated heterocycles. These were coupled to the tricyanopyrroline (TCP) acceptor by a simple vinylic bridge to identify new high  $\beta$ , high number density materials. Saturated heterocycles were found to offer the largest improvements over traditional dialkyl donors, with the predicted systems rivaling much longer polyene-based chromophores with a trifluoromethyl, phenyl-tricyanofuran ( $\text{CF}_3\text{PhTCF}$ ). Other potential candidates were based on diaryl amines donors which are a natural progression from previous heteroaryl chromophores. These systems were typified by a greater degree of localized electron density – by as much as 20% – at the donor and were found to exhibit characteristics that might be described as a double-donor. Several novel chromophores based on these new donors were synthesized to verify the theoretical results and evaluate their potential for use in EO devices.

## TABLE OF CONTENTS

	Page
List of Figures . . . . .	iii
List of Tables . . . . .	viii
Nomenclature . . . . .	viii
Chapter 1: Introduction to Organic Electro-Optics and Chromophore Design . . .	1
1.1 Beyond textiles: Organic Dyes and Photonics . . . . .	1
1.2 Organic Electro-Optic Materials . . . . .	5
1.3 Aim and scope of this thesis . . . . .	14
REFERENCES . . . . .	16
Chapter 2: Understanding the Effects of Structure and Substituents on Donor Strength	25
2.1 Introduction . . . . .	25
2.2 Computational Methodology . . . . .	29
2.3 Results and Discussion . . . . .	31
2.4 Conclusion . . . . .	41
2.5 Experimental . . . . .	42
REFERENCES . . . . .	44
Chapter 3: Synthesis of Dihydropyrazine Donor . . . . .	51
3.1 Introduction . . . . .	51
3.2 Results and Discussion . . . . .	51
3.3 Conclusion . . . . .	64
3.4 Experimental Section . . . . .	65



REFERENCES . . . . .	69
Chapter 4: Synthesis of Diaminotriphenylamine(DATPA) Donor . . . . .	71
4.1 Introduction . . . . .	71
4.2 Results and Discussion . . . . .	72
4.3 Conclusion . . . . .	82
4.4 Experimental . . . . .	82
REFERENCES . . . . .	87
Bibliography . . . . .	91
Appendix A: Complete Structures and Calculated Properties . . . . .	111
Appendix B: Python code for gdr.py . . . . .	155

## LIST OF FIGURES

Figure Number	Page	
1.1	Skeletal structure diagrams of Mauvine A(left) and Mauvine B(right), dyes synthesized by Sir William Henry Perkin in 1856 while trying to synthesize quinine from aniline. . . . .	1
1.2	A commercial Mach-Zehnder modulator based on gallium arsenide that operates at 40 GHz (source: aXenic) and Basic electro-optic modulator based on a Mach-Zehnder interferometer. Source: ref. <sup>[19]</sup> . . . . .	4
1.3	The half-wave voltage of EO modulators based on inorganic crystals from Thor Labs. . . . .	5
1.4	Classic dielectric model of electric field interaction with an atom (top, a-c) and the linear and nonlinear response of $\pi$ -conjugated system with electron donating and withdrawing end groups. a) Neutral atom in the absence of an electric field. b) As an electric field is applied, the electron cloud shifts in a direction opposite of the field. This leads to c) an induced dipole, $\mu_i$ , that is in the same direction as the electric field. The electric field is denoted by the blue arrow and the dipole by the red arrow. d) Following excitation by an optical field, an asymmetric electronic response arises due to polarization. The electron cloud favors the acceptor (A) end over the donor (D) end, resulting in a transition dipole and the nonlinearity. . . . .	6
1.5	a) In an unpoled systems, the molecules are randomly arranged and the EO activity is negligible. Upon applying heat and an electric field, the molecules are able to move so that their dipolar axis can align with the electric field. b) The amount of alignment is expressed in the term $\langle \cos^3(\theta) \rangle$ where $\theta$ is the angle between the dipolar axis and the external electric field. . . . .	8
1.6	The chromophore, YLD124, and a schematic showing the asymmetric donor- $\pi$ -acceptor motif generally followed when designing neutral ground-state dyes for use in EO applications. . . . .	9
1.7	Several acceptors (top) and donor-bridges (bottom) used in $D - \pi - A$ chromophores. . . . .	10

1.8	a) Bond-length alternation as described by Marder <i>et al.</i> . For any given donor/acceptor pair, there is a certain amount of alternation between single- and double-bonds that maximizes the molecular hyperpolarizability. There also exist a point where both the bond-length alternation and molecular hyperpolarizability will be zero and this is referred to as the cyanine limit. b) The relationship between bond length alternation and $\beta$ (—), $(\mu_{ee} - \mu_{gg})(- - -)$ , $(\mu_{ge})^2(- - -)$ and $1/\Delta E_{ge}$ ( $\cdot \cdot \cdot$ ) from equation 1.13. . . . .	12
1.9	The left is a schematic description of the effects of substituents to the HOMO and LUMO levels according to Dewar's rules. A CLD-type chromophore is shown on the right with substitution positions on the conjugated backbone. These are divided into starred and unstarred groups with the positions 3(*) and 5(*) denoting substitution of the isophorone ring. . . . .	13
2.1	Donors studied Kwon <i>et. al.</i> <sup>[7]</sup> , seperated into 4 basic donor structures: Alkyl (DA), Locked Ring (LR), Ring (R) and Aryl (DAAP). These basic structure types will serve as the basis for all structures investigated in this study. . . .	26
2.2	The structures of three CLD chromophores with the CF3Ph-TCF acceptor and different donors. . . . .	26
2.3	Representative diaryl chromophore based on FTC (A-C) <sup>[19]</sup> or CLD (B3-4) <sup>[9]</sup> bridges. . . . .	28
2.4	Structures used as guidance in the evaluation of new donors. YLD124TMS contains a bis(2-((trimethylsilyl)oxy)ethyl)amine donor while YLD124M contains a 2-methoxy- <i>N</i> -methylethylamine donor. Chromophore DA-00 shows the general structure of all chromophores to be evaluated. This chromophore contains a diethylamine donor and will serve as a basis against which all other donors are compared. . . . .	29
2.5	A comparison of $\beta_{zzz}(0)$ calculated at the CAM-B3LYP and M06-2x levels of theory <i>in vacuo</i> and in chloroform. On the left is a comparisons of CAM-B3LYP vs M06-2x in vacuum( $\diamond$ ) and chloroform( $\circ$ ). On the right, we compare Vacuum vs chloroform for CAM-B3LYP( $\circ$ ) and M06-2x( $\square$ ) . . . . .	31
2.6	Structures of the chromophores evaluated in this study. They are broken down according to the categories listed in figure Fig. 2.1. . . . .	33
2.7	The change in $\beta_{zzz}^{sys}$ from DA-00 of chromophores <i>in vacuo</i> and in chloroform. The shaded area represents the range between YLD124M (bottom) and YLD124TMS (top). Properties were calculated with Gaussian 09d at the CAM-B3LYP/6-31+G*//CAM-B3LYP/6-31+G* level of theory. . . . .	34

2.8	Theoretical (top) and experimental (bottom) optical spectra comparing the effects of silyl ethers on the intramolecular charge transfer band. The vertical lines in the theoretical spectra represent the relative oscillator strength of the transition(s) responsible for the observed peak. . . . .	36
2.9	Calculated $\beta_{zzz}$ of the shown dialkyl donor plotted against $\beta_{zzz}$ of a diaryl donor (left) or pyrazine donor (right) bearing the same donor. . . . .	39
2.10	Frontier molecular orbitals of chromophores DA-02, DAAP-09 and R-03. Shown below the orbitals. . . . .	40
3.1	Initial structures proposed for evaluating the dihydropyrazine donor. . . . .	52
3.2	Structures of new chromophores with a dihydropyrazine donor. Chromophores <b>DHPz-TCF-1</b> and <b>DHPz-TCF-2</b> were synthesized by Dr. Delwin Elder. . . . .	55
3.3	UV-Vis absorption spectra of chromophores <b>DHPz-MN-1</b> , <b>DHPz-MN-2</b> (left), <b>DHPz-TCF-1</b> and <b>DHPz-TCF-2</b> (right) in chloroform. . . . .	56
3.4	Cyclic voltammograms of chromophores DEA-MN, DEA-TCF, <b>DHPz-MN-1</b> and <b>DHPz-TCF-1</b> (left) and <b>DHPz-MN-1</b> and <b>DHPz-TCF-1</b> (right). Voltammograms were recorded in acetonitrile solutions containing a 0.1 M $\text{Bu}_4\text{NPF}_6$ supporting electrolyte at a scan rate of 50 $\text{mV s}^{-1}$ . . . . .	58
3.5	Differential Scanning Calorimetry plot of <b>DHPz-TCF-2</b> with a heating rate of $10^\circ\text{C min}^{-1}$ in a nitrogen environment. . . . .	60
3.6	Thermogravimetric analysis curve of <b>DHPz-TCF-2</b> with a heating rate of $10^\circ\text{C min}^{-1}$ in a nitrogen environment. $T_d = 265.7^\circ\text{C}$ . . . . .	61
3.7	Electro-optic coefficients of <b>DHPz-TCF-2</b> films, $\circ$ 25 wt.% in PMMA and $\diamond$ neat film, at different poling voltages. Poling efficiencies, $r_{33}/E_p = 0.14\text{nm}^2 \cdot \text{V}^{-2}$ for the guest-host system and $r_{33}/E_p = 0.16\text{nm}^2 \cdot \text{V}^{-2}$ for the monolithic film. . . . .	63
4.1	Top left, optical spectra of chromophores in chloroform. Top right, comparison with chromophores with a 2 carbon and 4 carbon bridge. Bottom left, comparison with <b>JRD2</b> in chloroform and as a film. Bottom right, optical constants, n and k, obtained from VASE measurements. . . . .	74
4.2	Cyclic voltammetry of CF3Ph-TCF chromophores. The bottom has a 2-carbon bridge with a diethylamine donor, the middle has a 4-carbon bridge with a diethylamine donor and the top has the DATPA donor. . . . .	76
4.3	Differential Scanning Calorimetry plot of <b>4Bn-DATPA-2</b> with a heating rate of $10^\circ\text{C min}^{-1}$ in a nitrogen environment. $T_g = 76.7^\circ\text{C}$ . . . . .	78
4.4	Thermogravimetric analysis curve of <b>4Bn-DATPA-2</b> with a heating rate of $10^\circ\text{C min}^{-1}$ in a nitrogen environment. $T_d = 194.3^\circ\text{C}$ . . . . .	79

4.5 Electro-optic coefficients of **4Bn-DATPA-2** monolithic films at different poling voltages. Poling efficiency,  $r_{33}/E_p = 0.47nm^2 \cdot V^{-2}$ . . . . . 81

## LIST OF SCHEMES

2.1	Synthesis of Butyl-TCP. . . . .	42
2.2	Synthesis of TBDPS-TCP. . . . .	43
3.1	Formylation of dihydropyrazine donor. Reagents and conditions: (a) 1 equiv of aniline, 2.2 equiv halide, 4 equiv base, H <sub>2</sub> O, reflux 24 h; (b) 3 equiv aniline, 5% v/v 1:1 trifluoroacetic acid/acetic acid, toluene, reflux, 6h; (c) 1–1.5 equiv POCl <sub>3</sub> , DMF, rt, 0.5h, 90°C, 0.75h. . . . .	53
3.2	Vilsmeier-Haack formylation of the 1,4-dihydropyrazine system. Instead of formylating the phenyl ring, formylation occurred at the 2 position of the pyrazine ring. . . . .	54
3.3	Synthesis of DHPz dyes. a) Ethanol or isopropanol, reflux, 30 minutes. . . . .	55
4.1	Synthesis of DATPA chromophores. . . . .	73

## LIST OF TABLES

Table Number		Page
2.1	Mulliken population analysis of representative chromophores, calculated from Gaussian 09d with the pop=Full keyword and the GaussSum program. $\Delta E = E_{LUMO} + E_{HOMO}$ . Values for $\beta_{zzz}$ where calculated in vacuum. . . . .	39
3.1	Dipole moment ( $\mu_z$ ), hyperpolarizability ( $\beta_{zzz}$ ) and number density ( $\rho_N$ ) of chromophores. <sup>a</sup> The number density was calculated based on an estimated density of 1.00 g/cc. <sup>b</sup> values taken from reference <sup>[8]</sup> . . . . .	52
3.2	Electrochemical and optical properties of chromophores in study. . . . .	58
4.1	Electrochemical and optical properties of chromophores in study. . . . .	77

## NOMENCLATURE

### List of Abbreviations

LiNbO<sub>3</sub> Lithium Niobate

CF<sub>3</sub>Ph-TCF 5-trifluoromethyl-5-phenyl-tricyanonofuran

DAAP 4-(diarylamino)phenyl

DATPA Diaminotriphenylamine

DFT Density Functional Theory

DNTPA Dinitrotriphenylamine

EO Electro-Optic

KDP Potassium Dihydrogen Phosphate

MN Malononitrile, CH<sub>2</sub>(CN)<sub>2</sub>

MND Malononitrile dimer, 2-Amino-1,1,3-propenetricarbonitrile

MPA Mulliken Population Analysis

NLO Nonlinear Optics

ONLO Organic Nonlinear Optics

OTN Optical Transport Network



TBDMS tert-butyldimethylsilyl

TBDPS tert-butyldiphenylsilyl

TCF 5,5-dimethyl-tricyanonofuran

TCP 5-trifluoromethyl-5-phenyl-tricyanonofuran

### Physical Symbols

$\beta_{ijk}$  First molecular hyperpolarizability, usually denoted as  $\beta_{vec}$  or  $\beta_{zzz}$  to indicate that it is in the direction of the dipolar axis

$\Delta E_{ge}$  Transition energy from the ground to the excited state.

$\Delta\mu_{ge}$   $\mu_{ee} - \mu_{gg}$

$\mu_r$  Relative permeability of a material

$\mu_{ee}$  Excited state dipole moment

$\mu_{ge}$  Transition dipole moment

$\mu_{gg}$  Ground state dipole moment

$\varepsilon_r$  Relative permittivity of a material

$r_{ij}$  Linear electro-optic coefficient

$V_\pi$  Half-wave voltage, the voltage required to induce a phase change of  $\pi$

n Index of refraction

## ACKNOWLEDGMENTS

First and foremost, I would like to thank my advisor, Prof. Larry Dalton, without whose help and support none of this would be possible. I would also like to thank Prof. Phil Reid and Prof. Bruce Robinson for their patience, insight, and guidance over the course of this project.

Over the course of my graduate career, many people aided in my personal and scientific growth. Dr. Meghana Rawal provided countless hours of insightful discussion, encouragement and greatly aided in my transition to a synthetic chemist. Dr. Andreas Tillack helped me to find value where I thought there was none. Without the help and knowledge of Drs. Bruce Eichinger, Lewis Johnson, and Kerry Garrett, the theoretical studies that guided much of my graduate synthetic work would not have been possible.

I would like to thank Brandon Henry for his constant friendship and support, the undergrads I have worked with and the staff of the Chemistry department. I would also like offer a special thanks to Dr. Delwin Elder. He has been a great mentor and font of knowledge as I worked through some rather tricky synthetic issues. He has tirelessly, and graciously, offered his time in assisting with characterizing many of the molecules presented in this work, and for that I am eternally grateful.

This material is based upon work supported by the National Science Foundation under Grant Number (DMR-1303080, DMR-1005819, DMR-0905686 and DMR-0120967). Any opinions, findings, and conclusions or recommendations expressed in this material are those of the author(s) and do not necessarily reflect the views of the National Science Foundation. The authors acknowledge partial financial support from the Air Force Office of Scientific Research (FA9550-10-1-0558, FA9550-15-1-0319, and FA9550-09-1- 0682).

## DEDICATION

To Malia, you keep me (mostly) sane  
and  
to my mother,  
who taught me the importance of an education.

## Chapter 1

# INTRODUCTION TO ORGANIC ELECTRO-OPTICS AND CHROMOPHORE DESIGN

## 1.1 Beyond textiles: Organic Dyes and Photonics

### 1.1.1 Synthetic dyes and Photonics

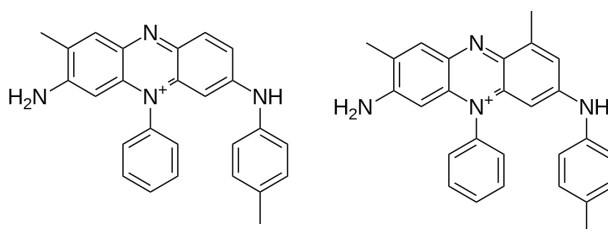


**Fig. 1.1** Skeletal structure diagrams of Mauvine A(left) and Mauvine B(right), dyes synthesized by Sir William Henry Perkin in 1856 while trying to synthesize quinine from aniline.

The first synthetic dye was discovered in 1856<sup>[1,2]</sup>. It was synthesized from aniline (and isomeric toluidine impurities found in aniline) while trying to synthesize the antimalarial drug, quinine<sup>[3]</sup>. This marked the beginning of the synthetic dye industry, the reaches of which have had impact far beyond the textile industry. Organic dyes have been used in medicine<sup>[4,5]</sup>, sensing<sup>[6]</sup>, optical recording<sup>[7]</sup> and power generation<sup>[8,9]</sup>. One thing that all of these applications have in common is the use of light; be it for the acquisition, storage, transmission and processing of data or for conversion into electricity, all of these applications fall under the broader field of photonics.

Photonics is the optical equivalent of electronics, where light and photons are used in place of electricity and electrons. As transistors become smaller, packing density starts to become an issue as interconnect crosstalk and power demands increase. Photonic offer one

possible way to overcome the inherent limits of electronics<sup>[10–12]</sup>. One industry that relies heavily on photonic devices is the telecommunications industry.

### 1.1.2 Photonics in Telecommunications

Telecommunications has become an integral part of modern business and society. Growth is being seen across all sectors and in all markets<sup>[13]</sup> as technological advances fundamentally change how traditional services are delivered. By the year 2020, the average internet household is predicted to generate 117.8 gigabytes of traffic per month and global IP traffic will reach an annual run rate of 2.3 zettabytes<sup>[13]</sup>. Most telecommunication networks have seen their older, copper-based, transmission lines replaced by optical fibers, but these networks are limited by the hardware used to transduce electrical signals on to optical carriers. These devices operate under the principle of the electro-optic effect.

### 1.1.3 The Electro-Optic Effect

The electro-optic effect (EO) is a change in the optical properties of a material by an electric field<sup>[14]</sup>. This change may be a change in absorption or a change in permittivity<sup>[15,16]</sup>, but for the purposes of this text, the latter shall remain the focus. We can define the refractive index of a material as

$$n = \sqrt{\varepsilon_r \mu_r}, \quad (1.1)$$

where  $\varepsilon_r$  is the relative permittivity of the material and  $\mu_r$  is the relative permeability<sup>[17]</sup>. For most cases, the relative permeability can be ignored for materials at optical frequencies – as they are non-magnetic so  $\mu_r \approx 1$  – so the index of refraction can be expressed as  $\sqrt{\varepsilon_r}$ . For an electro-optic material, the index of refraction is a function of the applied electric, which changes very little with the electric field,  $E$ . We can then expand this in a Taylor's series about  $E = 0$  such that,

$$n(E) = n + a_1 E + \frac{1}{2} a_2 E^2 + \dots, \quad (1.2)$$

and the coefficients of expansion are  $n = n(0)$ ,  $a_1 = (dn/dE)|_{E=0}$  and  $a_2 = (d^2n/dE^2)|_{E=0}$ . We can now define the two new coefficients,  $r$  and  $K$ , as

$$r = -\frac{2a_1}{n^3}, \quad (1.3)$$

and

$$K = -\frac{a_2}{n^3}, \quad (1.4)$$

and recast equation 1.2 as

$$n(E) = n - \frac{1}{2}rn^3E - \frac{1}{2}Kn^3E^2 + \dots. \quad (1.5)$$

We have now defined our linear EO coefficient, which corresponds to the Pockels effect, and the quadratic EO coefficient, which corresponds to the Kerr effect<sup>1</sup>.

Both the Pockels coefficient and the Kerr coefficient are tensors, so the direction of the applied electric field is important in determining the change in the refractive index. The Kerr effect occurs in all materials and has no special symmetry requirements so it will be ignored cite(Boyd:2013aa). For an applied field,  $E(E_x, E_y, E_z)$ , the change in refractive index is

$$\Delta \left( \frac{1}{n^2} \right)_i = \sum_{j=1}^3 r_{ij} E_j, \quad (1.6)$$

and  $i = 1, \dots, 6$  and  $j = 1, \dots, 3$ . In a centrosymmetric crystal, all of the tensor elements  $r_{ij}$  are zero. For a non-centrosymmetric crystal, such as LiNbO<sub>3</sub>, many of the off-diagonal elements vanish due to symmetry leaving only a few that are non-zero. From this, we learn that for a material to show a linear EO effect, it must be asymmetric or have a non-centrosymmetric crystal. Lithium niobate is a uniaxial crystal where  $n_x = n_y = n_o$ ,  $n_z = n_e$ <sup>2</sup>, and the important electro-optic coefficients are  $r_{33} = 30.9 \text{ pm/V}$  and  $r_{13} = 9.6 \text{ pm/V}$ . Thus,

---

<sup>1</sup>There is also a magneto-optic effect<sup>[18]</sup> that shares the same name. This refers strictly with the electro-optic Kerr effect.

<sup>2</sup> $n_o$  and  $n_e$  are the ordinary and extraordinary refractive indices and the birefringence of a material is given as  $\Delta n = n_e - n_o$

if an electric field is applied parallel to the  $E_z$  axis, a change in the refractive index will occur in either  $n_z \propto n_e r_{33} E_z$  or  $n_x = n_y \propto n_o r_{13} E_z$ . For optimal device performance, it is advantageous to orient the crystal such that linearly polarized light is parallel to the optical axis.

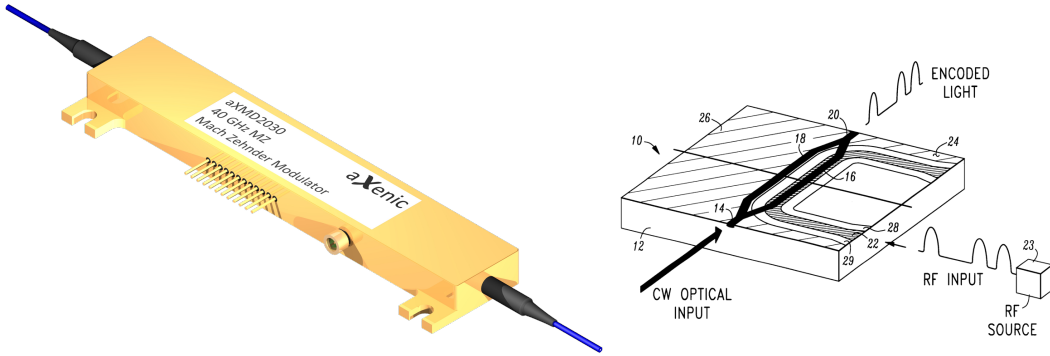


**Fig. 1.2** A commercial Mach-Zehnder modulator based on gallium arsenide that operates at 40 GHz (source: aXenic) and Basic electro-optic modulator based on a Mach-Zehnder interferometer. Source: ref. [19]

One of the devices commonly used to transduce light onto optical carriers is a Mach-Zehnder modulator. This is shown in figure Fig. 1.2. They operate by splitting light from a single source into two arms. In a simple configuration(right side of figure Fig. 1.2), one arm allows the light to pass unperturbed. The other arm is passed through an EO material and depending on the applied voltage, passes unperturbed or has an induced phase change of  $\pi$ . When the two arms recombine, there is either constructive or destructive interference resulting in an optical 1 or 0. The half-wave voltage,  $V_\pi$ , is the voltage required to induce a phase change of  $\pi$  and is defined as

$$V_\pi = \frac{\lambda_0 d}{n^3 r L}, \quad (1.7)$$

where  $\lambda_0$  is the operating wavelength,  $d$  is the active material thickness and  $L$  is the length of the active material. There is a trade-off between minimizing  $V_\pi$  and keeping optical losses at a minimum. Figure Fig. 1.3 shows typical half-wave voltages for EO modulators. Devices based on inorganic crystals have relatively low EO coefficients, necessitating longer

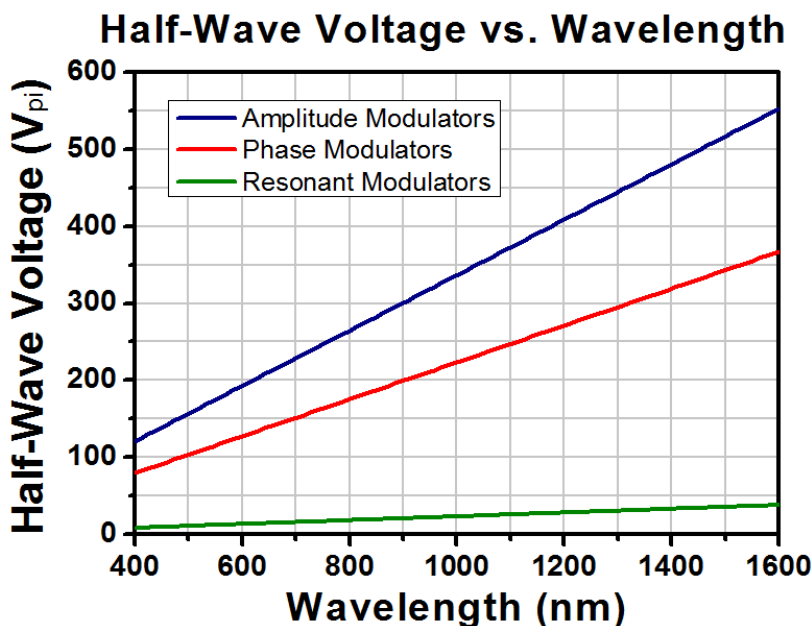


**Fig. 1.3** The half-wave voltage of EO modulators based on inorganic crystals from Thor Labs.

devices and high half-wave voltages. Synthetic organic dyes have been shown to have high EO coefficients<sup>[11,12]</sup>, high operating frequencies<sup>[20–22]</sup>, and low half-wave voltages.<sup>[11]</sup> These attributes make organic dyes ideal candidates for replacing inorganics in EO applications.

## 1.2 Organic Electro-Optic Materials

### 1.2.1 Nonlinear Polarization in Organic Molecules

Before discussing what makes a good dye for use in EO applications, one must first know how the nonlinear optical (NLO) response in organic dyes arise<sup>3</sup>. Light is composed of both electric and magnetic components that are orthogonal to each other. The electric field is capable of interacting with electrons in organic molecules such that

$$p_i = \alpha_{ij} E_j, \quad (1.8)$$

---

<sup>2</sup>The units for equations in this section are assumed to be in cgs or atomic units, unless stated or generally understood to be otherwise. Many of the equations are missing a factor of  $\epsilon_0$  that must be added if SI units are desired.



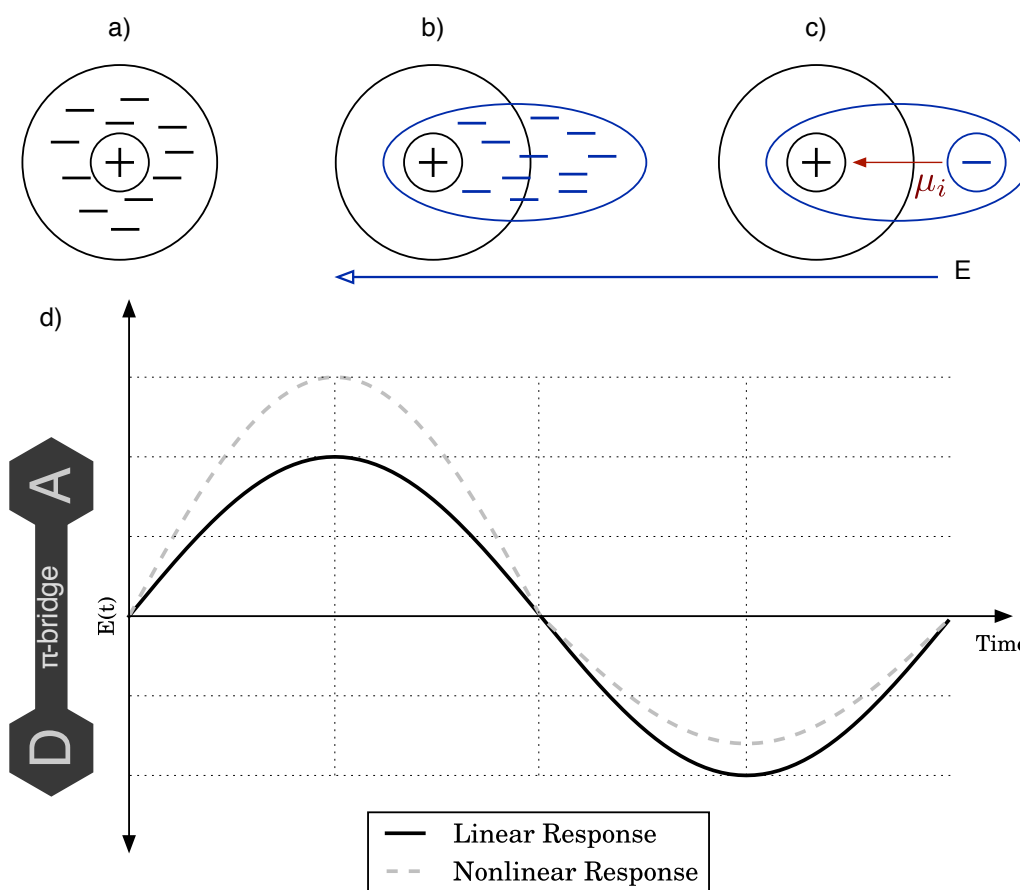


**Fig. 1.4** Classic dielectric model of electric field interaction with an atom (top, a–c) and the linear and nonlinear response of  $\pi$ -conjugated system with electron donating and withdrawing end groups. a) Neutral atom in the absence of an electric field. b) As an electric field is applied, the electron cloud shifts in a direction opposite of the field. This leads to c) an induced dipole,  $\mu_i$ , that is in the same direction as the electric field. The electric field is denoted by the blue arrow and the dipole by the red arrow. d) Following excitation by an optical field, an asymmetric electronic response arises due to polarization. The electron cloud favors the acceptor (A) end over the donor (D) end, resulting in a transition dipole and the nonlinearity.

where  $P_i$  is the induced polarization,  $\alpha_{ij}$  is the linear polarizability, and  $i$  and  $j$  refer to coordinates in the molecular frame. Shown in figure Fig. 1.4, we see the results of polarization on a simple atom under the classic dielectric model. In the absence of an external field, the electrons are arranged around the positive atom core. When the atom is placed in a field, the electron cloud shifts in a direction opposite of the field to form an induced dipole. This induced dipole is equal to the polarization so equation 1.8 becomes

$$\mu_i = p_i = \alpha_{ij}E_j, \quad (1.9)$$

which is linearly proportional to the strength of the electric field. This holds true for cases of low intensity light, but as the intensity is increased, so does the strength of the electric field and nonlinearities start to appear. The induced dipole is then a function of the field strength and we can express the nonlinear dependence with a Taylor expansion of equation 1.9:

$$\mu_i(E) = \mu_{g,i} + \alpha_{ij}E_j + \frac{1}{2!}\beta_{ijk}E_jE_k + \frac{1}{3!}\gamma_{ijkl}E_jE_kE_l + \dots \quad (1.10)$$

We now have the first hyperpolarizability,  $\beta$ , and the second hyperpolarizability,  $\gamma$ , of the molecule. We can also define the linear and nonlinear susceptibilities as

$$P = P_0 + \chi^{(1)}E + \chi^{(2)}E^2 + \chi^{(3)}E^3 + \dots \quad (1.11)$$

The first hyperpolarizability and second-order nonlinear susceptibility are at a maximum along the dipolar axis of the molecule, which we will define as the z-direction. We can now define the linear EO coefficient as

$$r_{33} = \frac{2f(\omega)}{n^4} \rho_N \beta_{zzz} \langle \cos^3(\theta) \rangle, \quad (1.12)$$

where  $f(\omega)$  is the local field arising from the host dielectric permittivity,  $n$  is the refractive index,  $\rho_N$  is the molecular number density,  $\beta_{zzz}$  is the first molecular hyperpolarizability and  $\langle \cos^3(\theta) \rangle$  is the anisotropy order parameter. Of course, this is assuming that the assumptions in the oriented-gas model hold true<sup>[23]</sup>. Our focus will be on improving  $r_{33}$  by improving  $\beta_{zzz}$  and possible  $\rho_N$  in small organic dyes that we will refer to as EO or nonlinear optical (NLO) chromophores so as to distinguish them from other uses.

### 1.2.2 Electric Field Poling

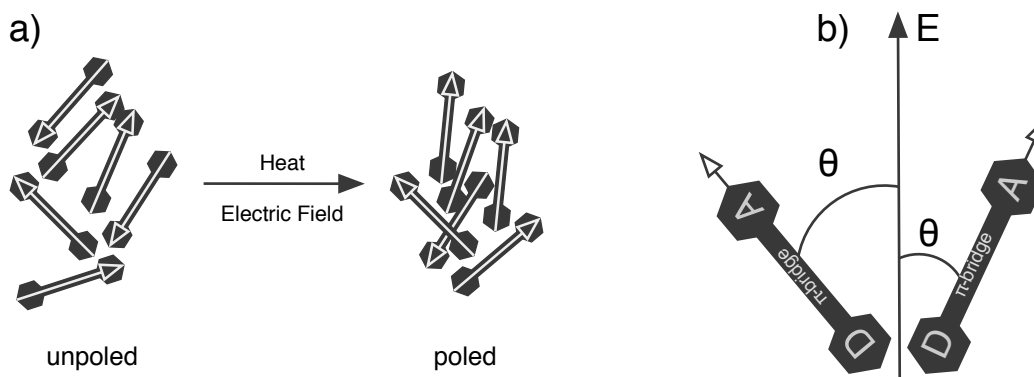


**Fig. 1.5** a) In an unpoled systems, the molecules are randomly arranged and the EO activity is negligible. Upon applying heat and an electric field, the molecules are able to move so that their dipolar axis can align with the electric field. b) The amount of alignment is expressed in the term  $\langle \cos^3(\theta) \rangle$  where  $\theta$  is the angle between the dipolar axis and the external electric field.

As discussed before, the linear EO response requires noncentrosymmetric symmetry. To achieve this, a technique known as electric field poling is used. In figure Fig. 1.5 is a simple schematic showing the results of poling. First, the system is unordered with all the dipolar axes of the molecules pointing in random directions. Due to strong dipole-dipole interactions, many of these molecules are likely to be aligned antiparallel to minimize the overall energy of the ensemble. These interactions may be mitigated with shape engineering, guest-host polymer systems<sup>[24-27]</sup>, binary systems<sup>[28]</sup> and side-chain interactions<sup>[29]</sup>, among others. The unordered system is heated to allow for movement of the molecules. This temperature is typically just above the glass transition temperature and an external electric field is applied. A typical field strength is  $100 \text{ V}/\mu\text{m}$  and once poling is complete, the achieved order is retained by allowing the system to cool. Activity may be measured by Teng and Man simple reflection ellipsometry<sup>[30,31]</sup>, second harmonic generation<sup>[32]</sup>, attenuated total reflection (ATR)<sup>[33,34]</sup>, Fabry-Perot interferometry<sup>[35,36]</sup>, and Mach-Zehnder interferometry<sup>[37,38]</sup>.

### 1.2.3 Nonlinear Optical Chromophores

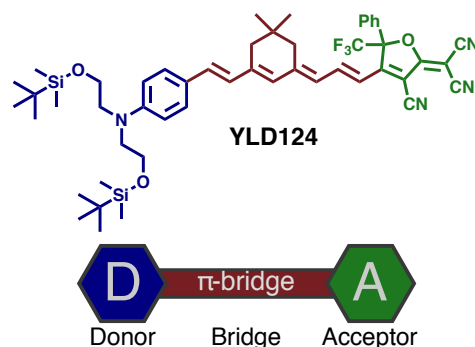


**Fig. 1.6** The chromophore, YLD124, and a schematic showing the asymmetric donor- $\pi$ -acceptor motif generally followed when designing neutral ground-state dyes for use in EO applications.

Dipolar, push-pull, chromophores for EO applications come in numerous shapes and sizes<sup>[39–48]</sup>. They may be either a neutral ground state (NGS) or be zwitterionic (ZWI) molecules. Regardless, these chromophores share many similarities such as a rod-like design with a donor and acceptor connected by a  $\pi$ -conjugated bridge. We have shown a simple schematic of this D- $\pi$ -A structure in figure Fig. 1.6 along with the structure for the chromophore YLD124. It is composed of a dialkyl donor and CF<sub>3</sub>-PhTCF acceptor linked by a CLD-type polyene bridge. The CLD polyene bridge in YLD124 and similar chromophores was developed to improve the loss in photo- and thermal stability often associated long, conjugated chains<sup>[49–53]</sup>. By incorporating the ring-locked isophorone unit in the bridge, the bridge length was extended to provide better charge separation. Another popular bridge is the FTC bridge, based on a thienyl-vinylene linker between the donor and acceptor. Chromophores based on this bridge often possess higher thermal and photo stabilities than their CLD counterparts, but at the cost of lower  $\beta$ <sup>[28,52,54]</sup>. These bridge moieties, along with several permutations, are shown in figure Fig. 1.7.

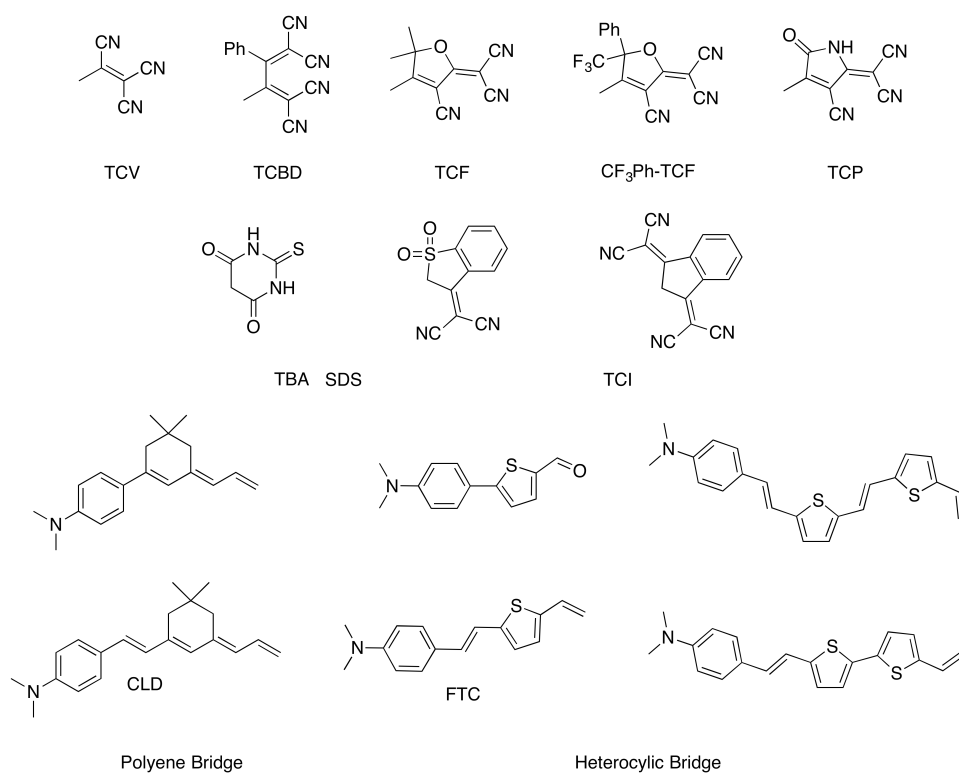


**Fig. 1.7** Several acceptors (top) and donor-bridges (bottom) used in  $D - \pi - A$  chromophores.

### 1.2.4 Structure and the effects on hyperpolarizability

#### *The Two-State Model*

Many early attempts at improving chromophore performance were based on permutations of 4-(*N,N*-dimethylamino)-4'-nitrostilbene (DANS). Oudar and Chemla put forth that the hyperpolarizability was dominated by a single intramolecular charge transfer process, greatly simplifying the sum-over-states(SOS) approach developed by Ward<sup>[55,56]</sup>. The SOS approach takes into account the admixing of the ground state and charge transfer state that arises from polarization caused by an external electric field. It accounted for all states and not just the dominant charge transfer state. But Oudar and Chemla were able to show that the contributions from the other states were negligible and that in these small  $D - \pi - A$  systems, only the frontier orbitals made any significant contribution to the electric field polarized state. From this model,

$$\beta_{vec} \propto \frac{(\mu_{ee} - \mu_{gg})(\mu_{ge})^2}{(\Delta E_{ge})^2}, \quad (1.13)$$

where  $\beta_{vec}$  is the element of the hyperpolarizability tensor in the direction of the dipolar axis,  $\mu_{gg}$  and  $\mu_{ee}$  are the ground state and excited state dipole moments,  $\mu_{ge}$  is the transition dipole moment and  $\Delta E_{ge}$  denotes the difference between the ground and first excited state orbitals. The terms  $\Delta E_{ge}$  and  $\mu_{ge}$  may be obtained from UV-Vis absorption spectroscopy;  $\mu_{ge}$  is related to the oscillator strength,  $\varepsilon$ , and  $\Delta E_{ge}$  can be found from the onset of the low energy absorption(the ICT band). This simplified model gave much needed structural insight into chromophore design. As only the frontier orbitals makes major contributions to the polarized state, attention could be given to lowering the lowest occupied molecular orbital(LUMO) by increasing the acceptor strength and raising the highest occupied molecular orbital(HOMO) by increasing donor strength. This would lower  $\Delta E_{ge}$  and an increase in  $\beta_{vec}$  according to equation 1.13. But if  $\Delta E_{ge}$  is too low and the transition dipole,  $\mu_{ge}$ , high, there will be significant electron density localized along the bridge. This would subsequently lower the term  $(\mu_{ee} - \mu_{gg})$ , hinting at the underlying structure-property relationship.

## Bond-Length Alternation

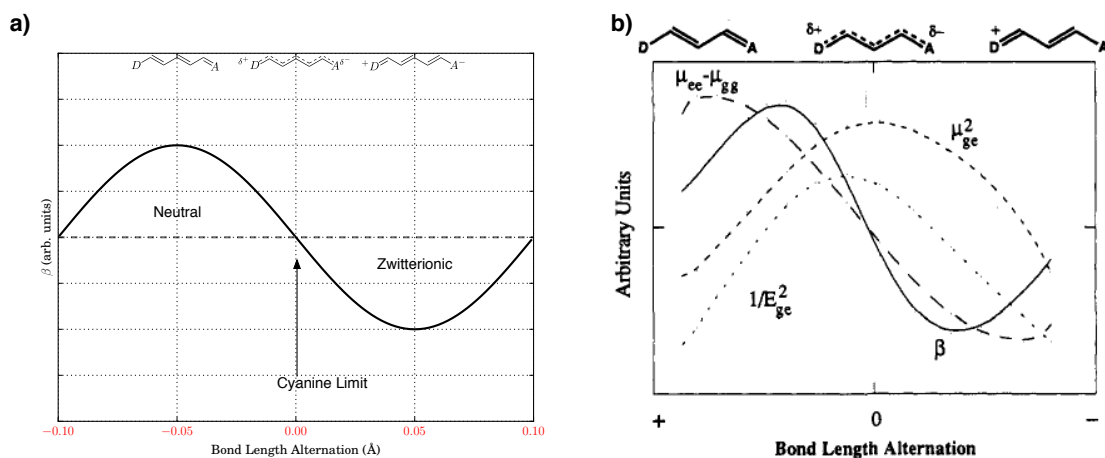


**Fig. 1.8** a) Bond-length alternation as described by Marder *et al.*. For any given donor/acceptor pair, there is a certain amount of alternation between single- and double-bonds that maximizes the molecular hyperpolarizability. There also exist a point where both the bond-length alternation and molecular hyperpolarizability will be zero and this is referred to as the cyanine limit. b) The relationship between bond length alternation and  $\beta$  (—),  $(\mu_{ee} - \mu_{gg})$  (---),  $(\mu_{ge})^2$  (- · - ·) and  $1/\Delta E_{ge}$  (· · ·) from equation 1.13.

Expanding upon the notion of the structure-property, Marder *et al.*, who showed that there was a mutual exclusion between the admixing of the HOMO and LUMO levels and the charge localization of the ground and polarized states. This was shown through the concepts of bond-length alternation (BLA) and bond-order alternation (BOA)<sup>[45]</sup>. Using a simple polyene system and varying the strength of an external electric field, Marder showed that  $\beta$  followed a sinusoidal dependence on the ground state polarization. Under this theory, the average difference between adjacent carbons in a polyene chain is calculated. For a molecule such as acetylene, the BLA should be (+11 Å), a carbon  $sp^2$ - $sp^2$  single bond is 1.45 Å and a double bond is 1.34 Å. This system would have a  $\beta$  of zero, but as acceptors and donors are added to the polyene chain, the degree of bond length polarization changes and there exist an optimal amount of ground state polarization to maximize  $\beta$ . If the ground state is too polarized, you reach the cyanine limit and  $\beta$  is minimized before crossing over

into a zwitterionic ground state regime. This is shown in figure Fig. 1.8 and demonstrates the importance of the structure-property relationship.

*Dewar's Rule and Chromophore Engineering*

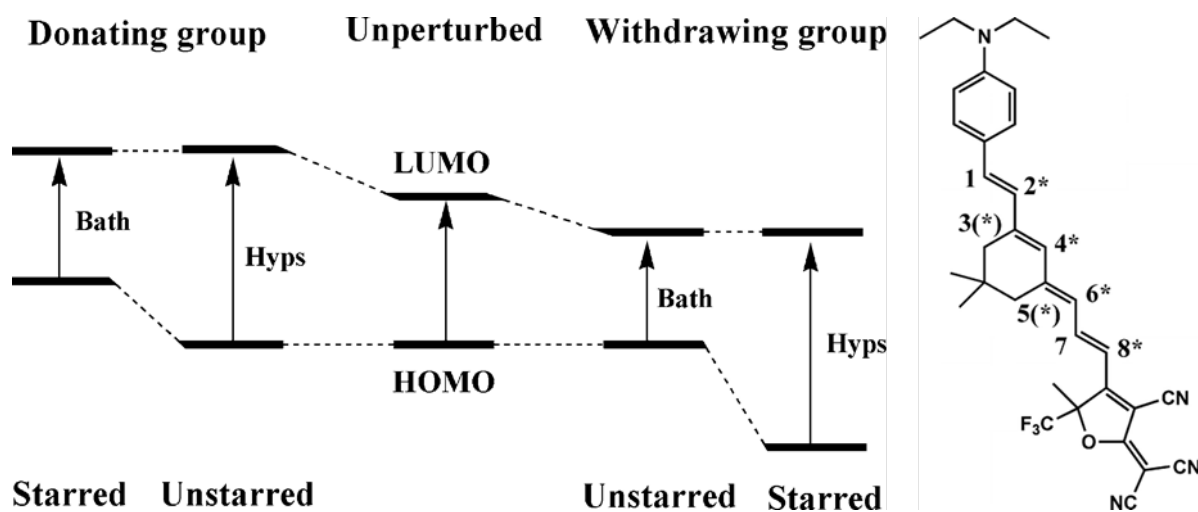


**Fig. 1.9** The left is a schematic description of the effects of substituents to the HOMO and LUMO levels according to Dewar's rules. A CLD-type chromophore is shown on the right with substitution positions on the conjugated backbone. These are divided into starred and unstarred groups with the positions 3(\*) and 5(\*) denoting substitution of the isophorone ring.

Bond-length alternation has been helpful in optimizing chromophore design<sup>[57]</sup>, but some have shown that it may not be applicable to all chromophore designs<sup>[58]</sup>. In attempts to engineer better chromophores, many schemes have been attempted. These attempts have run the gamut, from exotic shapes<sup>[59,60]</sup>, modified bridges<sup>[61–63]</sup> and donors<sup>[64,65]</sup> to mixed-state and bichromophore systems<sup>[64,66,67]</sup>. Most modifications have centered around attempts to provide better site-isolation while minimizing the effects on  $\beta$ .

One promising paradigm are chromophores based on Dewar's rules<sup>[68]</sup>. He found that for  $D - \pi - A$  type molecules, there was a pattern of alternating electronegativities along the  $\pi$ -conjugated backbone. As shown in Fig. 1.9, he proposed that this behavior can be used to predict the effects of substituents on the molecular energy levels based on the nature



of the substituent and location of the substitution. His work was based on perturbational molecular orbital theory, but in 2008, Chafin and Lindsay examined a polyene dye scaffold using density functional theory<sup>[69]</sup>. From their work, they found that the optimal pattern for optimizing the first molecular hyperpolarizability was substitute electron donating groups at the odd-numbered methine carbons and electron withdrawing groups at the even-numbered methine carbons. Their results mirrored Dewar’s finding. Following the guidance on where to place substituents and what types of substituents to substitute has allowed chromophores to be synthesized that exhibit higher hyperpolarizabilities and thermal stabilities than their unsubstituted counterparts<sup>[70–73]</sup>.

### **1.3 Aim and scope of this thesis**

The research described in this thesis aims to understand the structure-property relationship of donor groups, and by doing so, improve upon donor design for inclusion in EO chromophores. While much attention has been given to the  $\pi$ -conjugated bridge and acceptors<sup>[74]</sup>, there have been few systematic studies of electron donors<sup>[75]</sup>. That is not to say that donors beyond dialkyl amines do not exist in the literature, but they often arise as a consequence of trying to optimize other parts of the chromophore and are oft-times, neglected.

This work aims to remedy this, in part, by investigating a large body of donors with small perturbations. In doing so, a better understanding of the role of substituents on donor strength may be gleaned. Much like how the work of Chafin and Lindsay<sup>[69]</sup> offered guidance in how and where to substitute polyene bridges, this work aims to offer insight in to how and where to substitute donors. In doing so, better donors may be designed and current worst practices may be avoided in the future. Beyond that, this work aims to identify new potential donors that move beyond dialkyl and diaryl systems.

Much emphasis has been placed on the shape engineering of chromophores, but not necessarily on functional shape engineering. By functional, it is meant that substituents, if possible, should aid in the function of localizing the electron density at the donor in the ground state while not impeding overall polarization of the molecule. The molecular

hyperpolarizability of organic chromophores is dependent upon electron motion along the dipolar axis of the material from the donor, in the ground state, to the acceptor in the acceptor in the electronically excited state. Using density functional theory, donor structures will be investigated to discover how the molecular hyperpolarizability is affected by variations to i) how it is substituted and ii) how it is structured. Attempts will be made to identify trends that will lead to improvements in  $\beta$  and apply that to lessons learned from shape engineering. When possible, theoretical results will be compared to experimental work and attempts to synthesize new donors based on the study results shall be made.

**REFERENCES**

- [1] Anthony S. Travis. Perkin's mauve: Ancestor of the organic chemical industry. *Technology and Culture*, 31(1):51–82, 1990.
- [2] Karl Hübner. 150 jahre mauvein. *Chemie in unserer Zeit*, 40(4):274–275, 2006.
- [3] W. H. CLIFFE. In the footsteps of perkin. *Journal of the Society of Dyers and Colourists*, 72(12):563–566, 1956.
- [4] Paolo Zucca, Carla Vinci, Antonio Rescigno, Emil Dumitriu, and Enrico Sanjust. Is the bleaching of phenosafranine by hydrogen peroxide oxidation catalyzed by silica-supported 5,10,15,20-tetrakis-(sulfonatophenyl)porphine-mn(iii) really biomimetic? *Journal of Molecular Catalysis A: Chemical*, 321(1–2):27 – 33, 2010.
- [5] Peter Buchwald, Emilio Margolles-Clark, Norma S Kenyon, and Camillo Ricordi. Organic dyes as small molecule protein-protein interaction inhibitors for the cd40-cd154 costimulatory interaction. *J Mol Recognit*, 23(1):65–73, Jan-Feb 2010.
- [6] Ute Resch-Genger, Markus Grabolle, Sara Cavaliere-Jaricot, Roland Nitschke, and Thomas Nann. Quantum dots versus organic dyes as fluorescent labels. *Nat Meth*, 5(9):763–775, 09 2008.
- [7] Masaru Matsuoka. Dyes for optical recording. *Molecular Crystals and Liquid Crystals Science and Technology. Section A. Molecular Crystals and Liquid Crystals*, 224(1):85–94, 1993.
- [8] Agostina L. Capodilupo, Eduardo Fabiano, Luisa De Marco, Giuseppe Ciccarella, Giuseppe Gigli, et al. [1]benzothieno[3,2-b]benzothiophene-based organic dyes for dye-sensitized solar cells. *The Journal of Organic Chemistry*, 81(8):3235–3245, 2016. PMID: 26986652.

- [9] Brian O'Regan and Michael Gratzel. A low-cost, high-efficiency solar cell based on dye-sensitized colloidal  $\text{TiO}_2$  films. *Nature*, 353(6346):737–740, 10 1991.
- [10] K. Sano, K. Murata, T. Otsuji, T. Akeyoshi, N. Shimizu, et al. An 80-gb/s optoelectronic delayed flip-flop ic using resonant tunneling diodes and uni-traveling-carrier photodiode. *IEEE Journal of Solid-State Circuits*, 36(2):281–289, Feb 2001.
- [11] Larry R. Dalton, William H. Steier, Bruce H. Robinson, Chang Zhang, Albert Ren, et al. From molecules to opto-chips: organic electro-optic materials. *J. Mater. Chem.*, 9:1905–1920, 1999.
- [12] *Organic electro-optic/silicon photonic materials and devices*, volume 6638, 2007.
- [13] Cisco Systems Inc. Cisco visual networking index: Global mobile data traffic forecast update, 2015–2020, 2016.
- [14] Robert W. Boyd. *Nonlinear Optics*. Academic Press, 2013.
- [15] Paras N. Prasad and David J. Williams. *Introduction to Nonlinear Optical Effects in Molecules and Polymers*. John Wiley & Sons, Inc., 1991.
- [16] Bahaa E. A. Saleh and Malvin Carl Teich. *Fundamentals of Photonics*. John Wiley & Sons, Inc., 1991.
- [17] B. Bleaney and B.I Bleaney. *Electricity and Magnetism*, volume 3rd. Oxford University Press, 1976.
- [18] J Hamrle, S Blomeier, O Gaier, B Hillebrands, H Schneider, et al. Huge quadratic magneto-optical kerr effect and magnetization reversal in the  $\text{Co}_2\text{FeSi}$  heusler compound. *Journal of Physics D: Applied Physics*, 40(6):1563, 2007.
- [19] V.A.G.I.I. John, D.M. Gill, and R.W. Smith. Chirp compensated mach-zehnder electro-optic modulator, December 31 2002. US Patent 6,501,867.

- [20] Matthias Lauermann, Stefan Wolf, Philipp C. Schindler, Robert Palmer, Sebastian Koeber, et al. 40 gbd 16qam signaling at 160 gb/s in a silicon-organic hybrid modulator. *J. Lightwave Technol.*, 33(6):1210–1216, Mar 2015.
- [21] Luca Alloatti, Robert Palmer, Sebastian Diebold, Kai Philipp Pahl, Baoquan Chen, et al. 100 ghz silicon-organic hybrid modulator. *Light Sci Appl*, 3:e173–, 05 2014.
- [22] J. Leuthold, C. Koos, W. Freude, L. Alloatti, R. Palmer, et al. Silicon-organic hybrid electro-optical devices. *IEEE Journal of Selected Topics in Quantum Electronics*, 19(6):114–126, Nov 2013.
- [23] J. Zyss and J. L. Oudar. Relations between microscopic and macroscopic lowest-order optical nonlinearities of molecular crystals with one- or two-dimensional units. *Phys. Rev. A*, 26:2028–2048, Oct 1982.
- [24] Honghong Chen, Qi Ma, Yuqiao Zhou, Zhou Yang, Mojca Jazbinsek, et al. Engineering of organic chromophores with large second-order optical nonlinearity and superior crystal growth ability. *Crystal Growth & Design*, 15(11):5560–5567, 2015.
- [25] B.H. Robinson, L.R. Dalton, A.W. Harper, A. Ren, F. Wang, et al. The molecular and supramolecular engineering of polymeric electro-optic materials. *Chemical Physics*, 245(1–3):35 – 50, 1999.
- [26] Marco Ronchi, Alessio Orbelli Biroli, Daniele Marinotto, Maddalena Pizzotti, M. Chiara Ubaldi, et al. The role of the chromophore size and shape on the shg stability of pmma films with embedded nlo active macrocyclic chromophores based on a cyclotetrasiloxane scaffold. *The Journal of Physical Chemistry C*, 115(10):4240–4246, 2011.
- [27] Cheng Zhang, Lianjie Zhang, Stephanie J. Benight, Benjamin C. Olbricht, Lewis E. Johnson, et al. Shape engineering to promote head-tail interactions of electro-optic chromophores, 2013.

- [28] *An Extraordinary New Class of Electro-Optic Materials: Binary Chromophore Glasses*, July 2007.
- [29] Stephanie J. Benight, Daniel B. Knorr, Lewis E. Johnson, Philip A. Sullivan, David Lao, et al. Nano-engineering lattice dimensionality for a soft matter organic functional material. *Advanced Materials*, 24(24):3263–3268, 2012.
- [30] Jay S. Schildkraut. Determination of the electrooptic coefficient of a poled polymer film. *Appl. Opt.*, 29(19):2839–2841, Jul 1990.
- [31] C. C. Teng and H. T. Man. Simple reflection technique for measuring the electro-optic coefficient of poled polymers. *Applied Physics Letters*, 56(18):1734–1736, 1990.
- [32] Yoshito Shuto and Michiyuki Amano. Reflection measurement technique of electro-optic coefficients in lithium niobate crystals and poled polymer films. *Journal of Applied Physics*, 77(9):4632–4638, 1995.
- [33] V. Dentan, Y. Lévy, M. Dumont, P. Robin, and E. Chastaing. Electrooptic properties of a ferroelectric polymer studied by attenuated total reflection. *Optics Communications*, 69(5):379 – 383, 1989.
- [34] S. Herminghaus, Barton A. Smith, and J. D. Swalen. Electro-optic coefficients in electric-field-poled polymer waveguides. *J. Opt. Soc. Am. B*, 8(11):2311–2317, Nov 1991.
- [35] Ph. Prêtre, L.-M. Wu, R. A. Hill, and A. Knoesen. Characterization of electro-optic polymer films by use of decal-deposited reflection fabry–perot microcavities. *J. Opt. Soc. Am. B*, 15(1):379–392, Jan 1998.
- [36] Hisao Uchiki and Takayoshi Kobayashi. New determination method of electro-optic constants and relevant nonlinear susceptibilities and its application to doped polymer. *Journal of Applied Physics*, 64(5):2625–2629, 1988.

- [37] R. A. Norwood, M. G. Kuzyk, and R. A. Keosian. Electro-optic tensor ratio determination of side-chain copolymers with electro-optic interferometry. *Journal of Applied Physics*, 75(4):1869–1874, 1994.
- [38] K. D. Singer, M. G. Kuzyk, W. R. Holland, J. E. Sohn, S. J. Lalama, et al. Electro-optic phase modulation and optical second-harmonic generation in corona-poled polymer films. *Applied Physics Letters*, 53(19):1800–1802, 1988.
- [39] Christian Bosshard, Georg Knoepfle, Philippe Pretre, Stephan Follonier, Christophe Serbutoviez, et al. Molecular crystals and polymers for nonlinear optics. *Optical Engineering*, 34(7):1951–1960, 1995.
- [40] Christian Bosshard, Man Shing Wong, Feng Pan, Peter Günter, and Volker Gramlich. Self-assembly of an acentric co-crystal of a highly hyperpolarizable merocyanine dye with optimized alignment for nonlinear optics. *Advanced Materials*, 9(7):554–557, 1997.
- [41] Christian Bosshard, Ulrich Gubler, Phil Kaatz, Witold Mazerant, and Urs Meier. Non-phase-matched optical third-harmonic generation in noncentrosymmetric media: Cascaded second-order contributions for the calibration of third-order nonlinearities. *Phys. Rev. B*, 61:10688–10701, Apr 2000.
- [42] B.J. Coe, J.A. Harris, I. Asselberghs, K. Wostyn, K. Clays, et al. Quadratic optical nonlinearities of n-methyl and n-aryl pyridinium salts. *Advanced Functional Materials*, 13(5):347–357, 2003.
- [43] Larry R. Dalton, Philip A. Sullivan, and Denise H. Bale. Electric field poled organic electro-optic materials: State of the art and future prospects. *Chemical Reviews*, 110(1):25–55, 2010. PMID: 19848381.
- [44] Mark G. Kuzyk. Physical limits on electronic nonlinear molecular susceptibilities. *Phys. Rev. Lett.*, 85:1218–1221, Aug 2000.

- [45] Seth R. Marder, Lap-Tak Cheng, Bruce G. Tiemann, Andrienne C. Friedli, Mireille Blanchard-Desce, et al. Large first hyperpolarizabilities in push-pull polyenes by tuning of the bond length alternation and aromaticity. *Science*, 263(5146):511–514, 1994.
- [46] F. Meyers, S.R. Marder, B.M. Pierce, and J.L. Brédas. Tuning of large second hyperpolarizabilities in organic conjugated compounds. *Chemical Physics Letters*, 228(1):171 – 176, 1994.
- [47] Bruce G. Tiemann, Lap-Tak Cheng, and Seth R. Marder. The effect of varying ground-state aromaticity on the first molecular electronic hyperpolarizabilities of organic donor-acceptor molecules. *J. Chem. Soc., Chem. Commun.*, pages 735–737, 1993.
- [48] Joseph Zyss and Isabelle Ledoux. Nonlinear optics in multipolar media: theory and experiments. *Chemical Reviews*, 94(1):77–105, 1994.
- [49] Larry R. Dalton, Philip A. Sullivan, Denise H. Bale, and Ben C. Olbricht. Theory-inspired nano-engineering of photonic and electronic materials: Noncentrosymmetric charge-transfer electro-optic materials. *Solid-State Electronics*, 51(10):1263 – 1277, 2007. Special Issue: Papers Selected from the {NGC2007} Conference.
- [50] Yongqiang Shi, Cheng Zhang, Hua Zhang, James H. Bechtel, Larry R. Dalton, et al. Low (sub-1-volt) halfwave voltage polymeric electro-optic modulators achieved by controlling chromophore shape. *Science*, 288(5463):119–122, 2000.
- [51] Philip A. Sullivan and Larry R. Dalton. Theory-inspired development of organic electro-optic materials. *Accounts of Chemical Research*, 43(1):10–18, 2010. PMID: 19663413.
- [52] Cheng Zhang, , Larry R. Dalton, Min-Cheol Oh, Hua Zhang, et al. Low  $v\pi$  electrooptic modulators from cld-1: Chromophore design and synthesis, material processing, and characterization. *Chemistry of Materials*, 13(9):3043–3050, 2001.
- [53] *Synthesis of new second-order nonlinear optical chromophores: implementing lessons learned from theory and experiment*, volume 4114, 2000.



- [54] Yi Liao, Cyrus A. Anderson, Philip A. Sullivan, Andrew J. P. Akelaitis, Bruce H. Robinson, et al. Electro-optical properties of polymers containing alternating nonlinear optical chromophores and bulky spacers. *Chemistry of Materials*, 18(4):1062–1067, 2006.
- [55] J. L. Oudar and D. S. Chemla. Hyperpolarizabilities of the nitroanilines and their relations to the excited state dipole moment. *The Journal of Chemical Physics*, 66(6):2664–2668, 1977.
- [56] J. F. WARD. Calculation of nonlinear optical susceptibilities using diagrammatic perturbation theory. *Rev. Mod. Phys.*, 37:1–18, Jan 1965.
- [57] M. Blanchard-Desce, V. Alain, P. V. Bedworth, S. R. Marder, A. Fort, et al. Large quadratic hyperpolarizabilities with donor–acceptor polyenes exhibiting optimum bond length alternation: Correlation between structure and hyperpolarizability. *Chemistry – A European Journal*, 3(7):1091–1104, 1997.
- [58] Venkatakrisnan Parthasarathy, Ravindra Pandey, Matthias Stolte, Sampa Ghosh, Frédéric Castet, et al. Combination of cyanine behaviour and giant hyperpolarisability in novel merocyanine dyes: Beyond the bond length alternation (bla) paradigm. *Chemistry – A European Journal*, 21(40):14211–14217, 2015.
- [59] Parmeshwar Solanke, Filip Bureš, Oldřich Pytela, Milan Klikar, Tomáš Mikysek, et al. T-shaped (donor– $\pi$ )<sub>2</sub>acceptor– $\pi$ –donor push–pull systems based on indan-1,3-dione. *European Journal of Organic Chemistry*, 2015(24):5339–5349, 2015.
- [60] Yuhui Yang, Hongyan Xiao, Haoran Wang, Fenggang Liu, Shuhui Bo, et al. Synthesis and optical nonlinear properties of novel y-shaped chromophores with excellent electro-optic activity. *J. Mater. Chem. C*, 3:11423–11431, 2015.
- [61] Chaolei Hu, Fenggang Liu, Hua Zhang, Fuyang Huo, Yuhui Yang, et al. Synthesis of novel nonlinear optical chromophores: achieving excellent electro-optic activity by

- introducing benzene derivative isolation groups into the bridge. *Journal of Materials Chemistry C*, 3(44):11595–11604, 2015.
- [62] Fenggang Liu, Yuhui Yang, Shengyu Cong, Haoran Wang, Maolin Zhang, et al. Comparison of second-order nonlinear optical chromophores with d-[small pi]-a, d-a-[small pi]-a and d-d-[small pi]-a architectures: diverse nlo effects and interesting optical behavior. *RSC Adv.*, 4:52991–52999, 2014.
- [63] Fenggang Liu, Haoran Wang, Yuhui Yang, Hua jun Xu, Maolin Zhang, et al. Nonlinear optical chromophores containing a novel pyrrole-based bridge: optimization of electro-optic activity and thermal stability by modifying the bridge. *J. Mater. Chem. C*, 2:7785–7795, 2014.
- [64] Shengyu Cong, Airui Zhang, Fenggang Liu, Dan Yang, Maolin Zhang, et al. Improving poling efficiency by synthesizing a nonlinear optical chromophore containing two asymmetric non-conjugated d-[small pi]-a chains. *RSC Adv.*, 5:10497–10504, 2015.
- [65] Yuhui Yang, Jialei Liu, Maolin Zhang, Fenggang Liu, Haoran Wang, et al. The important role of the location of the alkoxy group on the thiophene ring in designing efficient organic nonlinear optical materials based on double-donor chromophores. *J. Mater. Chem. C*, 3:3913–3921, 2015.
- [66] Yi Liao, Sanchali Bhattacharjee, Kimberly A. Firestone, Bruce E. Eichinger, Rajan Paranj, et al. Antiparallel-aligned neutral-ground-state and zwitterionic chromophores as a nonlinear optical material. *Journal of the American Chemical Society*, 128(21):6847–6853, 2006. PMID: 16719465.
- [67] Victoria Peddie, Jack Anderson, Joanne E. Harvey, Gerald J. Smith, and Andrew Kay. Synthesis and solution aggregation studies of a suite of mixed neutral and zwitterionic chromophores for second-order nonlinear optics. *The Journal of Organic Chemistry*, 79(21):10153–10169, 2014. PMID: 25265243.

- [68] M. J. S. Dewar. 478. colour and constitution. part i. basic dyes. *J. Chem. Soc.*, pages 2329–2334, 1950.
- [69] Andrew P. Chafin and Geoffrey A. Lindsay. A pattern for increasing the first hyperpolarizability of a push–pull polyene dye as indicated from dft calculations. *The Journal of Physical Chemistry C*, 112(21):7829–7835, 2008.
- [70] Yen-Ju Cheng, Jingdong Luo, Su Huang, Xinghua Zhou, Zhengwei Shi, et al. Donor–acceptor thiolated polyenic chromophores exhibiting large optical nonlinearity and excellent photostability. *Chemistry of Materials*, 20(15):5047–5054, 2008.
- [71] Jane Hung, Wenkel Liang, Jingdong Luo, Zhengwei Shi, Alex K.-Y. Jen, et al. Rational design using dewar’s rules for enhancing the first hyperpolarizability of nonlinear optical chromophores. *The Journal of Physical Chemistry C*, 114(50):22284–22288, 2010.
- [72] Jingdong Luo, Su Huang, Yen-Ju Cheng, Tae-Dong Kim, Zhengwei Shi, et al. Phenyltetraene-based nonlinear optical chromophores with enhanced chemical stability and electrooptic activity. *Organic Letters*, 9(22):4471–4474, 10 2007.
- [73] Huaajun Xu, Dan Yang, Fenggang Liu, Mingkai Fu, Shuhui Bo, et al. Nonlinear optical chromophores based on dewar’s rules: enhancement of electro-optic activity by introducing heteroatoms into the donor or bridge. *Phys. Chem. Chem. Phys.*, 17:29679–29688, 2015.
- [74] Karin Schmidt, Stephen Barlow, Amalia Leclercq, Egbert Zojer, Sei-Hum Jang, et al. Efficient acceptor groups for nlo chromophores: competing inductive and resonance contributions in heterocyclic acceptors derived from 2-dicyanomethylidene-3-cyano-4,5,5-trimethyl-2,5-dihydrofuran. *J. Mater. Chem.*, 17:2944–2949, 2007.
- [75] Ohyun Kwon, Stephen Barlow, Susan A. Odom, Luca Beverina, Natalie J. Thompson, et al. Aromatic amines: A comparison of electron-donor strengths. *The Journal of Physical Chemistry A*, 109(41):9346–9352, 2005. PMID: 16833276.

## Chapter 2

# UNDERSTANDING THE EFFECTS OF STRUCTURE AND SUBSTITUENTS ON DONOR STRENGTH

### 2.1 Introduction

A rigorous investigation of the structure-property relationship of donors by purely synthetic means would be a daunting undertaking given the near endless possibilities of what is currently achievable current synthetic knowledge. For the affect of substituents on donor strength to be truly sussed out, many permutations would have to be explored making very minor changes with each iteration. Thankfully, there are other methods available to explore this structure-property relationship: namely computational chemistry. Given the advancements in modern computers, the matter of interrogating a large number of molecules bearing minor differences becomes almost trivial.

To study the structure-property relationship at the molecular level, Density functional theory (DFT)<sup>[1,2]</sup> has become an valuable tool as one can gain insight on both the linear and nonlinear properties of the target molecule<sup>[1-5]</sup>. For larger ensembles, Monte-Carlo simulations have been proven to lend insight in to how structural differences affect bulk properties<sup>[1,6]</sup>. It should also be mentioned that pioneering work by Kerry Garrett on small clusters—orientations obtained from both crystal structures and Monte-Carlo simulations—using DFT has offered insight into what might expected from bulk systems of EO chromophores<sup>[2]</sup>.

Typical EO chromophores contain a substituted amine attached to an aromatic ring<sup>[8-12]</sup>. While variants of this scheme exist, most donors still contain an aniline-like structure. This is, perhaps, best exemplified by the donors studied by Kwon *et al.* and shown in Fig. 2.1<sup>[7]</sup>. These structures have consistently been found to offer the best performance in EO applications and can be categorized in to one of four groups: alkyl (DA), ring-locked (RL), ring (R)

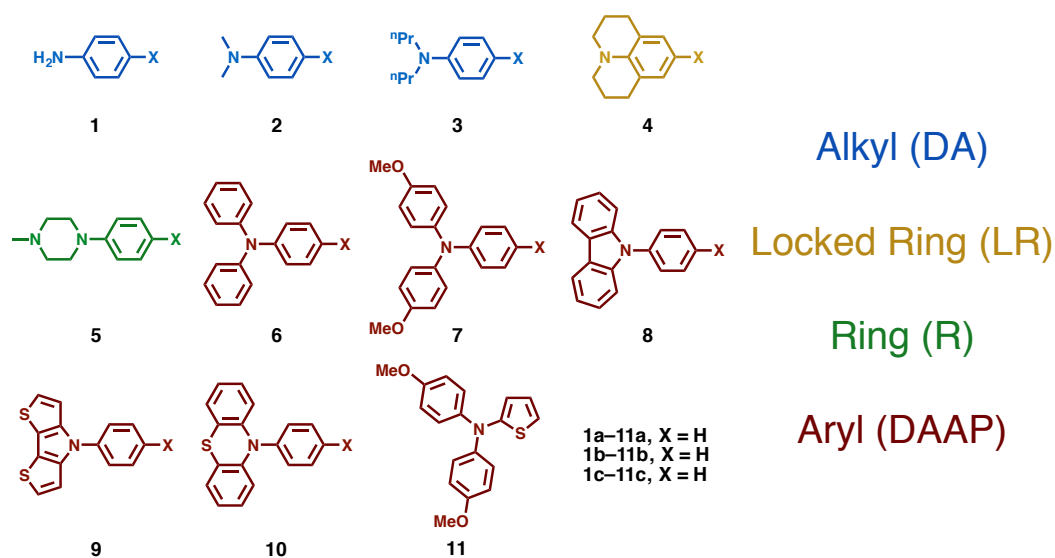


**Fig. 2.1** Donors studied Kwon *et. al.*<sup>[7]</sup>, separated into 4 basic donor structures: Alkyl (DA), Locked Ring (LR), Ring (R) and Aryl (DAAP). These basic structure types will serve as the basis for all structures investigated in this study.

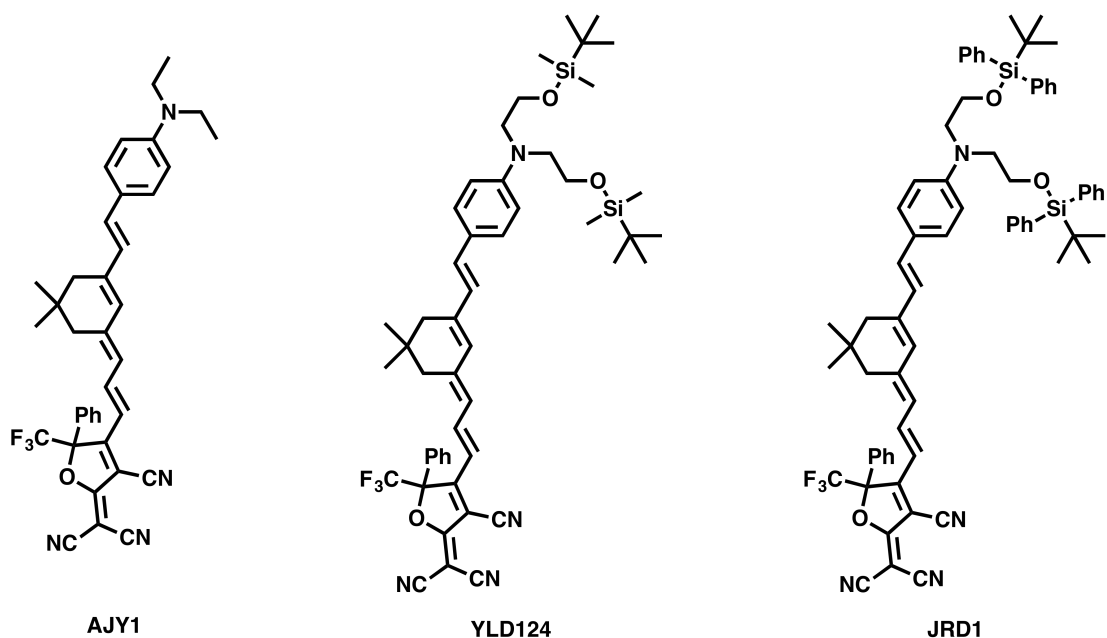


**Fig. 2.2** The structures of three CLD chromophores with the  $\text{CF}_3\text{Ph-TCF}$  acceptor and different donors.

and aryl (DAAP). During this study, they concluded that alkyl donors were the overall better choice for use with EO chromophores<sup>[7]</sup>. This conclusion was based partly on the C—X (where X is either O or N) bond distances of their CHO or CN acceptors. They used the C—X bond distance as a measure of the donor's ability to contribute to the charge-separated structure and they found a linear correlation between the C—O and C—N distances for 10 of the 11 molecules in the test set<sup>[7]</sup>. Due to sterics, many of the aryl donors were inferior to alkyl donors, despite being more thermally stable<sup>[13–16]</sup>. They did suggest that an aryl donor based on bis(4-methoxyphenyl)amine might be a workable compromise as it would offer the thermal stability of an aryl donor with a donor strength similar to N,N-dimethylaniline<sup>[7]</sup>.

Alkyl donors have been the most widely studied group of donors and a number of motifs have been introduced that improve upon simple dialkylamines (such as dimethyl or diethylamine). Recently, advances in this class of donor have allowed for translation of molecular hyperpolarizabilities to macroscopic susceptibilities<sup>[17]</sup>. In moving from tert-butyldimethylsilyl (TBDMS) ethers to tert-butyldiphenylsilyl (TBDPS) ethers, JRD1 was able to realize high macroscopic efficiencies in a neat chromophore system despite having a lower number density than neat YLD124<sup>[17]</sup>. These structures are shown in Fig. 2.2 to illustrate the subtle changes between AJY1, YLD124 and JRD1, all chromophores with identical bridges and acceptors and slightly different donors. The static hyperpolarizabilities, in vacuum, for the series were calculated to be  $444 \times 10^{-30} \text{ esu}$ ,  $460 \times 10^{-30} \text{ esu}$  and  $483 \times 10^{-30} \text{ esu}$ <sup>[17]</sup>. This shows the effects of subtle changes to the donor on the properties of chromophores and suggests that the silyloxy groups contribute to the electronic properties, contrary to the findings of Oudar and Chemla. In their work with para-nitroaniline, they found a negligible effect on  $\beta$  when the amine was replaced by a methylalaninate and concluded that additional  $\sigma$  and non-conjugated  $\pi$  bonds had no effect<sup>[18]</sup>.

In 2004, Spraul and coworkers had presented a number of chromophores based on a bis(4-methoxyphenyl)amine donor with an FTC-type bridge<sup>[20]</sup> and the following year, the same group presented chromophores with a CLD-type bridge<sup>[21]</sup>. Their choice was based on work previously performed by Pierre-Bonhote on Ruthenium dyes for solar cell applica-

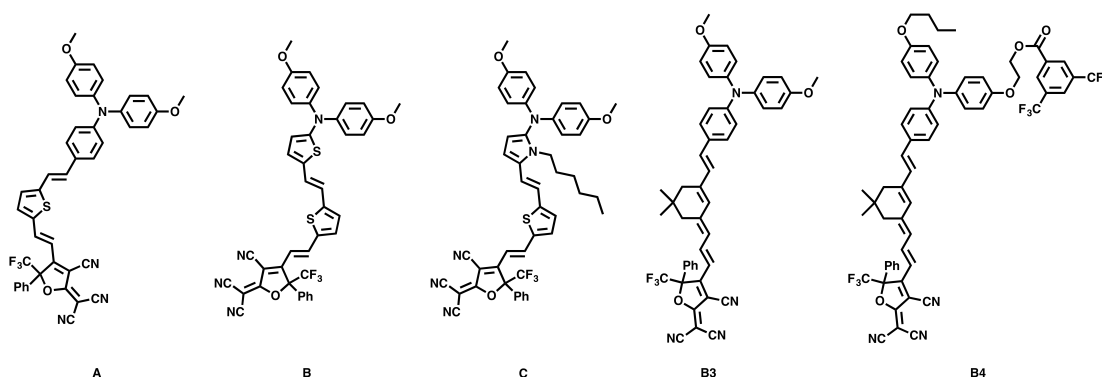


**Fig. 2.3** Representative di-aryl chromophore based on FTC (A–C)<sup>[19]</sup> or CLD (B3–4)<sup>[9]</sup> bridges.

tions<sup>[22]</sup>, who found the donor to possess a long-lived light-induced charge separated state. As previously reported for DAAP chromophore, those of Spraul, Suresh *et al.* had high decomposition temperatures near or above 300°C and exceptional measured hyperpolarizabilities. New DAAP chromophores with both FTC- and CLD-type bridges and the CF<sub>3</sub>Ph-TCF acceptor were later explored by the Cheng and coworkers and were found to have both large  $\beta$  values and EO coefficients in poled polymer systems (see Fig. 2.3)<sup>[9]</sup>. A point of interest, the chromophore with 4-methoxyphenyl (B3) aryl units had a higher measured hyperpolarizability – as determined by Hyper-Rayleigh Scattering – than one with a 4-butoxyphenyl and 4-(2-phenoxyethyl 3,5-bis(trifluoromethyl)benzoate) (B4) aryl units, but lower device performance. This may be contributed to enhanced compatibility of B4 with its polymer host by switching from two methoxy groups to a butyloxy group and ethoxy 3,5-bis(trifluoromethyl)benzoate group. This improvement might be compared to that observed when the TBDMS group on YLD124 was replaced by TBDPS. Further improvements were made with these systems by Davies *et al.* in 2008 by replacing the donor phenyl ring with thiophene and pyrrole<sup>[19]</sup>.

The following work will explore the structure-property relationship of EO chromophores to explore how structural changes to the donor affect the predicted hyperpolarizability. All

chromophores contain a simple vinyl bridge coupled to the TCP acceptor, unless otherwise noted (see structure DA-00 in Fig. 2.4). Donor structures falling, roughly, into one of the four groups shown in Fig. 2.1 are evaluated using DFT compared to (DA-00), as a baseline, and YLD124TMS and YLD124M will serve as target goals.

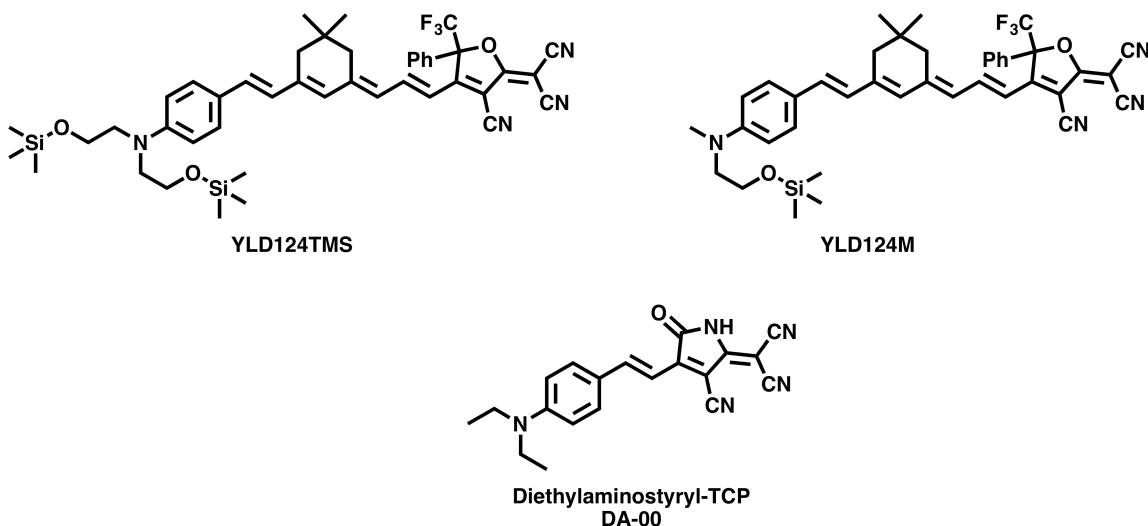


**Fig. 2.4** Structures used as guidance in the evaluation of new donors. YLD124TMS contains a bis(2-((trimethylsilyl)oxy)ethyl)amine donor while YLD124M contains a 2-methoxy-*N*-methylethylamine donor. Chromophore DA-00 shows the general structure of all chromophores to be evaluated. This chromophore contains a diethylamine donor and will serve as a basis against which all other donors are compared.

## 2.2 Computational Methodology

All structure and property calculation for the chromophores found in this study were calculated using the Gaussian 09 program<sup>[23]</sup>. The CAM-B3LYP hybrid exchange–correlation functional<sup>[24]</sup> and the 6-31+G\* basis set were used for all geometry optimizations in the gas phase. Frequency analysis of the minimized geometries was performed to confirm the absence of imaginary vibration modes. The vertical excitation energies were calculated using time-dependent DFT (TDDFT) formalism with the dispersion-corrected version of the range-separated  $\omega$ B97X functional<sup>[25]</sup>. Solvent effects on the excitation energies were sim-



ulated using the polarized continuum model as implemented in Gaussian 09<sup>[26,27]</sup> and calculated for the first 6 excited states. Population analysis was determined using Mulliken Population Analysis<sup>[28]</sup> as implemented in the GaussSum package<sup>[29]</sup>.

Molecular hyperpolarizabilities were calculated from the gas phase optimized structures *in vacuo* and in chloroform using the finite-field method<sup>[30-33]</sup>. Two DFT functionals were used for these calculations to verify the validity of the observed trends. The first was hybrid functional that utilizes the meta generalized-gradient approximation (GGA)<sup>[34]</sup> from the Minnesota 06 family<sup>[35]</sup>. Hybrid functionals incorporate some amount of exact exchange from Hartree-Fock(HF) theory that is constant at all points in space. The amount of HF exchange in the M06-2x functional 54% and this family of functionals have been shown to be superior to other hybrid functionals such as B3LYP in calculations where long-range self-interaction error (SIE) is a problem<sup>[36]</sup>. The other functional was a long-range corrected functional. Functionals from this class have partitioning parameters that allow the amount of HF exchange to be increased as larger inter-electronic distances, thus limiting SIE at large distances where it is known to dominate. The second functional used in this work was the CAM-B3LYP functional with the default partitioning parameters. The 6-31+G\* basis set was used for all calculations and static hyperpolarizabilities were deconvoluted from Gaussian output using MATLAB code originally developed by Bruce Eichinger. It has been updated and converted to Python using numpy and appears in Appendix B. All values are reported according to the Perturbation convention using cgs units. To aid in comparing donor strength, absolute hyperpolarizabilities have been converted to relative changes in hyperpolarizability from structure **DA-00** according to

$$\beta_{rel} = \frac{\beta_{zzz}^{sys} - \beta_{zzz}^{DA-00}}{\beta_{zzz}^{DA-00}} \quad (2.1)$$

where  $\beta_{zzz}^{sys}$  bears the donor of interest and  $\beta_{zzz}^{DA-00}$  has a N,N-diethylamine donor.

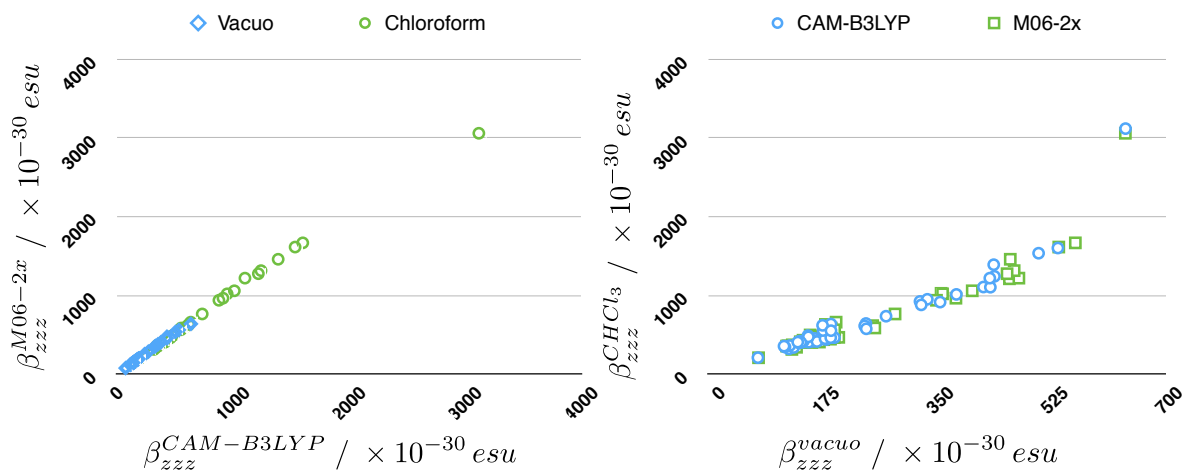


**Fig. 2.5** A comparison of  $\beta_{zzz}(0)$  calculated at the CAM-B3LYP and M06-2x levels of theory *in vacuo* and in chloroform. On the left is a comparisons of CAM-B3LYP vs M06-2x in vacuum( $\diamond$ ) and chloroform( $\circ$ ). On the right, we compare Vacuum vs chloroform for CAM-B3LYP( $\circ$ ) and M06-2x( $\square$ )

## 2.3 Results and Discussion

### 2.3.1 A brief comparison of methods

In general, DFT is good at predicting the general trends that are observed in experimental measurements, but fails to get the magnitude<sup>[37]</sup> of the molecular hyperpolarizability. It also fails to capture the gains experimentally observed by moving from an FTC-type bridge to a CLD-type bridge. The structures within this study all contain short bridges of two to four carbon units, but it should be noted that some of the presented predictions may not fully represent the full potential of an actual chromophore. For a given set of conditions, we would expect the property predictions from several methods to yield the same trend. To verify this, the hyperpolarizabilities predicted by CAM-B3LYP and M06-2x, both *in vacuo* and in chloroform were compared. These comparisons are shown in Fig. 2.5. There was a strong correlation found when keeping the solvent system the same, but changing the DFT functional. When comparing the trend of *in vacuo* values to those in chloroform, there was not a strong correlation. It is known that the hyperpolarizability of a molecule will vary

with solvent environment<sup>[38]</sup>, as the ground state structure adopts different conformations based on the dielectric environment. In a study of the effects of the dielectric environment,  $\beta_{HRS}^{1907}$  was observed to increase as the dielectric increased with one odd peculiarity: in dichloromethane, the values decreased for both measured chromophore systems<sup>[38]</sup>. For this study, the predicted values in chloroform are higher than those *in vacuo*, but the trends do not correlate well with each other as might be expected.

### 2.3.2 Change in relative static hyperpolarizabilities of donor structures

Due to the similarities between the values predicted by CAM-B3LYP and M06-2x, the focus will be on those produced by CAM-B3LYP and the properties predicted with M06-2x will not be presented in Fig. 2.7 but may be found in Appendix ???. In comparing the predicted values, we find that the improvements from the reference system in chloroform are often worse than in vacuum. In fact, some structures, such as DA-05, DA-06, DA-09, DA-17, DA-19–20 and DA-23, have a negative enhancement in chloroform. Furthermore, many of the structures that had a negative change in vacuum appear to become more negative in chloroform. The structures based on a bis(2-hydroxyethyl)amine donor (DA-05–DA-08) or (2-hydroxyethyl)methylamine were of particular interest due to their common use in chromophores. The asymmetric donor, DA-15 has very poor performance based on these calculations. One might expect DA-15 to be closer to DA-07, but there is a 15% difference between the two and latter is predicted to be a weaker donor than the reference diethylamine donor. For other asymmetric donors with longer alkyl chains, the performance is predicted to be better than the reference structure and even the base bis(2-hydroxyethyl)amine donor is predicted to be higher than the reference donor. Based on these observations, the decrease in  $\beta$  can reasonably be attributed to the smaller methyl unit on DA-15.

It is important to check theoretical predictions against experimental data, whenever possible, to ensure that the results are valid. The molecular hyperpolarizability is closely tied to the intramolecular charge transfer process. This relationship between the major component of the first-order hyperpolarizability along the dipolar axis and the spectroscopic

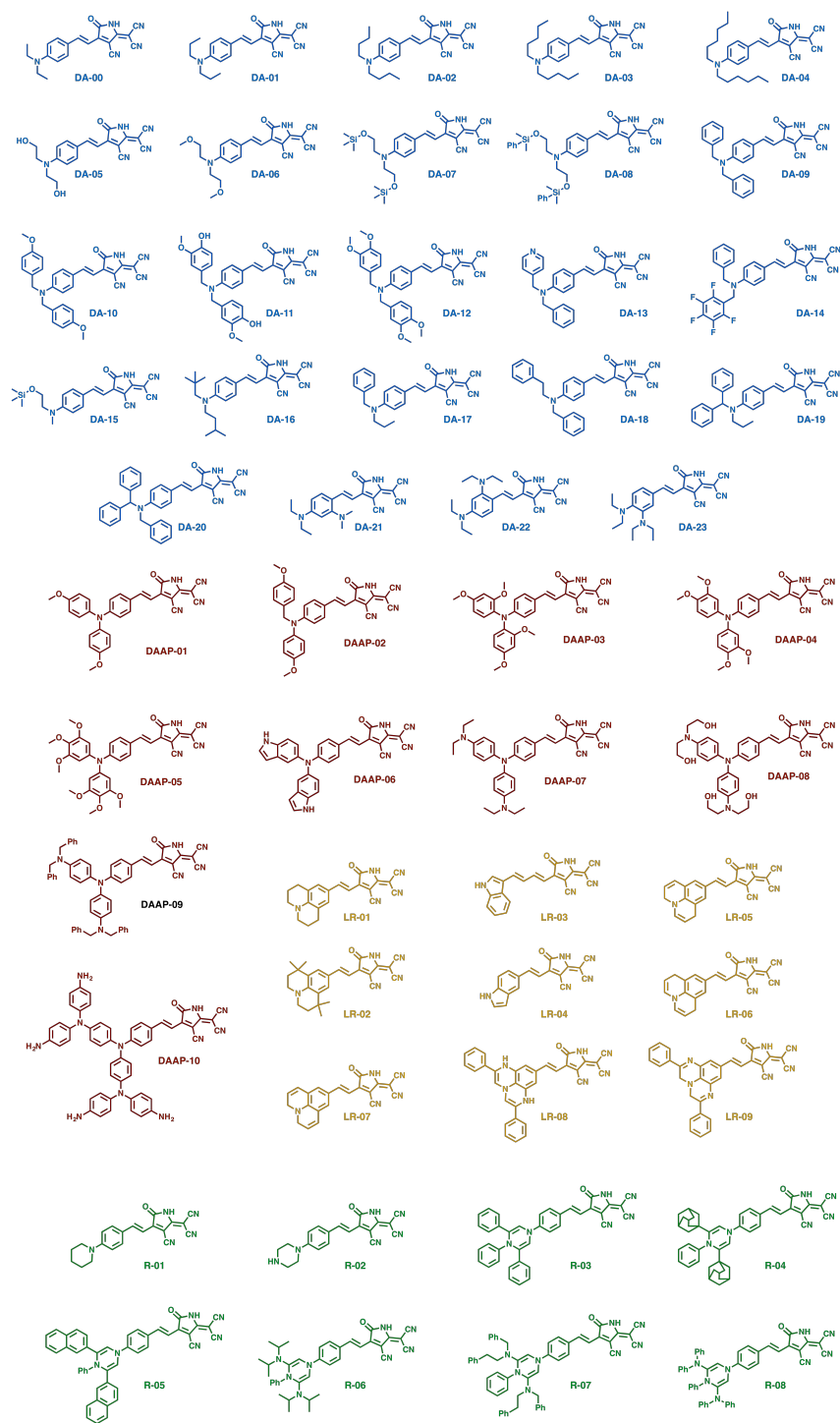


**Fig. 2.6** Structures of the chromophores evaluated in this study. They are broken down according to the categories listed in figure Fig. 2.1.

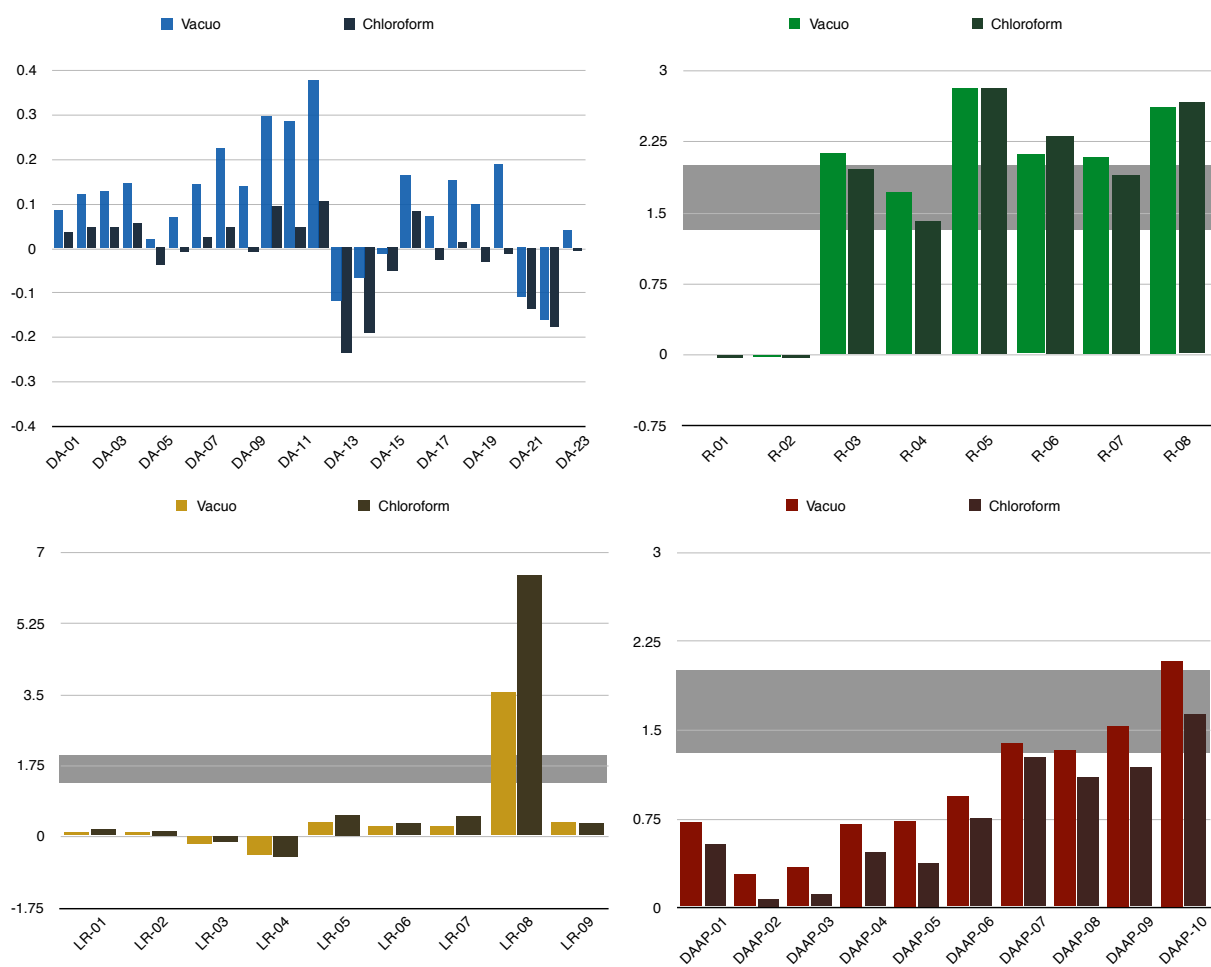


**Fig. 2.7** The change in  $\beta_{zzz}^{sys}$  from DA-00 of chromophores *in vacuo* and in chloroform. The shaded area represents the range between YLD124M (bottom) and YLD124TMS (top). Properties were calculated with Gaussian 09d at the CAM-B3LYP/6-31+G\*\*/CAM-B3LYP/6-31+G\* level of theory.

properties of a molecule was proposed by Oudar and Chemla<sup>[18]</sup>. They observed that the ground state was strongly coupled to a single electronic excited (charge transfer) state, allowing a simplification of the sum-over-states approach to just include these two states such that

$$\beta_{zzz} = \frac{\Delta\mu_{ge}\mu_{ge}^2}{E_{ge}^2} \quad (2.2)$$

where  $\Delta\mu_{ge}$  is the change in dipole moment,  $\mu_{ge}$  is the transition state dipole and  $E_{ge}$  is the transition energy from the ground to the CT excited state. The term  $E_{ge}$  is directly related to the position of the CT band, and if it is assumed that structures DA-02, DA-07 and DA-08 have similar dipole moments and transition dipole moments, then  $\beta_{zzz}$  can be estimated by the position of the CT band with longer wavelengths meaning a higher first-order hyperpolarizability. The optical spectra were calculated using TD-DFT using PCM to simulate the solvent (chloroform) environment and are presented in Fig. 2.8. The CT band for DA-02 is red-shifted from both DA-07 and DA-08. This follows well with the predictions for DA-02 and DA-07, but not for DA-08. In the simulated spectra, there is no change in the position of the CT band for DA-07 and DA-08. Comparing experimental data for three similar chromophores, we find the dibutylamine donor red shifted from either of the bis(silyloxyethyl)amines. The *tert*-butyldimethylsilyloxy have the largest hypsochromic shift, but replacing the methyl groups with phenyl groups decreases this shift and brings the CT band closest to the dibutyl donor. This is in agreement with the predicted trends in  $\beta$ . The same trend is present for chromophores with an extended bridge, such as AJY1(810 nm), YLD124(786 nm)<sup>[38]</sup> and JRD-1(788 nm)<sup>[17]</sup>, and are shown in ??.

Overall, comparing the group of alkyl donors, the straight-chain donors merit further study as there was no observed decrease or plateau in  $\beta$  as the chain length was increased. This suggest that there may be some contribution from longer chains that goes beyond two carbons, but the data also suggest that these contributions may be masked by the solvent environment. A solvent whose trends match those in vacuum might be a better solvent for future HRS measurements, but without extensive testing this cannot be concluded with any

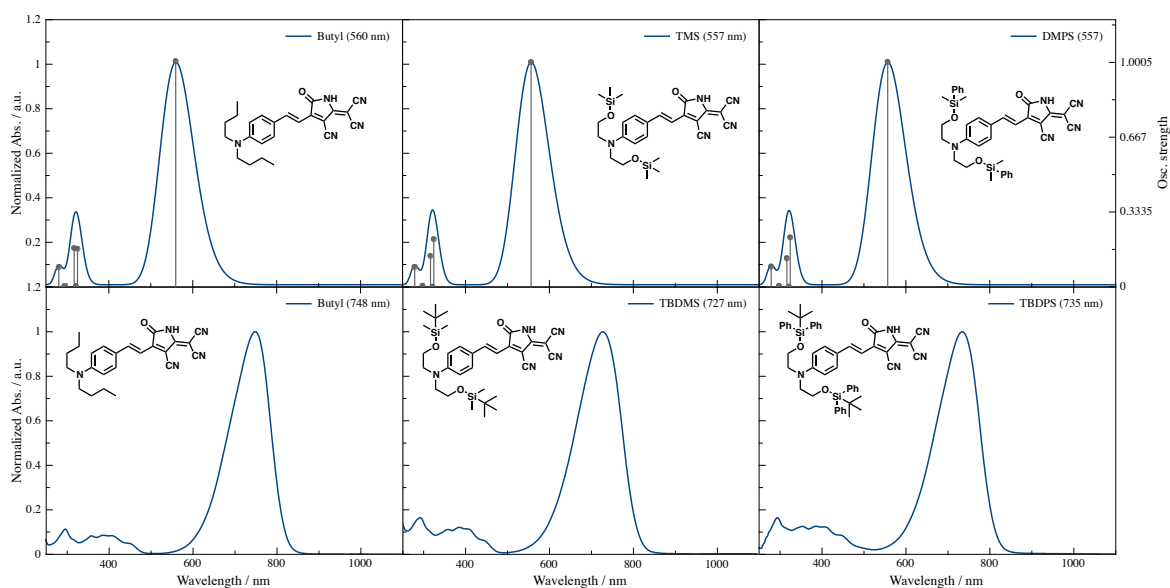


**Fig. 2.8** Theoretical (top) and experimental (bottom) optical spectra comparing the effects of silyl ethers on the intramolecular charge transfer band. The vertical lines in the theoretical spectra represent the relative oscillator strength of the transition(s) responsible for the observed peak.

certainty. In designing donors for future chromophores, methyl groups should be avoided as should electron withdrawing groups placed close to the donor. In coupling to hydroxyl groups, ethers are recommended over esters and benzyl or substituted benzyl moieties may be better than the current regime of hydroxyethyl based donors.

The trends observed from locked ring and ring-type donors followed very similar patterns. For fused rings, unsaturated six-member rings fused to benzene exhibited better gains than their five member ring analogs. Donors based on indole were among the worst chromophores tested (LR-03–04). Julolidine based donors (LR-01–02) closely matched dipropylamine (DA-01), showing no difference between flexible or rigid propyl groups. There did not appear to be any back-donation from these units into phenyl ring until the saturation was reduced. This improved donor strength, with the increase dependent on the location of the allylic site (LR-05–07). If the carbons in the 3- and 5-positions on the benzene ring are replaced by amines, there is a dramatic increase in the hyperpolarizability resulting in a small chromophore that should be better than a YLD124-class chromophore. Again, the location of the double-bonds matters as the gain seen in LR-08 is reduced considerably in the isomer LR-09.

With ring donors, the same process was followed to realize significant gains in this class of donor. There is no difference from the reference donor and one based on piperazine (R-01). A negative gain was found if the terminal amine is replaced by oxygen or thiophene (R-02), similar to what was observed in going from DA-01 to DA-05. Going back to R-01, if the degree of saturation is decreased and piperazine is converted to a substituted 1,4-dihydropyrazine, there is an improvement comparable to that seen for LR-08. To further investigate this donor, the substituents in the 3- and 5-positions of the pyrazine ring were changed to see how this might affect the donor strength. In structures R-03–08, there is a clear substituent effect on the donating ability of the pyrazine ring. For R-04, replacing the phenyl rings with adamantane reduces the properties to 80% of DA-03, but if those same rings are replaced with naphthyl rings, we see an improvement over DA-03. In fact, we find that the properties can be tuned quite readily by changing these groups, with naphthyl and diphenylamine providing the largest improvements over R-03, and DA-01.



Diaryl donors have already been shown to be better than dialkyl donors in previous studies<sup>[7]</sup>, but these donors were based on anisole. Further explorations to see if additional gains might be realized with this class of donor have been few and only recently have new chromophores been introduced<sup>[39]</sup>. Placing additional methoxy groups on anisole (DAAP-03–05) yielded little improvement over DAAP-01. This is in contrast to what was observed with DA-10 and DA-12. With the dibenzyl donors, improvements were found with additions of the first and second methoxy groups. Even the asymmetric donor, DAAP-02, failed to perform better than DA-10. The difference between DAAP-03 and DAAP-04 can be explained with sterics. Placing the methoxy groups ortho to the amine inhibits the ring from being able to properly rotate, keeping it from adopting an optimal configuration to allow efficient electron transfer. Why additional methoxy groups on a phenyl ring show a weaker effect on donor strength than those on a benzyl ring is harder to explain and warrants further investigation. Replacing oxygen with an amine has the expected effect as shown in DAAP-06–10. Donors based on indole had the lowest enhancement, but this was still better than the anisole based donor, DAAP-01. Much like what was seen with the dihydropyrazine ring, the substituents off the auxiliary amines affects the overall performance of the donors. Examination of the data suggests that these groups serve as auxiliary donors and that the stronger the auxiliary donor, the stronger the overall donor will be. To test this theory, the molecular hyperpolarizability of the DAAP or R chromophore was plotted as a function of the corresponding DA hyperpolarizability. If donors bearing chalcogens are ignored, there is a linear relationship between the structures shown in Fig. 2.9. This suggest that these are acting as double donor systems and that relative strength of new donors with these basic structures can be predicted by looking at the relative strengths of the auxiliary donors.

As discussed earlier, the first molecular hyperpolarizability can be explained as the change in electron densities of the molecule in going from the HOMO to the LUMO, so it is important to know how these new donors behave in comparison to a more traditional alkyl donor. The visualizations of these orbitals for DA-02, DAAP-09 and R-03 are presented in Fig. 2.10. There are noticeable differences between the three structures. For the bottom two, the

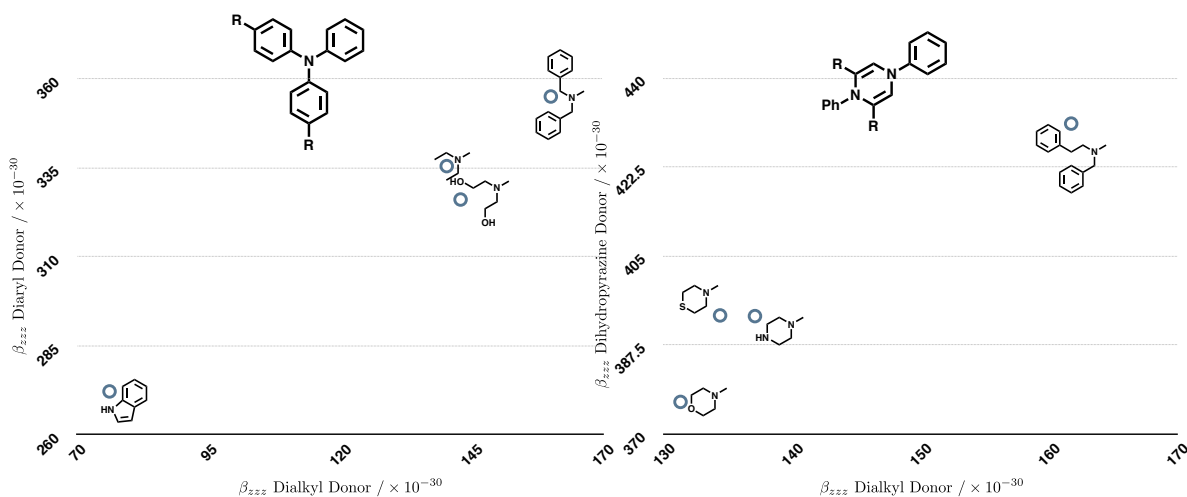


**Fig. 2.9** Calculated  $\beta_{zzz}$  of the shown dialkyl donor plotted against  $\beta_{zzz}$  of a diaryl donor (left) or pyrazine donor (right) bearing the same donor.

**Table 2.1** Mulliken population analysis of representative chromophores, calculated from Gaussian 09d with the pop=Full keyword and the GaussSum program.  $\Delta E = E_{LUMO} + E_{HOMO}$ . Values for  $\beta_{zzz}$  were calculated in vacuum.

		Donor	Bridge	Acceptor	$\Delta E / \text{eV}$	$\beta_{zzz}(0) / \times 10^{-30} \text{ esu}$
DA-02	LUMO	67%	14%	19%	4.15	157.2
	HOMO	12%	14%	74%		
DAAP-09	LUMO	13%	15%	72%	3.66	355.0
	HOMO	86%	6%	8%		
R-03	LUMO	12%	14%	74%	3.51	438.1
	HOMO	88%	5%	7%		

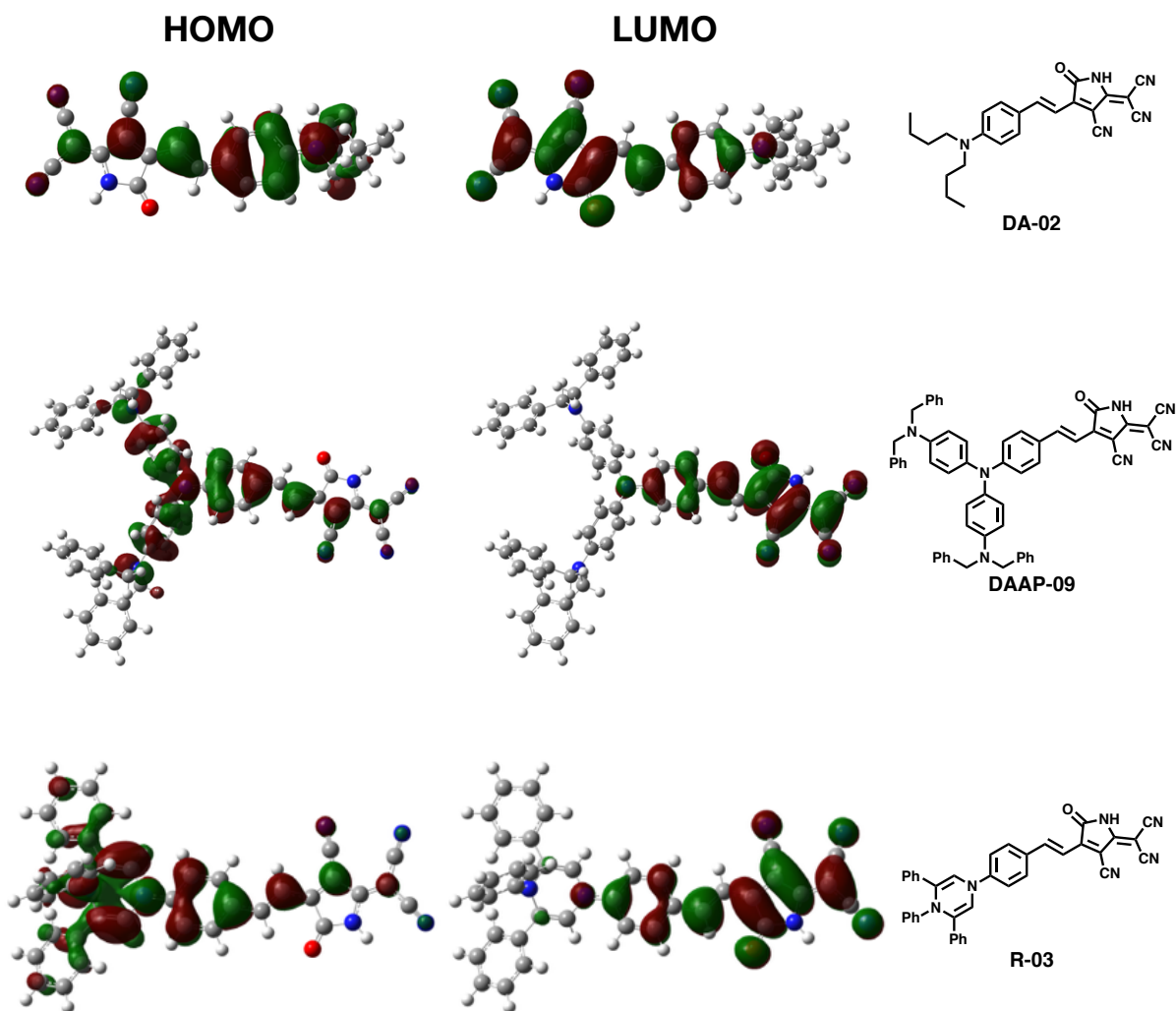


**Fig. 2.10** Frontier molecular orbitals of chromophores DA-02, DAAP-09 and R-03. Shown below the orbitals.

HOMO electron density extends further into the expanded structure of the donor, but it is difficult to tell with any clarity if this has had an effect on the electron density of the bridge or acceptor. To answer this, a Mulliken population analysis was performed and the results are presented in table ???. The chromophores all have the same acceptor and bridge, so there are no expectations for large differences in the LUMO electron density, as this is mostly determined by the acceptor, and we see that there is little to no change across the three molecules. In all cases, for the LUMO, nearly 72% of the electron density is centered around the acceptor. If this were not the case, a simple argument based on improved donor strength would no longer be possible. While the LUMO has not changed across the structures, there is a discernible change in the HOMO. For the new donors, more than 85% of the electron density is centered on the donor. This is a change of nearly 20% from the dibutyl donor. As mentioned above, this density extends into the expanded structure of the donor and corroborates what was seen in Fig. 2.9.

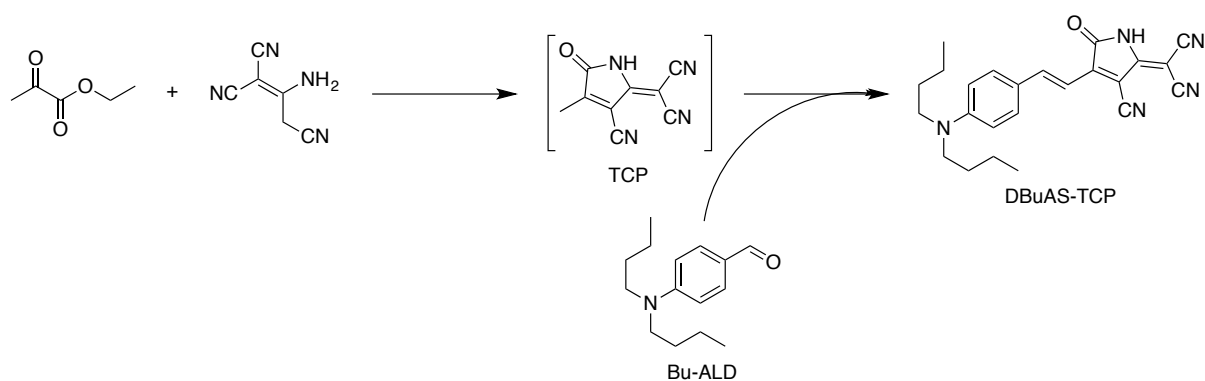
## **2.4 Conclusion**

An extensive study of chromophores with a small vinylic bridge and the TCP acceptor has been conducted to identify motifs that might be employed in designing next-generation donors. The study examined the effects of subtle changes in the donor structure on the overall predicted hyperpolarizability of the chromophore. Systems with chalcogens attached to alkyl chains, whether in a ring formation or not, were found to negatively affect  $\beta$  as compared to an alkyl chain of similar length (ethanol vs propane). Differences between esters, ethers, silyl ethers and silyl ethers bearing arenes was observed and it is recommended that the ethers and aryl-silyl ethers be employed with these types of donors to minimize the impact to  $\beta$ . Several new classes of donors have been identified as potential candidates for use in small chromophore systems with high hyperpolarizability and number density. Chromophores with these new donors had predicted properties that place them close to YLD124 type chromophores. If chromophores can be synthesized with these new donors and the improvements in hyperpolarizability translated from the microscopic to the macroscopic

regimes, this could be an important development in the design of future chromophores.

## 2.5 Experimental

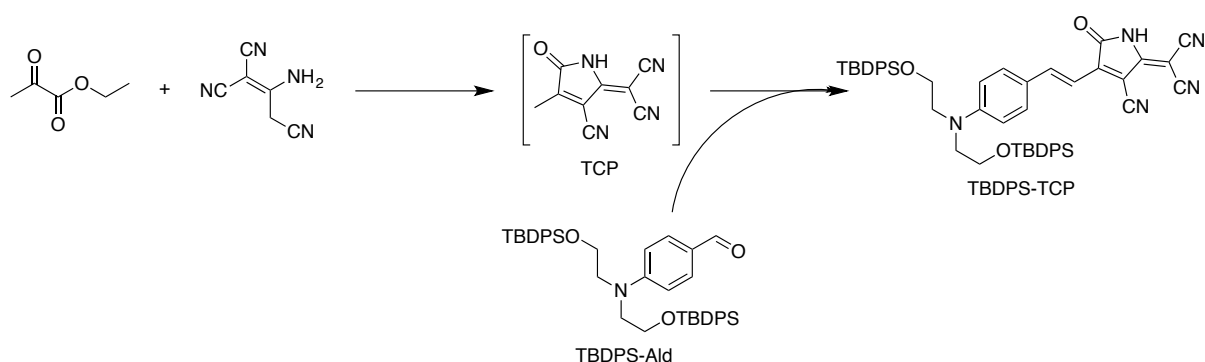
**General information:** Chemicals used were purchased from Sigma Aldrich, Alfa Aesar or TCI and used without further purification unless otherwise noted. UV-visible Absorption Spectroscopy was obtained on a Shimadzu 1601.  $^1\text{H}$  NMR spectra were acquired using a Bruker AVance series instrument running at 300 MHz.



**Scheme 2.1** Synthesis of Butyl-TCP.

### *Synthesis of (Butyl-TCP)*

To a 20 mL vial containing a magnetic stir bar was placed malononitrile dimer (1 eq), ethyl pyruvate (1.1 eq.) and ethanol (2 mL/mmol). The vial was sealed and heated at 85°C for 0.5 hours at which point, **Bu-ALD** (0.9 eq) was added in one portion and heating continued for an additional 6 hours. Once cool, the precipitated product was collected via filtration and washed with isopropanol, ethanol and chloroform until the filtrate ran clear. The solid was dried under vacuum at 60°C overnight to yield 0.56g (54%) Butyl-TCP as a green microcrystals.  $^1\text{H}$  NMR (300 MHz, DMSO- $d_6$ )  $\delta$  9.30 (1H, d), 8.76 (1H, d), 7.86 (2H, d), 7.77 (1H, d), 6.97 (2H, d), 4.20 (4H, t), 3.74 (4H, t), 1.97 (6H, s). MS (ESI) 398.4 (M-H).



**Scheme 2.2** Synthesis of TBDPS-TCP.

*Synthesis of (TBDPS-TCP)*

Chromophore **TBDPS-TCP** was synthesized exactly as **Butyl-TCP**, substituting **TBDPS-ALD** for **Bu-ALD**. The solvent was removed from by rotary evaporation and the residue was dissolved in a minimal amount of chloroform and the product precipitated from cold petroleum ether. This process was repeated three times to yield 0.49g (42%) **TBDPS-TCP** as a blue-green solid.  $^1\text{H}$  NMR (300 MHz, Acetone- $d_6$ )  $\delta$  8.50 (d,  $J = 15.3$  Hz, 1H), 7.65 (d,  $J = 6.4$  Hz, 8H), 7.42 (dd,  $J = 15.0, 7.3$  Hz, 14H), 7.06 (d,  $J = 15.3$  Hz, 1H), 6.79 (d,  $J = 9.0$  Hz, 2H), 3.89 (dd,  $J = 21.9, 5.2$  Hz, 8H), 1.03 (s, 18H).. MS (ESI) 853.6 (M+H).

**REFERENCES**

- [1] Lewis E. Johnson. *Multi-Scale Modeling of Organic Electro-Optic Materials*. Ph.D. thesis, University of Washington, 2012.
- [2] Kerry Garrett. *Computational Study of Linear and Nonlinear Optical Properties of Single Molecules and Clusters of Organic Electro-Optic Chromophores*. Ph.D. thesis, University of Washington, 2015.
- [3] Jan Andzelm, Berend C. Rinderspacher, Adam Rawlett, Joseph Dougherty, Roi Baer, et al. Performance of dft methods in the calculation of optical spectra of tcf-chromophores. *Journal of Chemical Theory and Computation*, 5(10):2835–2846, 2009. PMID: 26631795.
- [4] Muneaki Kamiya, Hideo Sekino, Takao Tsuneda, and Kimihiko Hirao. Nonlinear optical property calculations by the long-range-corrected coupled-perturbed kohn–sham method. *The Journal of Chemical Physics*, 122(23):234111, 2005.
- [5] Kyrill Yu. Suponitsky, Yi Liao, and Artëm E. Masunov. Electronic hyperpolarizabilities for donor-acceptor molecules with long conjugated bridges: Calculations versus experiment. *The Journal of Physical Chemistry A*, 113(41):10994–11001, 2009. PMID: 19772332.
- [6] Andreas F. Tillack. *Electro-Optic Material Design Criteria Derived from Condensed Matter Simulations Using the Level-of-Detail Coarse-Graining Approach*. Ph.D. thesis, University of Washington, 2015.
- [7] Ohyun Kwon, Stephen Barlow, Susan A. Odom, Luca Beverina, Natalie J. Thompson, et al. Aromatic amines: A comparison of electron-donor strengths. *The Journal of Physical Chemistry A*, 109(41):9346–9352, 2005. PMID: 16833276.
- [8] Delwin L. Elder, Stephanie J. Benight, Jinsheng Song, Bruce H. Robinson, and Larry R.

- Dalton. Matrix-assisted poling of monolithic bridge-disubstituted organic nlo chromophores. *Chemistry of Materials*, 26(2):872–874, 2014.
- [9] Yen-Ju Cheng, Jingdong Luo, Steven Hau, Denise H. Bale, Tae-Dong Kim, et al. Large electro-optic activity and enhanced thermal stability from diarylaminophenyl-containing high- $\beta$  nonlinear optical chromophores. *Chemistry of Materials*, 19(5):1154–1163, 2007.
- [10] Ergin Yalçın, Sylvain Achelle, Yasmina Bayrak, Nurgül Seferoğlu, Alberto Barsella, et al. Styryl-based NLO chromophores: synthesis, spectroscopic properties, and theoretical calculations. *Tetrahedron Letters*, 56(20):2586 – 2589, 2015.
- [11] Mohamed Ashraf, Ayele Teshome, Andrew J. Kay, Graeme J. Gainsford, M. Delower H. Bhuiyan, et al. Synthesis and optical properties of NLO chromophores containing an indoline donor and azo linker. *Dyes and Pigments*, 95(3):455 – 464, 2012.
- [12] Xiaohua Ma, Fei Ma, Zhenhua Zhao, Naiheng Song, and Jianping Zhang. Toward highly efficient nlo chromophores: Synthesis and properties of heterocycle-based electronically gradient dipolar nlo chromophores chromophores. *J. Mater. Chem.*, 20:2369–2380, 2010.
- [13] Christopher R. Moylan, Robert J. Twieg, Victor Y. Lee, Sally A. Swanson, Kathleen M. Betterton, et al. Nonlinear optical chromophores with large hyperpolarizabilities and enhanced thermal stabilities. *Journal of the American Chemical Society*, 115(26):12599–12600, 1993.
- [14] Peter V. Bedworth, Yongming Cai, Alex Jen, , and Seth R. Marder. Synthesis and relative thermal stabilities of diphenylamino- vs piperidinyl-substituted bithiophene chromophores for nonlinear optical materials. *The Journal of Organic Chemistry*, 61(6):2242–2246, 1996.
- [15] Christopher R. Moylan, Susan Ermer, Steven M. Lovejoy, I-Heng McComb, Doris S. Leung, et al. (dicyanomethylene)pyran derivatives with c<sub>2v</sub> symmetry: An unusual



- class of nonlinear optical chromophores. *Journal of the American Chemical Society*, 118(51):12950–12955, 1996.
- [16] S. Thayumanavan, Jeffrey Mendez, , and Seth R. Marder. Synthesis of functionalized organic second-order nonlinear optical chromophores for electrooptic applications. *The Journal of Organic Chemistry*, 64(12):4289–4297, 1999.
- [17] Wenwei Jin, Peter V. Johnston, Delwin L. Elder, Karl T. Manner, Kerry E. Garrett, et al. Structure-function relationship exploration for enhanced thermal stability and electro-optic activity in monolithic organic nlo chromophores. *J. Mater. Chem. C*, 4:3119–3124, 2016.
- [18] J. L. Oudar and D. S. Chemla. Hyperpolarizabilities of the nitroanilines and their relations to the excited state dipole moment. *The Journal of Chemical Physics*, 66(6):2664–2668, 1977.
- [19] Joshua A. Davies, Arumugasamy Elangovan, Philip A. Sullivan, Benjamin C. Olbricht, Denise H. Bale, et al. Rational enhancement of second-order nonlinearity: Bis-(4-methoxyphenyl)hetero-aryl-amino donor-based chromophores: Design, synthesis, and electrooptic activity. *Journal of the American Chemical Society*, 130(32):10565–10575, 2008.
- [20] Bryan K. Spraul, S. Suresh, Takafumi Sassa, M. Ángeles Herranz, Luis Echegoyen, et al. Thermally stable triaryl amino chromophores with high molecular hyperpolarizabilities. *Tetrahedron Letters*, 45(16):3253 – 3256, 2004.
- [21] S. Suresh, Huseyin Zengin, Bryan K. Spraul, Takafumi Sassa, Tatsuo Wada, et al. Synthesis and hyperpolarizabilities of high temperature triarylamine-polyene chromophores. *Tetrahedron Letters*, 46(22):3913 – 3916, 2005.
- [22] Pierre Bonhôte, Jacques-E. Moser, Robin Humphry-Baker, Nicolas Vlachopoulos, Shaik M. Zakeeruddin, et al. Long-lived photoinduced charge separation and redox-

- type photochromism on mesoporous oxide films sensitized by molecular dyads. *Journal of the American Chemical Society*, 121(6):1324–1336, 1999.
- [23] M. J. Frisch, G. W. Trucks, H. B. Schlegel, G. E. Scuseria, M. A. Robb, et al. Gaussian 09 Revision D.01. Gaussian Inc. Wallingford CT 2009.
- [24] Takeshi Yanai, David P Tew, and Nicholas C Handy. A new hybrid exchange-correlation functional using the coulomb-attenuating method (cam-b3lyp). *Chemical Physics Letters*, 393(1-3):51 – 57, 2004.
- [25] Jeng-Da Chai and Martin Head-Gordon. Long-range corrected hybrid density functionals with damped atom-atom dispersion corrections. *Phys. Chem. Chem. Phys.*, 10:6615–6620, 2008.
- [26] Jacopo Tomasi, Benedetta Mennucci, and Roberto Cammi. Quantum mechanical continuum solvation models. *Chemical Reviews*, 105(8):2999–3094, 2005. PMID: 16092826.
- [27] Giovanni Scalmani and Michael J. Frisch. Continuous surface charge polarizable continuum models of solvation. i. general formalism. *The Journal of Chemical Physics*, 132(11):114110, 2010.
- [28] R. S. Mulliken. Electronic population analysis on lcao-àimo molecular wave functions. i. *The Journal of Chemical Physics*, 23(10):1833–1840, 1955.
- [29] Noel M. O’boyle, Adam L. Tenderholt, and Karol M. Langner. cclib: A library for package-independent computational chemistry algorithms. *Journal of Computational Chemistry*, 29(5):839–845, 2008.
- [30] Howard D. Cohen and C. C. J. Roothaan. Electric dipole polarizability of atoms by the hartree—fock method. i. theory for closed-shell systems. *The Journal of Chemical Physics*, 43(10):S34–S39, 1965.

- [31] Pratibha Chopra, Louis Carlacci, Harry F. King, and Paras N. Prasad. Ab initio calculations of polarizabilities and second hyperpolarizabilities in organic molecules with extended  $\pi$ -electron conjugation. *The Journal of Physical Chemistry*, 93(20):7120–7130, 1989.
- [32] Masayoshi Nakano, Isamu Shigemoto, Satoru Yamada, and Kizashi Yamaguchi. Size-consistent approach and density analysis of hyperpolarizability: Second hyperpolarizabilities of polymeric systems with and without defects. *The Journal of Chemical Physics*, 103(10):4175–4191, 1995.
- [33] Dennis M. Elking, Lalith Perera, Robert Duke, Thomas Darden, and Lee G. Pedersen. A finite field method for calculating molecular polarizability tensors for arbitrary multipole rank. *Journal of Computational Chemistry*, 32(15):3283–3295, 2011.
- [34] Jianmin Tao, John P. Perdew, Viktor N. Staroverov, and Gustavo E. Scuseria. Climbing the density functional ladder: Nonempirical meta-generalized gradient approximation designed for molecules and solids. *Phys. Rev. Lett.*, 91:146401, Sep 2003.
- [35] Yan Zhao and Donald G. Truhlar. The m06 suite of density functionals for main group thermochemistry, thermochemical kinetics, noncovalent interactions, excited states, and transition elements: two new functionals and systematic testing of four m06-class functionals and 12 other functionals. *Theoretical Chemistry Accounts*, 120(1):215–241, 2008.
- [36] Yan Zhao, , and Donald G. Truhlar. Density functional for spectroscopy: No long-range self-interaction error, good performance for rydberg and charge-transfer states, and better performance on average than b3lyp for ground states. *The Journal of Physical Chemistry A*, 110(49):13126–13130, 2006. PMID: 17149824.
- [37] Larry R. Dalton, Peter Günter, Mojca Jazbinsek, O-Pil Kwon, and Philip A. Sullivan. *Organic Electro-Optics and Photonics: Molecules, Polymers and Crystals*. Cambridge University Press, 2015.

- [38] Denise H. Bale. *Nonlinear Optical Materials Characterization Studies Employing Photostability, Hyper-Rayleigh Scattering, and Electric Field Induced Second Harmonic Generation Techniques*. Ph.D. thesis, University of Washington, 2008.
- [39] Yuhui Yang, Hongyan Xiao, Haoran Wang, Fenggang Liu, Shuhui Bo, et al. Synthesis and optical nonlinear properties of novel y-shaped chromophores with excellent electro-optic activity. *J. Mater. Chem. C*, 3:11423–11431, 2015.
- [40] J. F. WARD. Calculation of nonlinear optical susceptibilities using diagrammatic perturbation theory. *Rev. Mod. Phys.*, 37:1–18, Jan 1965.
- [41] Manthos G. Papadopoulos, Andrzej J. Sadlej, and Jerzy Leszczynski, editors. *Non-Linear Optical Properties of Matter: From molecules to condensed phases*, volume 1. Springer Netherlands, 2006.
- [42] Sei-Hum Jang, Jingdong Luo, Neil M. Tucker, Amalia Leclercq, Egbert Zojer, et al. Pyrroline chromophores for electro-optics. *Chemistry of Materials*, 18(13):2982–2988, 2006.
- [43] L. R. Dalton, A. W. Harper, R. Ghosn, W. H. Steier, M. Ziari, et al. Synthesis and processing of improved organic second-order nonlinear optical materials for applications in photonics. *Chemistry of Materials*, 7(6):1060–1081, 1995.
- [44] Seth R. Marder, Lap-Tak Cheng, Bruce G. Tiemann, Andrienne C. Friedli, Mireille Blanchard-Desce, et al. Large first hyperpolarizabilities in push-pull polyenes by tuning of the bond length alternation and aromaticity. *Science*, 263(5146):511–514, 1994.
- [45] Marco Tarini, Paolo Cignoni, and Claudio Montani. Ambient occlusion and edge cueing for enhancing real time molecular visualization. *IEEE Transactions on Visualization and Computer Graphics*, 12(5):1237–1244, 2006.

- [46] Xiaohua Ma, Fei Ma, Zhenhua Zhao, Naiheng Song, and Jianping Zhang. Synthesis and properties of nlo chromophores with fine-tuned gradient electronic structures. *J. Mater. Chem.*, 19:2975–2985, 2009.
- [47] Jessica Sinness, Olivier Clot, Scott R. Hammond, Nishant Bhatambrekar, Harrison L. Rommel, et al. Synthesis of dendridic nlo chromophores for the improvement of order in electro-optics. In *Symposium DD – Organic and Nanocomposite Optical Materials*, volume 846 of *MRS Proceedings*, page DD6.3 (6 pages). 2004.

## Chapter 3

# SYNTHESIS OF DIHYDROPYRAZINE DONOR

### **3.1 Introduction**

Pyrazines and, particularly 1,4-dihydropyrazines, are known compounds<sup>[1]</sup>, but a reliable synthesis for the latter had not been reported until the early 1970s, thanks to the work of Fowler and Chen<sup>[2,3]</sup>. Their work identified possibly the first confirmed synthesis of 1,4-dihydropyrazine— as opposed to 1,2- dihydropyrazine<sup>[4]</sup> – through the acetylation of a substituted 5,6-dihydropyrazine<sup>[3]</sup>. Later, Fourrey reported the synthesis of stable N-aryl dihydropyrazines<sup>[5]</sup>. Without proper substitution, 1,4-dihydropyrazines are known to undergo a [1,3] alkyl shift<sup>[6,7]</sup>, so by moving from benzyl amine to aniline and avoiding strong Lewis acids, Fourrey reported the successful synthesis of stable ring systems from phenacyl bromide. Following the approaches laid out by Fowler, Chen and Fourrey<sup>[2,3,5]</sup> and based on the results of theoretical calculations presented in Chapter 2, attempts were made to synthesize a donor based on substituted 1,4-dihydropyrazines for use as electron donors in EO chromophores.

### **3.2 Results and Discussion**

Small molecules hold promise for realizing large EO coefficients,  $r_{33}$  by virtue of their small size when compared to traditional FTC and CLD based chromophores. One problem with realizing this has been that no donors, when coupled to known acceptors by a small vinylic bridge, have shown performance capable of matching or exceeding current systems. Several donors from the study performed in Chapter 2, when coupled with the TCP acceptor, meet or exceed molecular hyperpolarizabilities of some CLD-class chromophores bearing a CF<sub>3</sub>Ph-TCF acceptor. Looking at table Table 3.1, a case can be argued for these small chromophores

**Table 3.1** Dipole moment ( $\mu_z$ ), hyperpolarizability ( $\beta_{zzz}$ ) and number density ( $\rho_N$ ) of chromophores. <sup>a</sup>The number density was calculated based on an estimated density of 1.00 g/cc. <sup>b</sup>values taken from reference<sup>[8]</sup>

	$\mu_z$ (D)	$\beta_{zzz}(0)$ ( $\times 10^{30} esu$ )	$\rho_N$ ( $\times 10^{20} molecules/cc$ ) <sup>a</sup>
YLD124 <sup>b</sup>	22.0	460	6.83
JRD1 <sup>b</sup>	21.4	483	5.33
DAAP-01		242	12.06
R-03	15.0	438	10.37
DAAP-07	18.5	335	10.35
DAAP-09	17.7	355	7.26

as they all have higher than number densities ( $\rho_N$ ) than the CLD class chromophores with hyperpolarizabilities that range from 51% to 93% of the average  $\beta$  or YLD124 and JRD1.

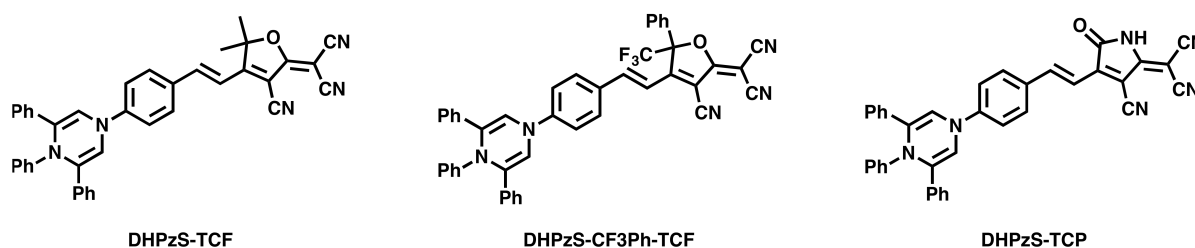
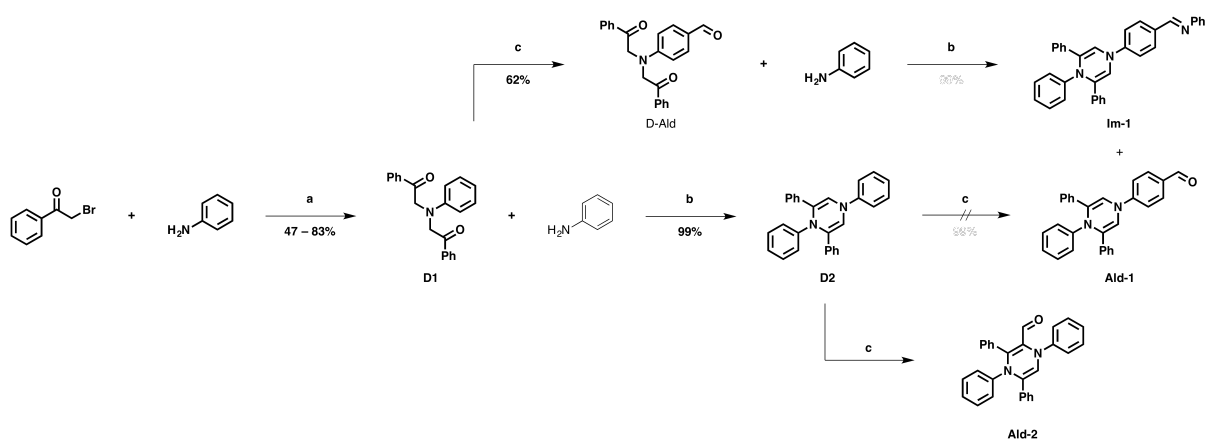


**Fig. 3.1** Initial structures proposed for evaluating the dihydropyrazine donor.

### 3.2.1 Synthesis of 1,4-dihydropyrazine donor

Three chromophores with a dihydropyrazine donor were proposed for initial studies and are shown in figure Fig. 3.1. This class of donor showed the largest improvement in  $\beta$ , a large number density,  $\rho_N$ , for a high  $\beta$  chromophore and, had lowest dipole moment of any of the possible donor candidates detailed in table Table 3.1. The synthetic scheme for the formylation of the dihydropyrazine donor is shown in Scheme 3.1, and to the best of the



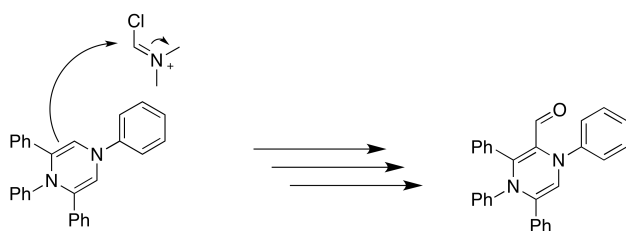
**Scheme 3.1** Formylation of dihydropyrazine donor. Reagents and conditions: (a) 1 equiv of aniline, 2.2 equiv halide, 4 equiv base, H<sub>2</sub>O, reflux 24 h; (b) 3 equiv aniline, 5% v/v 1:1 trifluoroacetic acid/acetic acid, toluene, reflux, 6h; (c) 1–1.5 equiv POCl<sub>3</sub>, DMF, rt, 0.5h, 90°C, 0.75h.

author's knowledge, this is the first time such a structure has been synthesized. Phenacyl bromide is commercially available, but may also be prepared by the Friedel-Crafts reaction between bromoacetyl bromide and any appropriate arene using AlCl<sub>3</sub> in dichloromethane or carbon sulfide. It may also be prepared from chloroacetyl chloride, but reactions between phenacyl chloride and aniline were found to yield only the monoacylated product. To force di-acetylation, an *in situ* Finkelstein reaction was required to convert the chloride to a bromide or iodide first. The reaction of aniline with phenacyl bromide, to produce D1 was performed in several protic and aprotic solvents. In all cases, sodium or potassium carbonates or bicarbonates gave the best results. Attempts with sodium hydroxide and sodium hydride as the base produced unidentifiable products and required an external cooling bath during addition or the halide to maintain control of an exothermic reaction. Triethylamine also required cooling during the initial stages of the reaction and produced a mixture of mono- and di-alkylated products, even when a large excess of the halide was employed. These were not issues when a milder base was employed. Reactions performed in acetone, propanol, isopropanol, DMF and water all gave the di-alkylated species as the major product. The highest yields were observed when water was used as a solvent and product isolation was



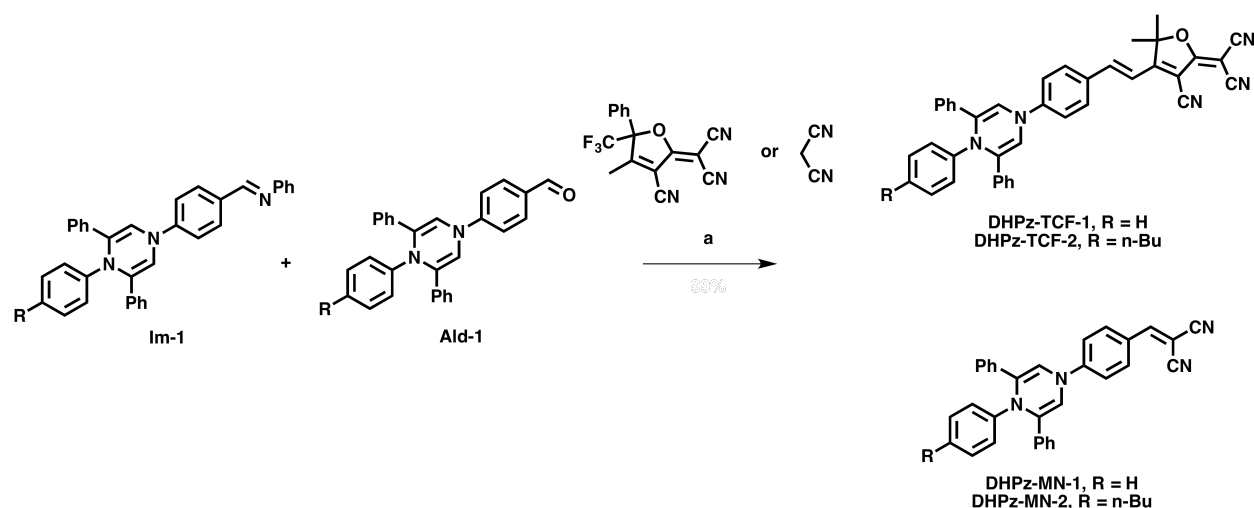
greatly simplified, requiring the precipitated product to be washed with water, dilute acid and aqueous isopropanol for product that was  $\geq 95\%$  pure by NMR.

Ring closure was accomplished by a catalytic system of 1:1 trifluoroacetic acid (TFA) and acetic acid (AcOH) in toluene. Attempts with p-toluenesulfonic acid (PTSA) in toluene had lower yields than the TFA:AcOH system and trace amounts were found to contaminate the final product, even after separation by silica gel and recrystallization from ethanol. It was also found that TFA, on its own, was not a good catalyst for ring closing procedure whereas acetic acid was. Yields were lower than with the 1:1 catalyst, but reactions could be done in toluene or just acetic acid with little to no effect on yield and product isolation from acetic acid could be achieved by inducing crystallization following aqueous dilution.



**Scheme 3.2** Vilsmeier-Haack formylation of the 1,4-dihydropyrazine system. Instead of formylating the phenyl ring, formylation occurred at the 2 position of the pyrazine ring.

The Vilsmeier-Haack formylation of D2 did not yield Ald-1, as expected. Instead, the isolated product was found to be Ald-2. The proposed mechanism is shown in Illustration Scheme 3.2. Instead of the arene reacting with the Vilsmeier reagent, the heteroarene at the position ortho to the amine. The Vilsmeier-Haack formylation requires an electron rich arene and the fact that the pyrazine ring reacted preferentially to either of the two arenes in the 1 or 4 position suggest that the pyrazine ring is more electron rich than a phenyl ring. Another reaction with tetracyanoethylene (TCNE) produced the same results with the electrophilic substitution occurring ortho at the 2- or 6-position<sup>1</sup>. To get around this, formylation of bis(phenacyl)aniline was done before closing the pyrazine ring. Following this route and the original ring closing procedure, the Schiff base was found to be the major



**Scheme 3.3** Synthesis of DHPz dyes. a) Ethanol or isopropanol, reflux, 30 minutes.

product. Reducing the amount of aniline present during the ring closing reaction produced both the aldehyde and the Schiff base, which were difficult to separate. An attempt was made to convert the aldehyde to a nitrile prior to ring-closure, but these reactions were low yielding and ring-closure of the resulting nitrile did not proceed in toluene, but was found to work in chloroform or dichloromethane using 30% acetic acid that contained 5% trifluoroacetic acid. Reversion of the nitrile back to the aldehyde, following ring closure, was accomplished by diisobutylaluminium hydride in dichloromethane at 0°C.

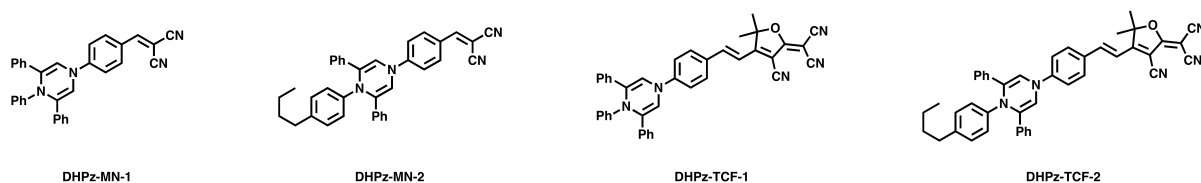


**Fig. 3.2** Structures of new chromophores with a dihydropyrazine donor. Chromophores **DHPz-TCF-1** and **DHPz-TCF-2** were synthesized by Dr. Delwin Elder.

<sup>1</sup>This was determined qualitatively by comparing the spectrum of the product from this reaction to the spectrum of a chromophore known to have been substituted on the arene para to the the pyrazine ring.

The Knoevenagel condensation reactions (see scheme Scheme 3.3) of acceptors with either the pure aldehyde or mixed aldehyde/Schiff base appeared to proceed as other acceptor/aldehyde condensations. A color change was noticed within minutes following addition of ethanol to the reaction vessel containing the CF<sub>3</sub>Ph-TCF acceptor and aldehyde and the reactions were allowed to proceed, under reflux, for 30 minutes at which time TLC showed near complete consumption of the starting material. It was during a typical workup and isolation using silica gel that the dihydropyrazine ring was found to be unstable. For the CF<sub>3</sub>Ph-TCF chromophore, the ring was removed so that the only isolated product was the chromophore with a free amine. Chromophores with the TCP acceptor were found to decompose even more quickly than those with the CF<sub>3</sub>Ph-TCF acceptor. Doctor Delwin Elder was able to isolate two chromophores with the TCF acceptor and condensation of the aldehyde with malononitrile in refluxing isopropanol was found to proceed smoothly and without any of the problems experienced with the stronger acceptors. All of the synthesized DHPz dyes are shown in figure Fig. 3.2.

### 3.2.2 Optical Properties

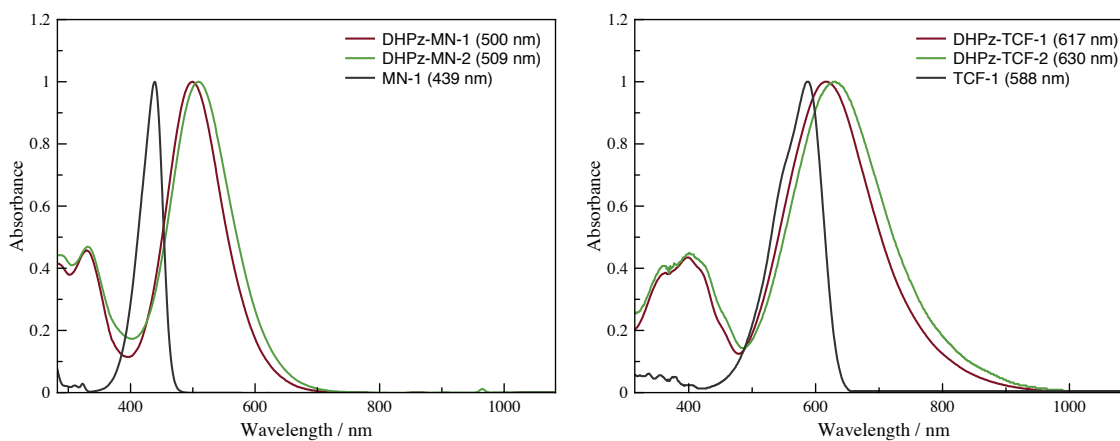


**Fig. 3.3** UV-Vis absorption spectra of chromophores **DHPz-MN-1**, **DHPz-MN-2** (left), **DHPz-TCF-1** and **DHPz-TCF-2** (right) in chloroform.

Optical absorption spectra allow us to probe the effects of structural changes on the intramolecular charge transfer band of dipolar chromophores. Per the theoretical calculations performed in Chapter 2, we expect the DHPz structure to be a better donor than diethyl amine. In figure Fig. 3.3 are the UV-Vis spectra of the DHPz chromophores and chromophores Mn-1 and TCF-1 for comparison. All chromophores exhibit a similar low energy transition which accounts for the  $\pi \rightarrow \pi^*$  transition, that is primarily responsible for the NLO response. For the DHPz chromophores, this ICT band is shifted to higher energies and suggest that the DHPz donor is better than the diethyl amine donor. For **DHPz-MN-1** and **DHPz-MN-2**, these shifts are +61 nm and +70 nm, respectively<sup>2</sup>. The addition of the butyl group in **DHPz-MN-2**, along with aiding in solubility, appears to also increase donor strength as evidenced by the +9 nm shift from **DHPz-MN-1**. A similar picture is observed for the TCF chromophores, with **DHPz-TCF-1** having a bathochromic shift of 29 nm from TCF-1 and **DHPz-TCF-2** having a shift of +42 nm. Again, their is a bathochromic shift (of +13 nm) when going from **DHPz-TCF-1** to **DHPz-TCF-2**. Based on theoretical calculations performed for R-03, this high energy transition is primarily attributed to a HOMO-10 $\rightarrow$ LUMO transition. Based on the large bathochromic shifts (61–70 nm for the Mn acceptor and 29–42nm for the TCF acceptor), it is concluded that the DHPz donor is better than the diethylamine donor.

### 3.2.3 Cyclic Voltammetry Measurements

To confirm the results of the UV-Vis study, cyclic voltammetry was performed to ascertain the ionization potential (IP) and electron affinity (EA). These values can be obtained from the oxidation peak and reduction peak onset potentials and are directly related to the HOMO and LUMO levels of the chromophore<sup>[9]</sup>. With this information, we can determine the energy gap( $LUMO - HOMO$ ) for comparison with our UV-Vis results and directly compare the HOMO levels of each chromophore. The cyclic voltammograms are shown in figure Fig. 4.2

---

<sup>2</sup>The +/- sign convention is used to indicate either a bathochromic (+) or hypsochromic (-) shift. The presence of the sign holds no other significance.

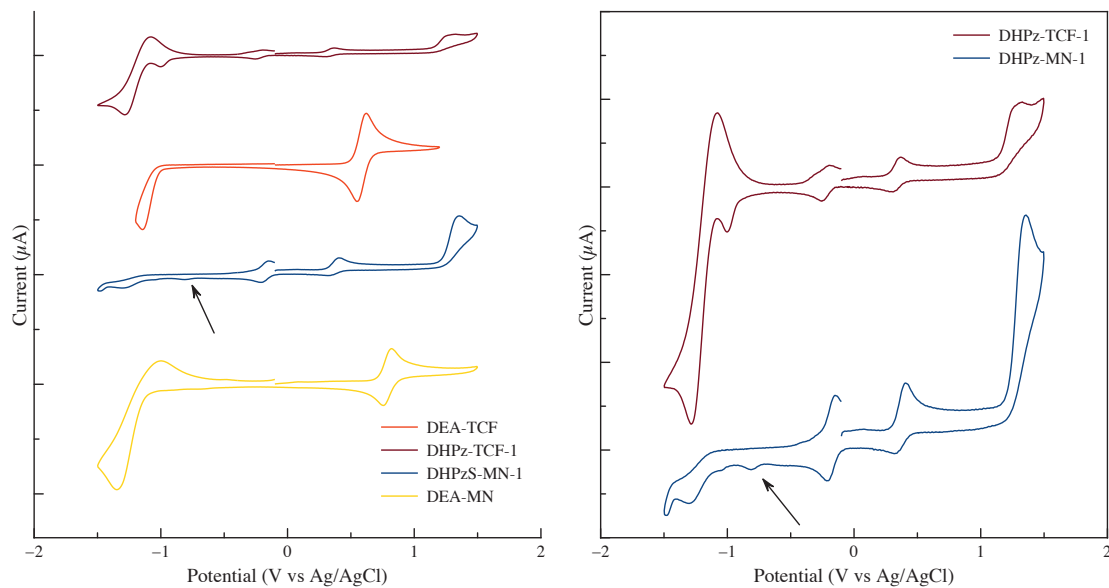


**Fig. 3.4** Cyclic voltammograms of chromophores DEA-MN, DEA-TCF, **DHPz-MN-1** and **DHPz-TCF-1** (left) and **DHPz-MN-1** and **DHPz-TCF-1** (right). Voltammograms were recorded in acetonitrile solutions containing a 0.1 M  $\text{Bu}_4\text{NPF}_6$  supporting electrolyte at a scan rate of  $50 \text{ mV s}^{-1}$ .

**Table 3.2** Electrochemical and optical properties of chromophores in study.

	$\lambda_{max}^{CHCl_3}$	$E_{ox}^{HOMO}$	$E_{red}^{LUMO}$	$E_g^{CV}$	$E_g^{Opt}$	$\beta_{zzz}(0)$
	nm	(eV)	(eV)	(eV)	(eV)	( $\times 10^{-30}$ esu)
DEA-MN	439	-5.11	-3.26	1.85	2.66	21.1
DEA-TCF		-4.99	-3.61	1.38		65.7
DHPz-MN-1	500	-4.71	-3.67	1.03	2.04	79.4
DHPz-TCF-1	616	-4.00	-3.49	0.51	1.59	194.2
DHPz-MN-2	509	—	—	—	1.98	—
DHPz-TCF-2	630	—	—	—	1.54	—

and the results tabulated in table Table 4.1. It is clear from the voltammograms that the HOMO level has shifted to a lower potential in the chromophores **DHPz-MN-1** and **DHPz-TCF-1** compared to MN-1 and TCF-1. The DHPz chromophores have two reversible oxidation peaks, the first one occurring near -0.2 V (vs Ag/AgCl). From this onset potential, the HOMO energy can be found from

$$E_{ox}^{HOMO} = -e[E_{ox}^{onset} + 4.4] eV \quad (3.1)$$

and similarly, the LUMO energy can be determined from

$$E_{red}^{LUMO} = -e[E_{red}^{onset} + 4.4] eV \quad (3.2)$$

where  $E_{ox}^{onset}$  and  $E_{red}^{onset}$  are in volts and  $e = 1\text{eV/V}^{[9]}$ . In going from a DEA donor to a DHPz donor, the HOMO energies for **DHPz-MN-1** and **DHPz-TCF-1** change by 0.40eV and 0.99eV, respectively. The effects on the energy gaps where a change from 1.85eV for MN-1 to 1.03eV for **DHPz-MN-1** and 1.03eV for TCF-1 to 0.51eV for **DHPz-TCF-1**. This further suggests that the DHPz donor is better than the DEA donor and that the theoretical predictions were correct.

### 3.2.4 Thermal Analysis

Thermal properties of **DHPz-TCF-2** were measured by differential scanning calorimetry (DSC)(Fig. 4.3) and thermogravimetric analysis (TGA)(Fig. 4.4). The first scan of the DSC plot shows a small feature near 90°C and a more pronounced, endothermic, feature at 160°C. The feature at 90°C was interpreted as the glass transition temperature based on the temperature at which neat films of the chromophore were poled. Interpretation of the feature at 160°C was not as clear as the feature did not reappear during the repeat scan. The presence of a glass transition temperature ( $T_g$ ) near 90°C suggests that this material may exist in an amorphous state, but any final conclusions are complicated by the additional endothermic peak. This peak may represent a crystallization event, some unknown solid-

Sample: DLE-14-114-4  
Size: 7.2600 mg  
Method: Heat/Cool/Heat

DSC

File: C:\...DLE-14-114-4-DSC-2nd.001  
Operator: DLE  
Run Date: 04-Aug-2016 10:14  
Instrument: DSC Q200 V24.11 Build 124

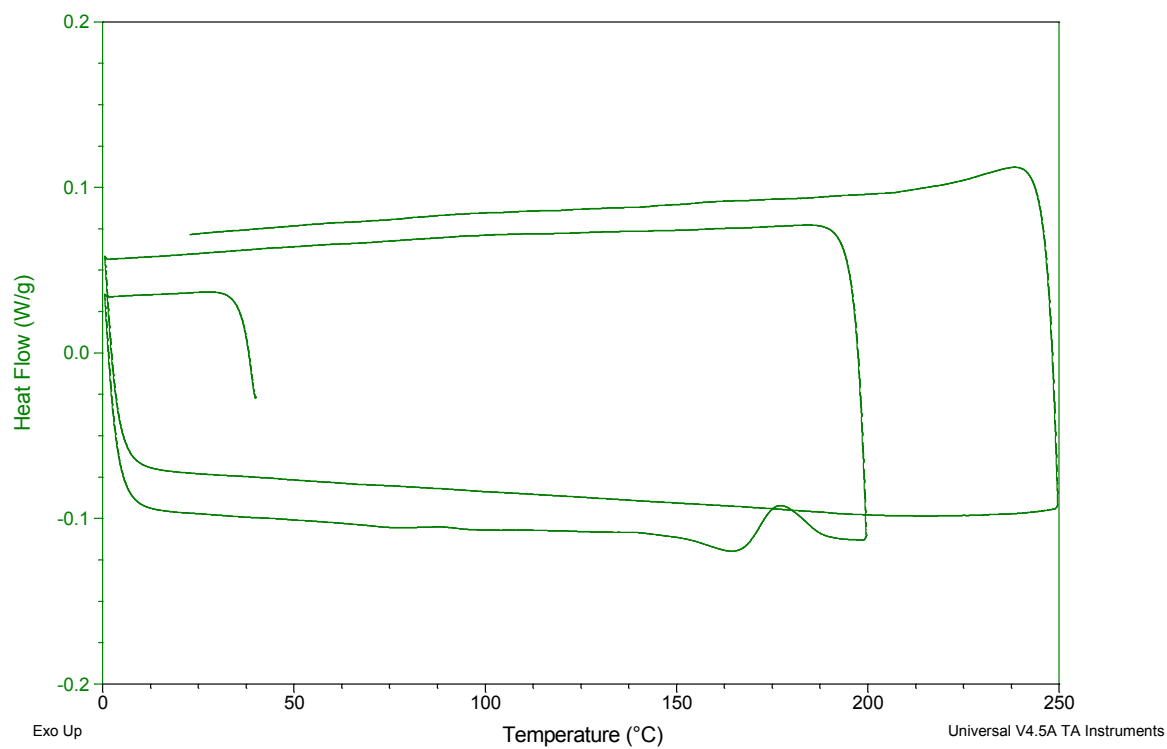


**Fig. 3.5** Differential Scanning Calorimetry plot of **DHPz-TCF-2** with a heating rate of  $10^{\circ}\text{C min}^{-1}$  in a nitrogen environment.

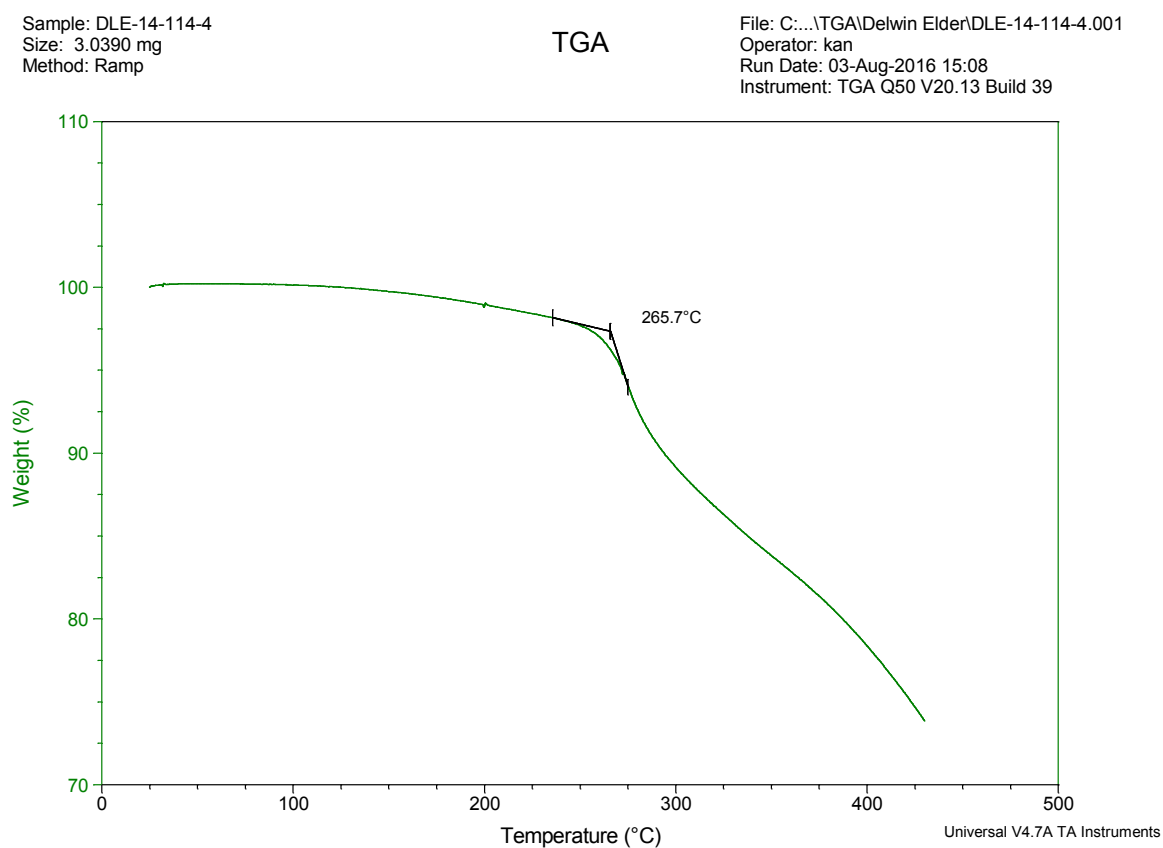


**Fig. 3.6** Thermogravimetric analysis curve of **DHPz-TCF-2** with a heating rate of  $10^{\circ}\text{C min}^{-1}$  in a nitrogen environment.  $T_d = 265.7^{\circ}\text{C}$ .



state transition or decomposition<sup>[10,11]</sup>. The absence of the peak, or any discernible features in the repeat scan, also indicate this may be a decomposition event, but this is contrary to what was revealed by thermogravimetric analysis.

The decomposition temperature,  $T_d$ , was found to be 265.7°C. This is higher than any of the diaryl chromophores reported by Cheng *et al.*<sup>[12]</sup>, and much higher than the endotherm observed by DSC. The aryl substituents on the dihydropyrazine ring would appear to be offering the same enhancement to thermal stability that is observed with the alkyl units are replaced with aryl moieties in more traditional chromophore donors. All of the diaryl chromophores had glass transition temperatures that ranged from 75°C for **B4** on the low end to 114°C for **B4**. With the exception of **A1**, all systems showed only a  $T_g$ , but **A1**, which contained a diphenylamine donor, had a  $T_g$  at 90°C a crystallization,  $T_c$ , at 158°C and a melting point,  $T_m$ , at 234°C<sup>[12]</sup>. No repeat scans over the range of interest were shown, but based on this it would appear that **DHPz-TCF-2** has a similar  $T_g$  are 90°C followed by a  $T_c$  at 160°C. No melting point was observed, but this may be due to the initial scan ending at 200°C and never reaching the  $T_m$  of the material. This may also explain why there are no discernible features in the second scan as the material was locked in a crystalline state following the initial scan. Additional thermal characterization of both **DHPz-TCF-1** and **DHPz-TCF-2** should be more revealing.

### 3.2.5 Electric Field Poling Experiments

Electric field poling experiments<sup>3</sup> were performed to evaluate the performance of **DHPz-TCF-2** in a simple EO device. The EO activity was measured in a guest-host polymer system using PMMA with 25% chromophore loading and also as a monolithic film. For the guest-host films, the solids were dissolved in 1,1,2-trichloroethane(TCE) to prepare a solution that was 12.5% total solids by weight. This solution was filtered through a 0.2 $\mu$ m PTFE filter and the filtered solution was spin-coated onto glass slides containing a thin layer of ITO on one half as an electrode. The films were baked in an oven, under vacuum, at 65°C overnight to ensure complete removal of any residual solvent. A gold electrode was sputtered on top

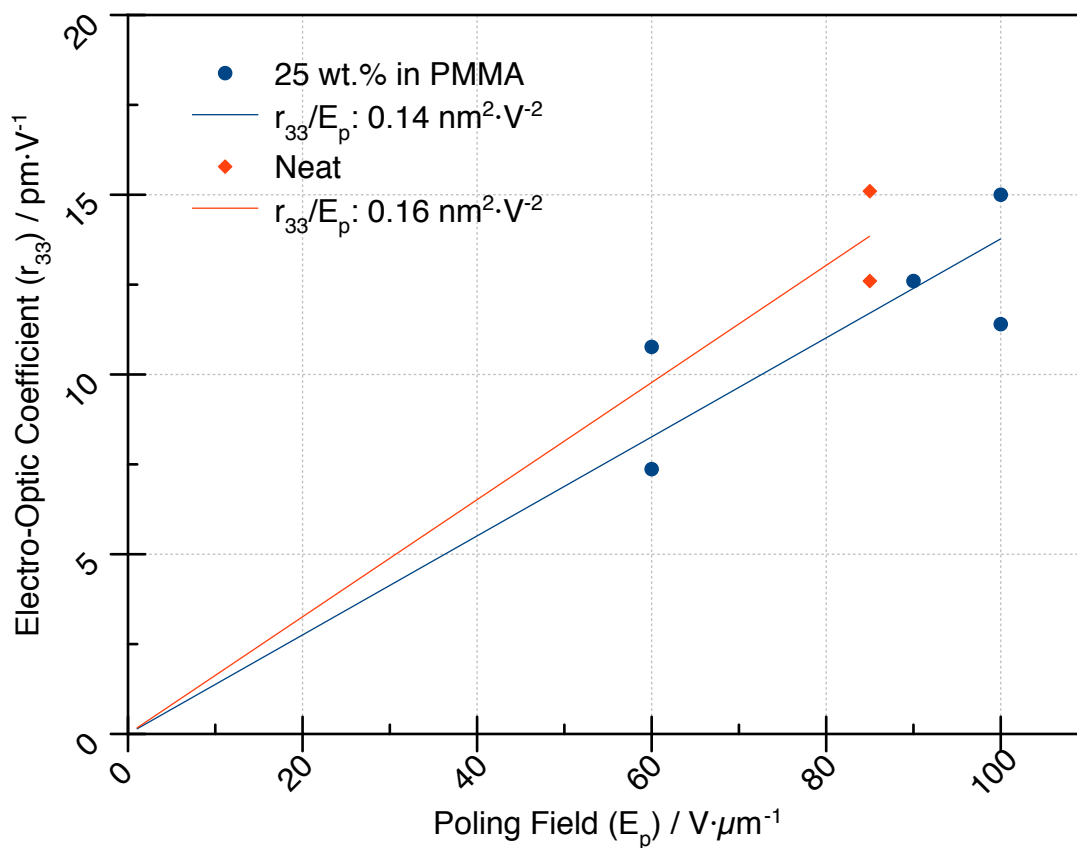


**Fig. 3.7** Electro-optic coefficients of **DHPz-TCF-2** films,  $\circ$  25 wt.% in PMMA and  $\diamond$  neat film, at different poling voltages. Poling efficiencies,  $r_{33}/E_p = 0.14 nm^2 \cdot V^{-2}$  for the guest-host system and  $r_{33}/E_p = 0.16 nm^2 \cdot V^{-2}$  for the monolithic film.

of the polymer film to supply a top electrode for contact poling. Monolithic chromophore films were prepared in a similar fashion to the guest-host systems. Initial films prepared from a 7.8 wt.% solution of chromophore in TCE were found to be of very poor quality due to the low solubility of the chromophore in solution. Film quality was improved for films prepared from a 1:1 mixture of **DHPz-TCF-2** with **EZ-FTC**, but the film thickness was much lower and there was still a large amount of solids that did not fully go into solution. All devices prepared from this solution shorted as a result of the very thin films. Changing the solvent from TCE to cyclopentanone yielded much better results. Initial films from a 7.8 wt.% solution produced films that were 550nm and based on previous results, new solutions of a higher concentration were prepared to produce thicker films. The concentration was increased to 12 wt.% to produce films that were 887nm thick.

Electro-optic coefficients,  $r_{33}$ , were measured by the Teng-Man simple reflection technique at 1310nm<sup>[13]</sup>. The results of the poling experiments are shown in figure Fig. 4.5. The films in PMMA had a maximum  $r_{33}$  of 15<sup>pm</sup>/v obtained at a poling field of 100V/ $\mu$ m. This equates to a maximum poling efficiency ( $r_{33}/E_p$ ) of 0.15<sup>nm</sup><sup>2</sup>/v<sup>2</sup> and an average poling efficiency of 0.14<sup>nm</sup><sup>2</sup>/v<sup>2</sup>. The neat chromophore system had a maximum  $r_{33}$  of 15.1<sup>pm</sup>/v obtained at a poling field of 85V/ $\mu$ m for a maximum poling efficiency ( $r_{33}/E_p$ ) of 0.18<sup>nm</sup><sup>2</sup>/v<sup>2</sup> and an average poling efficiency of 0.16<sup>nm</sup><sup>2</sup>/v<sup>2</sup>. Chromophore **A2**, with a diphenylamine donor, FTC bridge and CF3Ph-TCF acceptor has a reported  $r_{33}$  of 19<sup>pm</sup>/v obtained at a poling field of 100V/ $\mu$ m, as measured by Teng-Man<sup>[12]</sup>. **DHPz-TCF-2**, with a shorter bridge and weaker acceptor compares quite favorably and this is attributed to the DHPz donor.

### 3.3 Conclusion

We present, for the first time, several novel chromophores with a 1,4-dihydropyrazine donor for the use in electro-optic applications. Four chromophore were prepared with either the malononitrile or TCF acceptors. This family of chromophores exhibit large bathochromic

---

<sup>3</sup>The poling field correction as explained in ref<sup>[14]</sup> where not applied during this study.

shifts compared to their diethyl amine donor counterparts and were readily soluble in a range of solvents. The HOMO and LUMO levels were determined using Cyclic Voltammetry and were found to be  $E_{ox}^{HOMO} = -4.71 eV$  and  $E_{red}^{LUMO} = -3.67 eV$  for DHPz-MN-A and,  $E_{ox}^{HOMO} = -4.00 eV$  and  $E_{red}^{LUMO} = -3.49 eV$  for **DHPz-TCF-1**. The energy gap for the HOMO→LUMO transition  $0.82 eV$  and  $0.87 eV$  lower than their respective diethylamine donor counterparts. Devices were made from the **DHPz-TCF-2** chromophore in PMMA at 25 wt% and as monolithic films. The polymer guest-host system had a poling efficiency of  $0.14 \text{ nm}^2/\text{V}^2$  and a maximum  $r_{33}$  of 15.2 at a field strength of  $100 \text{ V}/\mu\text{m}$ . The neat chromophore system had a poling efficiency of  $0.16 \text{ nm}^2/\text{V}^2$  and a maximum  $r_{33}$  of 15.1 at a field strength of  $85 \text{ V}/\mu\text{m}$ . Attempts to attach stronger acceptors such as the CF3Ph-TCF or TCP acceptor failed due to decomposition of the dihydropyrazine ring. If these issues can be addressed, chromophores based on the DHPz donor may prove quite competitive as even with a weaker acceptor, the performance of **DHPz-TCF-2** was on par with an FTC-class chromophore with a CF3Ph-TCF acceptor.

### 3.4 Experimental Section

**General information:** Chemicals used were purchased from Sigma Aldrich, Alfa Aesar or TCI and used without further purification unless otherwise noted. UV-visible Absorption Spectroscopy was obtained on a Shimadzu 1601 or a Varian Cary 5000 spectrometer. Differential Scanning Calorimetry (DSC) data was acquired on a TA Instruments Q100 with heating and cooling under nitrogen at rates of  $10^\circ\text{C}$  per min. Thermogravimetric Analysis (TGA) data was acquired on a TA Instruments Q500 with heating under nitrogen at a rate of  $10^\circ\text{C}$  per min.  $^1\text{H}$  NMR spectra were acquired using a Bruker AVance series instrument running at 300 MHz. 1,1,2 trichloroethane (TCE) and cyclopentanone were purified via vacuum distillation prior to use. ITO/glass slides were purchased from Thin FilmDevices, Inc. Optical profilometry measurements were carried out on a WYKO NT-2000 model profilometer. In situ Teng-Man ellipsometry was carried out on a home built device<sup>[15]</sup>. The compounds IM-1-Bu/Ald-1-Bu, **DHPz-TCF-1** and **DHPz-TCF-2** were prepared by Dr.

Delwin Elder.

*Synthesis of 4-(3,4,5-triphenylpyrazin-1(4H)-yl)benzaldehyde (D1)*

A solution of 2,2'-(phenylazanediy)bis(1-phenylethanone) (1 eq.) in DMF (5 mL/mmol) was cooled to -20°C and to this was added POCl<sub>3</sub> (1 eq.) in one portion. The solution was kept at -20°C overnight and heated briefly to 60°C before being poured into ice water containing sodium acetate. The solid was filtered, washed with water, a small amount of isopropanol and diethyl ether. The product was air dried overnight to yield 0.58g (53%) 1,3,4,5-tetraphenyl-1,4-dihydropyrazine-2-carbaldehyde and 4-(3,4,5-triphenylpyrazin-1(4H)-yl)benzaldehyde as a red-orange solid. <sup>1</sup>H NMR (300 MHz, Acetone-d<sub>6</sub>) δ 9.18 (s, 1H), 7.81 (dd, J = 6.6, 3.1 Hz, 2H), 7.63 (dd, J = 8.2, 1.5 Hz, 3H), 7.54 – 7.47 (m, 3H), 7.38 – 7.22 (m, 6H), 7.15 (dd, J = 8.8, 1.2 Hz, 2H), 7.04 – 6.99 (m, 4H), 6.92 (s, 1H).

*Synthesis of 1,2,4,6-tetraphenyl-1,4-dihydropyrazine (D2)*

To a 20mL vial containing a stirbar, 2,2'-(phenylazanediy)bis(1-phenylethanone) (1 eq.) and aniline (1.4 eq.) was added a 5% solution of trifluoroacetic acid and acetic acid in toluene (5 mL/mmol). The vial was capped and placed in a bead bath held at 90°C for 6 hours. The vial was removed from the bath, allowed to cool and the contents transferred to a round bottom flask. The solvent was stripped under reduced pressure and the residue was treated with a hot mixture of ethanol or isopropanol and an aqueous solution of saturated sodium bicarbonate. The contents were filtered and washed with alcohol and diethyl ether. The product was air dried overnight to yield 0.89g (99%) 1,2,4,6-tetraphenyl-1,4-dihydropyrazine as a yellow crystalline solid. <sup>1</sup>H NMR (300 MHz, DMSO-d<sub>6</sub>) δ 8.10 (s, 2H), 7.93 – 7.79 (m, 4H), 7.49 (d, J = 8.1 Hz, 2H), 7.39 (q, J = 8.7, 8.3 Hz, 6H), 7.26 (d, J = 7.3 Hz, 2H), 7.15 – 6.95 (m, 3H), 6.71 (dd, J = 17.5, 7.8 Hz, 3H). MS (ESI) 387 (M+H).

*Synthesis of 4-(bis(2-oxo-2-phenylethyl)amino)benzaldehyde (D-Ald)*

To a cooled solution of 2,2'-(phenylazanediyl)bis(1-phenylethanone) (1 eq.) in DMF (5 mL/mmol) was added POCl<sub>3</sub> (1.5 eq.), dropwise, over 1 minute. The solution was stirred at room temperature for 30 minutes and heated to 90°C for 45 minutes. The cooled solution was neutralized with solid sodium acetate, diluted with ice water and allowed to sit overnight. The solid was filtered, washed with water, a small amount of isopropanol and diethyl ether. The product was air dried overnight to yield 4.15g (62%) 4-(bis(2-oxo-2-phenylethyl)amino)benzaldehyde as dark tan powder. <sup>1</sup>H NMR (300 MHz, Acetone-d<sub>6</sub>) δ 9.72 (s, 1H), 8.11 (d, J = 7.1 Hz, 4H), 7.74 – 7.63 (m, 4H), 7.62 – 7.52 (m, 4H), 6.75 (d, J = 8.9 Hz, 2H), 5.23 (s, 4H).

*Synthesis of N-(4-(3,4,5-triphenylpyrazin-1(4H)-yl)benzylidene)aniline (IM-1) and 4-(3,4,5-triphenylpyrazin-1(4H)-yl)benzaldehyde (Ald-1)*

To a 20mL vial containing a stirbar, 4-(bis(2-oxo-2-phenylethyl)amino)benzaldehyde (1 eq.) and aniline (3 eq.) was added a 5% solution of trifluoroacetic acid and acetic acid in toluene (5 mL/mmol). The vial was capped and placed in a bead bath held at 90°C for 6 hours. The vial was removed from the bath, allowed to cool and the contents transferred to a round bottom flask. The solvent was stripped under reduced pressure and the residue was treated with a hot mixture of ethanol or isopropanol and an aqueous solution of saturated sodium bicarbonate. The contents were filtered and washed with alcohol and diethyl ether. The product was air dried overnight to yield 0.31g (76%) N-(4-(3,4,5-triphenylpyrazin-1(4H)-yl)benzylidene)aniline as a yellow/orange solid. <sup>1</sup>H NMR (300 MHz, Acetone-d<sub>6</sub>) δ 8.53 (s, 1H), 8.03 (s, 2H), 8.01 – 7.90 (m, 7H), 7.60 (d, J = 8.9 Hz, 2H), 7.49 – 7.35 (m, 6H), 7.34 – 7.18 (m, 4H), 7.08 – 6.98 (m, 2H), 6.86 (d, J = 8.2 Hz, 2H), 6.76 (t, J = 7.2 Hz, 1H). MS (ESI) 415, 490 (M+H).

*Synthesis of 2-(4-(3,4,5-triphenylpyrazin-1(4H)-yl)benzylidene)malononitrile (**DHPz-MN-1**)*

To a vial containing a stir bar and IM-1/Ald-1 (1 eq.) in ethanol (1 ml/mmol) was added malononitrile (1.1 eq). The vial was capped and placed in a bead bath held at 90°C for 30 minutes. Once cool, the precipitate was filtered and washed with isopropanol and ethanol to yield 0.36g (76%) **DHPz-MN-1** as a maroon solid. <sup>1</sup>H NMR (300 MHz, Acetone-d<sub>6</sub>) δ 8.11–8.04 (m, 3H), 7.94 (d, J = 7.2 Hz, 4H), 7.85 (s, 2H), 7.64 (d, J = 9.1 Hz, 2H), 7.44 (t, J = 7.5 Hz, 4H), 7.33 (t, J = 7.3 Hz, 2H), 7.03 (dd, J = 8.6, 7.3 Hz, 2H), 6.91 (d, J = 7.9 Hz, 2H), 6.80 (t, J = 7.2 Hz, 1H). MS (ESI) 462 (M<sup>+</sup>).

*Synthesis of 2-(4-(4-(4-butylphenyl)-3,5-diphenylpyrazin-1(4H)-yl)benzylidene)malononitrile (**DHPz-MN-2**)*

**DHPz-MN-2** was synthesized exactly the same as **DHPz-MN-1** from Im-1-Bu/Ald-1-Bu. **DHPz-MN-2** as a maroon solid. <sup>1</sup>H NMR (300 MHz, Acetone-d<sub>6</sub>) δ 8.07 (d, J = 7.4 Hz, 3H), 7.93 (d, J = 7.4 Hz, 4H), 7.75 (s, 2H), 7.61 (d, J = 9.1 Hz, 2H), 7.43 (t, J = 7.5 Hz, 4H), 7.33 (t, J = 6.8 Hz, 2H), 6.87 (s, 4H), 2.47–2.32 (m, 2H), 1.43 (p, J = 7.8, 7.4 Hz, 2H), 1.24 (dt, J = 14.9, 7.2 Hz, 2H), 1.15 (s, 1H), 0.83 (t, J = 7.3 Hz, 2H). MS (ESI) 519 (M<sup>+</sup>H).

**REFERENCES**

- [1] R. C. Elderfield. *Heterocyclic compounds*. Wiley : University Microfilms International, New York; Ann Arbor, Mich., 1957.
- [2] Shue-Jen. Chen and Frank W. Fowler. Structures of alleged 1,4-dihydropyrazines. *The Journal of Organic Chemistry*, 35(11):3987–3989, 1970.
- [3] Frank W. Fowler and Shue-Jen Chen. Synthesis of the 1,4-dihydropyrazine ring system. stable 8.pi.-electron heterocycle. *The Journal of Organic Chemistry*, 36(26):4025–4028, 1971.
- [4] Arthur T. Mason and Goodlatte R. Winder. Xcix.-syntheses of piazine derivatives. interaction of benzylamine and phenacyl bromide. *J. Chem. Soc., Trans.*, 63:1355–1375, 1893.
- [5] Jean-Louis Fourrey, Josiane Beauhaire, and Chun Wei Yuan. Preparation of stable 1,4-dihydropyrazines. *J. Chem. Soc., Perkin Trans. 1*, pages 1841–1843, 1987.
- [6] J. William Lown and M. Humayoun Akhtar. Self-condensation and rearrangement of n-alkylphenacylamines. *J. Chem. Soc., Perkin Trans. 1*, pages 683–686, 1973.
- [7] J. William Lown, M. Humayoun Akhtar, and Robert S. McDaniel. Stereochemistry and mechanism of the thermal [1,3] alkyl shift of stable 1,4-dialkyl-1,4-dihydropyrazines. *The Journal of Organic Chemistry*, 39(14):1998–2006, 1974.
- [8] Wenwei Jin, Peter V. Johnston, Delwin L. Elder, Karl T. Manner, Kerry E. Garrett, et al. Structure-function relationship exploration for enhanced thermal stability and electro-optic activity in monolithic organic nlo chromophores. *J. Mater. Chem. C*, 4:3119–3124, 2016.
- [9] J. L. Bredas, R. Silbey, D. S. Boudreaux, and R. R. Chance. Chain-length dependence of electronic and electrochemical properties of conjugated systems: polyacetylene,



- polyphenylene, polythiophene, and polypyrrole. *Journal of the American Chemical Society*, 105(22):6555–6559, 1983.
- [10] John A. Dean. *Analytical chemistry handbook*. McGraw-Hill, New York, 1995.
- [11] Douglas A. Skoog, F. James. Holler, and Timothy A. Nieman. *Principles of instrumental analysis*. Saunders College Pub. ; Harcourt Brace College Publishers, Philadelphia; Orlando, Fla., 1998.
- [12] Yen-Ju Cheng, Jingdong Luo, Steven Hau, Denise H. Bale, Tae-Dong Kim, et al. Large electro-optic activity and enhanced thermal stability from diarylaminophenyl-containing high- $\beta$  nonlinear optical chromophores. *Chemistry of Materials*, 19(5):1154–1163, 2007.
- [13] C. C. Teng and H. T. Man. Simple reflection technique for measuring the electro-optic coefficient of poled polymers. *Applied Physics Letters*, 56(18):1734–1736, 1990.
- [14] Wenwei Jin, Peter V. Johnston, Delwin L. Elder, Andreas F. Tillack, Benjamin C. Olbricht, et al. Benzocyclobutene barrier layer for suppressing conductance in nonlinear optical devices during electric field poling. *Applied Physics Letters*, 104(24):243304, 2014.
- [15] Ben C. Olbricht. *Characterization and Processing of Organic Nonlinear Optical Materials using Ellipsometric, Waveguiding, and Absorption Spectroscopy Techniques*. Ph.D. thesis, University of Washington, 2010.

## Chapter 4

# SYNTHESIS OF DIAMINOTRIPHENYLAMINE(DATPA) DONOR

### 4.1 Introduction

One of the difficulties in designing new donors is developing a feasible synthetic scheme to give the desired product in the fewest steps possible with an adequate yield. With diaryl donors, one of these synthetic steps invariably involves the coupling of a functionalized aryl ring to an aryl amine<sup>[1-4]</sup>. This reaction is nontrivial as typical nucleophilic substitutions tend to fail except for in a few select cases<sup>[5]</sup>. Aryl amines are an important feedstock as they can be found in a number of natural products and pharmaceuticals, so to address these needs, a number of synthetic methods have been developed.

The Buchwald-Hartwig amination (BHA) is one of the more popular methods owing to its mild conditions and moderate-to-high yields<sup>[5]</sup>. This is a palladium catalyzed synthesis of aryl amines from aryl halides and primary or secondary amines. The efficacy of this reaction can depend upon the type of ligand used and a whole field of chemistry has emerged around the optimization of these ligands. To date, the most effective systems have involved palladium with bulky phosphine ligands<sup>[6-10]</sup>. This system has allowed the breadth and scope of C-N coupling reactions to expand to include a wider variety of substrates such that virtual any transformation may now be achieved with the proper ligand. Disadvantages of this class of reaction is that not all ligands perform equally, potentially requiring an assortment of ligands for work with several substrates, and these reactions tend to perform better with electron-poor aryl halides.

The Goldberg reaction<sup>[11]</sup>, or Ullmann condensation<sup>[12]</sup>, is another type of C-N coupling reaction. This reaction relies on copper or copper salts and aryl halides. Traditionally, this

method required stoichiometric amounts of copper and harsh reaction conditions, but recent advances have been made that allow catalytic amounts of copper(I) chloride or copper(I) iodide to be used in conjunction with diamine ligands<sup>[13-16]</sup>. This reaction works well for both electron-rich and electron-poor aryl halides, but can require large amounts of base and is used almost exclusively with aryl iodides.

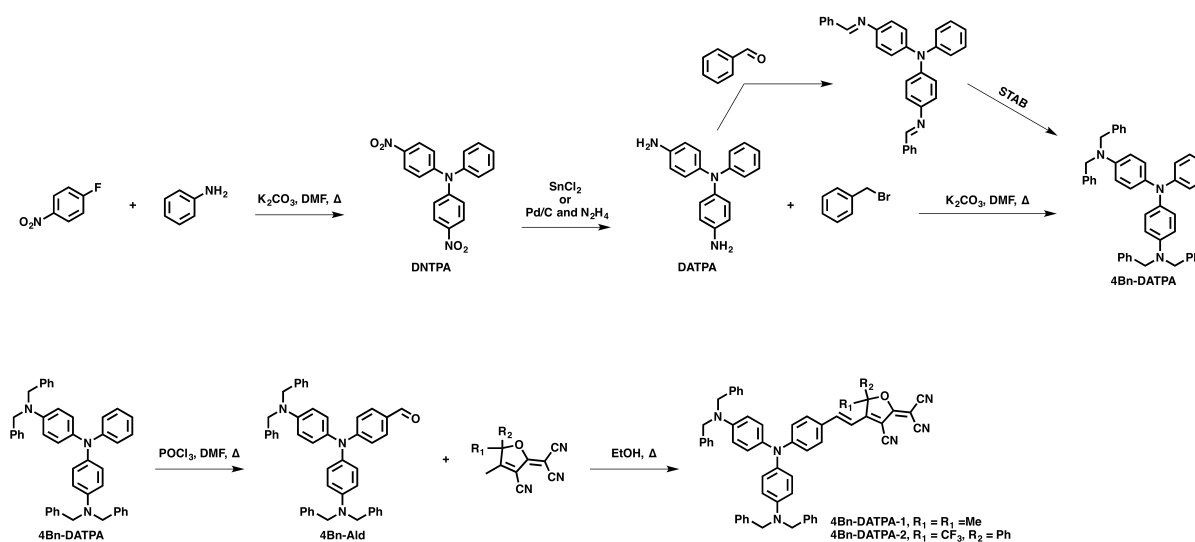
Other reactions include the Chan-Lam coupling which allows boronic acids, stannanes or siloxanes to be oxidatively coupled to amines at room temperature in air. The reaction can be performed with stoichiometric or catalytic amounts of copper, but the requirement of boronic acids introduces an additional step not required in the previous methods. Reductive aminations, such as the Eschweiler-Clarke reaction, are a facile method for converting carbonyls to amines, but the reactions are typically not employed in the synthesis of triaryl amines<sup>[17-22]</sup>.

## **4.2 Results and Discussion**

The triaryl amines in this work were synthesized from deactivated aryl fluorides in the presence of a mild base. This method offered the advantage of not requiring any specialized ligands, handling or transition metal catalyst. The conditions for these reactions are similar to nucleophilic substitution reactions between amines and alkyl halides and are known to proceed with excellent yields. This method also allows the possibility to investigate many systems from one common starting point using commercially available starting reagents.

### *4.2.1 Synthesis of 4',4-Diaminotriphenylamine Donor*

Synthesis of 4',4-diaminotriphenylamine (DATPA) was performed in two steps from 4-fluoronitrobenzene and aniline and the overall synthesis is shown in scheme Scheme 4.1. In the first step, 4-fluoronitrobenzene was reacted with aniline in the presence of potassium carbonate in dimethylformamide. The aniline/potassium carbonate slurry was activated by sonication for 5 minutes before addition of 4-fluoronitrobenzene. The reaction proceeded smoothly and 4',4-dinitrotriphenylamine (DNTPA) converted to DATPA by reduction with tin(II) chloride



**Scheme 4.1** Synthesis of DATPA chromophores.

dihydrate in ethanol or 10% Pd/C and hydrazine hydrate in ethanol. Both reactions gave the desired product in excellent yields, but tin salts were a constant problem with the tin(II) chloride reductions. No such problems were encountered during reductions with hydrazine. **4Bn-DATPA** was achieved via two methods. The first method was a direct nucleophilic substitution of DATPA with benzyl bromide. The second method was a reductive amination with benzyl bromide and sodium triacetoxyborohydride (STAB). Product isolation from the reductive amination was not as clean as the nucleophilic substitution due to difficulty in isolating the fully substituted product from the partially substituted products. **4Bn-Ald** was prepared by a Vilsmeier-Haack reaction using phosphorous oxychloride in dimethylformamide. Chromophores **4B-DATPA-TCF-1** and **4B-DATPA-TCF-2** were obtained *via* Knoevenagel condensation reactions with the TCF or CF<sub>3</sub>Ph-TCF acceptors in refluxing ethanol.

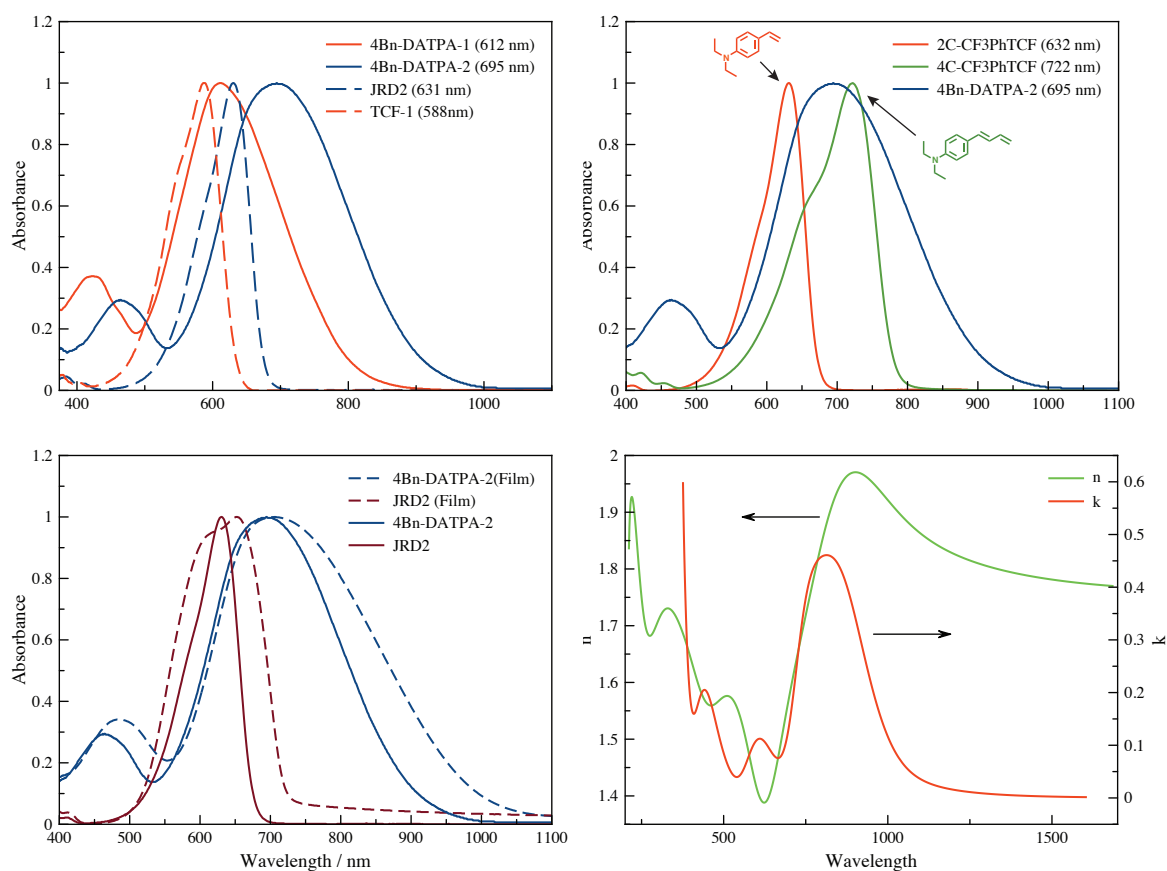


**Fig. 4.1** Top left, optical spectra of chromophores in chloroform. Top right, comparison with chromophores with a 2 carbon and 4 carbon bridge. Bottom left, comparison with **JRD2** in chloroform and as a film. Bottom right, optical constants,  $n$  and  $k$ , obtained from VASE measurements.

### 4.2.2 Optical Properties

The optical absorption spectra of chromophores **4Bn-DATPA-1** and **4Bn-DATPA-2** were measured in chloroform and compared to chromophores **JRD2**<sup>[23]</sup>, TCF-1 (labeled GIM2), **2C-CF3PhTCF** and **4C-CF3PhTCF** (see figure ??). The  $\lambda_{max}$  of these chromophores are 612nm, 695nm, 631nm, 588nm, 632nm and 722nm, respectively. The DATPA donor caused the ICT band to shift to lower energies for both chromophores. For **4Bn-DATPA-1**, this shift is +24nm<sup>1</sup>, and places it very close to **JRD2** and **2C-CF3PhTCF**, both with the stronger CF3PhTCF acceptor. **4Bn-DATPA-2** is red-shifted 64nm from **JRD2** and 63nm from **2C-CF3PhTCF**. The bathochromic shifts in the DATPA chromophores can be attributed to the new diary system contributing more to the donating strength of the conjugated system. To gauge how large this effect is, **4Bn-DATPA-2** was compared to chromophores have a 2 carbon bridge and a 4 carbon bridge. Extension of the bridge increases  $\beta$  due to greater charge separation and **4Bn-DATPA-2** is blue-shifted from **4C-CF3PhTCF** by 27nm. This suggests that **4Bn-DATPA-2** and **4C-CF3PhTCF** should have similar values of  $\beta$  and illustrates the enhanced donating ability of the DATPA donor. Neat films cast from 1,1,2-trichloroethane solutions were prepared from both **JRD2** and **4Bn-DATPA-2**. Chromophores capable of forming glassy materials are of great interest as they allow for higher number densities than is typically possible in guest-host polymer systems. One issue that becomes more apparent in these glassy materials is aggregation, as seen by the appearance of a shoulder on the ICT transition. This can be seen clearly in the neat film prepared from **JRD2** as a low energy shoulder. There is no apparent shoulder in the neat film of **4Bn-DATPA-2**, but it is not clear if one is present due to line broadening of the peak transition. Optical constants,  $n$  and  $k$ , were obtained from the thin film of **4Bn-DATPA-2** using a VASE® ellipsometer.

---

<sup>1</sup>The +/- sign convention is used to indicate either a bathochromic (+) or hypsochromic (-) shift. The presence of the sign holds no other significance.

### 4.2.3 Cyclic Voltammetry Measurements

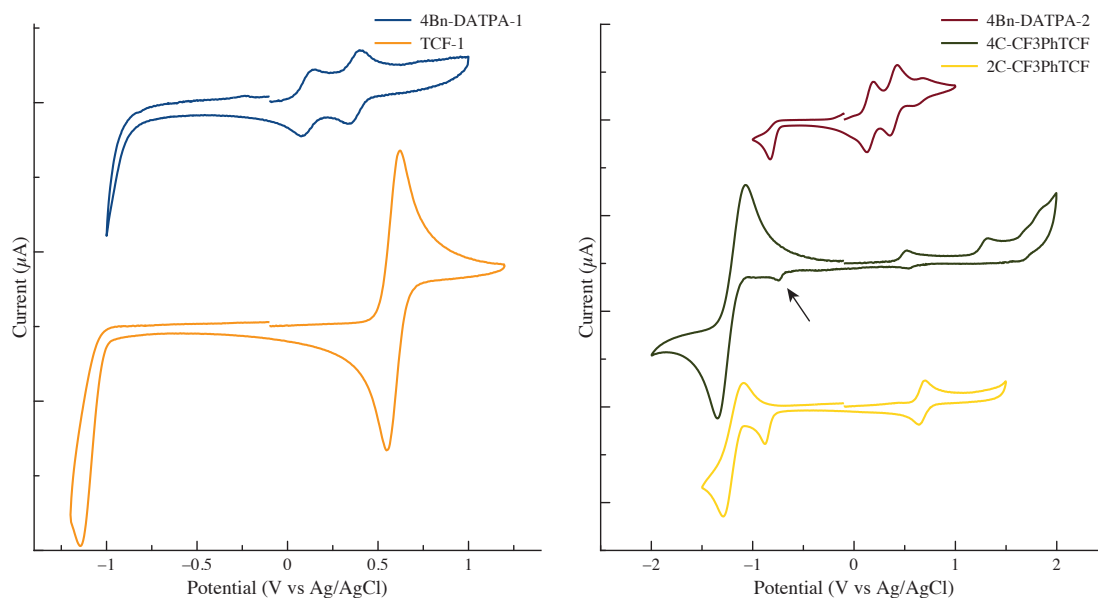


**Fig. 4.2** Cyclic voltammetry of CF<sub>3</sub>Ph-TCF chromophores. The bottom has a 2-carbon bridge with a diethylamine donor, the middle has a 4-carbon bridge with a diethylamine donor and the top has the DATPA donor.

The redox properties of chromophores **4Bn-DATPA-1** and **4Bn-DATPA-2** were determined by cyclic voltammetry in degassed acetonitrile solutions containing a 0.1 M tetrabutylammonium hexafluorophosphate as the supporting electrolyte at a scan rate of 50 mV s<sup>-1</sup>. The voltammograms are shown in figure Fig. 4.2 and the relevant data is tabulated in table Table 4.1. **4Bn-DATPA-1** had two reversible oxidation peaks and one irreversible reduction peak. Both oxidation peaks occurred at much lower potentials than **TCF-1**, suggesting an increase in the HOMO energies. The energy gap was determined to be 1.51eV for **TCF-1** with an  $E_{ox}^{HOMO}$  at about -4.90eV and an  $E_{red}^{LUMO}$  at -3.39eV. **4Bn-DATPA-1** had an energy gap of 0.90eV with an  $E_{ox}^{HOMO}$  at -4.43eV and an  $E_{red}^{LUMO}$  at -3.52eV. For **4Bn-DATPA-2**, a third reversible oxidation peak appeared and  $E_{ox}^{HOMO}$  was found to be -4.48eV and  $E_{red}^{LUMO}$  was -3.66eV for an energy gap of 0.82eV. This was smaller than both

**Table 4.1** Electrochemical and optical properties of chromophores in study.

	$\lambda_{max}^{CHCl_3}$	$E_{ox}$	$E_{red}$	$E_g^{CV}$	$E_g^{Opt}$	$\beta_{zzz}(0)$
	nm	(eV)	(eV)	(eV)	(eV)	( $\times 10^{-30}$ esu)
TCF-1		-4.90	-3.39	1.51		65.7
4Bn-DATPA-1	612	-4.43	-3.52	0.90	1.37	164.1 <sup>a</sup>
2C-CF3PhTCF	632	-4.99	-3.62	1.37	1.85	
4C-CF3PhTCF	722	-4.82	-3.73	1.09	1.58	
4Bn-DATPA-2	695	-4.48	-3.66	0.82	1.56	193.6 <sup>a</sup>

**2C-CF3PhTCF** (1.37eV) and **4C-CF3PhTCF** (1.09eV). This trend followed what was observed with the optical energy gap. The data confirms the theoretical results that the DATPA donors are improvements over dialkyl donors as in all cases, the HOMO energies for the DATPA chromophores are higher than their dialkyl counterparts. Further more, **4Bn-DATPA-2** has a HOMO that is higher than **4C-CF3PhTCF** which has had its bridge extended by two carbons.

#### 4.2.4 Thermal Analysis

Thermal properties of **4Bn-DATPA-2** were measure by differential scanning calorimetry (DSC)(figure Fig. 4.3) thermogravimetric analysis (TGA)(figure Fig. 4.4). This chromophore only exhibits a glass transition temperature ( $T_g$ ) 76.7°C, suggesting that it is an amorphous glassy material. We see this transition on both the first and second scans suggesting that the amorphous state is thermodynamically stable. The combination of benzyl groups and the diaryl structure of the donor are most likely responsible for this. The non-planar nature of the triphenyl donor and the benzyl groups likely prevent close packing of the molecules, thus inhibiting crystallization??. The extended aryl system may also interact favorably with each other through dipole-quadrupole or quadrapole-quadrupole interactions leading to an



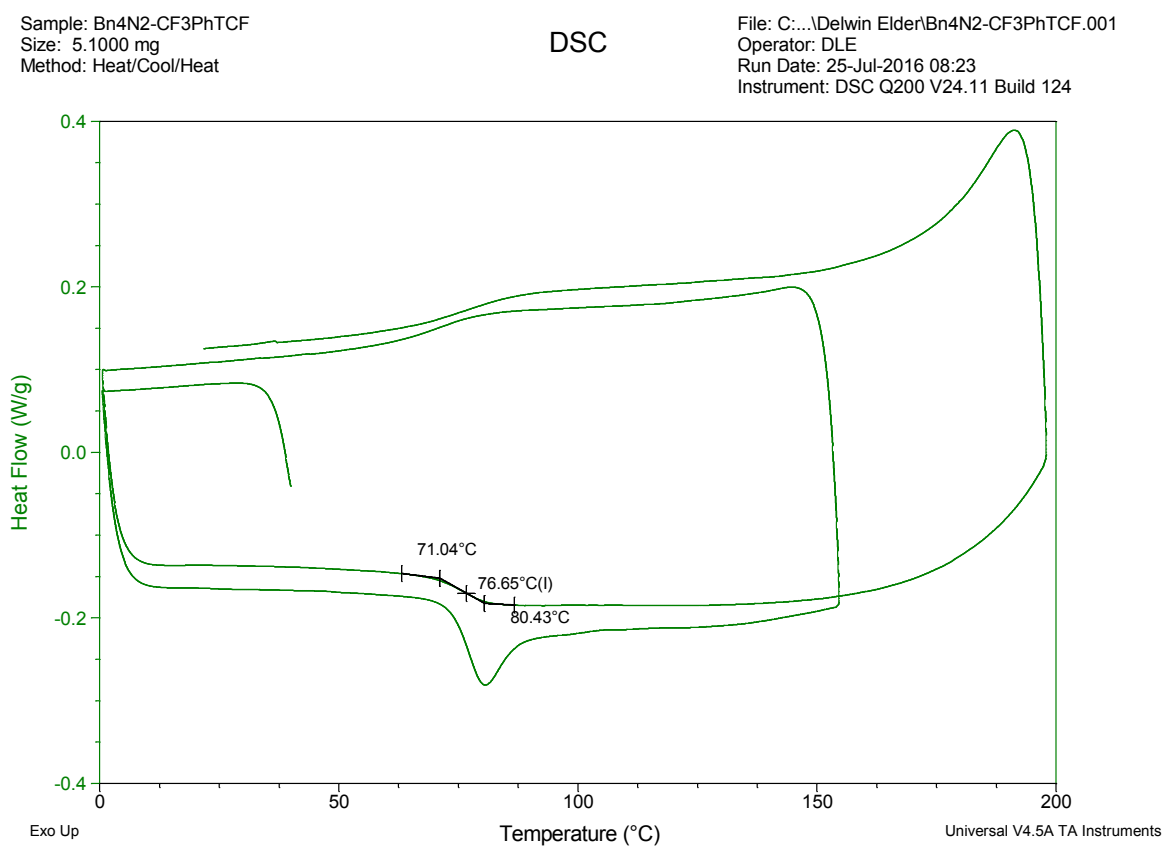


**Fig. 4.3** Differential Scanning Calorimetry plot of **4Bn-DATPA-2** with a heating rate of  $10^{\circ}\text{C min}^{-1}$  in a nitrogen environment.  $T_g = 76.7^{\circ}\text{C}$ .

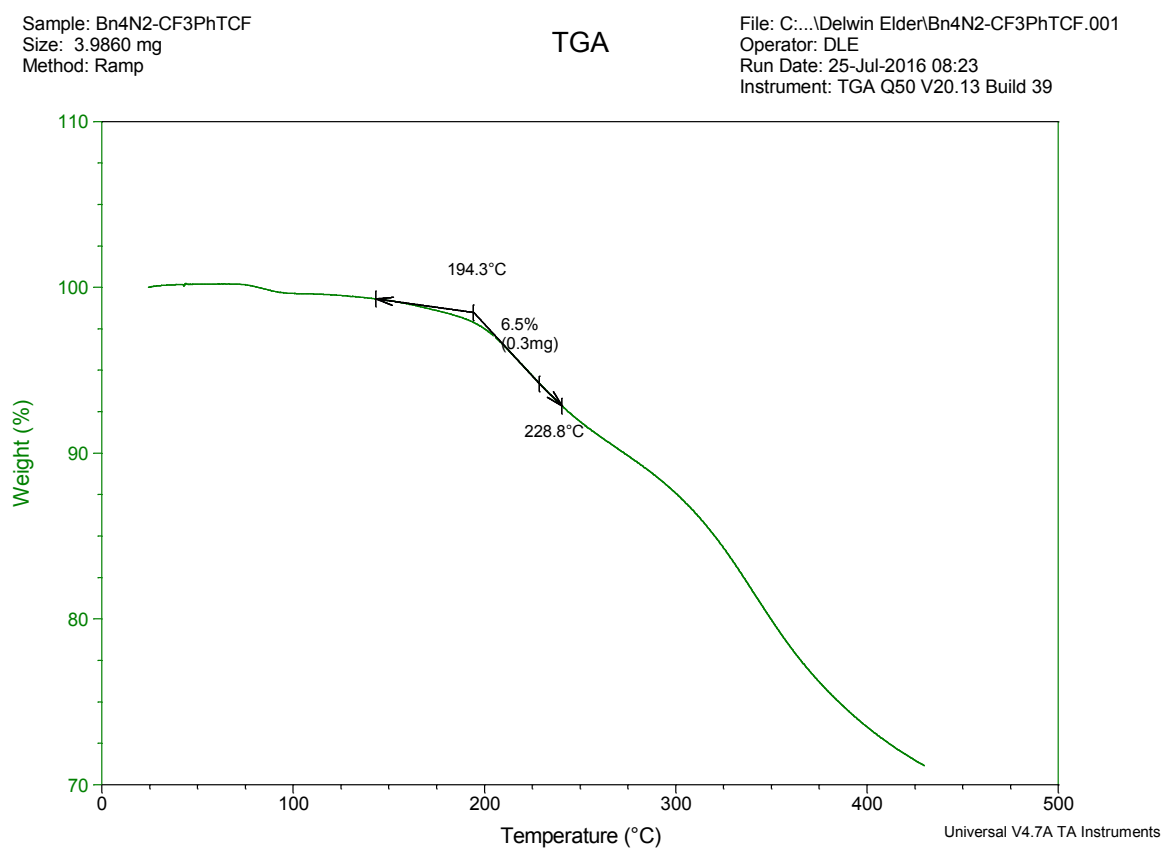


**Fig. 4.4** Thermogravimetric analysis curve of **4Bn-DATPA-2** with a heating rate of  $10^{\circ}\text{C min}^{-1}$  in a nitrogen environment.  $T_d = 194.3^{\circ}\text{C}$ .

extended network that behaves as a much large system. A more systematic study of these systems are likely to reveal both the role of the diaryl and benzyl moieties and offer incite as to what role they play in the organization of this chromophore. It should also be noted that this  $T_g$  is higher than **JRD2**<sup>[23]</sup> which exhibits similar behavior.

The decomposition temperature,  $T_d$ , is 194°C. This is lower than what has been reported for other diaryl chromophores<sup>[1]</sup>, but is similar to what is seen for dialkylamino donors. This reduction in  $T_d$  is likely caused by the 4 benzyl groups. By reducing their number or replacing them altogether, it should be possible to raise the  $T_d$  but the effects on the other, aforementioned, properties are not yet known and it may be more beneficial to leave the benzyl rings as the  $T_d$  is still on par with typical chromophores such as **YLD124**<sup>[1,23]</sup>.

#### 4.2.5 Electric Field Poling Experiments

Electric field poling experiments were performed to evaluate the performance of **4Bn-DATPA-2** in a simple EO device. The EO activity was measured from a monolithic organic glass(neat film). The chromophore was dissolved in 1,1,2-trichloroethane to prepare a solution that was 8.5 wt% and filtered through a 0.2 $\mu$ m PTFE filter. The filtered solution was spin-coated onto glass slides containing a thin layer of ITO on one half as an electrode. The films were baked in an oven, under vacuum, at 65°C overnight to ensure complete removal of any residual solvent. A gold electrode was sputtered on top of the polymer film to supply a top electrode for contact poling. The  $r_{33}$  values were measured by the Teng-Man simple reflection technique at 1310nm<sup>[24]</sup>. The results of the poling experiments are shown in figure Fig. 4.5.

**4Bn-DATPA-2** performed well as a neat system with a maximum  $r_{33}$  of 49<sup>pm/v</sup> at a poling field of 72V/ $\mu$ m. Poled films of **JRD2**, another small chromophore monolithic glassy material, had a maximum  $r_{33}$  of 22<sup>pm/v</sup> at a poling field of 54V/ $\mu$ m<sup>[23,25]</sup>. The  $r_{33}$  of the DATPA chromophore was more than twice **JRD2** and the poling efficiency,  $r_{33}/E_p$ , nearly doubled. This, along with a  $T_g$  that is 22°C higher than **JRD2** suggest that the 4Bn-DATPA donor may be a good replacement for the shaped-modified dialkyl donor present on

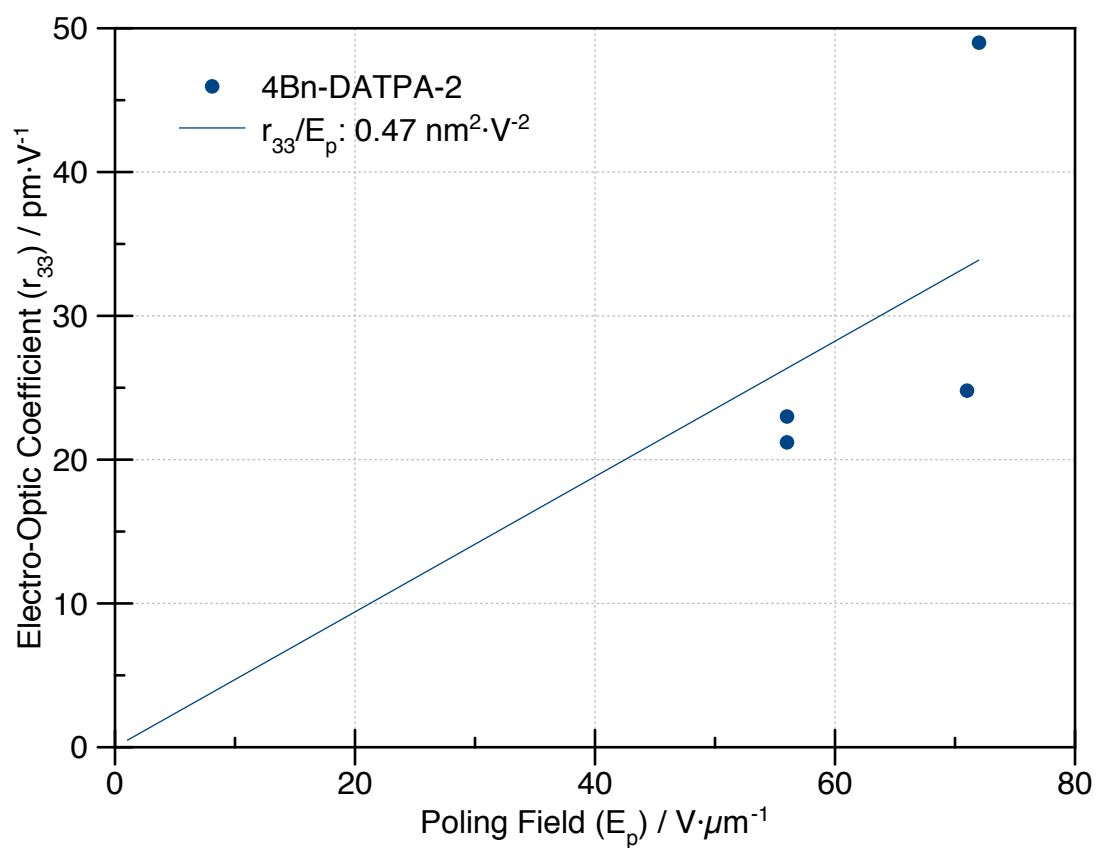


**Fig. 4.5** Electro-optic coefficients of **4Bn-DATPA-2** monolithic films at different poling voltages. Poling efficiency,  $r_{33}/E_p = 0.47 \text{ nm}^2 \cdot V^{-2}$ .

**JRD2.** These results demonstrate that the 4Bn-DATPA donor appears to be offering the same benefits as the shape-modified donor while also improving  $\beta$  and  $T_g$ . More data and testing are required before any conclusive determinations can be made, but what is presented here is very promising and indicates that this functional donor motif may be superior.

### 4.3 Conclusion

Two new chromophores containing benzylated DATPA donors have been synthesized. The CF3Ph-TCF chromophore forms an amorphous solid with excellent film forming qualities on par with those bearing TBDPS groups<sup>[23]</sup>. Use of benzyl groups has lowered the thermal decomposition temperature, compared to that reported for other diaryl chromophores, to 194°C, but the glass transition temperature is improved over a similar chromophore to TBDPS groups from 60°C to 77°C. Poled films of **4Bn-DATPA-2** had a maximum  $r_{33}$  of 49.0 pm/V, measured for a monolithic film poled under a field of 72 V/ $\mu\text{m}$  for a poling efficiency of 0.68 nm<sup>2</sup>/V<sup>2</sup>. These results are higher than what has previously been reported for the small chromophore-neat film system, **JRD2**. As both chromophores have similar number densities, and assuming around the same order, this improvement can be explained as an increase in the first molecular hyperpolarizability. Increasing the bridge length should allow for even higher performing chromophores, ones that have the benefits of the TBDPS groups introduced to **JRD2**, but with a stronger donor that can be easily modified to include crosslinking or other moieties without decreasing donor strength.

### 4.4 Experimental

**General information:** Chemicals used were purchased from Sigma Aldrich, Alfa Aesar or TCI and used without further purification unless otherwise noted. UV-visible Absorption Spectroscopy was obtained on a Shimadzu 1601 or a Varian Cary 5000 spectrometer. Differential Scanning Calorimetry (DSC) data was acquired on a TA Instruments Q100 with heating and cooling under nitrogen at rates of 10°C per min. Thermogravimetric Analysis (TGA) data was acquired on a TA Instruments Q500 with heating under nitrogen at a rate of

10°C per min.  $^1\text{H}$  NMR spectra were acquired using a Bruker AVance series instrument running at 300 MHz. 1,1,2 trichloroethane (TCE) and cyclopentanone were purified via vacuum distillation prior to use. ITO/glass slides were purchased from Thin FilmDevices, Inc. Optical profilometry measurements were carried out on a WYKO NT-2000 model profilometer. In situ Teng-Man ellipsometry was carried out on a home built device<sup>[26]</sup>.

*Synthesis of 4-nitro-N-(4-nitrophenyl)-N-phenylaniline (DNTPA)*

A solution of aniline (1 eq.) and potassium carbonate (4 eq.) in DMF (5 ml/mmol) were sonicated for five minutes. To this solution was added 4-fluorobenzaldehyde (2.2 eq.) and the solution was heated to 100°C for 24 hours. Once cool, the solution was diluted with ice water and allowed to settle overnight. The solid was collected on a filter and washed with excess warm water, isopropyl alcohol and hexanes. The solid was dried under vacuum at 60°C overnight to yield 8.84g (87%) 4-nitro-N-(4-nitrophenyl)-N-phenylaniline. MS (ESI) 335.7 (M+).  $^1\text{H}$  NMR (300 MHz, Acetone-d<sub>6</sub>)  $\delta$  10.00 (d, J = 19.7 Hz, 1H), 8.34 – 8.22 (m, 2H), 8.20 – 8.13 (m, 1H), 8.02 – 7.95 (m, 1H), 7.93 – 7.86 (m, 2H), 7.47 (dd, J = 14.1, 8.1 Hz, 1H), 7.42 – 7.37 (m, 3H), 7.31 (dd, J = 8.3, 6.4 Hz, 2H), 7.22 – 7.13 (m, 1H).

*Synthesis of N<sup>1</sup>-(4-aminophenyl)-N<sup>1</sup>-phenylbenzene-1,4-diamine (DATPA) (Method 1)*

To a stirred solution of **DNTPA** (1 eq.) in ethanol (100 mL) was added  $\text{SnCl}_2 \cdot 2\text{H}_2\text{O}$  (5 eq). The flask was attached to a condenser and heated under reflux for 8 hours and allowed to cool to room temperature. The cooled solution was poured onto ice and neutralized with a saturated solution of  $\text{NaHCO}_3$  to a pH of 7–8. The mixture was immediately filtered and washed with excess water and a 50% aqueous isopropanol solution. The product was air dried to yield 0.81g (73–99%) N<sup>1</sup>-(4-aminophenyl)-N<sup>1</sup>-phenylbenzene-1,4-diamine which was used directly in the next step.  $^1\text{H}$  NMR (300 MHz, Acetone-d<sub>6</sub>)  $\delta$  7.07 (dd, J = 8.8, 7.2 Hz, 2H), 6.85 (d, J = 8.6 Hz, 4H), 6.78–6.67 (m, 3H), 6.64 (d, J = 8.7 Hz, 4H), 4.51 (s, 4H). MS (ESI) 275.2 (M+).

*Synthesis of N<sup>1</sup>-(4-aminophenyl)-N<sup>1</sup>-phenylbenzene-1,4-diamine (DATPA) (Method 2)*

To a solution of **DNTPA** (1 eq.) in ethanol (100 mL) was added 10%Pd/C (10mg/mmol). The solution was heated to reflux under a nitrogen and hydrazine monohydrate was slowly added (16 eq.). The addition took approximately 10 minutes to ensure the gas evolution did not get out of control. Reflux was continued for 8 hours and the contents were filtered through celite to remove the catalyst while still hot. The celite was washed with additional ethanol followed by a small amount of THF. This solution was left to cool overnight and the resulting crystals were collected by filtration and washed by a small amount of 85% cold ethanol. The product was air dried to yield 0.81g (96%) N<sup>1</sup>-(4-aminophenyl)-N<sup>1</sup>-phenylbenzene-1,4-diamine which was used directly in the next step. <sup>1</sup>H NMR (300 MHz, Acetone-d<sub>6</sub>)  $\delta$  7.07 (dd, J = 8.8, 7.2 Hz, 2H), 6.85 (d, J = 8.6 Hz, 4H), 6.78–6.67 (m, 3H), 6.64 (d, J = 8.7 Hz, 4H), 4.51 (s, 4H). MS (ESI) 276.3 (M+H).

*Synthesis of N<sup>1</sup>,N<sup>1</sup>-dibenzyl-N<sup>4</sup>-(4-(dibenzylamino)phenyl)-N<sup>4</sup>-phenylbenzene-1,4-diamine (4Bn-DATPA)*

A stirred solution of **DATPA** (1 eq.) and potassium carbonate(4 eq.) in DMF (5 ml/mmol) was placed in a ice bath (0–5°C) and benzyl bromide (2.2 eq.) was added over the course of five minutes. The ice bath was removed and the solution was heated to 100°C for 24 hours. Once cool, the solution was diluted with ice water and allowed to settle overnight. The solid was collected on a filter and washed with excess warm water, cold hexanes and air dried overnight. The crude material was purified via a short column of silica with a gradient elution of 4:1 to 1:4 hexanes/toluene. The solvent was stripped under reduced pressure and the solid dried under vacuum at 60°C overnight to yield 0.67g (83%) N<sup>1</sup>-(4-(dibenzylamino)phenyl)-N<sup>4</sup>,N<sup>4</sup>-dimethyl-N<sup>1</sup>-phenylbenzene-1,4-diamine as an off-white solid. <sup>1</sup>H NMR (300 MHz, Acetone-d<sub>6</sub>)  $\delta$  7.30 (s, 16H), 7.27–7.19 (m, 3H), 7.06 (dd, J = 8.4, 6.9 Hz, 2H), 6.89 (d, J = 8.9 Hz, 4H), 6.77–6.64 (m, 8H), 4.67 (s, 8H). MS (ESI) 636.5 (M+H).

*Synthesis of 4-(bis(4-(dibenzylamino)phenyl)amino)benzaldehyde (**4Bn-Ald**)*

To a cooled solution of **4Bn-DATPA** (1 eq.) in DMF (5 mL/mmol) was added POCl<sub>3</sub> (1.5 eq.), dropwise, over 1 minute. The solution was stirred at room temperature for 30 minutes and heated to 80°C for 8 hours. The cooled solution was neutralized with solid sodium acetate, diluted with water and extracted with chloroform. The organic extract was dried over sodium sulphate and the solvent removed under reduced pressure. The residue was dissolved in a minimal amount of 1:1 hexane/toluene and purified by a short column of silica gel eluting with toluene. (46%) 4-(bis(4-(dibenzylamino)phenyl)amino)benzaldehyde as a semi-solid. <sup>1</sup>H NMR (300 MHz, Acetone-d<sub>6</sub>) δ 9.69 (s, 1H), 7.57 (d, J = 8.9 Hz, 2H), 7.31 (d, J = 2.8 Hz, 16H), 7.29–7.19 (m, 2H), 7.03 (s, 4H), 6.81–6.74 (m, 4H), 6.72 (t, J = 4.6 Hz, 2H), 6.65 (d, J = 8.8 Hz, 2H), 4.74 (s, 8H). MS (ESI) 664.8 (M+H).

*Synthesis of (E)-2-(4-(4-(bis(4-(dibenzylamino)phenyl)amino)styryl)-3-cyano-5,5-dimethylfuran-2(5H)-ylidene)malononitrile (**4Bn-DATPA-1**)*

To a vial containing a stir bar and **4Bn-Ald** (1 eq.) in ethanol (1 mL/mmol) was added TCF acceptor (1.1 eq.). The vial was capped and placed in a bead bath held at 90°C for 45 minutes to 1 hour. Once cool, the solvent was stripped by rotary evaporation and the residue loaded onto a column of silica gel with a toluene followed by a gradient elution with 1:1 toluene in chloroform to 100% chloroform. (53%) **4Bn-DATPA-1** as a dark blue solid. <sup>1</sup>H NMR (300 MHz, Acetone-d<sub>6</sub>) δ 8.39 (d, J = 8.7 Hz, 2H), 8.06 (d, J = 15.4 Hz, 1H), 7.74 (d, J = 5.2 Hz, 2H), 7.58–7.50 (m, 16H), 7.29 (d, J = 8.9 Hz, 2H), 7.03 (d, J = 3.5 Hz, 2H), 7.00 (d, J = 9.1 Hz, 4H), 6.61 (d, J = 9.1 Hz, 4H), 6.15 (d, J = 15.4 Hz, 1H), 4.75 (s, 8H), 2.80 (s, 6H). MS (ESI) 846.3 (M+H).



*Synthesis of (E)-2-(4-(4-(bis(4-(dibenzylamino)phenyl)amino)styryl)-3-cyano-5-phenyl-5-(trifluoromethyl)-2(5H)-ylidene)malononitrile (4Bn-DATPA-2)*

**4Bn-DATPA-2** was synthesized in a manner similar to **4Bn-DATPA-1** from CF<sub>3</sub>Ph-TCF acceptor and **4Bn-Ald**. **4Bn-DATPA-2** as a dark green solid. <sup>1</sup>H NMR (300 MHz, Acetone-d<sub>6</sub>) δ 7.73 (dd, J = 9.2, 5.7 Hz, 4H), 7.59 (dd, J = 5.1, 1.6 Hz, 4H), 7.49 (d, J = 8.9 Hz, 2H), 7.29 (dt, J = 11.4, 7.6 Hz, 16H), 7.03 (d, J = 8.9 Hz, 4H), 6.90 (d, J = 15.6 Hz, 1H), 6.78 (d, J = 9.0 Hz, 4H), 6.70 (d, J = 8.9 Hz, 2H), 6.64 (d, J = 8.9 Hz, 2H), 4.75 (s, 8H). MS (ESI) 961.3 (M<sup>+</sup>).

**REFERENCES**

- [1] Yen-Ju Cheng, Jingdong Luo, Steven Hau, Denise H. Bale, Tae-Dong Kim, et al. Large electro-optic activity and enhanced thermal stability from diarylamino-phenyl-containing high- $\beta$  nonlinear optical chromophores. *Chemistry of Materials*, 19(5):1154–1163, 2007.
- [2] Joshua A. Davies, Arumugasamy Elangovan, Philip A. Sullivan, Benjamin C. Olbricht, Denise H. Bale, et al. Rational enhancement of second-order nonlinearity: Bis-(4-methoxyphenyl)hetero-aryl-amino donor-based chromophores: Design, synthesis, and electrooptic activity. *Journal of the American Chemical Society*, 130(32):10565–10575, 2008.
- [3] Bryan K. Spraul, S. Suresh, Takafumi Sassa, M. Ángeles Herranz, Luis Echegoyen, et al. Thermally stable triaryl amino chromophores with high molecular hyperpolarizabilities. *Tetrahedron Letters*, 45(16):3253 – 3256, 2004.
- [4] S. Suresh, Huseyin Zengin, Bryan K. Spraul, Takafumi Sassa, Tatsuo Wada, et al. Synthesis and hyperpolarizabilities of high temperature triarylamine-polyene chromophores. *Tetrahedron Letters*, 46(22):3913 – 3916, 2005.
- [5] Alfredo Ricci, editor. *Modern Amination Methods*. John Wiley & Sons, Inc., 2008.
- [6] John F. Hartwig. Transition metal catalyzed synthesis of arylamines and aryl ethers from aryl halides and triflates: Scope and mechanism. *Angewandte Chemie International Edition*, 37(15):2046–2067, 1998.
- [7] Brett P. Fors and Stephen L. Buchwald. A multiligand based pd catalyst for c–n cross-coupling reactions. *Journal of the American Chemical Society*, 132(45):15914–15917, 2010. PMID: 20979367.
- [8] Qilong Shen and John F. Hartwig. [(cypf-tbu)pdcl<sub>2</sub>]: An air-stable, one-component, highly efficient catalyst for amination of heteroaryl and aryl halides. *Organic Letters*, 10(18):4109–4112, 2008. PMID: 18715012.

- [9] David S. Surry and Stephen L. Buchwald. Dialkylbiaryl phosphines in pd-catalyzed amination: a user's guide. *Chem. Sci.*, 2:27–50, 2011.
- [10] Bennett J. Tardiff, Robert McDonald, Michael J. Ferguson, and Mark Stradiotto. Rational and predictable chemoselective synthesis of oligoamines via buchwald–hartwig amination of (hetero)aryl chlorides employing mor-dalpos. *The Journal of Organic Chemistry*, 77(2):1056–1071, 2012. PMID: 22195727.
- [11] Iram Goldberg. Ueber phenylirungen bei gegenwart von kupfer als katalysator. *Berichte der deutschen chemischen Gesellschaft*, 39(2):1691–1692, 1906.
- [12] Fritz Ullmann and Paul Sponagel. Ueber die phenylirung von phenolen. *Berichte der deutschen chemischen Gesellschaft*, 38(2):2211–2212, 1905.
- [13] Henri-Jean Cristau, Pascal P. Cellier, Jean-Francis Spindler, and Marc Taillefer. Highly efficient and mild copper-catalyzed n- and c-arylations with aryl bromides and iodides. *Chemistry – A European Journal*, 10(22):5607–5622, 2004.
- [14] Steven V. Ley and Andrew W. Thomas. Modern synthetic methods for copper-mediated c(aryl)–o, c(aryl)–n, and c(aryl)–s bond formation. *Angewandte Chemie International Edition*, 42(44):5400–5449, 2003.
- [15] Yunyun Liu and Jie-Ping Wan. Advances in copper-catalyzed c–c coupling reactions and related domino reactions based on active methylene compounds. *Chemistry – An Asian Journal*, 7(7):1488–1501, 2012.
- [16] Florian Monnier and Marc Taillefer. Catalytic c–c, c–n, and c–o ullmann-type coupling reactions. *Angewandte Chemie International Edition*, 48(38):6954–6971, 2009.
- [17] Wilhelm Eschweiler. Ersatz von an stickstoff gebundenen wasserstoffatomen durch die methylgruppe mit hülfe von formaldehyd. *Berichte der deutschen chemischen Gesellschaft*, 38(1):880–882, 1905.

- [18] H. T. Clarke, H. B. Gillespie, and S. Z. Weisshaus. The action of formaldehyde on amines and amino acids. *Journal of the American Chemical Society*, 55(11):4571–4587, 1933.
- [19] Maurice L. Moore, editor. *The Leuckart Reaction*. John Wiley & Sons, Inc., 2004.
- [20] Ahmed F. Abdel-Magid, Kenneth G. Carson, Bruce D. Harris, Cynthia A. Maryanoff, and Rekha D. Shah. Reductive amination of aldehydes and ketones with sodium triacetoxyborohydride. studies on direct and indirect reductive amination procedures. *The Journal of Organic Chemistry*, 61(11):3849–3862, 1996. PMID: 11667239.
- [21] Douglas C. Beshore, , and Christopher J. Dinsmore. Preparation of substituted piperazinones via tandem reductive amination–(n,n’-acyl transfer)–cyclization. *Organic Letters*, 4(7):1201–1204, 2002. PMID: 11922818.
- [22] Onkar S. Nayal, Vinod Bhatt, Sushila Sharma, and Neeraj Kumar. Chemoselective reductive amination of carbonyl compounds for the synthesis of tertiary amines using  $\text{SnCl}_2 \cdot 2\text{H}_2\text{O}$ /pmhs/meoh. *The Journal of Organic Chemistry*, 80(11):5912–5918, 2015. PMID: 25938581.
- [23] Wenwei Jin, Peter V. Johnston, Delwin L. Elder, Karl T. Manner, Kerry E. Garrett, et al. Structure-function relationship exploration for enhanced thermal stability and electro-optic activity in monolithic organic nlo chromophores. *J. Mater. Chem. C*, 4:3119–3124, 2016.
- [24] C. C. Teng and H. T. Man. Simple reflection technique for measuring the electro-optic coefficient of poled polymers. *Applied Physics Letters*, 56(18):1734–1736, 1990.
- [25] Peter V. Johnston. *Structure Function Paradigms of Organic Electrooptic Materials*. Ph.D. thesis, University of Washington, 2016.
- [26] Ben C. Olbricht. *Characterization and Processing of Organic Nonlinear Optical Materials using Ellipsometric, Waveguiding, and Absorption Spectroscopy Techniques*. Ph.D. thesis, University of Washington, 2010.

- [27] Wenwei Jin, Peter V. Johnston, Delwin L. Elder, Andreas F. Tillack, Benjamin C. Olbricht, et al. Benzocyclobutene barrier layer for suppressing conductance in nonlinear optical devices during electric field poling. *Applied Physics Letters*, 104(24):243304, 2014.
- [28] Douglas A. Skoog, F. James. Holler, and Timothy A. Nieman. *Principles of instrumental analysis*. Saunders College Pub. ; Harcourt Brace College Publishers, Philadelphia; Orlando, Fla., 1998.
- [29] Marina Yu. Balakina. Polymer matrix effects on the nonlinear optical response of incorporated chromophore: New analytical models. *ChemPhysChem*, 7(10):2115–2125, 2006.

**BIBLIOGRAPHY**

Ahmed F. Abdel-Magid, Kenneth G. Carson, Bruce D. Harris, Cynthia A. Maryanoff, and Rekha D. Shah. Reductive amination of aldehydes and ketones with sodium triacetoxyborohydride. studies on direct and indirect reductive amination procedures<sup>1</sup>. *The Journal of Organic Chemistry*, 61(11):3849–3862, 1996. PMID: 11667239.

Luca Alloatti, Robert Palmer, Sebastian Diebold, Kai Philipp Pahl, Baoquan Chen, Raluca Dinu, Maryse Fournier, Jean-Marc Fedeli, Thomas Zwick, Wolfgang Freude, Christian Koos, and Juerg Leuthold. 100 ghz silicon–organic hybrid modulator. *Light Sci Appl*, 3:e173–, 05 2014.

Raquel Andreu, Elena Galán, Jesús Orduna, Belén Villacampa, Raquel Alicante, Juan T. López Navarrete, Juan Casado, and Javier Garín. Aromatic/proaromatic donors in 2-dicyanomethylenethiazole merocyanines: From neutral to strongly zwitterionic nonlinear optical chromophores. *Chemistry – A European Journal*, 17(3):826–838, 2011.

Jan Andzelm, Berend C. Rinderspacher, Adam Rawlett, Joseph Dougherty, Roi Baer, and Niranjana Govind. Performance of dft methods in the calculation of optical spectra of tcf-chromophores. *Journal of Chemical Theory and Computation*, 5(10):2835–2846, 2009. PMID: 26631795.

Mohamed Ashraf, Ayele Teshome, Andrew J. Kay, Graeme J. Gainsford, M. Delower H. Bhuiyan, Inge Asselberghs, and Koen Clays. Synthesis and optical properties of NLO chromophores containing an indoline donor and azo linker. *Dyes and Pigments*, 95(3):455 – 464, 2012.

Marina Yu. Balakina. Polymer matrix effects on the nonlinear optical response of incorporated chromophore: New analytical models. *ChemPhysChem*, 7(10):2115–2125, 2006.

Denise H. Bale. *Nonlinear Optical Materials Characterization Studies Employing Photostability, Hyper-Rayleigh Scattering, and Electric Field Induced Second Harmonic Generation Techniques*. PhD thesis, University of Washington, 2008.

Peter V. Bedworth, Yongming Cai, Alex Jen, , and Seth R. Marder. Synthesis and relative thermal stabilities of diphenylamino- vs piperidinyl-substituted bithiophene chromophores for nonlinear optical materials. *The Journal of Organic Chemistry*, 61(6):2242–2246, 1996.

Stephanie J. Benight, Daniel B. Knorr, Lewis E. Johnson, Philip A. Sullivan, David Lao, Jianing Sun, Lakshmi S. Kocherlakota, Arumugasamy Elangovan, Bruce H. Robinson, Rene M. Overney, and Larry R. Dalton. Nano-engineering lattice dimensionality for a soft matter organic functional material. *Advanced Materials*, 24(24):3263–3268, 2012.

Douglas C. Beshore, , and Christopher J. Dinsmore. Preparation of substituted piperazinones via tandem reductive amination–(n,n’-acyl transfer)–cyclization. *Organic Letters*, 4(7):1201–1204, 2002. PMID: 11922818.

M. Blanchard-Desce, V. Alain, P. V. Bedworth, S. R. Marder, A. Fort, C. Runser, M. Barzoukas, S. Lebus, and R. Wortmann. Large quadratic hyperpolarizabilities with donor–acceptor polyenes exhibiting optimum bond length alternation: Correlation between structure and hyperpolarizability. *Chemistry – A European Journal*, 3(7):1091–1104, 1997.

B. Bleaney and B.I Bleaney. *Electricity and Magnetism*, volume 3rd. Oxford University Press, 1976.

Pierre Bonhôte, Jacques-E. Moser, Robin Humphry-Baker, Nicolas Vlachopoulos, Shaik M. Zakeeruddin, Lorenz Walder, and Michael Grätzel. Long-lived photoinduced charge separation and redox-type photochromism on mesoporous oxide films sensitized by molecular dyads. *Journal of the American Chemical Society*, 121(6):1324–1336, 1999.

Christian Bosshard, Ulrich Gubler, Phil Kaatz, Witold Mazerant, and Urs Meier. Non-phase-matched optical third-harmonic generation in noncentrosymmetric media: Cascaded

second-order contributions for the calibration of third-order nonlinearities. *Phys. Rev. B*, 61:10688–10701, Apr 2000.

Christian Bosshard, Georg Knoepfle, Philippe Pretre, Stephan Follonier, Christophe Serbutoviez, and Peter Guenter. Molecular crystals and polymers for nonlinear optics. *Optical Engineering*, 34(7):1951–1960, 1995.

Christian Bosshard, Man Shing Wong, Feng Pan, Peter Günter, and Volker Gramlich. Self-assembly of an acentric co-crystal of a highly hyperpolarizable merocyanine dye with optimized alignment for nonlinear optics. *Advanced Materials*, 9(7):554–557, 1997.

Robert W. Boyd. *Nonlinear Optics*. Academic Press, 2013.

J. L. Bredas, R. Silbey, D. S. Boudreaux, and R. R. Chance. Chain-length dependence of electronic and electrochemical properties of conjugated systems: polyacetylene, polyphenylene, polythiophene, and polypyrrole. *Journal of the American Chemical Society*, 105(22):6555–6559, 1983.

Peter Buchwald, Emilio Margolles-Clark, Norma S Kenyon, and Camillo Ricordi. Organic dyes as small molecule protein-protein interaction inhibitors for the cd40-cd154 costimulatory interaction. *J Mol Recognit*, 23(1):65–73, Jan-Feb 2010.

Agostina L. Capodilupo, Eduardo Fabiano, Luisa De Marco, Giuseppe Ciccarella, Giuseppe Gigli, Carmela Martinelli, and Antonio Cardone. [1]benzothieno[3,2-b]benzothiophene-based organic dyes for dye-sensitized solar cells. *The Journal of Organic Chemistry*, 81(8):3235–3245, 2016. PMID: 26986652.

Andrew P. Chafin and Geoffrey A. Lindsay. A pattern for increasing the first hyperpolarizability of a push-pull polyene dye as indicated from dft calculations. *The Journal of Physical Chemistry C*, 112(21):7829–7835, 2008.



Jeng-Da Chai and Martin Head-Gordon. Long-range corrected hybrid density functionals with damped atom-atom dispersion corrections. *Phys. Chem. Chem. Phys.*, 10:6615–6620, 2008.

Honghong Chen, Qi Ma, Yuqiao Zhou, Zhou Yang, Mojca Jazbinsek, Yongzhong Bian, Ning Ye, Dong Wang, Hui Cao, and Wanli He. Engineering of organic chromophores with large second-order optical nonlinearity and superior crystal growth ability. *Crystal Growth & Design*, 15(11):5560–5567, 2015.

Shue-Jen. Chen and Frank W. Fowler. Structures of alleged 1,4-dihydropyrazines. *The Journal of Organic Chemistry*, 35(11):3987–3989, 1970.

Yen-Ju Cheng, Jingdong Luo, Steven Hau, Denise H. Bale, Tae-Dong Kim, Zhengwei Shi, David B. Lao, Neil M. Tucker, Yanqing Tian, Larry R. Dalton, Philip J. Reid, , and Alex K-Y. Jen. Large electro-optic activity and enhanced thermal stability from diarylaminophenyl-containing high- $\beta$  nonlinear optical chromophores. *Chemistry of Materials*, 19(5):1154–1163, 2007.

Yen-Ju Cheng, Jingdong Luo, Su Huang, Xinghua Zhou, Zhengwei Shi, Tae-Dong Kim, Denise H. Bale, Satsuki Takahashi, Andrew Yick, Brent M. Polishak, Sei-Hum Jang, Larry R. Dalton, Philip J. Reid, William H. Steier, and Alex K.-Y. Jen. Donor–acceptor thiolated polyenic chromophores exhibiting large optical nonlinearity and excellent photostability. *Chemistry of Materials*, 20(15):5047–5054, 2008.

Pratibha Chopra, Louis Carlacci, Harry F. King, and Paras N. Prasad. Ab initio calculations of polarizabilities and second hyperpolarizabilities in organic molecules with extended  $\pi$ -electron conjugation. *The Journal of Physical Chemistry*, 93(20):7120–7130, 1989.

Cisco Systems Inc. Cisco visual networking index: Global mobile data traffic forecast update, 2015–2020, 2016.

H. T. Clarke, H. B. Gillespie, and S. Z. Weisshaus. The action of formaldehyde on amines and amino acids<sup>1</sup>. *Journal of the American Chemical Society*, 55(11):4571–4587, 1933.

W. H. CLIFFE. In the footsteps of perkin. *Journal of the Society of Dyers and Colourists*, 72(12):563–566, 1956.

B.J. Coe, J.A. Harris, I. Asselberghs, K. Wostyn, K. Clays, A. Persoons, B.S. Brunshwig, S.J. Coles, T. Gelbrich, M.E. Light, M.B. Hursthouse, and K. Nakatani. Quadratic optical nonlinearities of n-methyl and n-aryl pyridinium salts. *Advanced Functional Materials*, 13(5):347–357, 2003.

Howard D. Cohen and C. C. J. Roothaan. Electric dipole polarizability of atoms by the hartree—fock method. i. theory for closed-shell systems. *The Journal of Chemical Physics*, 43(10):S34–S39, 1965.

Shengyu Cong, Airui Zhang, Fenggang Liu, Dan Yang, Maolin Zhang, Shuhui Bo, Xinhou Liu, Ling Qiu, and Zhen Zhen. Improving poling efficiency by synthesizing a nonlinear optical chromophore containing two asymmetric non-conjugated d-[small pi]-a chains. *RSC Adv.*, 5:10497–10504, 2015.

Henri-Jean Cristau, Pascal P. Cellier, Jean-Francis Spindler, and Marc Taillefer. Highly efficient and mild copper-catalyzed n- and c-arylations with aryl bromides and iodides. *Chemistry – A European Journal*, 10(22):5607–5622, 2004.

L. R. Dalton, A. W. Harper, R. Ghosn, W. H. Steier, M. Ziari, H. Fetterman, Y. Shi, R. V. Mustacich, A. K.-Y. Jen, and K. J. Shea. Synthesis and processing of improved organic second-order nonlinear optical materials for applications in photonics. *Chemistry of Materials*, 7(6):1060–1081, 1995.

Larry R. Dalton, Peter Günter, Mojca Jazbinsek, O-Pil Kwon, and Philip A. Sullivan. *Organic Electro-Optics and Photonics: Molecules, Polymers and Crystals*. Cambridge University Press, 2015.

Larry R. Dalton, Philip A. Sullivan, and Denise H. Bale. Electric field poled organic electro-optic materials: State of the art and future prospects. *Chemical Reviews*, 110(1):25–55, 2010. PMID: 19848381.

Larry R. Dalton, Philip A. Sullivan, Denise H. Bale, and Ben C. Olbricht. Theory-inspired nano-engineering of photonic and electronic materials: Noncentrosymmetric charge-transfer electro-optic materials. *Solid-State Electronics*, 51(10):1263 – 1277, 2007. Special Issue: Papers Selected from the {NGC2007} Conference.

Joshua A. Davies, Arumugasamy Elangovan, Philip A. Sullivan, Benjamin C. Olbricht, Denise H. Bale, Todd R. Ewy, Christine M. Isborn, Bruce E. Eichinger, Bruce H. Robinson, Philip J. Reid, Xiaosong Li, and Larry R. Dalton. Rational enhancement of second-order nonlinearity: Bis-(4-methoxyphenyl)hetero-aryl-amino donor-based chromophores: Design, synthesis, and electrooptic activity. *Journal of the American Chemical Society*, 130(32):10565–10575, 2008.

John A. Dean. *Analytical chemistry handbook*. McGraw-Hill, New York, 1995.

V. Dentan, Y. Lévy, M. Dumont, P. Robin, and E. Chastaing. Electrooptic properties of a ferroelectric polymer studied by attenuated total reflection. *Optics Communications*, 69(5):379 – 383, 1989.

M. J. S. Dewar. 478. colour and constitution. part i. basic dyes. *J. Chem. Soc.*, pages 2329–2334, 1950.

Delwin L. Elder, Stephanie J. Benight, Jinsheng Song, Bruce H. Robinson, and Larry R. Dalton. Matrix-assisted poling of monolithic bridge-disubstituted organic nlo chromophores. *Chemistry of Materials*, 26(2):872–874, 2014.

R. C. Elderfield. *Heterocyclic compounds*. Wiley : University Microfilms International, New York; Ann Arbor, Mich., 1957.

Dennis M. Elking, Lalith Perera, Robert Duke, Thomas Darden, and Lee G. Pedersen. A finite field method for calculating molecular polarizability tensors for arbitrary multipole rank. *Journal of Computational Chemistry*, 32(15):3283–3295, 2011.

Wilhelm Eschweiler. Ersatz von an stickstoff gebundenen wasserstoffatomen durch die methylgruppe mit hülfe von formaldehyd. *Berichte der deutschen chemischen Gesellschaft*, 38(1):880–882, 1905.

Brett P. Fors and Stephen L. Buchwald. A multiligand based pd catalyst for c–n cross-coupling reactions. *Journal of the American Chemical Society*, 132(45):15914–15917, 2010. PMID: 20979367.

Jean-Louis Fourrey, Josiane Beauhaire, and Chun Wei Yuan. Preparation of stable 1,4-dihydropyrazines. *J. Chem. Soc., Perkin Trans. 1*, pages 1841–1843, 1987.

Frank W. Fowler and Shue-Jen Chen. Synthesis of the 1,4-dihydropyrazine ring system. stable 8. $\pi$ -electron heterocycle. *The Journal of Organic Chemistry*, 36(26):4025–4028, 1971.

M. J. Frisch, G. W. Trucks, H. B. Schlegel, G. E. Scuseria, M. A. Robb, J. R. Cheeseman, G. Scalmani, V. Barone, B. Mennucci, G. A. Petersson, H. Nakatsuji, M. Caricato, X. Li, H. P. Hratchian, A. F. Izmaylov, J. Bloino, G. Zheng, J. L. Sonnenberg, M. Hada, M. Ehara, K. Toyota, R. Fukuda, J. Hasegawa, M. Ishida, T. Nakajima, Y. Honda, O. Kitao, H. Nakai, T. Vreven, J. A. Montgomery, Jr., J. E. Peralta, F. Ogliaro, M. Bearpark, J. J. Heyd, E. Brothers, K. N. Kudin, V. N. Staroverov, R. Kobayashi, J. Normand, K. Raghavachari, A. Rendell, J. C. Burant, S. S. Iyengar, J. Tomasi, M. Cossi, N. Rega, J. M. Millam, M. Klene, J. E. Knox, J. B. Cross, V. Bakken, C. Adamo, J. Jaramillo, R. Gomperts, R. E. Stratmann, O. Yazyev, A. J. Austin, R. Cammi, C. Pomelli, J. W. Ochterski, R. L. Martin, K. Morokuma, V. G. Zakrzewski, G. A. Voth, P. Salvador, J. J. Dannenberg, S. Dapprich, A. D. Daniels, Ö. Farkas, J. B. Foresman, J. V. Ortiz, J. Cioslowski, and D. J. Fox. Gaussian 09 Revision D.01. Gaussian Inc. Wallingford CT 2009.

Kerry Garrett. *Computational Study of Linear and Nonlinear Optical Properties of Single Molecules and Clusters of Organic Electro-Optic Chromophores*. PhD thesis, University of Washington, 2015.

Iram Goldberg. Ueber phenylirungen bei gegenwart von kupfer als katalysator. *Berichte der deutschen chemischen Gesellschaft*, 39(2):1691–1692, 1906.

J Hamrle, S Blomeier, O Gaier, B Hillebrands, H Schneider, G Jakob, K Postava, and C Felser. Huge quadratic magneto-optical kerr effect and magnetization reversal in the co 2 fesi heusler compound. *Journal of Physics D: Applied Physics*, 40(6):1563, 2007.

John F. Hartwig. Transition metal catalyzed synthesis of arylamines and aryl ethers from aryl halides and triflates: Scope and mechanism. *Angewandte Chemie International Edition*, 37(15):2046–2067, 1998.

S. Herminghaus, Barton A. Smith, and J. D. Swalen. Electro-optic coefficients in electric-field-poled polymer waveguides. *J. Opt. Soc. Am. B*, 8(11):2311–2317, Nov 1991.

Chaolei Hu, Fenggang Liu, Hua Zhang, Fuyang Huo, Yuhui Yang, Haoran Wang, Hongyan Xiao, Zhuo Chen, Jialei Liu, Ling Qiu, Zhen Zhen, Xinhou Liu, and Shuhui Bo. Synthesis of novel nonlinear optical chromophores: achieving excellent electro-optic activity by introducing benzene derivative isolation groups into the bridge. *Journal of Materials Chemistry C*, 3(44):11595–11604, 2015.

Karl Hübner. 150 jahre mauvein. *Chemie in unserer Zeit*, 40(4):274–275, 2006.

Jane Hung, Wenkel Liang, Jingdong Luo, Zhengwei Shi, Alex K.-Y. Jen, and Xiaosong Li. Rational design using dewar’s rules for enhancing the first hyperpolarizability of nonlinear optical chromophores. *The Journal of Physical Chemistry C*, 114(50):22284–22288, 2010.

Sei-Hum Jang, Jingdong Luo, Neil M. Tucker, Amalia Leclercq, Egbert Zojer, Marnie A. Haller, Tae-Dong Kim, Jae-Wook Kang, Kimberly Firestone, Denise Bale, David Lao, Jason B. Benedict, Dawn Cohen, Werner Kaminsky, Bart Kahr, Jean-Luc Brédas, Philip Reid,

Larry R. Dalton, and Alex K. Y. Jen. Pyrroline chromophores for electro-optics. *Chemistry of Materials*, 18(13):2982–2988, 2006.

Wenwei Jin, Peter V. Johnston, Delwin L. Elder, Karl T. Manner, Kerry E. Garrett, Werner Kaminsky, Ruimin Xu, Bruce H. Robinson, and Larry R. Dalton. Structure-function relationship exploration for enhanced thermal stability and electro-optic activity in monolithic organic nlo chromophores. *J. Mater. Chem. C*, 4:3119–3124, 2016.

Wenwei Jin, Peter V. Johnston, Delwin L. Elder, Andreas F. Tillack, Benjamin C. Olbricht, Jinsheng Song, Philip J. Reid, Ruimin Xu, Bruce H. Robinson, and Larry R. Dalton. Benzocyclobutene barrier layer for suppressing conductance in nonlinear optical devices during electric field poling. *Applied Physics Letters*, 104(24), 2014.

V.A.G.I.I. John, D.M. Gill, and R.W. Smith. Chirp compensated mach-zehnder electro-optic modulator, December 31 2002. US Patent 6,501,867.

Lewis E. Johnson. *Multi-Scale Modeling of Organic Electro-Optic Materials*. PhD thesis, University of Washington, 2012.

Peter V. Johnston. *Structure Function Paradigms of Organic Electrooptic Materials*. PhD thesis, University of Washington, 2016.

Muneaki Kamiya, Hideo Sekino, Takao Tsuneda, and Kimihiko Hirao. Nonlinear optical property calculations by the long-range-corrected coupled-perturbed kohn–sham method. *The Journal of Chemical Physics*, 122(23), 2005.

Mark G. Kuzyk. Physical limits on electronic nonlinear molecular susceptibilities. *Phys. Rev. Lett.*, 85:1218–1221, Aug 2000.

Ohyun Kwon, Stephen Barlow, Susan A. Odom, Luca Beverina, Natalie J. Thompson, Egbert Zojer, Jean-Luc Brédas, and Seth R. Marder. Aromatic amines: A comparison of electron-donor strengths. *The Journal of Physical Chemistry A*, 109(41):9346–9352, 2005. PMID: 16833276.

Matthias Lauermann, Stefan Wolf, Philipp C. Schindler, Robert Palmer, Sebastian Koeber, Dietmar Korn, Luca Alloatti, Thorsten Wahlbrink, Jens Bolten, Michael Waldow, Michael Koenigsmann, Matthias Kohler, Dimitri Malsam, Delwin L. Elder, Peter V. Johnston, Nathaniel Phillips-Sylvain, Philip A. Sullivan, Larry R. Dalton, Juerg Leuthold, Wolfgang Freude, and Christian Koos. 40 gbd 16qam signaling at 160 gb/s in a silicon-organic hybrid modulator. *J. Lightwave Technol.*, 33(6):1210–1216, Mar 2015.

John E. Lesch, editor. *The First Miracle Drugs: How the Sulfa Drugs Transformed Medicine*. Oxford University Press, 2006.

J. Leuthold, C. Koos, W. Freude, L. Alloatti, R. Palmer, D. Korn, J. Pfeifle, M. Lauermann, R. Dinu, S. Wehrli, M. Jazbinsek, P. Günter, M. Waldow, T. Wahlbrink, J. Bolten, H. Kurz, M. Fournier, J. M. Fedeli, H. Yu, and W. Bogaerts. Silicon-organic hybrid electro-optical devices. *IEEE Journal of Selected Topics in Quantum Electronics*, 19(6):114–126, Nov 2013.

Steven V. Ley and Andrew W. Thomas. Modern synthetic methods for copper-mediated c(aryl)–o, c(aryl)–n, and c(aryl)–s bond formation. *Angewandte Chemie International Edition*, 42(44):5400–5449, 2003.

Yi Liao, Cyrus A. Anderson, Philip A. Sullivan, Andrew J. P. Akelaitis, Bruce H. Robinson, and Larry R. Dalton. Electro-optical properties of polymers containing alternating nonlinear optical chromophores and bulky spacers. *Chemistry of Materials*, 18(4):1062–1067, 2006.

Yi Liao, Sanchali Bhattacharjee, Kimberly A. Firestone, Bruce E. Eichinger, Rajan Paranj, Cyrus A. Anderson, Bruce H. Robinson, Philip J. Reid, and Larry R. Dalton. Antiparallel-aligned neutral-ground-state and zwitterionic chromophores as a nonlinear optical material. *Journal of the American Chemical Society*, 128(21):6847–6853, 2006. PMID: 16719465.

Fenggang Liu, Haoran Wang, Yuhui Yang, Huajun Xu, Maolin Zhang, Airui Zhang, Shuhui Bo, Zhen Zhen, Xinhou Liu, and Ling Qiu. Nonlinear optical chromophores containing a

novel pyrrole-based bridge: optimization of electro-optic activity and thermal stability by modifying the bridge. *J. Mater. Chem. C*, 2:7785–7795, 2014.

Fenggang Liu, Yuhui Yang, Shengyu Cong, Haoran Wang, Maolin Zhang, Shuhui Bo, Jialei Liu, Zhen Zhen, Xinhou Liu, and Ling Qiu. Comparison of second-order nonlinear optical chromophores with d-[small pi]-a, d-a-[small pi]-a and d-d-[small pi]-a architectures: diverse nlo effects and interesting optical behavior. *RSC Adv.*, 4:52991–52999, 2014.

Yunyun Liu and Jie-Ping Wan. Advances in copper-catalyzed c–c coupling reactions and related domino reactions based on active methylene compounds. *Chemistry – An Asian Journal*, 7(7):1488–1501, 2012.

J. William Lown and M. Humayoun Akhtar. Self-condensation and rearrangement of n-alkylphenacylamines. *J. Chem. Soc., Perkin Trans. 1*, pages 683–686, 1973.

J. William Lown, M. Humayoun Akhtar, and Robert S. McDaniel. Stereochemistry and mechanism of the thermal [1,3] alkyl shift of stable 1,4-dialkyl-1,4-dihydropyrazines. *The Journal of Organic Chemistry*, 39(14):1998–2006, 1974.

Jingdong Luo, Su Huang, Yen-Ju Cheng, Tae-Dong Kim, Zhengwei Shi, Xing-Hua Zhou, and Alex K. Y. Jen. Phenyltetraene-based nonlinear optical chromophores with enhanced chemical stability and electrooptic activity. *Organic Letters*, 9(22):4471–4474, 10 2007.

Xiaohua Ma, Fei Ma, Zhenhua Zhao, Naiheng Song, and Jianping Zhang. Synthesis and properties of nlo chromophores with fine-tuned gradient electronic structures. *J. Mater. Chem.*, 19:2975–2985, 2009.

Xiaohua Ma, Fei Ma, Zhenhua Zhao, Naiheng Song, and Jianping Zhang. Toward highly efficient nlo chromophores: Synthesis and properties of heterocycle-based electronically gradient dipolar nlo chromophores. *J. Mater. Chem.*, 20:2369–2380, 2010.

Seth R. Marder, Lap-Tak Cheng, Bruce G. Tiemann, Andrienne C. Friedli, Mireille Blanchard-Desce, Joseph W. Perry, and Jørgen Skindhøj. Large first hyperpolarizabilities



in push-pull polyenes by tuning of the bond length alternation and aromaticity. *Science*, 263(5146):511–514, 1994.

Arthur T. Mason and Goodlatte R. Winder. Xcix.-syntheses of piazine derivatives. interaction of benzylamine and phenacyl bromide. *J. Chem. Soc., Trans.*, 63:1355–1375, 1893.

Masaru Matsuoka. Dyes for optical recording. *Molecular Crystals and Liquid Crystals Science and Technology. Section A. Molecular Crystals and Liquid Crystals*, 224(1):85–94, 1993.

F. Meyers, S.R. Marder, B.M. Pierce, and J.L. Brédas. Tuning of large second hyperpolarizabilities in organic conjugated compounds. *Chemical Physics Letters*, 228(1):171 – 176, 1994.

Florian Monnier and Marc Taillefer. Catalytic c–c, c–n, and c–o ullmann-type coupling reactions. *Angewandte Chemie International Edition*, 48(38):6954–6971, 2009.

Maurice L. Moore, editor. *The Leuckart Reaction*. John Wiley & Sons, Inc., 2004.

Christopher R. Moylan, Susan Ermer, Steven M. Lovejoy, I-Heng McComb, Doris S. Leung, Rüdiger Wortmann, Peter Krdmer, , and Robert J. Twieg. (dicyanomethylene)pyran derivatives with c<sub>2v</sub> symmetry: An unusual class of nonlinear optical chromophores. *Journal of the American Chemical Society*, 118(51):12950–12955, 1996.

Christopher R. Moylan, Robert J. Twieg, Victor Y. Lee, Sally A. Swanson, Kathleen M. Betterton, and Robert D. Miller. Nonlinear optical chromophores with large hyperpolarizabilities and enhanced thermal stabilities. *Journal of the American Chemical Society*, 115(26):12599–12600, 1993.

R. S. Mulliken. Electronic population analysis on lcao-àimo molecular wave functions. i. *The Journal of Chemical Physics*, 23(10):1833–1840, 1955.

Masayoshi Nakano, Isamu Shigemoto, Satoru Yamada, and Kizashi Yamaguchi. Size-consistent approach and density analysis of hyperpolarizability: Second hyperpolarizabilities of polymeric systems with and without defects. *The Journal of Chemical Physics*, 103(10):4175–4191, 1995.

Onkar S. Nayal, Vinod Bhatt, Sushila Sharma, and Neeraj Kumar. Chemoselective reductive amination of carbonyl compounds for the synthesis of tertiary amines using  $\text{sncl}_2 \cdot 2\text{h}_2\text{o} / \text{pmhs} / \text{meoh}$ . *The Journal of Organic Chemistry*, 80(11):5912–5918, 2015. PMID: 25938581.

R. A. Norwood, M. G. Kuzyk, and R. A. Keosian. Electro-optic tensor ratio determination of side-chain copolymers with electro-optic interferometry. *Journal of Applied Physics*, 75(4):1869–1874, 1994.

Noel M. O’boyle, Adam L. Tenderholt, and Karol M. Langner. cclib: A library for package-independent computational chemistry algorithms. *Journal of Computational Chemistry*, 29(5):839–845, 2008.

Ben C. Olbricht. *Characterization and Processing of Organic Nonlinear Optical Materials using Ellipsometric, Waveguiding, and Absorption Spectroscopy Techniques*. PhD thesis, University of Washington, 2010.

Brian O’Regan and Michael Gratzel. A low-cost, high-efficiency solar cell based on dye-sensitized colloidal  $\text{tio}_2$  films. *Nature*, 353(6346):737–740, 10 1991.

J. L. Oudar and D. S. Chemla. Hyperpolarizabilities of the nitroanilines and their relations to the excited state dipole moment. *The Journal of Chemical Physics*, 66(6):2664–2668, 1977.

Mantios G. Papadopoulos, Andrzej J. Sadlej, and Jerzy Leszczynski, editors. *Non-Linear Optical Properties of Matter: From molecules to condensed phases*, volume 1. Springer Netherlands, 2006.

Venkatakrishnan Parthasarathy, Ravindra Pandey, Matthias Stolte, Sampa Ghosh, Frédéric Castet, Frank Würthner, Puspendu Kumar Das, and Mireille Blanchard-Desce. Combination of cyanine behaviour and giant hyperpolarisability in novel merocyanine dyes: Beyond the bond length alternation (bla) paradigm. *Chemistry – A European Journal*, 21(40):14211–14217, 2015.

Victoria Peddie, Jack Anderson, Joanne E. Harvey, Gerald J. Smith, and Andrew Kay. Synthesis and solution aggregation studies of a suite of mixed neutral and zwitterionic chromophores for second-order nonlinear optics. *The Journal of Organic Chemistry*, 79(21):10153–10169, 2014. PMID: 25265243.

Paras N. Prasad and David J. Williams. *Introduction to Nonlinear Optical Effects in Molecules and Polymers*. John Wiley & Sons, Inc., 1991.

Ph. Prêtre, L.-M. Wu, R. A. Hill, and A. Knoesen. Characterization of electro-optic polymer films by use of decal-deposited reflection fabry–perot microcavities. *J. Opt. Soc. Am. B*, 15(1):379–392, Jan 1998.

Larry R. Dalton, William H. Steier, Bruce H. Robinson, Chang Zhang, Albert Ren, Sean Garner, Antao Chen, Timothy Londergan, Lindsey Irwin, Brenden Carlson, Leonard Fifield, Gregory Phelan, Clint Kincaid, Joseph Amend, and Alex Jen. From molecules to opto-chips: organic electro-optic materials. *J. Mater. Chem.*, 9:1905–1920, 1999.

Ute Resch-Genger, Markus Grabolle, Sara Cavaliere-Jaricot, Roland Nitschke, and Thomas Nann. Quantum dots versus organic dyes as fluorescent labels. *Nat Meth*, 5(9):763–775, 09 2008.

Alfredo Ricci, editor. *Modern Amination Methods*. John Wiley & Sons, Inc., 2008.

B.H. Robinson, L.R. Dalton, A.W. Harper, A. Ren, F. Wang, C. Zhang, G. Todorova, M. Lee, R. Aniszfeld, S. Garner, A. Chen, W.H. Steier, S. Houbrecht, A. Persoons, I Ledoux,

J. Zyss, and A.K.Y. Jen. The molecular and supramolecular engineering of polymeric electro-optic materials. *Chemical Physics*, 245(1–3):35 – 50, 1999.

Marco Ronchi, Alessio Orbelli Biroli, Daniele Marinotto, Maddalena Pizzotti, M. Chiara Ubaldi, and Silvia M. Pietralunga. The role of the chromophore size and shape on the shg stability of pmma films with embedded nlo active macrocyclic chromophores based on a cyclotetrasiloxane scaffold. *The Journal of Physical Chemistry C*, 115(10):4240–4246, 2011.

Bahaa E. A. Saleh and Malvin Carl Teich. *Fundamentals of Photonics*. John Wiley & Sons, Inc., 1991.

K. Sano, K. Murata, T. Otsuji, T. Akeyoshi, N. Shimizu, and E. Sano. An 80-gb/s optoelectronic delayed flip-flop ic using resonant tunneling diodes and uni-traveling-carrier photodiode. *IEEE Journal of Solid-State Circuits*, 36(2):281–289, Feb 2001.

Giovanni Scalmani and Michael J. Frisch. Continuous surface charge polarizable continuum models of solvation. i. general formalism. *The Journal of Chemical Physics*, 132(11), 2010.

Jay S. Schildkraut. Determination of the electrooptic coefficient of a poled polymer film. *Appl. Opt.*, 29(19):2839–2841, Jul 1990.

Karin Schmidt, Stephen Barlow, Amalia Leclercq, Egbert Zojer, Sei-Hum Jang, Seth R. Marder, Alex K.-Y. Jen, and Jean-Luc Bredas. Efficient acceptor groups for nlo chromophores: competing inductive and resonance contributions in heterocyclic acceptors derived from 2-dicyanomethylidene-3-cyano-4,5,5-trimethyl-2,5-dihydrofuran. *J. Mater. Chem.*, 17:2944–2949, 2007.

Qilong Shen and John F. Hartwig. [(cypf-tbu)pdcl<sub>2</sub>]: An air-stable, one-component, highly efficient catalyst for amination of heteroaryl and aryl halides. *Organic Letters*, 10(18):4109–4112, 2008. PMID: 18715012.

Yongqiang Shi, Cheng Zhang, Hua Zhang, James H. Bechtel, Larry R. Dalton, Bruce H. Robinson, and William H. Steier. Low (sub-1-volt) halfwave voltage polymeric electro-optic modulators achieved by controlling chromophore shape. *Science*, 288(5463):119–122, 2000.

Yoshito Shuto and Michiyuki Amano. Reflection measurement technique of electro-optic coefficients in lithium niobate crystals and poled polymer films. *Journal of Applied Physics*, 77(9):4632–4638, 1995.

K. D. Singer, M. G. Kuzyk, W. R. Holland, J. E. Sohn, S. J. Lalama, R. B. Comizzoli, H. E. Katz, and M. L. Schilling. Electro-optic phase modulation and optical second-harmonic generation in corona-poled polymer films. *Applied Physics Letters*, 53(19):1800–1802, 1988.

Jessica Sinness, Olivier Clot, Scott R. Hammond, Nishant Bhatambrekar, Harrison L. Rommel, Bruce Robinson, Alex K-Y. Jen, and Larry Dalton. Synthesis of dendritic nlo chromophores for the improvement of order in electro-optics. In *Symposium DD – Organic and Nanocomposite Optical Materials*, volume 846 of *MRS Proceedings*, page DD6.3 (6 pages), 2004.

Douglas A. Skoog, F. James. Holler, and Timothy A. Nieman. *Principles of instrumental analysis*. Saunders College Pub. ; Harcourt Brace College Publishers, Philadelphia; Orlando, Fla., 1998.

Parmeshwar Solanke, Filip Bureš, Oldřich Pytela, Milan Klikar, Tomáš Mikysek, Loic Mager, Alberto Barsella, and Zdeňka Ružičková. T-shaped (donor– $\pi$ –)2acceptor– $\pi$ –donor push–pull systems based on indan-1,3-dione. *European Journal of Organic Chemistry*, 2015(24):5339–5349, 2015.

SPIE. *Synthesis of new second-order nonlinear optical chromophores: implementing lessons learned from theory and experiment*, volume 4114, 2000.

SPIE. *Systematic optimization of polymeric electro-optic materials*, volume 4114, 2000.

SPIE. *An Extraordinary New Class of Electro-Optic Materials: Binary Chromophore Glasses*, July 2007.

SPIE. *Organic electro-optic/silicon photonic materials and devices*, volume 6638, 2007.

Bryan K. Spraul, S. Suresh, Takafumi Sassa, M. Ángeles Herranz, Luis Echegoyen, Tatsuo Wada, Dvora Perahia, and Dennis W. Smith Jr. Thermally stable triaryl amino chromophores with high molecular hyperpolarizabilities. *Tetrahedron Letters*, 45(16):3253 – 3256, 2004.

Philip A. Sullivan and Larry R. Dalton. Theory-inspired development of organic electro-optic materials. *Accounts of Chemical Research*, 43(1):10–18, 2010. PMID: 19663413.

Kyrill Yu. Suponitsky, Yi Liao, and Artëm E. Masunov. Electronic hyperpolarizabilities for donor-acceptor molecules with long conjugated bridges: Calculations versus experiment. *The Journal of Physical Chemistry A*, 113(41):10994–11001, 2009. PMID: 19772332.

S. Suresh, Huseyin Zengin, Bryan K. Spraul, Takafumi Sassa, Tatsuo Wada, and Dennis W. Smith Jr. Synthesis and hyperpolarizabilities of high temperature triarylamine-polyene chromophores. *Tetrahedron Letters*, 46(22):3913 – 3916, 2005.

David S. Surry and Stephen L. Buchwald. Dialkylbiaryl phosphines in pd-catalyzed amination: a user’s guide. *Chem. Sci.*, 2:27–50, 2011.

Jianmin Tao, John P. Perdew, Viktor N. Staroverov, and Gustavo E. Scuseria. Climbing the density functional ladder: Nonempirical meta<sup>g</sup> generalized gradient approximation designed for molecules and solids. *Phys. Rev. Lett.*, 91:146401, Sep 2003.

Bennett J. Tardiff, Robert McDonald, Michael J. Ferguson, and Mark Stradiotto. Rational and predictable chemoselective synthesis of oligoamines via buchwald–hartwig amination of (hetero)aryl chlorides employing mor-dalphos. *The Journal of Organic Chemistry*, 77(2):1056–1071, 2012. PMID: 22195727.

Marco Tarini, Paolo Cignoni, and Claudio Montani. Ambient occlusion and edge cueing for enhancing real time molecular visualization. *IEEE Transactions on Visualization and Computer Graphics*, 12(5):1237–1244, 2006.

C. C. Teng and H. T. Man. Simple reflection technique for measuring the electro-optic coefficient of poled polymers. *Applied Physics Letters*, 56(18):1734–1736, 1990.

S. Thayumanavan, Jeffrey Mendez, , and Seth R. Marder. Synthesis of functionalized organic second-order nonlinear optical chromophores for electrooptic applications. *The Journal of Organic Chemistry*, 64(12):4289–4297, 1999.

Bruce G. Tiemann, Lap-Tak Cheng, and Seth R. Marder. The effect of varying ground-state aromaticity on the first molecular electronic hyperpolarizabilities of organic donor-acceptor molecules. *J. Chem. Soc., Chem. Commun.*, pages 735–737, 1993.

Andreas F. Tillack. *Electro-Optic Material Design Criteria Derived from Condensed Matter Simulations Using the Level-of-Detail Coarse-Graining Approach*. PhD thesis, University of Washington, 2015.

Jacopo Tomasi, Benedetta Mennucci, and Roberto Cammi. Quantum mechanical continuum solvation models. *Chemical Reviews*, 105(8):2999–3094, 2005. PMID: 16092826.

Anthony S. Travis. Perkin’s mauve: Ancestor of the organic chemical industry. *Technology and Culture*, 31(1):51–82, 1990.

Hisao Uchiki and Takayoshi Kobayashi. New determination method of electro-optic constants and relevant nonlinear susceptibilities and its application to doped polymer. *Journal of Applied Physics*, 64(5):2625–2629, 1988.

Fritz Ullmann and Paul Sponagel. Ueber die phenylirung von phenolen. *Berichte der deutschen chemischen Gesellschaft*, 38(2):2211–2212, 1905.

J. F. WARD. Calculation of nonlinear optical susceptibilities using diagrammatic perturbation theory. *Rev. Mod. Phys.*, 37:1–18, Jan 1965.

Huajun Xu, Dan Yang, Fenggang Liu, Mingkai Fu, Shuhui Bo, Xinhou Liu, and Yuan Cao. Nonlinear optical chromophores based on Dewar's rules: enhancement of electro-optic activity by introducing heteroatoms into the donor or bridge. *Phys. Chem. Chem. Phys.*, 17:29679–29688, 2015.

Ergin Yalçın, Sylvain Achelle, Yasmina Bayrak, Nurgül Seferoğlu, Alberto Barsella, and Zeynel Seferoğlu. Styryl-based NLO chromophores: synthesis, spectroscopic properties, and theoretical calculations. *Tetrahedron Letters*, 56(20):2586 – 2589, 2015.

Takeshi Yanai, David P Tew, and Nicholas C Handy. A new hybrid exchange-correlation functional using the coulomb-attenuating method (cam-b3lyp). *Chemical Physics Letters*, 393(1-3):51 – 57, 2004.

Yuhui Yang, Jialei Liu, Maolin Zhang, Fenggang Liu, Haoran Wang, Shuhui Bo, Zhen Zhen, Ling Qiu, and Xinhou Liu. The important role of the location of the alkoxy group on the thiophene ring in designing efficient organic nonlinear optical materials based on double-donor chromophores. *J. Mater. Chem. C*, 3:3913–3921, 2015.

Yuhui Yang, Hongyan Xiao, Haoran Wang, Fenggang Liu, Shuhui Bo, Jialei Liu, Ling Qiu, Zhen Zhen, and Xinhou Liu. Synthesis and optical nonlinear properties of novel y-shaped chromophores with excellent electro-optic activity. *J. Mater. Chem. C*, 3:11423–11431, 2015.

Cheng Zhang, , Larry R. Dalton, Min-Cheol Oh, Hua Zhang, , and William H. Steier. Low  $v\pi$  electrooptic modulators from cld-1: Chromophore design and synthesis, material processing, and characterization. *Chemistry of Materials*, 13(9):3043–3050, 2001.

Cheng Zhang, Albert S. Ren, Fang Wang, Jingsong Zhu, Larry R. Dalton, J. N. Wood-



ford, and C. H. Wang. Synthesis and characterization of sterically stabilized second-order nonlinear optical chromophores. *Chemistry of Materials*, 11(8):1966–1968, 1999.

Cheng Zhang, Lianjie Zhang, Stephanie J. Benight, Benjamin C. Olbricht, Lewis E. Johnson, Bruce H. Robinson, Robert A. Norwood, and Larry R. Dalton. Shape engineering to promote head-tail interactions of electro-optic chromophores, 2013.

Yan Zhao, , and Donald G. Truhlar. Density functional for spectroscopy: No long-range self-interaction error, good performance for rydberg and charge-transfer states, and better performance on average than b3lyp for ground states. *The Journal of Physical Chemistry A*, 110(49):13126–13130, 2006. PMID: 17149824.

Yan Zhao and Donald G. Truhlar. The m06 suite of density functionals for main group thermochemistry, thermochemical kinetics, noncovalent interactions, excited states, and transition elements: two new functionals and systematic testing of four m06-class functionals and 12 other functionals. *Theoretical Chemistry Accounts*, 120(1):215–241, 2008.

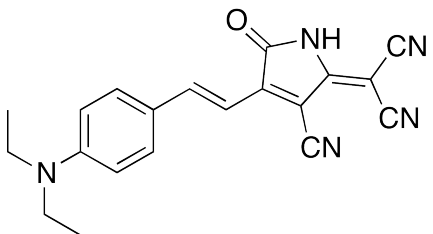
Paolo Zucca, Carla Vinci, Antonio Rescigno, Emil Dumitriu, and Enrico Sanjust. Is the bleaching of phenosafranine by hydrogen peroxide oxidation catalyzed by silica-supported 5,10,15,20-tetrakis-(sulfonatophenyl)porphine-mn(iii) really biomimetic? *Journal of Molecular Catalysis A: Chemical*, 321(1-2):27 – 33, 2010.

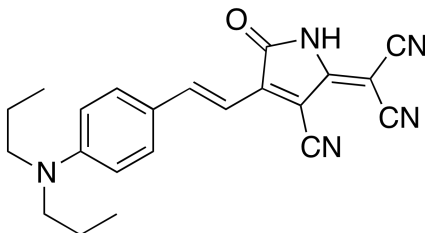
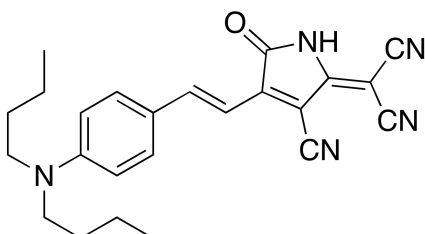
J. Zyss and J. L. Oudar. Relations between microscopic and macroscopic lowest-order optical nonlinearities of molecular crystals with one- or two-dimensional units. *Phys. Rev. A*, 26:2028–2048, Oct 1982.

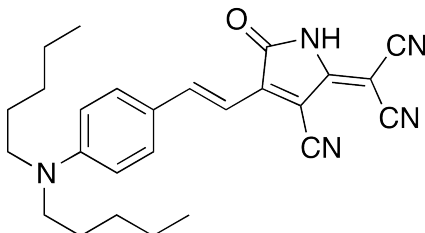
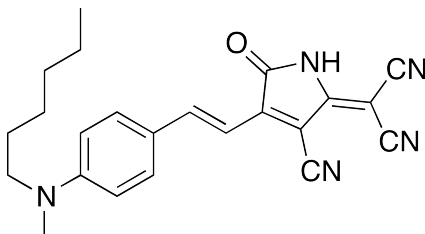
Joseph Zyss and Isabelle Ledoux. Nonlinear optics in multipolar media: theory and experiments. *Chemical Reviews*, 94(1):77–105, 1994.

## Appendix A

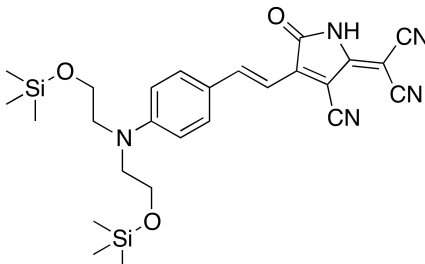
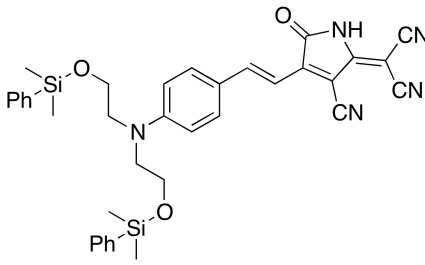
## COMPLETE STRUCTURES AND CALCULATED PROPERTIES

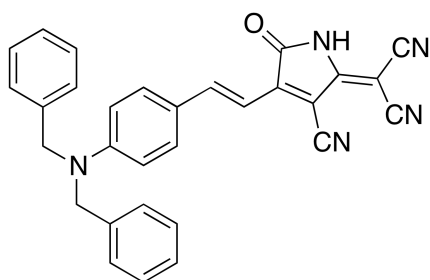
 <p style="text-align: center;">DA-00</p>	<i>Dipole</i>	14.9618	Debye
	<i>μβ</i>	1328.8084	$\times 10^{-48}$ esu
	<i>β<sub>HRS</sub></i>	64.3414	$\times 10^{-30}$ esu
	<i>β<sub>zzz</sub></i>	140.2909	$\times 10^{-30}$ esu
	<i>β<sub>avg</sub></i>	153.4608	$\times 10^{-30}$ esu
	<i>Dipole</i>	14.9620	Debye
<i>μβ</i>	3997.0782	$\times 10^{-48}$ esu	
<i>β<sub>HRS</sub></i>	193.2914	$\times 10^{-30}$ esu	
<i>β<sub>zzz</sub></i>	420.2842	$\times 10^{-30}$ esu	
	<i>β<sub>avg</sub></i>	461.7995	$\times 10^{-30}$ esu
	<i>Dipole</i>	14.9621	Debye
<i>μβ</i>	1374.4307	$\times 10^{-48}$ esu	
<i>β<sub>HRS</sub></i>	66.2848	$\times 10^{-30}$ esu	
<i>β<sub>zzz</sub></i>	145.2381	$\times 10^{-30}$ esu	
	<i>β<sub>avg</sub></i>	158.3922	$\times 10^{-30}$ esu
	<i>Dipole</i>	18.8429	Debye
<i>μβ</i>	5203.2717	$\times 10^{-48}$ esu	
<i>β<sub>HRS</sub></i>	199.7291	$\times 10^{-30}$ esu	
<i>β<sub>zzz</sub></i>	430.9754	$\times 10^{-30}$ esu	
	<i>β<sub>avg</sub></i>	478.2471	$\times 10^{-30}$ esu

 <p style="text-align: center;">DA-01</p>	<i>Dipole</i> $\mu\beta$ $\beta_{HRS}$ $\beta_{zzz}$ $\beta_{avg}$	14.5917 1414.2082 70.0630 151.9172 167.6915	Debye $\times 10^{-48}$ esu $\times 10^{-30}$ esu $\times 10^{-30}$ esu $\times 10^{-30}$ esu
	<i>Dipole</i> $\mu\beta$ $\beta_{HRS}$ $\beta_{zzz}$ $\beta_{avg}$	14.5915 4062.1252 201.1771 435.6815 481.6923	Debye $\times 10^{-48}$ esu $\times 10^{-30}$ esu $\times 10^{-30}$ esu $\times 10^{-30}$ esu
	<i>Dipole</i> $\mu\beta$ $\beta_{HRS}$ $\beta_{zzz}$ $\beta_{avg}$	14.5913 1465.2289 72.3444 157.5793 173.4139	Debye $\times 10^{-48}$ esu $\times 10^{-30}$ esu $\times 10^{-30}$ esu $\times 10^{-30}$ esu
	<i>Dipole</i> $\mu\beta$ $\beta_{HRS}$ $\beta_{zzz}$ $\beta_{avg}$	18.1961 5238.8422 208.2926 446.1836 499.6909	Debye $\times 10^{-48}$ esu $\times 10^{-30}$ esu $\times 10^{-30}$ esu $\times 10^{-30}$ esu
 <p style="text-align: center;">DA-02</p>	<i>Dipole</i> $\mu\beta$ $\beta_{HRS}$ $\beta_{zzz}$ $\beta_{avg}$	14.5174 1456.1930 72.5007 157.1621 173.5521	Debye $\times 10^{-48}$ esu $\times 10^{-30}$ esu $\times 10^{-30}$ esu $\times 10^{-30}$ esu
	<i>Dipole</i> $\mu\beta$ $\beta_{HRS}$ $\beta_{zzz}$ $\beta_{avg}$	14.5193 4082.2911 203.1949 439.8402 486.5401	Debye $\times 10^{-48}$ esu $\times 10^{-30}$ esu $\times 10^{-30}$ esu $\times 10^{-30}$ esu
	<i>Dipole</i> $\mu\beta$ $\beta_{HRS}$ $\beta_{zzz}$ $\beta_{avg}$	14.5190 1511.2841 74.9813 163.2701 179.7580	Debye $\times 10^{-48}$ esu $\times 10^{-30}$ esu $\times 10^{-30}$ esu $\times 10^{-30}$ esu
	<i>Dipole</i> $\mu\beta$ $\beta_{HRS}$ $\beta_{zzz}$ $\beta_{avg}$	18.0462 5248.5596 210.4882 450.2607 504.9729	Debye $\times 10^{-48}$ esu $\times 10^{-30}$ esu $\times 10^{-30}$ esu $\times 10^{-30}$ esu

 <p style="text-align: center;">DA-03</p>	<i>Dipole</i> $\mu\beta$ $\beta_{HRS}$ $\beta_{zzz}$ $\beta_{avg}$	14.7030 1482.3481 72.7728 158.0760 174.3112	Debye $\times 10^{-48}$ esu $\times 10^{-30}$ esu $\times 10^{-30}$ esu $\times 10^{-30}$ esu
	<i>Dipole</i> $\mu\beta$ $\beta_{HRS}$ $\beta_{zzz}$ $\beta_{avg}$	14.7022 4123.8707 202.5141 439.2655 485.0499	Debye $\times 10^{-48}$ esu $\times 10^{-30}$ esu $\times 10^{-30}$ esu $\times 10^{-30}$ esu
	<i>Dipole</i> $\mu\beta$ $\beta_{HRS}$ $\beta_{zzz}$ $\beta_{avg}$	14.7027 1537.2109 75.2194 164.1225 180.4299	Debye $\times 10^{-48}$ esu $\times 10^{-30}$ esu $\times 10^{-30}$ esu $\times 10^{-30}$ esu
	<i>Dipole</i> $\mu\beta$ $\beta_{HRS}$ $\beta_{zzz}$ $\beta_{avg}$	18.2476 5289.7988 209.6290 449.2077 503.0404	Debye $\times 10^{-48}$ esu $\times 10^{-30}$ esu $\times 10^{-30}$ esu $\times 10^{-30}$ esu
 <p style="text-align: center;">DA-04</p>	<i>Dipole</i> $\mu\beta$ $\beta_{HRS}$ $\beta_{zzz}$ $\beta_{avg}$	14.6320 1501.5863 74.0991 160.8698 177.4562	Debye $\times 10^{-48}$ esu $\times 10^{-30}$ esu $\times 10^{-30}$ esu $\times 10^{-30}$ esu
	<i>Dipole</i> $\mu\beta$ $\beta_{HRS}$ $\beta_{zzz}$ $\beta_{avg}$	14.6316 4148.3623 204.7623 443.9036 490.3604	Debye $\times 10^{-48}$ esu $\times 10^{-30}$ esu $\times 10^{-30}$ esu $\times 10^{-30}$ esu
	<i>Dipole</i> $\mu\beta$ $\beta_{HRS}$ $\beta_{zzz}$ $\beta_{avg}$	14.6324 1557.7532 76.6116 167.0676 183.7436	Debye $\times 10^{-48}$ esu $\times 10^{-30}$ esu $\times 10^{-30}$ esu $\times 10^{-30}$ esu
	<i>Dipole</i> $\mu\beta$ $\beta_{HRS}$ $\beta_{zzz}$ $\beta_{avg}$	18.1505 5317.6641 211.9352 453.7644 508.5156	Debye $\times 10^{-48}$ esu $\times 10^{-30}$ esu $\times 10^{-30}$ esu $\times 10^{-30}$ esu

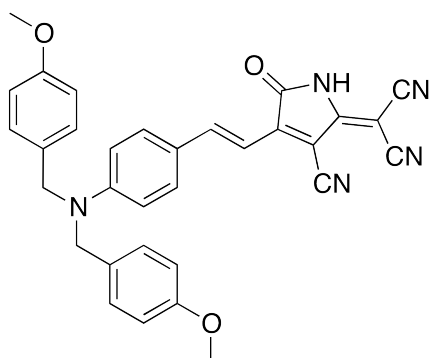
<p>DA-05</p>	<i>Dipole</i> $\mu\beta$ $\beta_{HRS}$ $\beta_{zzz}$ $\beta_{avg}$	16.8706 1527.7508 65.5450 142.9243 156.5167	Debye $\times 10^{-48}$ esu $\times 10^{-30}$ esu $\times 10^{-30}$ esu $\times 10^{-30}$ esu
	<i>Dipole</i> $\mu\beta$ $\beta_{HRS}$ $\beta_{zzz}$ $\beta_{avg}$	16.8696 4313.0492 184.5809 403.5118 441.2544	Debye $\times 10^{-48}$ esu $\times 10^{-30}$ esu $\times 10^{-30}$ esu $\times 10^{-30}$ esu
	<i>Dipole</i> $\mu\beta$ $\beta_{HRS}$ $\beta_{zzz}$ $\beta_{avg}$	16.8695 1578.3231 67.4855 147.7004 161.4280	Debye $\times 10^{-48}$ esu $\times 10^{-30}$ esu $\times 10^{-30}$ esu $\times 10^{-30}$ esu
	<i>Dipole</i> $\mu\beta$ $\beta_{HRS}$ $\beta_{zzz}$ $\beta_{avg}$	20.3227 5341.4210 190.5864 407.6723 456.5705	Debye $\times 10^{-48}$ esu $\times 10^{-30}$ esu $\times 10^{-30}$ esu $\times 10^{-30}$ esu
<p>DA-06</p>	<i>Dipole</i> $\mu\beta$ $\beta_{HRS}$ $\beta_{zzz}$ $\beta_{avg}$	16.4625 1553.2910 68.1739 150.0398 162.6032	Debye $\times 10^{-48}$ esu $\times 10^{-30}$ esu $\times 10^{-30}$ esu $\times 10^{-30}$ esu
	<i>Dipole</i> $\mu\beta$ $\beta_{HRS}$ $\beta_{zzz}$ $\beta_{avg}$	16.4632 4299.7875 188.0393 415.6387 449.1930	Debye $\times 10^{-48}$ esu $\times 10^{-30}$ esu $\times 10^{-30}$ esu $\times 10^{-30}$ esu
	<i>Dipole</i> $\mu\beta$ $\beta_{HRS}$ $\beta_{zzz}$ $\beta_{avg}$	16.4637 1601.0763 70.0171 154.6459 167.3032	Debye $\times 10^{-48}$ esu $\times 10^{-30}$ esu $\times 10^{-30}$ esu $\times 10^{-30}$ esu
	<i>Dipole</i> $\mu\beta$ $\beta_{HRS}$ $\beta_{zzz}$ $\beta_{avg}$	19.8448 5303.4050 193.3596 417.3568 462.8983	Debye $\times 10^{-48}$ esu $\times 10^{-30}$ esu $\times 10^{-30}$ esu $\times 10^{-30}$ esu

 <p style="text-align: center;">DA-07</p>	<i>Dipole</i> $\mu\beta$ $\beta_{HRS}$ $\beta_{zzz}$ $\beta_{avg}$	16.9389 1713.1778 73.1501 160.2791 174.5148	Debye $\times 10^{-48}$ esu $\times 10^{-30}$ esu $\times 10^{-30}$ esu $\times 10^{-30}$ esu
	<i>Dipole</i> $\mu\beta$ $\beta_{HRS}$ $\beta_{zzz}$ $\beta_{avg}$	16.9398 4584.5610 194.8771 430.1845 465.6230	Debye $\times 10^{-48}$ esu $\times 10^{-30}$ esu $\times 10^{-30}$ esu $\times 10^{-30}$ esu
	<i>Dipole</i> $\mu\beta$ $\beta_{HRS}$ $\beta_{zzz}$ $\beta_{avg}$	16.9394 1765.9128 75.1286 165.2705 179.5514	Debye $\times 10^{-48}$ esu $\times 10^{-30}$ esu $\times 10^{-30}$ esu $\times 10^{-30}$ esu
	<i>Dipole</i> $\mu\beta$ $\beta_{HRS}$ $\beta_{zzz}$ $\beta_{avg}$	20.3548 5631.7314 200.2823 431.2397 479.5746	Debye $\times 10^{-48}$ esu $\times 10^{-30}$ esu $\times 10^{-30}$ esu $\times 10^{-30}$ esu
 <p style="text-align: center;">DA-08</p>	<i>Dipole</i> $\mu\beta$ $\beta_{HRS}$ $\beta_{zzz}$ $\beta_{avg}$	17.2598 1870.9165 78.1912 171.5972 186.8726	Debye $\times 10^{-48}$ esu $\times 10^{-30}$ esu $\times 10^{-30}$ esu $\times 10^{-30}$ esu
	<i>Dipole</i> $\mu\beta$ $\beta_{HRS}$ $\beta_{zzz}$ $\beta_{avg}$	17.2606 4765.8374 198.5617 438.9478 474.7319	Debye $\times 10^{-48}$ esu $\times 10^{-30}$ esu $\times 10^{-30}$ esu $\times 10^{-30}$ esu
	<i>Dipole</i> $\mu\beta$ $\beta_{HRS}$ $\beta_{zzz}$ $\beta_{avg}$	17.2605 1926.0903 80.2582 176.7565 192.1021	Debye $\times 10^{-48}$ esu $\times 10^{-30}$ esu $\times 10^{-30}$ esu $\times 10^{-30}$ esu
	<i>Dipole</i> $\mu\beta$ $\beta_{HRS}$ $\beta_{zzz}$ $\beta_{avg}$	20.4437 5752.6617 203.6109 438.2575 487.7877	Debye $\times 10^{-48}$ esu $\times 10^{-30}$ esu $\times 10^{-30}$ esu $\times 10^{-30}$ esu



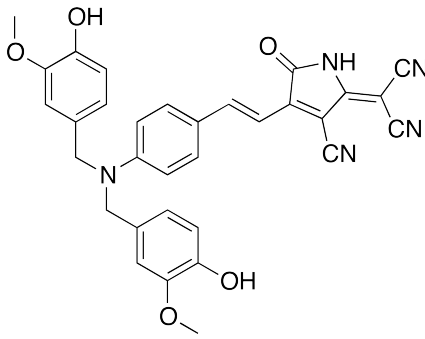
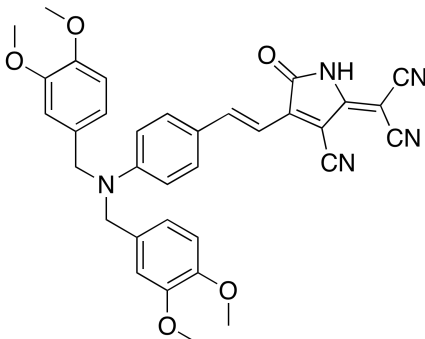
DA-09

<i>cam-b3lyp</i> (vacuo)	<i>Dipole</i>	14.7789	Debye
	$\mu\beta$	1515.1215	$\times 10^{-48}$ esu
	$\beta_{HRS}$	74.5805	$\times 10^{-30}$ esu
	$\beta_{zzz}$	160.0986	$\times 10^{-30}$ esu
	$\beta_{avg}$	178.0743	$\times 10^{-30}$ esu
<i>cam-b3lyp</i> (chloroform)	<i>Dipole</i>	14.7793	Debye
	$\mu\beta$	3913.0292	$\times 10^{-48}$ esu
	$\beta_{HRS}$	191.6849	$\times 10^{-30}$ esu
	$\beta_{zzz}$	416.0459	$\times 10^{-30}$ esu
	$\beta_{avg}$	457.9881	$\times 10^{-30}$ esu
$\Psi_{00}^{00}$	<i>Dipole</i>	14.7796	Debye
	$\mu\beta$	1564.7854	$\times 10^{-48}$ esu
	$\beta_{HRS}$	76.7509	$\times 10^{-30}$ esu
	$\beta_{zzz}$	165.3658	$\times 10^{-30}$ esu
	$\beta_{avg}$	183.5942	$\times 10^{-30}$ esu
<i>m062x</i> (chloroform)	<i>Dipole</i>	17.8511	Debye
	$\mu\beta$	4818.2132	$\times 10^{-48}$ esu
	$\beta_{HRS}$	197.0283	$\times 10^{-30}$ esu
	$\beta_{zzz}$	413.3774	$\times 10^{-30}$ esu
	$\beta_{avg}$	471.8021	$\times 10^{-30}$ esu

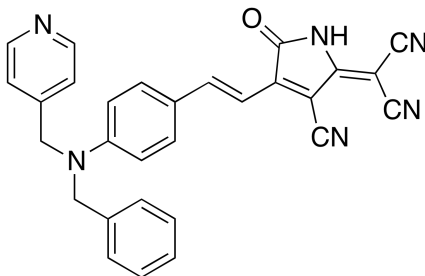
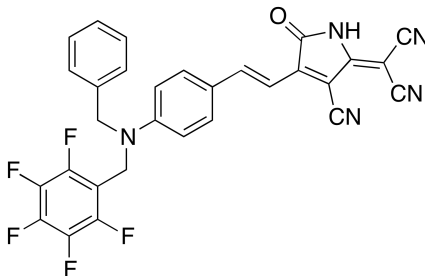


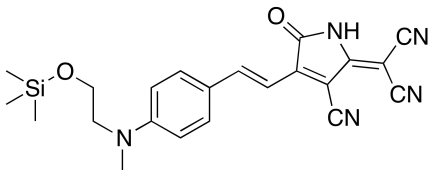
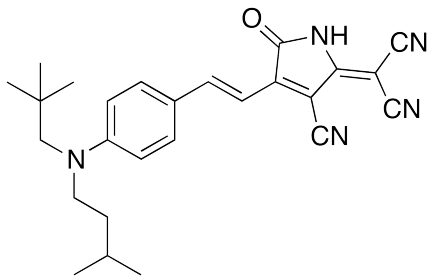
DA-10

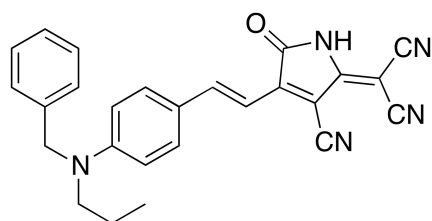
<i>cam-b3lyp</i> (vacuo)	<i>Dipole</i>	16.5376	Debye
	$\mu\beta$	1874.2067	$\times 10^{-48}$ esu
	$\beta_{HRS}$	81.3779	$\times 10^{-30}$ esu
	$\beta_{zzz}$	181.7489	$\times 10^{-30}$ esu
	$\beta_{avg}$	194.7211	$\times 10^{-30}$ esu
<i>cam-b3lyp</i> (chloroform)	<i>Dipole</i>	16.5369	Debye
	$\mu\beta$	4701.3902	$\times 10^{-48}$ esu
	$\beta_{HRS}$	203.0983	$\times 10^{-30}$ esu
	$\beta_{zzz}$	460.0917	$\times 10^{-30}$ esu
	$\beta_{avg}$	485.6811	$\times 10^{-30}$ esu
$\Psi_{00}^{00}$	<i>Dipole</i>	16.5360	Debye
	$\mu\beta$	1930.0207	$\times 10^{-48}$ esu
	$\beta_{HRS}$	83.5674	$\times 10^{-30}$ esu
	$\beta_{zzz}$	187.0380	$\times 10^{-30}$ esu
	$\beta_{avg}$	200.2760	$\times 10^{-30}$ esu
<i>m062x</i> (chloroform)	<i>Dipole</i>	19.6513	Debye
	$\mu\beta$	5683.8388	$\times 10^{-48}$ esu
	$\beta_{HRS}$	208.4333	$\times 10^{-30}$ esu
	$\beta_{zzz}$	456.2199	$\times 10^{-30}$ esu
	$\beta_{avg}$	499.4972	$\times 10^{-30}$ esu

 <p style="text-align: center;">DA-11</p>	<p><i>Dipole</i> 16.2879 Debye</p> <p><math>\mu\beta</math> 1969.4105 <math>\times 10^{-48}</math> esu</p> <p><math>\beta_{HRS}</math> 88.8068 <math>\times 10^{-30}</math> esu</p> <p><math>\beta_{zzz}</math> 180.5505 <math>\times 10^{-30}</math> esu</p> <p><math>\beta_{avg}</math> 214.0023 <math>\times 10^{-30}</math> esu</p>
	<p><i>Dipole</i> 16.2871 Debye</p> <p><math>\mu\beta</math> 4760.3430 <math>\times 10^{-48}</math> esu</p> <p><math>\beta_{HRS}</math> 214.1472 <math>\times 10^{-30}</math> esu</p> <p><math>\beta_{zzz}</math> 440.0002 <math>\times 10^{-30}</math> esu</p> <p><math>\beta_{avg}</math> 515.0611 <math>\times 10^{-30}</math> esu</p>
	<p><i>Dipole</i> 16.2874 Debye</p> <p><math>\mu\beta</math> 2041.4619 <math>\times 10^{-48}</math> esu</p> <p><math>\beta_{HRS}</math> 91.8912 <math>\times 10^{-30}</math> esu</p> <p><math>\beta_{zzz}</math> 187.0830 <math>\times 10^{-30}</math> esu</p> <p><math>\beta_{avg}</math> 221.6647 <math>\times 10^{-30}</math> esu</p>
	<p><i>Dipole</i> 19.2386 Debye</p> <p><math>\mu\beta</math> 5780.4880 <math>\times 10^{-48}</math> esu</p> <p><math>\beta_{HRS}</math> 221.3332 <math>\times 10^{-30}</math> esu</p> <p><math>\beta_{zzz}</math> 444.7866 <math>\times 10^{-30}</math> esu</p> <p><math>\beta_{avg}</math> 533.1746 <math>\times 10^{-30}</math> esu</p>
 <p style="text-align: center;">DA-12</p>	<p><i>Dipole</i> 15.8689 Debye</p> <p><math>\mu\beta</math> 1988.4582 <math>\times 10^{-48}</math> esu</p> <p><math>\beta_{HRS}</math> 90.6030 <math>\times 10^{-30}</math> esu</p> <p><math>\beta_{zzz}</math> 193.2379 <math>\times 10^{-30}</math> esu</p> <p><math>\beta_{avg}</math> 218.0783 <math>\times 10^{-30}</math> esu</p>
	<p><i>Dipole</i> 15.8704 Debye</p> <p><math>\mu\beta</math> 4731.8102 <math>\times 10^{-48}</math> esu</p> <p><math>\beta_{HRS}</math> 215.1258 <math>\times 10^{-30}</math> esu</p> <p><math>\beta_{zzz}</math> 463.5461 <math>\times 10^{-30}</math> esu</p> <p><math>\beta_{avg}</math> 517.0113 <math>\times 10^{-30}</math> esu</p>
	<p><i>Dipole</i> 15.8710 Debye</p> <p><math>\mu\beta</math> 2059.0105 <math>\times 10^{-48}</math> esu</p> <p><math>\beta_{HRS}</math> 93.6474 <math>\times 10^{-30}</math> esu</p> <p><math>\beta_{zzz}</math> 199.8795 <math>\times 10^{-30}</math> esu</p> <p><math>\beta_{avg}</math> 225.6413 <math>\times 10^{-30}</math> esu</p>
	<p><i>Dipole</i> 18.4968 Debye</p> <p><math>\mu\beta</math> 5662.3652 <math>\times 10^{-48}</math> esu</p> <p><math>\beta_{HRS}</math> 222.1085 <math>\times 10^{-30}</math> esu</p> <p><math>\beta_{zzz}</math> 467.6866 <math>\times 10^{-30}</math> esu</p> <p><math>\beta_{avg}</math> 534.6357 <math>\times 10^{-30}</math> esu</p>



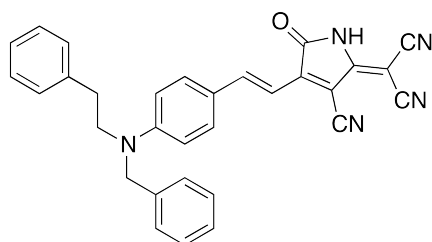
 <p style="text-align: center;">DA-13</p>	<i>Dipole</i> $\mu\beta$ $\beta_{HRS}$ $\beta_{zzz}$ $\beta_{avg}$	14.4870 1311.6766 70.2581 123.4936 167.7809	Debye $\times 10^{-48}$ esu $\times 10^{-30}$ esu $\times 10^{-30}$ esu $\times 10^{-30}$ esu
	<i>Dipole</i> $\mu\beta$ $\beta_{HRS}$ $\beta_{zzz}$ $\beta_{avg}$	14.4851 3369.6848 178.9696 321.3591 427.6870	Debye $\times 10^{-48}$ esu $\times 10^{-30}$ esu $\times 10^{-30}$ esu $\times 10^{-30}$ esu
	<i>Dipole</i> $\mu\beta$ $\beta_{HRS}$ $\beta_{zzz}$ $\beta_{avg}$	14.4840 1356.8902 72.3827 128.1106 173.1664	Debye $\times 10^{-48}$ esu $\times 10^{-30}$ esu $\times 10^{-30}$ esu $\times 10^{-30}$ esu
	<i>Dipole</i> $\mu\beta$ $\beta_{HRS}$ $\beta_{zzz}$ $\beta_{avg}$	17.7065 4178.4737 184.0426 314.4412 440.7609	Debye $\times 10^{-48}$ esu $\times 10^{-30}$ esu $\times 10^{-30}$ esu $\times 10^{-30}$ esu
 <p style="text-align: center;">DA-14</p>	<i>Dipole</i> $\mu\beta$ $\beta_{HRS}$ $\beta_{zzz}$ $\beta_{avg}$	14.0479 1255.0671 66.8228 130.8993 159.9242	Debye $\times 10^{-48}$ esu $\times 10^{-30}$ esu $\times 10^{-30}$ esu $\times 10^{-30}$ esu
	<i>Dipole</i> $\mu\beta$ $\beta_{HRS}$ $\beta_{zzz}$ $\beta_{avg}$	14.0490 3222.2927 170.5644 339.1578 408.1701	Debye $\times 10^{-48}$ esu $\times 10^{-30}$ esu $\times 10^{-30}$ esu $\times 10^{-30}$ esu
	<i>Dipole</i> $\mu\beta$ $\beta_{HRS}$ $\beta_{zzz}$ $\beta_{avg}$	14.0493 1294.7953 68.6697 135.2333 164.5961	Debye $\times 10^{-48}$ esu $\times 10^{-30}$ esu $\times 10^{-30}$ esu $\times 10^{-30}$ esu
	<i>Dipole</i> $\mu\beta$ $\beta_{HRS}$ $\beta_{zzz}$ $\beta_{avg}$	17.1330 4014.1631 174.7832 341.5018 419.0955	Debye $\times 10^{-48}$ esu $\times 10^{-30}$ esu $\times 10^{-30}$ esu $\times 10^{-30}$ esu

 <p style="text-align: center;">DA-15</p>	<i>Dipole</i> $\mu\beta$ $\beta_{HRS}$ $\beta_{zzz}$ $\beta_{avg}$	15.4556 1406.2311 67.0141 138.6888 159.9679	Debye $\times 10^{-48}$ esu $\times 10^{-30}$ esu $\times 10^{-30}$ esu $\times 10^{-30}$ esu
	<i>Dipole</i> $\mu\beta$ $\beta_{HRS}$ $\beta_{zzz}$ $\beta_{avg}$	15.4557 4067.7864 194.0138 398.1825 463.6440	Debye $\times 10^{-48}$ esu $\times 10^{-30}$ esu $\times 10^{-30}$ esu $\times 10^{-30}$ esu
	<i>Dipole</i> $\mu\beta$ $\beta_{HRS}$ $\beta_{zzz}$ $\beta_{avg}$	15.4562 1449.8994 68.7950 143.3699 164.4888	Debye $\times 10^{-48}$ esu $\times 10^{-30}$ esu $\times 10^{-30}$ esu $\times 10^{-30}$ esu
	<i>Dipole</i> $\mu\beta$ $\beta_{HRS}$ $\beta_{zzz}$ $\beta_{avg}$	19.1020 5168.1171 199.5796 405.4728 477.9506	Debye $\times 10^{-48}$ esu $\times 10^{-30}$ esu $\times 10^{-30}$ esu $\times 10^{-30}$ esu
 <p style="text-align: center;">DA-16</p>	<i>Dipole</i> $\mu\beta$ $\beta_{HRS}$ $\beta_{zzz}$ $\beta_{avg}$	15.3365 1577.5544 74.0875 163.0700 177.1593	Debye $\times 10^{-48}$ esu $\times 10^{-30}$ esu $\times 10^{-30}$ esu $\times 10^{-30}$ esu
	<i>Dipole</i> $\mu\beta$ $\beta_{HRS}$ $\beta_{zzz}$ $\beta_{avg}$	15.3382 4396.9005 206.2888 454.0170 493.5632	Debye $\times 10^{-48}$ esu $\times 10^{-30}$ esu $\times 10^{-30}$ esu $\times 10^{-30}$ esu
	<i>Dipole</i> $\mu\beta$ $\beta_{HRS}$ $\beta_{zzz}$ $\beta_{avg}$	15.3387 1632.7767 76.4177 168.8913 183.0115	Debye $\times 10^{-48}$ esu $\times 10^{-30}$ esu $\times 10^{-30}$ esu $\times 10^{-30}$ esu
	<i>Dipole</i> $\mu\beta$ $\beta_{HRS}$ $\beta_{zzz}$ $\beta_{avg}$	19.1051 5643.3849 212.9616 462.3110 510.5826	Debye $\times 10^{-48}$ esu $\times 10^{-30}$ esu $\times 10^{-30}$ esu $\times 10^{-30}$ esu



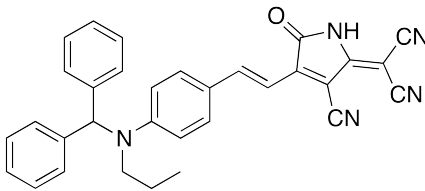
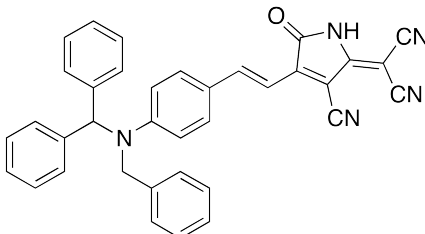
DA-17

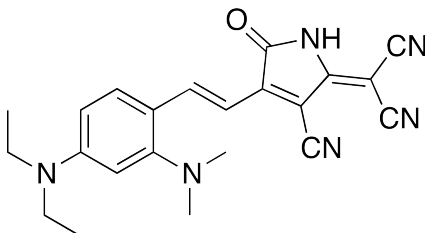
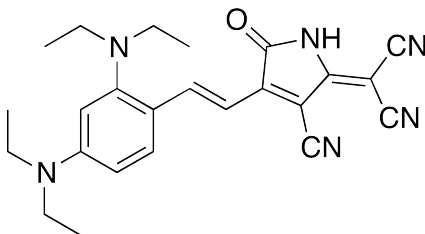
<i>cam-b3lyp</i> (vacuo)	<i>Dipole</i>	14.6320	Debye
	$\mu\beta$	1412.2094	$\times 10^{-48}$ esu
	$\beta_{HRS}$	70.1039	$\times 10^{-30}$ esu
	$\beta_{zzz}$	150.2747	$\times 10^{-30}$ esu
	$\beta_{avg}$	167.6031	$\times 10^{-30}$ esu
<i>cam-b3lyp</i> (chloroform)	<i>Dipole</i>	14.6325	Debye
	$\mu\beta$	3833.9712	$\times 10^{-48}$ esu
	$\beta_{HRS}$	189.8317	$\times 10^{-30}$ esu
	$\beta_{zzz}$	409.3118	$\times 10^{-30}$ esu
	$\beta_{avg}$	454.0291	$\times 10^{-30}$ esu
$\Psi_{0f}^{0f}$	<i>Dipole</i>	14.6321	Debye
	$\mu\beta$	1458.7988	$\times 10^{-48}$ esu
	$\beta_{HRS}$	72.1636	$\times 10^{-30}$ esu
	$\beta_{zzz}$	155.3631	$\times 10^{-30}$ esu
	$\beta_{avg}$	172.8196	$\times 10^{-30}$ esu
<i>m062x</i> (chloroform)	<i>Dipole</i>	18.0060	Debye
	$\mu\beta$	4834.3929	$\times 10^{-48}$ esu
	$\beta_{HRS}$	195.2835	$\times 10^{-30}$ esu
	$\beta_{zzz}$	412.6556	$\times 10^{-30}$ esu
	$\beta_{avg}$	468.0561	$\times 10^{-30}$ esu

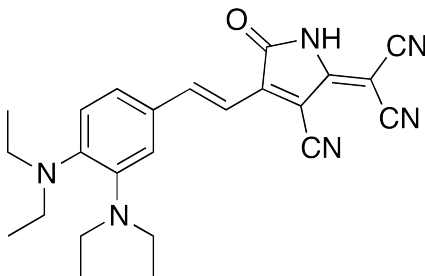
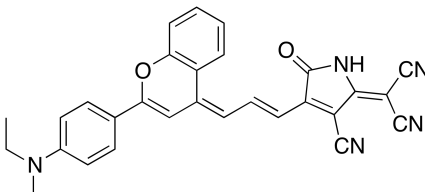


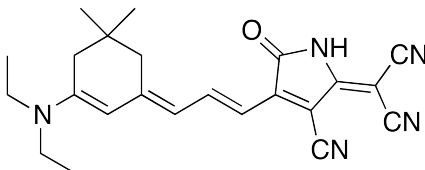
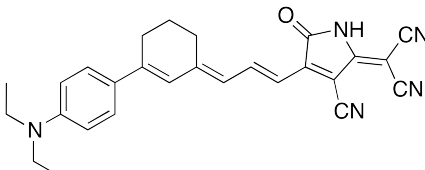
DA-18

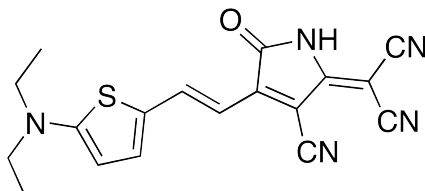
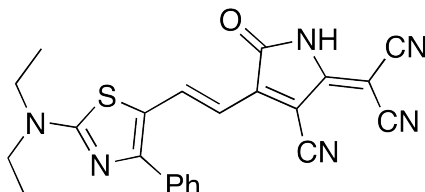
<i>cam-b3lyp</i> (vacuo)	<i>Dipole</i>	14.5505	Debye
	$\mu\beta$	1493.3353	$\times 10^{-48}$ esu
	$\beta_{HRS}$	74.3248	$\times 10^{-30}$ esu
	$\beta_{zzz}$	161.7415	$\times 10^{-30}$ esu
	$\beta_{avg}$	177.3623	$\times 10^{-30}$ esu
<i>cam-b3lyp</i> (chloroform)	<i>Dipole</i>	14.5514	Debye
	$\mu\beta$	3928.2494	$\times 10^{-48}$ esu
	$\beta_{HRS}$	195.0271	$\times 10^{-30}$ esu
	$\beta_{zzz}$	425.4445	$\times 10^{-30}$ esu
	$\beta_{avg}$	466.0347	$\times 10^{-30}$ esu
$\Psi_{0f}^{0f}$	<i>Dipole</i>	14.5517	Debye
	$\mu\beta$	1548.2303	$\times 10^{-48}$ esu
	$\beta_{HRS}$	76.7882	$\times 10^{-30}$ esu
	$\beta_{zzz}$	167.6708	$\times 10^{-30}$ esu
	$\beta_{avg}$	183.5781	$\times 10^{-30}$ esu
<i>m062x</i> (chloroform)	<i>Dipole</i>	17.8270	Debye
	$\mu\beta$	4945.5100	$\times 10^{-48}$ esu
	$\beta_{HRS}$	201.3345	$\times 10^{-30}$ esu
	$\beta_{zzz}$	429.3140	$\times 10^{-30}$ esu
	$\beta_{avg}$	482.1793	$\times 10^{-30}$ esu

 <p style="text-align: center;">DA-19</p>	<i>Dipole</i> $\mu\beta$ $\beta_{HRS}$ $\beta_{zzz}$ $\beta_{avg}$	14.7700 1466.1214 72.4306 153.8601 172.9231	Debye $\times 10^{-48}$ esu $\times 10^{-30}$ esu $\times 10^{-30}$ esu $\times 10^{-30}$ esu
	<i>Dipole</i> $\mu\beta$ $\beta_{HRS}$ $\beta_{zzz}$ $\beta_{avg}$	14.7696 3838.6384 188.5387 406.4311 450.4722	Debye $\times 10^{-48}$ esu $\times 10^{-30}$ esu $\times 10^{-30}$ esu $\times 10^{-30}$ esu
	<i>Dipole</i> $\mu\beta$ $\beta_{HRS}$ $\beta_{zzz}$ $\beta_{avg}$	14.7696 1510.6620 74.3782 158.5867 177.9000	Debye $\times 10^{-48}$ esu $\times 10^{-30}$ esu $\times 10^{-30}$ esu $\times 10^{-30}$ esu
	<i>Dipole</i> $\mu\beta$ $\beta_{HRS}$ $\beta_{zzz}$ $\beta_{avg}$	18.0712 4776.7247 193.4070 402.5404 463.1409	Debye $\times 10^{-48}$ esu $\times 10^{-30}$ esu $\times 10^{-30}$ esu $\times 10^{-30}$ esu
 <p style="text-align: center;">DA-20</p>	<i>Dipole</i> $\mu\beta$ $\beta_{HRS}$ $\beta_{zzz}$ $\beta_{avg}$	15.1932 1609.0046 76.7105 166.5638 183.2432	Debye $\times 10^{-48}$ esu $\times 10^{-30}$ esu $\times 10^{-30}$ esu $\times 10^{-30}$ esu
	<i>Dipole</i> $\mu\beta$ $\beta_{HRS}$ $\beta_{zzz}$ $\beta_{avg}$	14.6028 3842.3321 190.1035 414.7047 454.3519	Debye $\times 10^{-48}$ esu $\times 10^{-30}$ esu $\times 10^{-30}$ esu $\times 10^{-30}$ esu
	<i>Dipole</i> $\mu\beta$ $\beta_{HRS}$ $\beta_{zzz}$ $\beta_{avg}$	14.6027 1590.5472 78.8343 170.2475 188.6832	Debye $\times 10^{-48}$ esu $\times 10^{-30}$ esu $\times 10^{-30}$ esu $\times 10^{-30}$ esu
	<i>Dipole</i> $\mu\beta$ $\beta_{HRS}$ $\beta_{zzz}$ $\beta_{avg}$	17.5423 4681.7654 194.8463 407.8910 466.7664	Debye $\times 10^{-48}$ esu $\times 10^{-30}$ esu $\times 10^{-30}$ esu $\times 10^{-30}$ esu

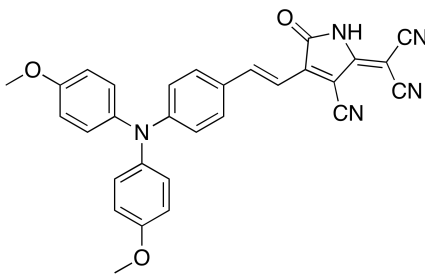
 <p style="text-align: center;">DA-21</p>	<i>Dipole</i> $\mu\beta$ $\beta_{HRS}$ $\beta_{zzz}$ $\beta_{avg}$	15.8301 1216.9027 55.1080 124.8018 131.4031	Debye $\times 10^{-48}$ esu $\times 10^{-30}$ esu $\times 10^{-30}$ esu $\times 10^{-30}$ esu
	<i>Dipole</i> $\mu\beta$ $\beta_{HRS}$ $\beta_{zzz}$ $\beta_{avg}$	15.8307 3560.9770 161.1272 363.0158 384.8403	Debye $\times 10^{-48}$ esu $\times 10^{-30}$ esu $\times 10^{-30}$ esu $\times 10^{-30}$ esu
	<i>Dipole</i> $\mu\beta$ $\beta_{HRS}$ $\beta_{zzz}$ $\beta_{avg}$	15.8311 1254.5323 56.5257 128.7675 135.0903	Debye $\times 10^{-48}$ esu $\times 10^{-30}$ esu $\times 10^{-30}$ esu $\times 10^{-30}$ esu
	<i>Dipole</i> $\mu\beta$ $\beta_{HRS}$ $\beta_{zzz}$ $\beta_{avg}$	20.2190 4700.2964 166.1792 372.4896 398.0388	Debye $\times 10^{-48}$ esu $\times 10^{-30}$ esu $\times 10^{-30}$ esu $\times 10^{-30}$ esu
 <p style="text-align: center;">DA-22</p>	<i>Dipole</i> $\mu\beta$ $\beta_{HRS}$ $\beta_{zzz}$ $\beta_{avg}$	16.0032 1240.5364 56.9910 117.5910 135.8666	Debye $\times 10^{-48}$ esu $\times 10^{-30}$ esu $\times 10^{-30}$ esu $\times 10^{-30}$ esu
	<i>Dipole</i> $\mu\beta$ $\beta_{HRS}$ $\beta_{zzz}$ $\beta_{avg}$	16.0040 3696.2493 170.5489 344.6027 407.3617	Debye $\times 10^{-48}$ esu $\times 10^{-30}$ esu $\times 10^{-30}$ esu $\times 10^{-30}$ esu
	<i>Dipole</i> $\mu\beta$ $\beta_{HRS}$ $\beta_{zzz}$ $\beta_{avg}$	16.0038 1284.7343 58.7092 122.0356 140.3051	Debye $\times 10^{-48}$ esu $\times 10^{-30}$ esu $\times 10^{-30}$ esu $\times 10^{-30}$ esu
	<i>Dipole</i> $\mu\beta$ $\beta_{HRS}$ $\beta_{zzz}$ $\beta_{avg}$	20.4389 4925.0752 176.9913 360.0533 423.9278	Debye $\times 10^{-48}$ esu $\times 10^{-30}$ esu $\times 10^{-30}$ esu $\times 10^{-30}$ esu

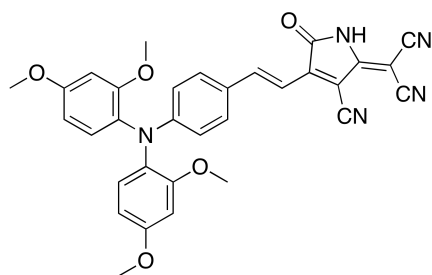
 <p style="text-align: center;">DA-23</p>	<i>Dipole</i> 12.7793 Debye $\mu\beta$ 1190.6438 $\times 10^{-48}$ esu $\beta_{HRS}$ 67.9149 $\times 10^{-30}$ esu $\beta_{zzz}$ 145.5862 $\times 10^{-30}$ esu $\beta_{avg}$ 162.0317 $\times 10^{-30}$ esu
	<i>Dipole</i> 12.7791 Debye $\mu\beta$ 3395.7418 $\times 10^{-48}$ esu $\beta_{HRS}$ 192.4842 $\times 10^{-30}$ esu $\beta_{zzz}$ 417.0472 $\times 10^{-30}$ esu $\beta_{avg}$ 460.0718 $\times 10^{-30}$ esu
	<i>Dipole</i> 12.7787 Debye $\mu\beta$ 1226.2707 $\times 10^{-48}$ esu $\beta_{HRS}$ 69.6865 $\times 10^{-30}$ esu $\beta_{zzz}$ 150.0542 $\times 10^{-30}$ esu $\beta_{avg}$ 166.5386 $\times 10^{-30}$ esu
	<i>Dipole</i> 15.8947 Debye $\mu\beta$ 4319.4549 $\times 10^{-48}$ esu $\beta_{HRS}$ 197.9204 $\times 10^{-30}$ esu $\beta_{zzz}$ 418.4359 $\times 10^{-30}$ esu $\beta_{avg}$ 474.0051 $\times 10^{-30}$ esu
 <p style="text-align: center;">DA-25</p>	<i>Dipole</i> 20.6622 Debye $\mu\beta$ 3075.1664 $\times 10^{-48}$ esu $\beta_{HRS}$ 112.8118 $\times 10^{-30}$ esu $\beta_{zzz}$ 214.6521 $\times 10^{-30}$ esu $\beta_{avg}$ 268.0687 $\times 10^{-30}$ esu
	<i>Dipole</i> 20.6611 Debye $\mu\beta$ 7509.5192 $\times 10^{-48}$ esu $\beta_{HRS}$ 296.4501 $\times 10^{-30}$ esu $\beta_{zzz}$ 504.8690 $\times 10^{-30}$ esu $\beta_{avg}$ 683.4432 $\times 10^{-30}$ esu
	<i>Dipole</i> 20.6612 Debye $\mu\beta$ 3320.5914 $\times 10^{-48}$ esu $\beta_{HRS}$ 119.7325 $\times 10^{-30}$ esu $\beta_{zzz}$ 233.0507 $\times 10^{-30}$ esu $\beta_{avg}$ 286.7732 $\times 10^{-30}$ esu
	<i>Dipole</i> 26.8849 Debye $\mu\beta$ 11308.7372 $\times 10^{-48}$ esu $\beta_{HRS}$ 329.1760 $\times 10^{-30}$ esu $\beta_{zzz}$ 586.8748 $\times 10^{-30}$ esu $\beta_{avg}$ 774.5636 $\times 10^{-30}$ esu

 <p style="text-align: center;">DA-24</p>	<i>Dipole</i> $\mu\beta$ $\beta_{HRS}$ $\beta_{zzz}$ $\beta_{avg}$	21.5320 1388.9019 50.4625 95.3157 117.5122	Debye $\times 10^{-48}$ esu $\times 10^{-30}$ esu $\times 10^{-30}$ esu $\times 10^{-30}$ esu
	<i>Dipole</i> $\mu\beta$ $\beta_{HRS}$ $\beta_{zzz}$ $\beta_{avg}$	21.5318 1745.1302 94.0341 91.3983 192.5457	Debye $\times 10^{-48}$ esu $\times 10^{-30}$ esu $\times 10^{-30}$ esu $\times 10^{-30}$ esu
	<i>Dipole</i> $\mu\beta$ $\beta_{HRS}$ $\beta_{zzz}$ $\beta_{avg}$	21.5323 1514.6575 53.4684 105.5676 125.9054	Debye $\times 10^{-48}$ esu $\times 10^{-30}$ esu $\times 10^{-30}$ esu $\times 10^{-30}$ esu
	<i>Dipole</i> $\mu\beta$ $\beta_{HRS}$ $\beta_{zzz}$ $\beta_{avg}$	29.5587 3119.1572 101.5433 134.8966 220.2002	Debye $\times 10^{-48}$ esu $\times 10^{-30}$ esu $\times 10^{-30}$ esu $\times 10^{-30}$ esu
 <p style="text-align: center;">DA-26</p>	<i>Dipole</i> $\mu\beta$ $\beta_{HRS}$ $\beta_{zzz}$ $\beta_{avg}$	18.2114 4400.4608 174.8114 372.5279 420.0797	Debye $\times 10^{-48}$ esu $\times 10^{-30}$ esu $\times 10^{-30}$ esu $\times 10^{-30}$ esu
	<i>Dipole</i> $\mu\beta$ $\beta_{HRS}$ $\beta_{zzz}$ $\beta_{avg}$	18.2122 14034.8958 556.8620 1193.3208 1337.5658	Debye $\times 10^{-48}$ esu $\times 10^{-30}$ esu $\times 10^{-30}$ esu $\times 10^{-30}$ esu
	<i>Dipole</i> $\mu\beta$ $\beta_{HRS}$ $\beta_{zzz}$ $\beta_{avg}$	18.2120 4707.4358 186.3468 398.5585 448.6461	Debye $\times 10^{-48}$ esu $\times 10^{-30}$ esu $\times 10^{-30}$ esu $\times 10^{-30}$ esu
	<i>Dipole</i> $\mu\beta$ $\beta_{HRS}$ $\beta_{zzz}$ $\beta_{avg}$	23.1126 19155.4907 599.4357 1269.4755 1443.2913	Debye $\times 10^{-48}$ esu $\times 10^{-30}$ esu $\times 10^{-30}$ esu $\times 10^{-30}$ esu

 <p style="text-align: center;">DA-27</p>	<i>Dipole</i> $\mu\beta$ $\beta_{HRS}$ $\beta_{zzz}$ $\beta_{avg}$	16.6385 1041.9628 46.5866 98.1978 109.7311	Debye $\times 10^{-48}$ esu $\times 10^{-30}$ esu $\times 10^{-30}$ esu $\times 10^{-30}$ esu
	<i>Dipole</i> $\mu\beta$ $\beta_{HRS}$ $\beta_{zzz}$ $\beta_{avg}$	16.6380 2780.2837 127.8902 258.1782 297.9029	Debye $\times 10^{-48}$ esu $\times 10^{-30}$ esu $\times 10^{-30}$ esu $\times 10^{-30}$ esu
	<i>Dipole</i> $\mu\beta$ $\beta_{HRS}$ $\beta_{zzz}$ $\beta_{avg}$	16.6377 1074.3517 47.5727 101.3833 112.5717	Debye $\times 10^{-48}$ esu $\times 10^{-30}$ esu $\times 10^{-30}$ esu $\times 10^{-30}$ esu
	<i>Dipole</i> $\mu\beta$ $\beta_{HRS}$ $\beta_{zzz}$ $\beta_{avg}$	21.9488 3818.2902 131.5545 266.0206 309.0472	Debye $\times 10^{-48}$ esu $\times 10^{-30}$ esu $\times 10^{-30}$ esu $\times 10^{-30}$ esu
 <p style="text-align: center;">DA-28</p>	<i>Dipole</i> $\mu\beta$ $\beta_{HRS}$ $\beta_{zzz}$ $\beta_{avg}$	14.2601 779.1824 38.8388 83.7025 93.6006	Debye $\times 10^{-48}$ esu $\times 10^{-30}$ esu $\times 10^{-30}$ esu $\times 10^{-30}$ esu
	<i>Dipole</i> $\mu\beta$ $\beta_{HRS}$ $\beta_{zzz}$ $\beta_{avg}$	14.2581 2098.4420 106.5923 224.1342 254.6760	Debye $\times 10^{-48}$ esu $\times 10^{-30}$ esu $\times 10^{-30}$ esu $\times 10^{-30}$ esu
	<i>Dipole</i> $\mu\beta$ $\beta_{HRS}$ $\beta_{zzz}$ $\beta_{avg}$	14.2580 819.1819 40.5290 88.2012 98.0884	Debye $\times 10^{-48}$ esu $\times 10^{-30}$ esu $\times 10^{-30}$ esu $\times 10^{-30}$ esu
	<i>Dipole</i> $\mu\beta$ $\beta_{HRS}$ $\beta_{zzz}$ $\beta_{avg}$	17.8717 2817.0153 113.0123 239.1405 271.9372	Debye $\times 10^{-48}$ esu $\times 10^{-30}$ esu $\times 10^{-30}$ esu $\times 10^{-30}$ esu

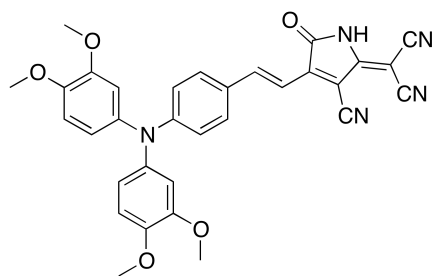


 <p style="text-align: center;">DAAP-01</p>	<i>Dipole</i> $\mu\beta$ $\beta_{HRS}$ $\beta_{zzz}$ $\beta_{avg}$	15.4062 2417.5513 113.2183 241.5123 272.7453	Debye $\times 10^{-48}$ esu $\times 10^{-30}$ esu $\times 10^{-30}$ esu $\times 10^{-30}$ esu
	<i>Dipole</i> $\mu\beta$ $\beta_{HRS}$ $\beta_{zzz}$ $\beta_{avg}$	15.4066 6435.3764 301.1697 643.5371 725.4265	Debye $\times 10^{-48}$ esu $\times 10^{-30}$ esu $\times 10^{-30}$ esu $\times 10^{-30}$ esu
	<i>Dipole</i> $\mu\beta$ $\beta_{HRS}$ $\beta_{zzz}$ $\beta_{avg}$	15.4066 2532.8203 118.3129 252.9634 285.4191	Debye $\times 10^{-48}$ esu $\times 10^{-30}$ esu $\times 10^{-30}$ esu $\times 10^{-30}$ esu
	<i>Dipole</i> $\mu\beta$ $\beta_{HRS}$ $\beta_{zzz}$ $\beta_{avg}$	16.6355 1880.5110 80.9450 178.8342 194.5018	Debye $\times 10^{-48}$ esu $\times 10^{-30}$ esu $\times 10^{-30}$ esu $\times 10^{-30}$ esu
	<i>Dipole</i> $\mu\beta$ $\beta_{HRS}$ $\beta_{zzz}$ $\beta_{avg}$	16.6367 4714.7168 202.7056 451.1963 486.2405	Debye $\times 10^{-48}$ esu $\times 10^{-30}$ esu $\times 10^{-30}$ esu $\times 10^{-30}$ esu
	<i>Dipole</i> $\mu\beta$ $\beta_{HRS}$ $\beta_{zzz}$ $\beta_{avg}$	16.6366 1942.5771 83.3606 184.7553 200.5987	Debye $\times 10^{-48}$ esu $\times 10^{-30}$ esu $\times 10^{-30}$ esu $\times 10^{-30}$ esu
	<i>Dipole</i> $\mu\beta$ $\beta_{HRS}$ $\beta_{zzz}$ $\beta_{avg}$	19.8950 5768.7860 208.7582 451.9857 501.7989	Debye $\times 10^{-48}$ esu $\times 10^{-30}$ esu $\times 10^{-30}$ esu $\times 10^{-30}$ esu



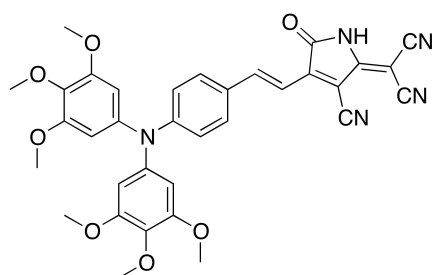
DAAP-03

<i>cam-b3lyp</i> (vacuo)	<i>Dipole</i>	17.6034	Debye
	$\mu\beta$	2098.3640	$\times 10^{-48}$ esu
	$\beta_{HRS}$	85.8297	$\times 10^{-30}$ esu
	$\beta_{zzz}$	187.5952	$\times 10^{-30}$ esu
	$\beta_{avg}$	205.7903	$\times 10^{-30}$ esu
<i>cam-b3lyp</i> (chloroform)	<i>Dipole</i>	17.6040	Debye
	$\mu\beta$	5179.3354	$\times 10^{-48}$ esu
	$\beta_{HRS}$	212.0979	$\times 10^{-30}$ esu
	$\beta_{zzz}$	463.2474	$\times 10^{-30}$ esu
	$\beta_{avg}$	507.9686	$\times 10^{-30}$ esu
$\Psi_{062x}$	<i>Dipole</i>	17.6036	Debye
	$\mu\beta$	2159.0590	$\times 10^{-48}$ esu
	$\beta_{HRS}$	88.0147	$\times 10^{-30}$ esu
	$\beta_{zzz}$	193.1015	$\times 10^{-30}$ esu
	$\beta_{avg}$	211.3697	$\times 10^{-30}$ esu
<i>m062x</i> (chloroform)	<i>Dipole</i>	20.4995	Debye
	$\mu\beta$	6164.3086	$\times 10^{-48}$ esu
	$\beta_{HRS}$	217.6168	$\times 10^{-30}$ esu
	$\beta_{zzz}$	465.6092	$\times 10^{-30}$ esu
	$\beta_{avg}$	522.3746	$\times 10^{-30}$ esu



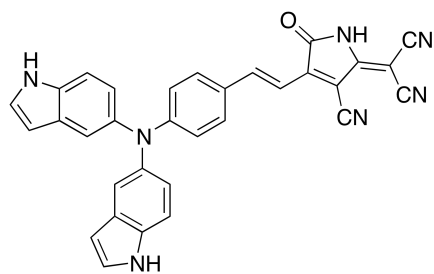
DAAP-04

<i>cam-b3lyp</i> (vacuo)	<i>Dipole</i>	14.9575	Debye
	$\mu\beta$	2452.1610	$\times 10^{-48}$ esu
	$\beta_{HRS}$	121.2624	$\times 10^{-30}$ esu
	$\beta_{zzz}$	239.5183	$\times 10^{-30}$ esu
	$\beta_{avg}$	292.4477	$\times 10^{-30}$ esu
<i>cam-b3lyp</i> (chloroform)	<i>Dipole</i>	14.9605	Debye
	$\mu\beta$	6269.2005	$\times 10^{-48}$ esu
	$\beta_{HRS}$	309.4806	$\times 10^{-30}$ esu
	$\beta_{zzz}$	613.2646	$\times 10^{-30}$ esu
	$\beta_{avg}$	746.1884	$\times 10^{-30}$ esu
$\Psi_{062x}$	<i>Dipole</i>	14.9606	Debye
	$\mu\beta$	2574.5651	$\times 10^{-48}$ esu
	$\beta_{HRS}$	126.9242	$\times 10^{-30}$ esu
	$\beta_{zzz}$	251.7031	$\times 10^{-30}$ esu
	$\beta_{avg}$	306.4990	$\times 10^{-30}$ esu
<i>m062x</i> (chloroform)	<i>Dipole</i>	17.5182	Debye
	$\mu\beta$	7617.8833	$\times 10^{-48}$ esu
	$\beta_{HRS}$	325.4603	$\times 10^{-30}$ esu
	$\beta_{zzz}$	616.1204	$\times 10^{-30}$ esu
	$\beta_{avg}$	786.0139	$\times 10^{-30}$ esu



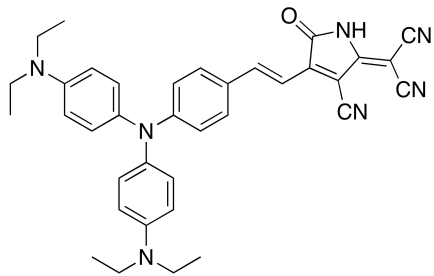
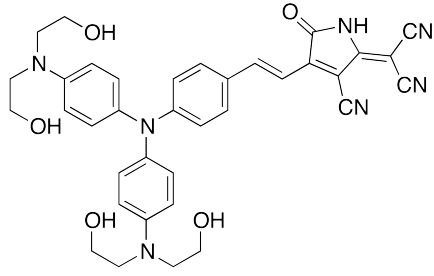
DAAP-05

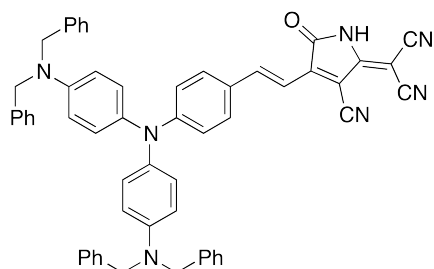
<i>cam-b3lyp</i> (vacuo)	<i>Dipole</i>	13.6566	Debye
	$\mu\beta$	2113.0355	$\times 10^{-48}$ esu
	$\beta_{HRS}$	111.3874	$\times 10^{-30}$ esu
	$\beta_{zzz}$	241.9286	$\times 10^{-30}$ esu
	$\beta_{avg}$	267.2147	$\times 10^{-30}$ esu
<i>cam-b3lyp</i> (chloroform)	<i>Dipole</i>	13.6582	Debye
	$\mu\beta$	5024.4275	$\times 10^{-48}$ esu
	$\beta_{HRS}$	264.3027	$\times 10^{-30}$ esu
	$\beta_{zzz}$	576.2219	$\times 10^{-30}$ esu
	$\beta_{avg}$	634.5148	$\times 10^{-30}$ esu
$\Psi_{00}^{00}$	<i>Dipole</i>	13.6577	Debye
	$\mu\beta$	2228.3711	$\times 10^{-48}$ esu
	$\beta_{HRS}$	117.1893	$\times 10^{-30}$ esu
	$\beta_{zzz}$	255.0378	$\times 10^{-30}$ esu
	$\beta_{avg}$	281.5175	$\times 10^{-30}$ esu
$\Psi_{00}^{00}$ (chloroform)	<i>Dipole</i>	15.8315	Debye
	$\mu\beta$	6078.5522	$\times 10^{-48}$ esu
	$\beta_{HRS}$	278.3052	$\times 10^{-30}$ esu
	$\beta_{zzz}$	586.7992	$\times 10^{-30}$ esu
	$\beta_{avg}$	669.2565	$\times 10^{-30}$ esu



DAAP-06

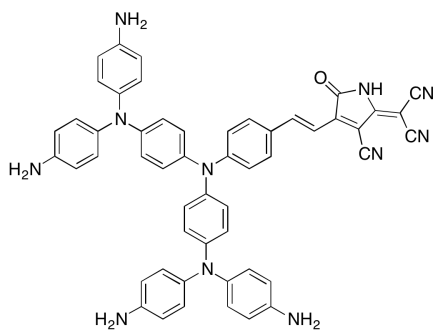
<i>cam-b3lyp</i> (vacuo)	<i>Dipole</i>	17.6455	Debye
	$\mu\beta$	2999.1703	$\times 10^{-48}$ esu
	$\beta_{HRS}$	120.7077	$\times 10^{-30}$ esu
	$\beta_{zzz}$	272.2086	$\times 10^{-30}$ esu
	$\beta_{avg}$	290.1538	$\times 10^{-30}$ esu
<i>cam-b3lyp</i> (chloroform)	<i>Dipole</i>	17.6444	Debye
	$\mu\beta$	8118.0918	$\times 10^{-48}$ esu
	$\beta_{HRS}$	326.1223	$\times 10^{-30}$ esu
	$\beta_{zzz}$	736.0851	$\times 10^{-30}$ esu
	$\beta_{avg}$	784.8853	$\times 10^{-30}$ esu
$\Psi_{00}^{00}$	<i>Dipole</i>	17.6447	Debye
	$\mu\beta$	3154.6331	$\times 10^{-48}$ esu
	$\beta_{HRS}$	126.6093	$\times 10^{-30}$ esu
	$\beta_{zzz}$	286.0199	$\times 10^{-30}$ esu
	$\beta_{avg}$	304.8918	$\times 10^{-30}$ esu
$\Psi_{00}^{00}$ (chloroform)	<i>Dipole</i>	20.9009	Debye
	$\mu\beta$	10125.5341	$\times 10^{-48}$ esu
	$\beta_{HRS}$	344.4271	$\times 10^{-30}$ esu
	$\beta_{zzz}$	764.5700	$\times 10^{-30}$ esu
	$\beta_{avg}$	830.6158	$\times 10^{-30}$ esu

 <p style="text-align: center;">DAAP-07</p>	<i>Dipole</i> $\mu\beta$ $\beta_{HRS}$ $\beta_{zzz}$ $\beta_{avg}$	18.5080 3871.9436 145.7741 335.4266 353.9823	Debye $\times 10^{-48}$ esu $\times 10^{-30}$ esu $\times 10^{-30}$ esu $\times 10^{-30}$ esu
	<i>Dipole</i> $\mu\beta$ $\beta_{HRS}$ $\beta_{zzz}$ $\beta_{avg}$	18.5060 10964.6713 412.8680 950.7737 1002.2392	Debye $\times 10^{-48}$ esu $\times 10^{-30}$ esu $\times 10^{-30}$ esu $\times 10^{-30}$ esu
	<i>Dipole</i> $\mu\beta$ $\beta_{HRS}$ $\beta_{zzz}$ $\beta_{avg}$	18.5059 4155.0557 155.9598 358.7063 379.7002	Debye $\times 10^{-48}$ esu $\times 10^{-30}$ esu $\times 10^{-30}$ esu $\times 10^{-30}$ esu
	<i>Dipole</i> $\mu\beta$ $\beta_{HRS}$ $\beta_{zzz}$ $\beta_{avg}$	22.0305 14173.0866 448.6621 1020.1341 1092.2233	Debye $\times 10^{-48}$ esu $\times 10^{-30}$ esu $\times 10^{-30}$ esu $\times 10^{-30}$ esu
 <p style="text-align: center;">DAAP-08</p>	<i>Dipole</i> $\mu\beta$ $\beta_{HRS}$ $\beta_{zzz}$ $\beta_{avg}$	19.4875 4002.2614 143.3468 326.0516 348.5788	Debye $\times 10^{-48}$ esu $\times 10^{-30}$ esu $\times 10^{-30}$ esu $\times 10^{-30}$ esu
	<i>Dipole</i> $\mu\beta$ $\beta_{HRS}$ $\beta_{zzz}$ $\beta_{avg}$	19.4946 10755.3166 385.6278 879.9269 935.8859	Debye $\times 10^{-48}$ esu $\times 10^{-30}$ esu $\times 10^{-30}$ esu $\times 10^{-30}$ esu
	<i>Dipole</i> $\mu\beta$ $\beta_{HRS}$ $\beta_{zzz}$ $\beta_{avg}$	19.4956 4298.7056 153.4178 349.3994 373.8817	Debye $\times 10^{-48}$ esu $\times 10^{-30}$ esu $\times 10^{-30}$ esu $\times 10^{-30}$ esu
	<i>Dipole</i> $\mu\beta$ $\beta_{HRS}$ $\beta_{zzz}$ $\beta_{avg}$	22.8115 13601.7744 417.6789 938.4234 1016.2056	Debye $\times 10^{-48}$ esu $\times 10^{-30}$ esu $\times 10^{-30}$ esu $\times 10^{-30}$ esu



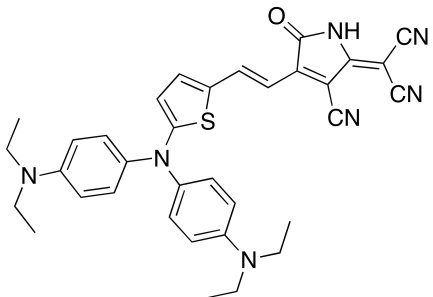
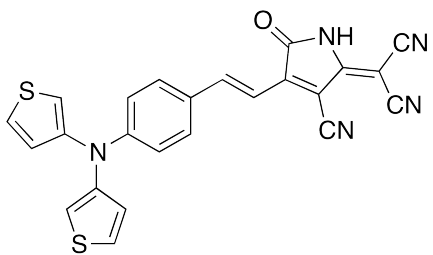
DAAP-09

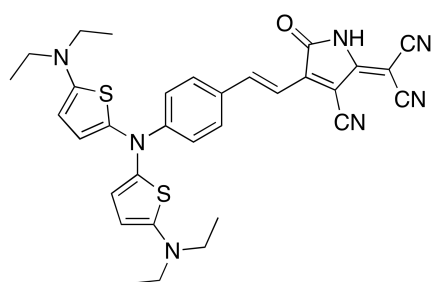
<i>cam-b3lyp</i> vacuo	<i>Dipole</i>	17.7129	Debye
	$\mu\beta$	3959.5700	$\times 10^{-48}$ esu
	$\beta_{HRS}$	156.1920	$\times 10^{-30}$ esu
	$\beta_{zzz}$	354.9586	$\times 10^{-30}$ esu
	$\beta_{avg}$	379.6719	$\times 10^{-30}$ esu
<i>cam-b3lyp</i> (chloroform)	<i>Dipole</i>	17.7134	Debye
	$\mu\beta$	10164.9910	$\times 10^{-48}$ esu
	$\beta_{HRS}$	401.4566	$\times 10^{-30}$ esu
	$\beta_{zzz}$	915.0796	$\times 10^{-30}$ esu
	$\beta_{avg}$	974.0340	$\times 10^{-30}$ esu
$\Psi_{000}^{00x}$	<i>Dipole</i>	17.7138	Debye
	$\mu\beta$	4240.4246	$\times 10^{-48}$ esu
	$\beta_{HRS}$	166.7184	$\times 10^{-30}$ esu
	$\beta_{zzz}$	379.1700	$\times 10^{-30}$ esu
	$\beta_{avg}$	406.2001	$\times 10^{-30}$ esu
$\Psi_{000}^{062x}$ (chloroform)	<i>Dipole</i>	20.6194	Debye
	$\mu\beta$	12681.3130	$\times 10^{-48}$ esu
	$\beta_{HRS}$	431.8442	$\times 10^{-30}$ esu
	$\beta_{zzz}$	964.7365	$\times 10^{-30}$ esu
	$\beta_{avg}$	1050.3921	$\times 10^{-30}$ esu



DAAP-10

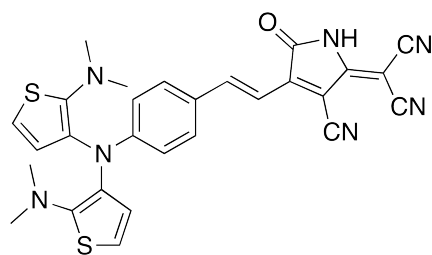
<i>cam-b3lyp</i> vacuo	<i>Dipole</i>	20.8387	Debye
	$\mu\beta$	5764.4938	$\times 10^{-48}$ esu
	$\beta_{HRS}$	190.3601	$\times 10^{-30}$ esu
	$\beta_{zzz}$	431.8559	$\times 10^{-30}$ esu
	$\beta_{avg}$	468.7162	$\times 10^{-30}$ esu
<i>cam-b3lyp</i> (chloroform)	<i>Dipole</i>	20.8388	Debye
	$\mu\beta$	14607.0371	$\times 10^{-48}$ esu
	$\beta_{HRS}$	483.9030	$\times 10^{-30}$ esu
	$\beta_{zzz}$	1104.1311	$\times 10^{-30}$ esu
	$\beta_{avg}$	1186.5383	$\times 10^{-30}$ esu
$\Psi_{000}^{00x}$	<i>Dipole</i>	20.8382	Debye
	$\mu\beta$	6396.0038	$\times 10^{-48}$ esu
	$\beta_{HRS}$	210.3250	$\times 10^{-30}$ esu
	$\beta_{zzz}$	475.5164	$\times 10^{-30}$ esu
	$\beta_{avg}$	520.0035	$\times 10^{-30}$ esu
$\Psi_{000}^{062x}$ (chloroform)	<i>Dipole</i>	24.0745	Debye
	$\mu\beta$	18972.4635	$\times 10^{-48}$ esu
	$\beta_{HRS}$	544.6266	$\times 10^{-30}$ esu
	$\beta_{zzz}$	1219.4868	$\times 10^{-30}$ esu
	$\beta_{avg}$	1341.3550	$\times 10^{-30}$ esu

 <p style="text-align: center;">DAAP-11</p>	<i>Dipole</i> $\mu\beta$ $\beta_{HRS}$ $\beta_{zzz}$ $\beta_{avg}$	20.1747 2550.1272 89.3927 205.3166 215.2461	Debye $\times 10^{-48}$ esu $\times 10^{-30}$ esu $\times 10^{-30}$ esu $\times 10^{-30}$ esu
	<i>Dipole</i> $\mu\beta$ $\beta_{HRS}$ $\beta_{zzz}$ $\beta_{avg}$	20.1759 6739.8232 239.0543 542.3055 572.2944	Debye $\times 10^{-48}$ esu $\times 10^{-30}$ esu $\times 10^{-30}$ esu $\times 10^{-30}$ esu
	<i>Dipole</i> $\mu\beta$ $\beta_{HRS}$ $\beta_{zzz}$ $\beta_{avg}$	20.1764 2693.7362 93.7961 215.8621 226.8685	Debye $\times 10^{-48}$ esu $\times 10^{-30}$ esu $\times 10^{-30}$ esu $\times 10^{-30}$ esu
	<i>Dipole</i> $\mu\beta$ $\beta_{HRS}$ $\beta_{zzz}$ $\beta_{avg}$	25.1198 9029.9530 256.6280 570.9052 618.8139	Debye $\times 10^{-48}$ esu $\times 10^{-30}$ esu $\times 10^{-30}$ esu $\times 10^{-30}$ esu
 <p style="text-align: center;">DAAP-12</p>	<i>Dipole</i> $\mu\beta$ $\beta_{HRS}$ $\beta_{zzz}$ $\beta_{avg}$	12.3824 1534.2193 90.7157 188.9442 217.1249	Debye $\times 10^{-48}$ esu $\times 10^{-30}$ esu $\times 10^{-30}$ esu $\times 10^{-30}$ esu
	<i>Dipole</i> $\mu\beta$ $\beta_{HRS}$ $\beta_{zzz}$ $\beta_{avg}$	12.3826 4143.6176 244.1091 510.1343 585.4650	Debye $\times 10^{-48}$ esu $\times 10^{-30}$ esu $\times 10^{-30}$ esu $\times 10^{-30}$ esu
	<i>Dipole</i> $\mu\beta$ $\beta_{HRS}$ $\beta_{zzz}$ $\beta_{avg}$	12.3826 1630.8200 96.1105 200.8072 230.4787	Debye $\times 10^{-48}$ esu $\times 10^{-30}$ esu $\times 10^{-30}$ esu $\times 10^{-30}$ esu
	<i>Dipole</i> $\mu\beta$ $\beta_{HRS}$ $\beta_{zzz}$ $\beta_{avg}$	15.0166 5335.6445 260.9882 530.1470 627.2227	Debye $\times 10^{-48}$ esu $\times 10^{-30}$ esu $\times 10^{-30}$ esu $\times 10^{-30}$ esu



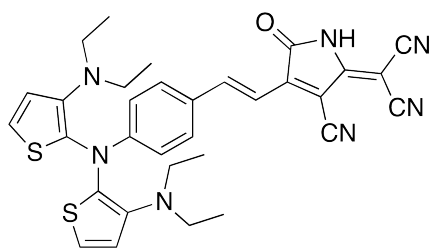
DAAP-13

<i>cam-b3lyp</i> (vacuum)	<i>Dipole</i>	17.1330	Debye
	$\mu\beta$	2055.2544	$\times 10^{-48}$ esu
	$\beta_{HRS}$	84.8537	$\times 10^{-30}$ esu
	$\beta_{zzz}$	192.2284	$\times 10^{-30}$ esu
	$\beta_{avg}$	204.4704	$\times 10^{-30}$ esu
<i>cam-b3lyp</i> (chloroform)	<i>Dipole</i>	17.1335	Debye
	$\mu\beta$	4632.3581	$\times 10^{-48}$ esu
	$\beta_{HRS}$	191.2559	$\times 10^{-30}$ esu
	$\beta_{zzz}$	434.7164	$\times 10^{-30}$ esu
	$\beta_{avg}$	460.2936	$\times 10^{-30}$ esu
$\Psi_{062x}$	<i>Dipole</i>	17.1335	Debye
	$\mu\beta$	2122.4471	$\times 10^{-48}$ esu
	$\beta_{HRS}$	87.3974	$\times 10^{-30}$ esu
	$\beta_{zzz}$	198.4930	$\times 10^{-30}$ esu
	$\beta_{avg}$	210.8879	$\times 10^{-30}$ esu
$m_{062x}$ (chloroform)	<i>Dipole</i>	19.7305	Debye
	$\mu\beta$	5438.1195	$\times 10^{-48}$ esu
	$\beta_{HRS}$	195.6930	$\times 10^{-30}$ esu
	$\beta_{zzz}$	436.5979	$\times 10^{-30}$ esu
	$\beta_{avg}$	471.9197	$\times 10^{-30}$ esu



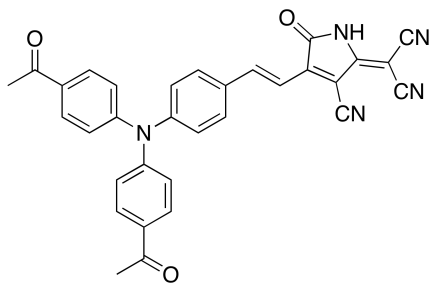
DAAP-14

<i>cam-b3lyp</i> (vacuum)	<i>Dipole</i>	14.4767	Debye
	$\mu\beta$	1931.1531	$\times 10^{-48}$ esu
	$\beta_{HRS}$	96.3549	$\times 10^{-30}$ esu
	$\beta_{zzz}$	209.3504	$\times 10^{-30}$ esu
	$\beta_{avg}$	230.7007	$\times 10^{-30}$ esu
<i>cam-b3lyp</i> (chloroform)	<i>Dipole</i>	14.4765	Debye
	$\mu\beta$	5024.8872	$\times 10^{-48}$ esu
	$\beta_{HRS}$	249.9975	$\times 10^{-30}$ esu
	$\beta_{zzz}$	544.3053	$\times 10^{-30}$ esu
	$\beta_{avg}$	599.4816	$\times 10^{-30}$ esu
$\Psi_{062x}$	<i>Dipole</i>	14.4762	Debye
	$\mu\beta$	2035.3655	$\times 10^{-48}$ esu
	$\beta_{HRS}$	101.2549	$\times 10^{-30}$ esu
	$\beta_{zzz}$	220.7073	$\times 10^{-30}$ esu
	$\beta_{avg}$	242.7919	$\times 10^{-30}$ esu
$m_{062x}$ (chloroform)	<i>Dipole</i>	17.3042	Debye
	$\mu\beta$	6311.8849	$\times 10^{-48}$ esu
	$\beta_{HRS}$	264.0967	$\times 10^{-30}$ esu
	$\beta_{zzz}$	561.9620	$\times 10^{-30}$ esu
	$\beta_{avg}$	634.4182	$\times 10^{-30}$ esu



DAAP-15

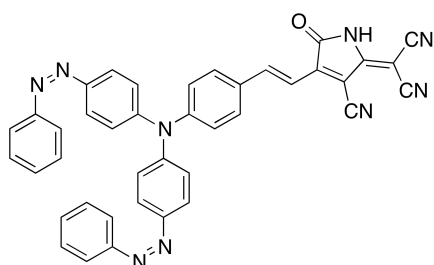
<i>cam-b3lyp</i> (vacuo)	<i>Dipole</i>	14.3918	Debye
	$\mu\beta$	1449.2904	$\times 10^{-48}$ esu
	$\beta_{HRS}$	72.7516	$\times 10^{-30}$ esu
	$\beta_{zzz}$	158.9150	$\times 10^{-30}$ esu
	$\beta_{avg}$	173.8525	$\times 10^{-30}$ esu
<i>cam-b3lyp</i> (chloroform)	<i>Dipole</i>	14.3920	Debye
	$\mu\beta$	3418.5834	$\times 10^{-48}$ esu
	$\beta_{HRS}$	171.2849	$\times 10^{-30}$ esu
	$\beta_{zzz}$	374.7650	$\times 10^{-30}$ esu
	$\beta_{avg}$	409.6318	$\times 10^{-30}$ esu
$\Psi_{000}^{000}$	<i>Dipole</i>	14.3920	Debye
	$\mu\beta$	1502.2880	$\times 10^{-48}$ esu
	$\beta_{HRS}$	75.1572	$\times 10^{-30}$ esu
	$\beta_{zzz}$	164.8325	$\times 10^{-30}$ esu
	$\beta_{avg}$	179.8910	$\times 10^{-30}$ esu
<i>m062x</i> (chloroform)	<i>Dipole</i>	17.0166	Debye
	$\mu\beta$	4134.4112	$\times 10^{-48}$ esu
	$\beta_{HRS}$	176.0151	$\times 10^{-30}$ esu
	$\beta_{zzz}$	376.6038	$\times 10^{-30}$ esu
	$\beta_{avg}$	421.8110	$\times 10^{-30}$ esu



DAAP-16

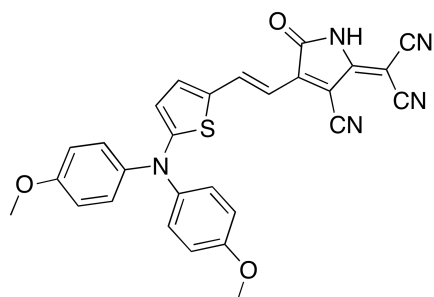
<i>cam-b3lyp</i> (vacuo)	<i>Dipole</i>	6.3993	Debye
	$\mu\beta$	594.6805	$\times 10^{-48}$ esu
	$\beta_{HRS}$	88.6992	$\times 10^{-30}$ esu
	$\beta_{zzz}$	82.8691	$\times 10^{-30}$ esu
	$\beta_{avg}$	206.0548	$\times 10^{-30}$ esu
<i>cam-b3lyp</i> (chloroform)	<i>Dipole</i>	6.3990	Debye
	$\mu\beta$	1379.6011	$\times 10^{-48}$ esu
	$\beta_{HRS}$	202.7902	$\times 10^{-30}$ esu
	$\beta_{zzz}$	195.9884	$\times 10^{-30}$ esu
	$\beta_{avg}$	474.4171	$\times 10^{-30}$ esu
$\Psi_{000}^{000}$	<i>Dipole</i>	6.3985	Debye
	$\mu\beta$	629.7725	$\times 10^{-48}$ esu
	$\beta_{HRS}$	93.3986	$\times 10^{-30}$ esu
	$\beta_{zzz}$	88.5443	$\times 10^{-30}$ esu
	$\beta_{avg}$	217.7229	$\times 10^{-30}$ esu
<i>m062x</i> (chloroform)	<i>Dipole</i>	7.7385	Debye
	$\mu\beta$	1621.5101	$\times 10^{-48}$ esu
	$\beta_{HRS}$	213.1686	$\times 10^{-30}$ esu
	$\beta_{zzz}$	156.4230	$\times 10^{-30}$ esu
	$\beta_{avg}$	500.3883	$\times 10^{-30}$ esu





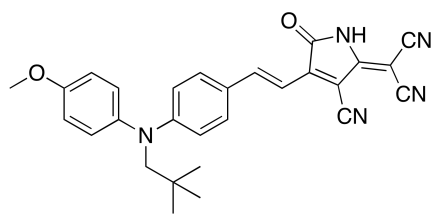
DAAP-17

<i>cam-b3lyp</i> (vacuo)	<i>Dipole</i>	12.2682	Debye
	$\mu\beta$	1708.1137	$\times 10^{-48}$ esu
	$\beta_{HRS}$	113.6209	$\times 10^{-30}$ esu
	$\beta_{zzz}$	176.0623	$\times 10^{-30}$ esu
	$\beta_{avg}$	268.4177	$\times 10^{-30}$ esu
<i>cam-b3lyp</i> (chloroform)	<i>Dipole</i>	12.2685	Debye
	$\mu\beta$	3874.9187	$\times 10^{-48}$ esu
	$\beta_{HRS}$	257.5898	$\times 10^{-30}$ esu
	$\beta_{zzz}$	395.1736	$\times 10^{-30}$ esu
	$\beta_{avg}$	610.0556	$\times 10^{-30}$ esu
$\Psi_{00}^{00}$	<i>Dipole</i>	12.2686	Debye
	$\mu\beta$	1816.3179	$\times 10^{-48}$ esu
	$\beta_{HRS}$	120.2555	$\times 10^{-30}$ esu
	$\beta_{zzz}$	187.4335	$\times 10^{-30}$ esu
	$\beta_{avg}$	284.8971	$\times 10^{-30}$ esu
$m^{062x}$ (chloroform)	<i>Dipole</i>	14.6603	Debye
	$\mu\beta$	4785.6034	$\times 10^{-48}$ esu
	$\beta_{HRS}$	272.5889	$\times 10^{-30}$ esu
	$\beta_{zzz}$	384.2930	$\times 10^{-30}$ esu
	$\beta_{avg}$	647.5315	$\times 10^{-30}$ esu



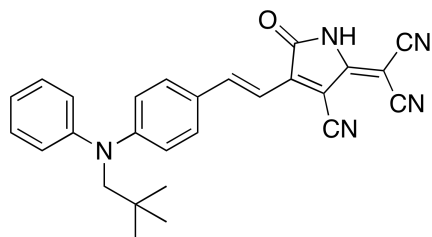
DAAP-18

<i>cam-b3lyp</i> (vacuo)	<i>Dipole</i>	17.3353	Debye
	$\mu\beta$	1841.1483	$\times 10^{-48}$ esu
	$\beta_{HRS}$	77.5457	$\times 10^{-30}$ esu
	$\beta_{zzz}$	165.2170	$\times 10^{-30}$ esu
	$\beta_{avg}$	185.3916	$\times 10^{-30}$ esu
<i>cam-b3lyp</i> (chloroform)	<i>Dipole</i>	17.3350	Debye
	$\mu\beta$	4892.9465	$\times 10^{-48}$ esu
	$\beta_{HRS}$	207.8904	$\times 10^{-30}$ esu
	$\beta_{zzz}$	439.8066	$\times 10^{-30}$ esu
	$\beta_{avg}$	494.3204	$\times 10^{-30}$ esu
$\Psi_{00}^{00}$	<i>Dipole</i>	17.3346	Debye
	$\mu\beta$	1904.7971	$\times 10^{-48}$ esu
	$\beta_{HRS}$	79.7469	$\times 10^{-30}$ esu
	$\beta_{zzz}$	170.8305	$\times 10^{-30}$ esu
	$\beta_{avg}$	191.2433	$\times 10^{-30}$ esu
$m^{062x}$ (chloroform)	<i>Dipole</i>	21.6035	Debye
	$\mu\beta$	6331.4862	$\times 10^{-48}$ esu
	$\beta_{HRS}$	216.3953	$\times 10^{-30}$ esu
	$\beta_{zzz}$	445.0195	$\times 10^{-30}$ esu
	$\beta_{avg}$	517.2187	$\times 10^{-30}$ esu



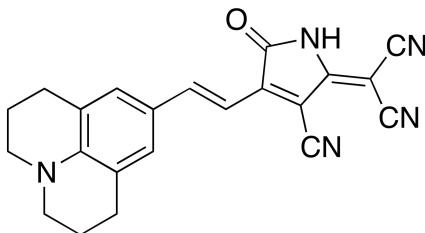
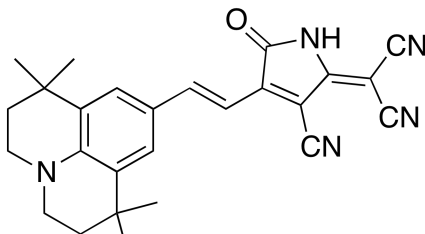
DAAP-19

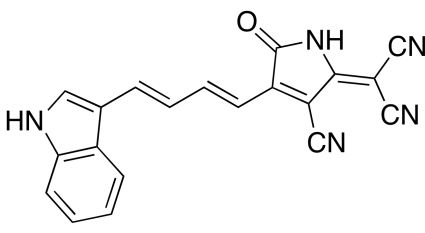
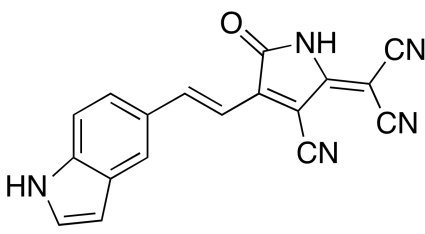
<i>cam-b3lyp</i> <i>vacuo</i>	<i>Dipole</i>	15.2894	Debye
	$\mu\beta$	1712.1933	$\times 10^{-48}$ esu
	$\beta_{HRS}$	80.4379	$\times 10^{-30}$ esu
	$\beta_{zzz}$	177.8932	$\times 10^{-30}$ esu
	$\beta_{avg}$	192.7885	$\times 10^{-30}$ esu
<i>cam-b3lyp</i> <i>(chloroform)</i>	<i>Dipole</i>	15.2897	Debye
	$\mu\beta$	4527.6441	$\times 10^{-48}$ esu
	$\beta_{HRS}$	212.1476	$\times 10^{-30}$ esu
	$\beta_{zzz}$	472.1855	$\times 10^{-30}$ esu
	$\beta_{avg}$	508.3347	$\times 10^{-30}$ esu
$\Psi_{000}^{xyz}$	<i>Dipole</i>	15.2895	Debye
	$\mu\beta$	1774.2588	$\times 10^{-48}$ esu
	$\beta_{HRS}$	83.1021	$\times 10^{-30}$ esu
	$\beta_{zzz}$	184.3164	$\times 10^{-30}$ esu
	$\beta_{avg}$	199.4754	$\times 10^{-30}$ esu
<i>m062x</i> <i>(chloroform)</i>	<i>Dipole</i>	18.5338	Debye
	$\mu\beta$	5632.2318	$\times 10^{-48}$ esu
	$\beta_{HRS}$	219.5058	$\times 10^{-30}$ esu
	$\beta_{zzz}$	472.7315	$\times 10^{-30}$ esu
	$\beta_{avg}$	527.0693	$\times 10^{-30}$ esu

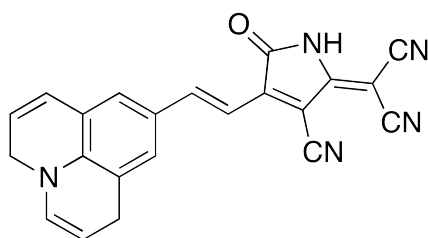


DAAP-20

<i>cam-b3lyp</i> <i>vacuo</i>	<i>Dipole</i>	14.4808	Debye
	$\mu\beta$	1536.4316	$\times 10^{-48}$ esu
	$\beta_{HRS}$	76.6893	$\times 10^{-30}$ esu
	$\beta_{zzz}$	167.1680	$\times 10^{-30}$ esu
	$\beta_{avg}$	183.2060	$\times 10^{-30}$ esu
<i>cam-b3lyp</i> <i>(chloroform)</i>	<i>Dipole</i>	14.4801	Debye
	$\mu\beta$	4123.5105	$\times 10^{-48}$ esu
	$\beta_{HRS}$	205.5788	$\times 10^{-30}$ esu
	$\beta_{zzz}$	448.1616	$\times 10^{-30}$ esu
	$\beta_{avg}$	491.6144	$\times 10^{-30}$ esu
$\Psi_{000}^{xyz}$	<i>Dipole</i>	14.4796	Debye
	$\mu\beta$	1594.3001	$\times 10^{-48}$ esu
	$\beta_{HRS}$	79.3398	$\times 10^{-30}$ esu
	$\beta_{zzz}$	173.5756	$\times 10^{-30}$ esu
	$\beta_{avg}$	189.8363	$\times 10^{-30}$ esu
<i>m062x</i> <i>(chloroform)</i>	<i>Dipole</i>	17.6764	Debye
	$\mu\beta$	5181.7754	$\times 10^{-48}$ esu
	$\beta_{HRS}$	212.9061	$\times 10^{-30}$ esu
	$\beta_{zzz}$	452.0313	$\times 10^{-30}$ esu
	$\beta_{avg}$	510.1808	$\times 10^{-30}$ esu

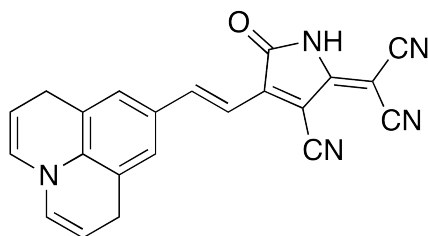
 <p style="text-align: center;">LR-01</p>	<i>Dipole</i> $\mu\beta$ $\beta_{HRS}$ $\beta_{zzz}$ $\beta_{avg}$	16.1399 1554.2843 69.5775 152.7118 166.0732	Debye $\times 10^{-48}$ esu $\times 10^{-30}$ esu $\times 10^{-30}$ esu $\times 10^{-30}$ esu
	<i>Dipole</i> $\mu\beta$ $\beta_{HRS}$ $\beta_{zzz}$ $\beta_{avg}$	16.1409 5020.7171 225.0691 490.0760 537.6387	Debye $\times 10^{-48}$ esu $\times 10^{-30}$ esu $\times 10^{-30}$ esu $\times 10^{-30}$ esu
	<i>Dipole</i> $\mu\beta$ $\beta_{HRS}$ $\beta_{zzz}$ $\beta_{avg}$	16.1407 1586.1938 70.7473 156.0854 169.1142	Debye $\times 10^{-48}$ esu $\times 10^{-30}$ esu $\times 10^{-30}$ esu $\times 10^{-30}$ esu
	<i>Dipole</i> $\mu\beta$ $\beta_{HRS}$ $\beta_{zzz}$ $\beta_{avg}$	20.8826 6619.5939 228.8400 497.8532 547.7498	Debye $\times 10^{-48}$ esu $\times 10^{-30}$ esu $\times 10^{-30}$ esu $\times 10^{-30}$ esu
 <p style="text-align: center;">LR-02</p>	<i>Dipole</i> $\mu\beta$ $\beta_{HRS}$ $\beta_{zzz}$ $\beta_{avg}$	16.1087 1552.2912 69.8795 153.3524 166.2830	Debye $\times 10^{-48}$ esu $\times 10^{-30}$ esu $\times 10^{-30}$ esu $\times 10^{-30}$ esu
	<i>Dipole</i> $\mu\beta$ $\beta_{HRS}$ $\beta_{zzz}$ $\beta_{avg}$	16.1080 4846.3455 218.3898 474.3558 520.6235	Debye $\times 10^{-48}$ esu $\times 10^{-30}$ esu $\times 10^{-30}$ esu $\times 10^{-30}$ esu
	<i>Dipole</i> $\mu\beta$ $\beta_{HRS}$ $\beta_{zzz}$ $\beta_{avg}$	16.1077 1581.9742 70.9438 156.5532 169.0855	Debye $\times 10^{-48}$ esu $\times 10^{-30}$ esu $\times 10^{-30}$ esu $\times 10^{-30}$ esu
	<i>Dipole</i> $\mu\beta$ $\beta_{HRS}$ $\beta_{zzz}$ $\beta_{avg}$	20.8447 6392.0283 221.9730 482.1291 530.3138	Debye $\times 10^{-48}$ esu $\times 10^{-30}$ esu $\times 10^{-30}$ esu $\times 10^{-30}$ esu

 <p style="text-align: center;">LR-03</p>	<i>Dipole</i> $\mu\beta$ $\beta_{HRS}$ $\beta_{zzz}$ $\beta_{avg}$	15.0645 1237.8168 62.5466 116.0599 149.5425	Debye $\times 10^{-48}$ esu $\times 10^{-30}$ esu $\times 10^{-30}$ esu $\times 10^{-30}$ esu
	<i>Dipole</i> $\mu\beta$ $\beta_{HRS}$ $\beta_{zzz}$ $\beta_{avg}$	15.0652 3775.3123 189.8873 356.2560 454.2037	Debye $\times 10^{-48}$ esu $\times 10^{-30}$ esu $\times 10^{-30}$ esu $\times 10^{-30}$ esu
	<i>Dipole</i> $\mu\beta$ $\beta_{HRS}$ $\beta_{zzz}$ $\beta_{avg}$	15.0652 1273.9506 63.9697 119.9632 153.3065	Debye $\times 10^{-48}$ esu $\times 10^{-30}$ esu $\times 10^{-30}$ esu $\times 10^{-30}$ esu
	<i>Dipole</i> $\mu\beta$ $\beta_{HRS}$ $\beta_{zzz}$ $\beta_{avg}$	19.3199 4929.6591 193.9857 356.5283 465.3445	Debye $\times 10^{-48}$ esu $\times 10^{-30}$ esu $\times 10^{-30}$ esu $\times 10^{-30}$ esu
 <p style="text-align: center;">LR-04</p>	<i>Dipole</i> $\mu\beta$ $\beta_{HRS}$ $\beta_{zzz}$ $\beta_{avg}$	12.4413 589.5190 33.8658 76.1266 81.0644	Debye $\times 10^{-48}$ esu $\times 10^{-30}$ esu $\times 10^{-30}$ esu $\times 10^{-30}$ esu
	<i>Dipole</i> $\mu\beta$ $\beta_{HRS}$ $\beta_{zzz}$ $\beta_{avg}$	12.4426 1626.7391 93.0392 209.8092 223.1544	Debye $\times 10^{-48}$ esu $\times 10^{-30}$ esu $\times 10^{-30}$ esu $\times 10^{-30}$ esu
	<i>Dipole</i> $\mu\beta$ $\beta_{HRS}$ $\beta_{zzz}$ $\beta_{avg}$	12.4426 596.7852 34.0952 77.0940 81.8228	Debye $\times 10^{-48}$ esu $\times 10^{-30}$ esu $\times 10^{-30}$ esu $\times 10^{-30}$ esu
	<i>Dipole</i> $\mu\beta$ $\beta_{HRS}$ $\beta_{zzz}$ $\beta_{avg}$	15.1979 1993.2717 93.2331 208.6528 224.2296	Debye $\times 10^{-48}$ esu $\times 10^{-30}$ esu $\times 10^{-30}$ esu $\times 10^{-30}$ esu



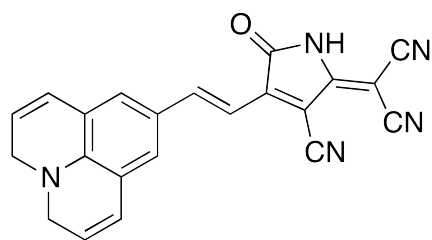
LR-05

<i>cam-b3lyp</i> (vacuo)	<i>Dipole</i>	13.1782	Debye
	$\mu\beta$	1531.9707	$\times 10^{-48}$ esu
	$\beta_{HRS}$	83.1091	$\times 10^{-30}$ esu
	$\beta_{zzz}$	187.9063	$\times 10^{-30}$ esu
	$\beta_{avg}$	198.5351	$\times 10^{-30}$ esu
<i>cam-b3lyp</i> (chloroform)	<i>Dipole</i>	13.1792	Debye
	$\mu\beta$	5207.6085	$\times 10^{-48}$ esu
	$\beta_{HRS}$	281.1318	$\times 10^{-30}$ esu
	$\beta_{zzz}$	636.9900	$\times 10^{-30}$ esu
	$\beta_{avg}$	673.8147	$\times 10^{-30}$ esu
$\Psi_{00}^{00}$	<i>Dipole</i>	13.1793	Debye
	$\mu\beta$	1597.2578	$\times 10^{-48}$ esu
	$\beta_{HRS}$	86.3812	$\times 10^{-30}$ esu
	$\beta_{zzz}$	195.7979	$\times 10^{-30}$ esu
	$\beta_{avg}$	206.7190	$\times 10^{-30}$ esu
<i>m062x</i> (chloroform)	<i>Dipole</i>	16.6326	Debye
	$\mu\beta$	6875.8481	$\times 10^{-48}$ esu
	$\beta_{HRS}$	294.5544	$\times 10^{-30}$ esu
	$\beta_{zzz}$	660.3976	$\times 10^{-30}$ esu
	$\beta_{avg}$	707.1208	$\times 10^{-30}$ esu



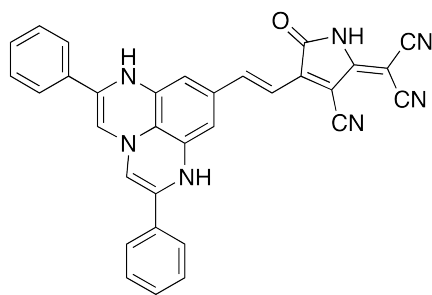
LR-06

<i>cam-b3lyp</i> (vacuo)	<i>Dipole</i>	11.6234	Debye
	$\mu\beta$	1337.8230	$\times 10^{-48}$ esu
	$\beta_{HRS}$	84.9348	$\times 10^{-30}$ esu
	$\beta_{zzz}$	175.8631	$\times 10^{-30}$ esu
	$\beta_{avg}$	202.2286	$\times 10^{-30}$ esu
<i>cam-b3lyp</i> (chloroform)	<i>Dipole</i>	11.6239	Debye
	$\mu\beta$	4217.3147	$\times 10^{-48}$ esu
	$\beta_{HRS}$	266.0068	$\times 10^{-30}$ esu
	$\beta_{zzz}$	553.8394	$\times 10^{-30}$ esu
	$\beta_{avg}$	635.8876	$\times 10^{-30}$ esu
$\Psi_{00}^{00}$	<i>Dipole</i>	11.6243	Debye
	$\mu\beta$	1433.9503	$\times 10^{-48}$ esu
	$\beta_{HRS}$	90.7031	$\times 10^{-30}$ esu
	$\beta_{zzz}$	188.2898	$\times 10^{-30}$ esu
	$\beta_{avg}$	216.4785	$\times 10^{-30}$ esu
<i>m062x</i> (chloroform)	<i>Dipole</i>	14.3271	Debye
	$\mu\beta$	5606.4999	$\times 10^{-48}$ esu
	$\beta_{HRS}$	288.5568	$\times 10^{-30}$ esu
	$\beta_{zzz}$	585.8299	$\times 10^{-30}$ esu
	$\beta_{avg}$	691.2497	$\times 10^{-30}$ esu



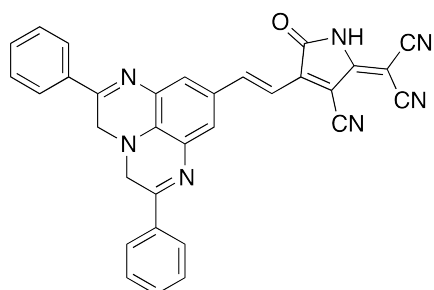
LR-07

<i>cam-b3lyp</i> (vacuo)	<i>Dipole</i>	15.1206	Debye
	$\mu\beta$	1667.4338	$\times 10^{-48}$ esu
	$\beta_{HRS}$	79.8937	$\times 10^{-30}$ esu
	$\beta_{zzz}$	175.0508	$\times 10^{-30}$ esu
	$\beta_{avg}$	190.3961	$\times 10^{-30}$ esu
<i>cam-b3lyp</i> (chloroform)	<i>Dipole</i>	15.1205	Debye
	$\mu\beta$	5943.9407	$\times 10^{-48}$ esu
	$\beta_{HRS}$	283.8586	$\times 10^{-30}$ esu
	$\beta_{zzz}$	620.0568	$\times 10^{-30}$ esu
	$\beta_{avg}$	678.7642	$\times 10^{-30}$ esu
$\Psi_{00}^{00}$	<i>Dipole</i>	15.1207	Debye
	$\mu\beta$	1708.0722	$\times 10^{-48}$ esu
	$\beta_{HRS}$	81.5550	$\times 10^{-30}$ esu
	$\beta_{zzz}$	179.3808	$\times 10^{-30}$ esu
	$\beta_{avg}$	194.6941	$\times 10^{-30}$ esu
<i>m062x</i> (chloroform)	<i>Dipole</i>	19.6705	Debye
	$\mu\beta$	7900.8032	$\times 10^{-48}$ esu
	$\beta_{HRS}$	289.5773	$\times 10^{-30}$ esu
	$\beta_{zzz}$	631.3961	$\times 10^{-30}$ esu
	$\beta_{avg}$	693.6357	$\times 10^{-30}$ esu



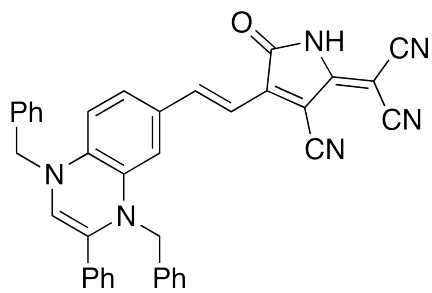
LR-08

<i>cam-b3lyp</i> (vacuo)	<i>Dipole</i>	13.8592	Debye
	$\mu\beta$	5617.8224	$\times 10^{-48}$ esu
	$\beta_{HRS}$	297.6600	$\times 10^{-30}$ esu
	$\beta_{zzz}$	638.7527	$\times 10^{-30}$ esu
	$\beta_{avg}$	704.6707	$\times 10^{-30}$ esu
<i>cam-b3lyp</i> (chloroform)	<i>Dipole</i>	13.8577	Debye
	$\mu\beta$	27712.9212	$\times 10^{-48}$ esu
	$\beta_{HRS}$	1446.6454	$\times 10^{-30}$ esu
	$\beta_{zzz}$	3118.2126	$\times 10^{-30}$ esu
	$\beta_{avg}$	3465.9939	$\times 10^{-30}$ esu
$\Psi_{00}^{00}$	<i>Dipole</i>	13.8576	Debye
	$\mu\beta$	5618.7443	$\times 10^{-48}$ esu
	$\beta_{HRS}$	297.7946	$\times 10^{-30}$ esu
	$\beta_{zzz}$	638.4755	$\times 10^{-30}$ esu
	$\beta_{avg}$	704.9660	$\times 10^{-30}$ esu
<i>m062x</i> (chloroform)	<i>Dipole</i>	18.2409	Debye
	$\mu\beta$	36023.3961	$\times 10^{-48}$ esu
	$\beta_{HRS}$	1431.9490	$\times 10^{-30}$ esu
	$\beta_{zzz}$	3058.8916	$\times 10^{-30}$ esu
	$\beta_{avg}$	3432.3455	$\times 10^{-30}$ esu



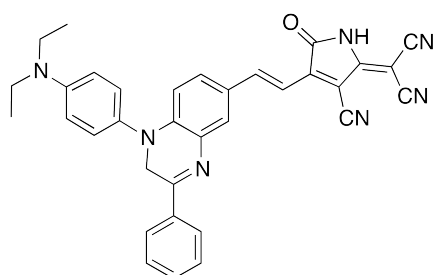
LR-09

<i>cam-b3lyp</i> (vacuo)	<i>Dipole</i>	16.2792	Debye
	$\mu\beta$	1852.9134	$\times 10^{-48}$ esu
	$\beta_{HRS}$	82.4258	$\times 10^{-30}$ esu
	$\beta_{zzz}$	187.9678	$\times 10^{-30}$ esu
	$\beta_{avg}$	194.4810	$\times 10^{-30}$ esu
<i>cam-b3lyp</i> (chloroform)	<i>Dipole</i>	16.2797	Debye
	$\mu\beta$	5494.5607	$\times 10^{-48}$ esu
	$\beta_{HRS}$	242.2101	$\times 10^{-30}$ esu
	$\beta_{zzz}$	552.3976	$\times 10^{-30}$ esu
	$\beta_{avg}$	575.5966	$\times 10^{-30}$ esu
$\Psi_{062x}$	<i>Dipole</i>	16.2798	Debye
	$\mu\beta$	1910.2359	$\times 10^{-48}$ esu
	$\beta_{HRS}$	84.6683	$\times 10^{-30}$ esu
	$\beta_{zzz}$	193.5631	$\times 10^{-30}$ esu
	$\beta_{avg}$	200.2021	$\times 10^{-30}$ esu
$m062x$ (chloroform)	<i>Dipole</i>	20.5852	Debye
	$\mu\beta$	7135.5624	$\times 10^{-48}$ esu
	$\beta_{HRS}$	248.5354	$\times 10^{-30}$ esu
	$\beta_{zzz}$	563.7089	$\times 10^{-30}$ esu
	$\beta_{avg}$	591.8813	$\times 10^{-30}$ esu



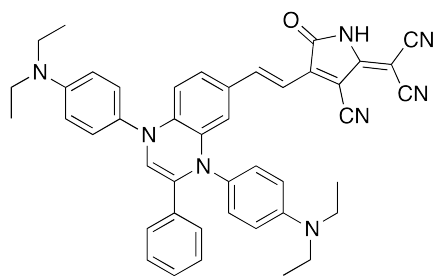
LR-10

<i>cam-b3lyp</i> (vacuo)	<i>Dipole</i>	14.3242	Debye
	$\mu\beta$	2319.4867	$\times 10^{-48}$ esu
	$\beta_{HRS}$	122.2438	$\times 10^{-30}$ esu
	$\beta_{zzz}$	231.8893	$\times 10^{-30}$ esu
	$\beta_{avg}$	291.7918	$\times 10^{-30}$ esu
<i>cam-b3lyp</i> (chloroform)	<i>Dipole</i>	14.3234	Debye
	$\mu\beta$	6905.8687	$\times 10^{-48}$ esu
	$\beta_{HRS}$	363.0641	$\times 10^{-30}$ esu
	$\beta_{zzz}$	689.6809	$\times 10^{-30}$ esu
	$\beta_{avg}$	869.2152	$\times 10^{-30}$ esu
$\Psi_{062x}$	<i>Dipole</i>	14.3229	Debye
	$\mu\beta$	2438.8903	$\times 10^{-48}$ esu
	$\beta_{HRS}$	128.3618	$\times 10^{-30}$ esu
	$\beta_{zzz}$	243.1217	$\times 10^{-30}$ esu
	$\beta_{avg}$	306.9209	$\times 10^{-30}$ esu
$m062x$ (chloroform)	<i>Dipole</i>	17.6227	Debye
	$\mu\beta$	8863.1915	$\times 10^{-48}$ esu
	$\beta_{HRS}$	383.3836	$\times 10^{-30}$ esu
	$\beta_{zzz}$	696.7219	$\times 10^{-30}$ esu
	$\beta_{avg}$	919.5729	$\times 10^{-30}$ esu



LR-11

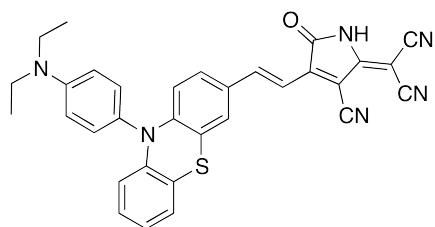
<i>cam-b3lyp</i> (vacuo)	<i>Dipole</i>	19.1843	Debye
	$\mu\beta$	2320.6592	$\times 10^{-48}$ esu
	$\beta_{HRS}$	89.5857	$\times 10^{-30}$ esu
	$\beta_{zzz}$	179.4981	$\times 10^{-30}$ esu
	$\beta_{avg}$	214.3232	$\times 10^{-30}$ esu
<i>cam-b3lyp</i> (chloroform)	<i>Dipole</i>	19.1847	Debye
	$\mu\beta$	6143.3178	$\times 10^{-48}$ esu
	$\beta_{HRS}$	238.3956	$\times 10^{-30}$ esu
	$\beta_{zzz}$	471.1685	$\times 10^{-30}$ esu
	$\beta_{avg}$	570.2608	$\times 10^{-30}$ esu
$\Psi_{00}^{00}$	<i>Dipole</i>	19.1846	Debye
	$\mu\beta$	2390.9604	$\times 10^{-48}$ esu
	$\beta_{HRS}$	91.8782	$\times 10^{-30}$ esu
	$\beta_{zzz}$	185.3308	$\times 10^{-30}$ esu
	$\beta_{avg}$	220.2140	$\times 10^{-30}$ esu
$\Psi_{00}^{02x}$ (chloroform)	<i>Dipole</i>	23.1720	Debye
	$\mu\beta$	7604.4631	$\times 10^{-48}$ esu
	$\beta_{HRS}$	244.0743	$\times 10^{-30}$ esu
	$\beta_{zzz}$	479.8148	$\times 10^{-30}$ esu
	$\beta_{avg}$	585.1387	$\times 10^{-30}$ esu



LR-12

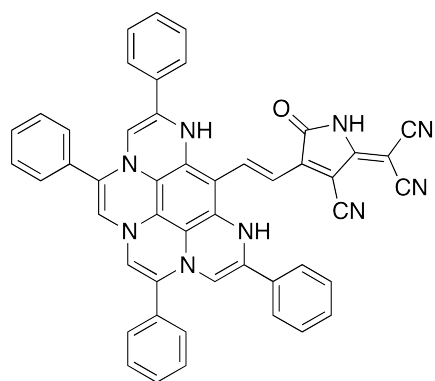
<i>cam-b3lyp</i> (vacuo)	<i>Dipole</i>	16.9394	Debye
	$\mu\beta$	3651.4400	$\times 10^{-48}$ esu
	$\beta_{HRS}$	161.4224	$\times 10^{-30}$ esu
	$\beta_{zzz}$	312.4962	$\times 10^{-30}$ esu
	$\beta_{avg}$	386.4935	$\times 10^{-30}$ esu
<i>cam-b3lyp</i> (chloroform)	<i>Dipole</i>	16.9406	Debye
	$\mu\beta$	12833.3728	$\times 10^{-48}$ esu
	$\beta_{HRS}$	568.0321	$\times 10^{-30}$ esu
	$\beta_{zzz}$	1095.7036	$\times 10^{-30}$ esu
	$\beta_{avg}$	1361.5245	$\times 10^{-30}$ esu
$\Psi_{00}^{00}$	<i>Dipole</i>	16.9402	Debye
	$\mu\beta$	3708.6612	$\times 10^{-48}$ esu
	$\beta_{HRS}$	163.6915	$\times 10^{-30}$ esu
	$\beta_{zzz}$	316.1961	$\times 10^{-30}$ esu
	$\beta_{avg}$	392.6989	$\times 10^{-30}$ esu
$\Psi_{00}^{02x}$ (chloroform)	<i>Dipole</i>	21.1011	Debye
	$\mu\beta$	16113.3661	$\times 10^{-48}$ esu
	$\beta_{HRS}$	574.9623	$\times 10^{-30}$ esu
	$\beta_{zzz}$	1087.6069	$\times 10^{-30}$ esu
	$\beta_{avg}$	1380.8533	$\times 10^{-30}$ esu





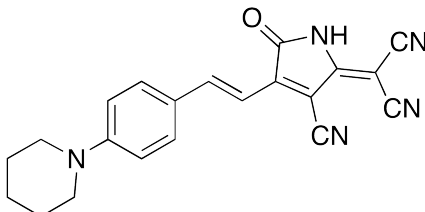
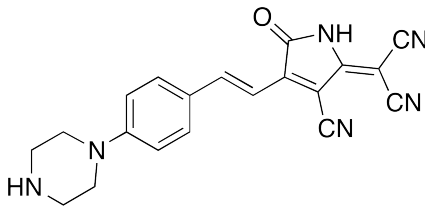
LR-13

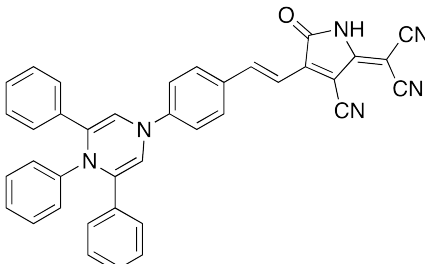
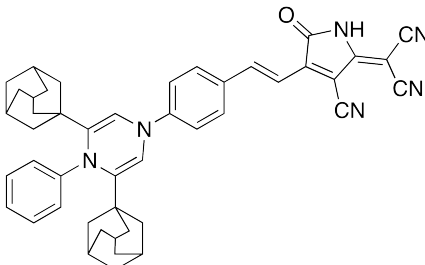
$\text{cam-b3lyp}$ (vacuo)	<i>Dipole</i>	16.8671	Debye
	$\mu\beta$	2170.4782	$\times 10^{-48}$ esu
	$\beta_{HRS}$	101.9228	$\times 10^{-30}$ esu
	$\beta_{zzz}$	162.9032	$\times 10^{-30}$ esu
	$\beta_{avg}$	244.9335	$\times 10^{-30}$ esu
$\text{cam-b3lyp}$ (chloroform)	<i>Dipole</i>	16.8677	Debye
	$\mu\beta$	5206.3120	$\times 10^{-48}$ esu
	$\beta_{HRS}$	247.1752	$\times 10^{-30}$ esu
	$\beta_{zzz}$	382.5686	$\times 10^{-30}$ esu
	$\beta_{avg}$	593.7504	$\times 10^{-30}$ esu
$\psi\Omega\Omega\Omega^x$	<i>Dipole</i>	16.8680	Debye
	$\mu\beta$	2299.2387	$\times 10^{-48}$ esu
	$\beta_{HRS}$	107.7084	$\times 10^{-30}$ esu
	$\beta_{zzz}$	172.6527	$\times 10^{-30}$ esu
	$\beta_{avg}$	259.2583	$\times 10^{-30}$ esu
$\text{m062x}$ (chloroform)	<i>Dipole</i>	19.7840	Debye
	$\mu\beta$	6401.2681	$\times 10^{-48}$ esu
	$\beta_{HRS}$	262.4467	$\times 10^{-30}$ esu
	$\beta_{zzz}$	388.6430	$\times 10^{-30}$ esu
	$\beta_{avg}$	631.6556	$\times 10^{-30}$ esu

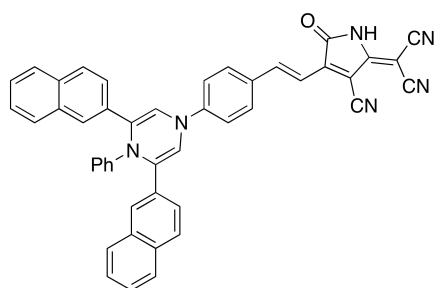


LR-14

$\text{cam-b3lyp}$ (vacuo)	<i>Dipole</i>	13.5019	Debye
	$\mu\beta$	4488.7698	$\times 10^{-48}$ esu
	$\beta_{HRS}$	251.9161	$\times 10^{-30}$ esu
	$\beta_{zzz}$	509.3259	$\times 10^{-30}$ esu
	$\beta_{avg}$	592.2387	$\times 10^{-30}$ esu
$\text{cam-b3lyp}$ (chloroform)	<i>Dipole</i>	13.4999	Debye
	$\mu\beta$	21507.7608	$\times 10^{-48}$ esu
	$\beta_{HRS}$	1182.2579	$\times 10^{-30}$ esu
	$\beta_{zzz}$	2402.4049	$\times 10^{-30}$ esu
	$\beta_{avg}$	2820.6460	$\times 10^{-30}$ esu
$\psi\Omega\Omega\Omega^x$	<i>Dipole</i>	13.4996	Debye
	$\mu\beta$	4740.5377	$\times 10^{-48}$ esu
	$\beta_{HRS}$	266.6150	$\times 10^{-30}$ esu
	$\beta_{zzz}$	534.1728	$\times 10^{-30}$ esu
	$\beta_{avg}$	627.5289	$\times 10^{-30}$ esu
$\text{m062x}$ (chloroform)	<i>Dipole</i>	17.4783	Debye
	$\mu\beta$	30919.2916	$\times 10^{-48}$ esu
	$\beta_{HRS}$	1318.8222	$\times 10^{-30}$ esu
	$\beta_{zzz}$	2626.8099	$\times 10^{-30}$ esu
	$\beta_{avg}$	3151.9458	$\times 10^{-30}$ esu

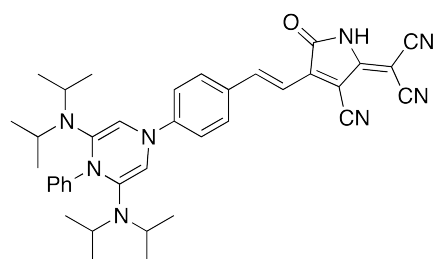
 <p style="text-align: center;">R-01</p>	<i>Dipole</i> $\mu\beta$ $\beta_{HRS}$ $\beta_{zzz}$ $\beta_{avg}$	13.8247 1250.1201 65.5773 141.6945 156.6432	Debye $\times 10^{-48}$ esu $\times 10^{-30}$ esu $\times 10^{-30}$ esu $\times 10^{-30}$ esu
	<i>Dipole</i> $\mu\beta$ $\beta_{HRS}$ $\beta_{zzz}$ $\beta_{avg}$	13.8247 3570.9921 187.0017 404.3007 447.1777	Debye $\times 10^{-48}$ esu $\times 10^{-30}$ esu $\times 10^{-30}$ esu $\times 10^{-30}$ esu
	<i>Dipole</i> $\mu\beta$ $\beta_{HRS}$ $\beta_{zzz}$ $\beta_{avg}$	13.8248 1283.2896 67.1058 145.4426 160.5535	Debye $\times 10^{-48}$ esu $\times 10^{-30}$ esu $\times 10^{-30}$ esu $\times 10^{-30}$ esu
	<i>Dipole</i> $\mu\beta$ $\beta_{HRS}$ $\beta_{zzz}$ $\beta_{avg}$	16.9732 4467.7846 191.0692 406.6638 457.7621	Debye $\times 10^{-48}$ esu $\times 10^{-30}$ esu $\times 10^{-30}$ esu $\times 10^{-30}$ esu
	<i>Dipole</i> $\mu\beta$ $\beta_{HRS}$ $\beta_{zzz}$ $\beta_{avg}$	14.9058 1349.3100 66.6225 137.1054 159.3151	Debye $\times 10^{-48}$ esu $\times 10^{-30}$ esu $\times 10^{-30}$ esu $\times 10^{-30}$ esu
 <p style="text-align: center;">R-02</p>	<i>Dipole</i> $\mu\beta$ $\beta_{HRS}$ $\beta_{zzz}$ $\beta_{avg}$	14.9071 4014.6329 198.1882 407.4014 473.9805	Debye $\times 10^{-48}$ esu $\times 10^{-30}$ esu $\times 10^{-30}$ esu $\times 10^{-30}$ esu
	<i>Dipole</i> $\mu\beta$ $\beta_{HRS}$ $\beta_{zzz}$ $\beta_{avg}$	14.9070 1385.9261 68.1757 140.9501 163.2952	Debye $\times 10^{-48}$ esu $\times 10^{-30}$ esu $\times 10^{-30}$ esu $\times 10^{-30}$ esu
	<i>Dipole</i> $\mu\beta$ $\beta_{HRS}$ $\beta_{zzz}$ $\beta_{avg}$	18.6424 5128.1217 202.7293 411.5850 485.8157	Debye $\times 10^{-48}$ esu $\times 10^{-30}$ esu $\times 10^{-30}$ esu $\times 10^{-30}$ esu
	<i>Dipole</i> $\mu\beta$ $\beta_{HRS}$ $\beta_{zzz}$ $\beta_{avg}$	18.6424 5128.1217 202.7293 411.5850 485.8157	Debye $\times 10^{-48}$ esu $\times 10^{-30}$ esu $\times 10^{-30}$ esu $\times 10^{-30}$ esu
	<i>Dipole</i> $\mu\beta$ $\beta_{HRS}$ $\beta_{zzz}$ $\beta_{avg}$	18.6424 5128.1217 202.7293 411.5850 485.8157	Debye $\times 10^{-48}$ esu $\times 10^{-30}$ esu $\times 10^{-30}$ esu $\times 10^{-30}$ esu

 <p style="text-align: center;">R-03</p>	<i>Dipole</i> $\mu\beta$ $\beta_{HRS}$ $\beta_{zzz}$ $\beta_{avg}$	15.0331 4231.8482 202.8892 438.1202 487.4065	Debye $\times 10^{-48}$ esu $\times 10^{-30}$ esu $\times 10^{-30}$ esu $\times 10^{-30}$ esu
	<i>Dipole</i> $\mu\beta$ $\beta_{HRS}$ $\beta_{zzz}$ $\beta_{avg}$	15.0347 12004.1417 573.9803 1242.4450 1380.8563	Debye $\times 10^{-48}$ esu $\times 10^{-30}$ esu $\times 10^{-30}$ esu $\times 10^{-30}$ esu
	<i>Dipole</i> $\mu\beta$ $\beta_{HRS}$ $\beta_{zzz}$ $\beta_{avg}$	15.0347 4526.8338 216.6612 468.2684 521.0551	Debye $\times 10^{-48}$ esu $\times 10^{-30}$ esu $\times 10^{-30}$ esu $\times 10^{-30}$ esu
	<i>Dipole</i> $\mu\beta$ $\beta_{HRS}$ $\beta_{zzz}$ $\beta_{avg}$	17.9851 15478.0871 623.0272 1314.7031 1500.5998	Debye $\times 10^{-48}$ esu $\times 10^{-30}$ esu $\times 10^{-30}$ esu $\times 10^{-30}$ esu
 <p style="text-align: center;">R-04</p>	<i>Dipole</i> $\mu\beta$ $\beta_{HRS}$ $\beta_{zzz}$ $\beta_{avg}$	14.8809 3614.8843 174.1973 379.8400 419.1649	Debye $\times 10^{-48}$ esu $\times 10^{-30}$ esu $\times 10^{-30}$ esu $\times 10^{-30}$ esu
	<i>Dipole</i> $\mu\beta$ $\beta_{HRS}$ $\beta_{zzz}$ $\beta_{avg}$	14.8804 9626.6846 463.4038 1012.7588 1115.2733	Debye $\times 10^{-48}$ esu $\times 10^{-30}$ esu $\times 10^{-30}$ esu $\times 10^{-30}$ esu
	<i>Dipole</i> $\mu\beta$ $\beta_{HRS}$ $\beta_{zzz}$ $\beta_{avg}$	14.8803 3846.2666 185.0877 404.1248 445.7370	Debye $\times 10^{-48}$ esu $\times 10^{-30}$ esu $\times 10^{-30}$ esu $\times 10^{-30}$ esu
	<i>Dipole</i> $\mu\beta$ $\beta_{HRS}$ $\beta_{zzz}$ $\beta_{avg}$	17.9192 12325.8525 495.9254 1058.8303 1194.7391	Debye $\times 10^{-48}$ esu $\times 10^{-30}$ esu $\times 10^{-30}$ esu $\times 10^{-30}$ esu



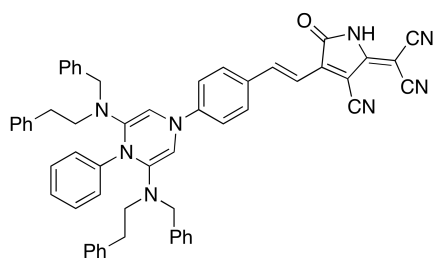
R-05

<i>cam-b3lyp</i> <i>vacuo</i>	<i>Dipole</i>	17.6370	Debye
	$\mu\beta$	5978.9423	$\times 10^{-48}$ esu
	$\beta_{HRS}$	241.9967	$\times 10^{-30}$ esu
	$\beta_{zzz}$	535.2172	$\times 10^{-30}$ esu
	$\beta_{avg}$	582.2997	$\times 10^{-30}$ esu
<i>cam-b3lyp</i> <i>(chloroform)</i>	<i>Dipole</i>	17.6373	Debye
	$\mu\beta$	17902.0007	$\times 10^{-48}$ esu
	$\beta_{HRS}$	723.7570	$\times 10^{-30}$ esu
	$\beta_{zzz}$	1602.0442	$\times 10^{-30}$ esu
	$\beta_{avg}$	1742.6122	$\times 10^{-30}$ esu
$\Psi_{000}^{000}$	<i>Dipole</i>	17.6376	Debye
	$\mu\beta$	6280.4734	$\times 10^{-48}$ esu
	$\beta_{HRS}$	253.9204	$\times 10^{-30}$ esu
	$\beta_{zzz}$	561.9125	$\times 10^{-30}$ esu
	$\beta_{avg}$	611.3990	$\times 10^{-30}$ esu
<i>m062x</i> <i>(chloroform)</i>	<i>Dipole</i>	21.2723	Debye
	$\mu\beta$	22756.9219	$\times 10^{-48}$ esu
	$\beta_{HRS}$	766.4004	$\times 10^{-30}$ esu
	$\beta_{zzz}$	1667.5167	$\times 10^{-30}$ esu
	$\beta_{avg}$	1846.7610	$\times 10^{-30}$ esu



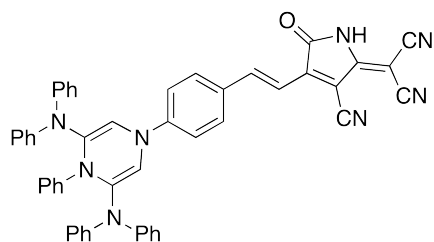
R-06

<i>cam-b3lyp</i> <i>vacuo</i>	<i>Dipole</i>	17.9994	Debye
	$\mu\beta$	4929.5485	$\times 10^{-48}$ esu
	$\beta_{HRS}$	194.1644	$\times 10^{-30}$ esu
	$\beta_{zzz}$	437.0060	$\times 10^{-30}$ esu
	$\beta_{avg}$	467.6857	$\times 10^{-30}$ esu
<i>cam-b3lyp</i> <i>(chloroform)</i>	<i>Dipole</i>	17.9995	Debye
	$\mu\beta$	15692.6728	$\times 10^{-48}$ esu
	$\beta_{HRS}$	617.6241	$\times 10^{-30}$ esu
	$\beta_{zzz}$	1390.1843	$\times 10^{-30}$ esu
	$\beta_{avg}$	1488.3651	$\times 10^{-30}$ esu
$\Psi_{000}^{000}$	<i>Dipole</i>	17.9992	Debye
	$\mu\beta$	5214.3137	$\times 10^{-48}$ esu
	$\beta_{HRS}$	205.0423	$\times 10^{-30}$ esu
	$\beta_{zzz}$	462.3333	$\times 10^{-30}$ esu
	$\beta_{avg}$	494.2998	$\times 10^{-30}$ esu
<i>m062x</i> <i>(chloroform)</i>	<i>Dipole</i>	22.2805	Debye
	$\mu\beta$	20580.4856	$\times 10^{-48}$ esu
	$\beta_{HRS}$	656.2575	$\times 10^{-30}$ esu
	$\beta_{zzz}$	1459.0319	$\times 10^{-30}$ esu
	$\beta_{avg}$	1583.0175	$\times 10^{-30}$ esu



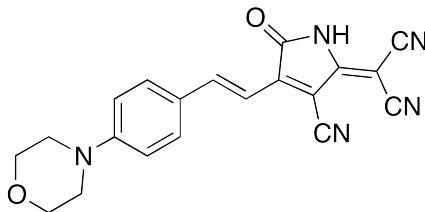
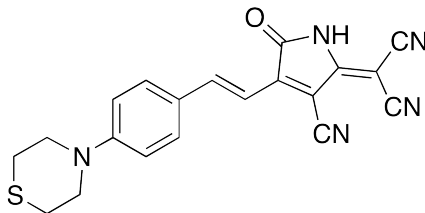
R-07

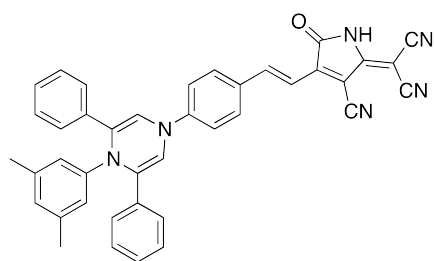
<i>cam-b3lyp</i> vacuo	<i>Dipole</i>	16.7839	Debye
	$\mu\beta$	4541.3585	$\times 10^{-48}$ esu
	$\beta_{HRS}$	192.0209	$\times 10^{-30}$ esu
	$\beta_{zzz}$	431.0212	$\times 10^{-30}$ esu
	$\beta_{avg}$	462.5451	$\times 10^{-30}$ esu
<i>cam-b3lyp</i> (chloroform)	<i>Dipole</i>	16.7898	Debye
	$\mu\beta$	12857.2029	$\times 10^{-48}$ esu
	$\beta_{HRS}$	543.4477	$\times 10^{-30}$ esu
	$\beta_{zzz}$	1219.4213	$\times 10^{-30}$ esu
	$\beta_{avg}$	1308.9277	$\times 10^{-30}$ esu
$\Psi_{000}^{000}$	<i>Dipole</i>	16.7901	Debye
	$\mu\beta$	4823.1327	$\times 10^{-48}$ esu
	$\beta_{HRS}$	203.5098	$\times 10^{-30}$ esu
	$\beta_{zzz}$	457.4616	$\times 10^{-30}$ esu
	$\beta_{avg}$	490.6831	$\times 10^{-30}$ esu
<i>m062x</i> (chloroform)	<i>Dipole</i>	20.2224	Debye
	$\mu\beta$	16408.4817	$\times 10^{-48}$ esu
	$\beta_{HRS}$	578.2939	$\times 10^{-30}$ esu
	$\beta_{zzz}$	1275.8686	$\times 10^{-30}$ esu
	$\beta_{avg}$	1394.3696	$\times 10^{-30}$ esu



R-08

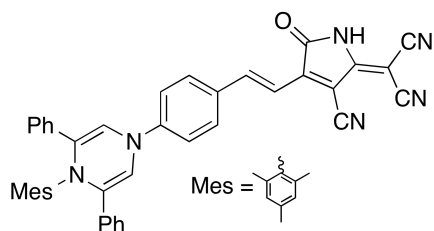
<i>cam-b3lyp</i> vacuo	<i>Dipole</i>	17.6049	Debye
	$\mu\beta$	5614.7279	$\times 10^{-48}$ esu
	$\beta_{HRS}$	226.1320	$\times 10^{-30}$ esu
	$\beta_{zzz}$	505.6874	$\times 10^{-30}$ esu
	$\beta_{avg}$	545.7172	$\times 10^{-30}$ esu
<i>cam-b3lyp</i> (chloroform)	<i>Dipole</i>	17.6079	Debye
	$\mu\beta$	17071.8348	$\times 10^{-48}$ esu
	$\beta_{HRS}$	687.2275	$\times 10^{-30}$ esu
	$\beta_{zzz}$	1535.9450	$\times 10^{-30}$ esu
	$\beta_{avg}$	1658.7923	$\times 10^{-30}$ esu
$\Psi_{000}^{000}$	<i>Dipole</i>	17.6089	Debye
	$\mu\beta$	5962.5082	$\times 10^{-48}$ esu
	$\beta_{HRS}$	239.6949	$\times 10^{-30}$ esu
	$\beta_{zzz}$	536.5857	$\times 10^{-30}$ esu
	$\beta_{avg}$	579.0374	$\times 10^{-30}$ esu
<i>m062x</i> (chloroform)	<i>Dipole</i>	21.2615	Debye
	$\mu\beta$	21947.3392	$\times 10^{-48}$ esu
	$\beta_{HRS}$	735.0094	$\times 10^{-30}$ esu
	$\beta_{zzz}$	1614.1386	$\times 10^{-30}$ esu
	$\beta_{avg}$	1776.0866	$\times 10^{-30}$ esu

 <p style="text-align: center;">R-09</p>	<i>Dipole</i> $\mu\beta$ $\beta_{HRS}$ $\beta_{zzz}$ $\beta_{avg}$	12.7036 1097.8441 63.4671 131.3071 151.8161	Debye $\times 10^{-48}$ esu $\times 10^{-30}$ esu $\times 10^{-30}$ esu $\times 10^{-30}$ esu
	<i>Dipole</i> $\mu\beta$ $\beta_{HRS}$ $\beta_{zzz}$ $\beta_{avg}$	12.7031 3235.8466 187.0028 386.7788 447.3735	Debye $\times 10^{-48}$ esu $\times 10^{-30}$ esu $\times 10^{-30}$ esu $\times 10^{-30}$ esu
	<i>Dipole</i> $\mu\beta$ $\beta_{HRS}$ $\beta_{zzz}$ $\beta_{avg}$	12.7031 1128.1124 64.9895 135.0687 155.6974	Debye $\times 10^{-48}$ esu $\times 10^{-30}$ esu $\times 10^{-30}$ esu $\times 10^{-30}$ esu
	<i>Dipole</i> $\mu\beta$ $\beta_{HRS}$ $\beta_{zzz}$ $\beta_{avg}$	16.0711 4185.4102 191.4758 391.1874 458.9644	Debye $\times 10^{-48}$ esu $\times 10^{-30}$ esu $\times 10^{-30}$ esu $\times 10^{-30}$ esu
 <p style="text-align: center;">R-10</p>	<i>Dipole</i> $\mu\beta$ $\beta_{HRS}$ $\beta_{zzz}$ $\beta_{avg}$	12.3868 1100.0321 65.4712 134.3893 156.4036	Debye $\times 10^{-48}$ esu $\times 10^{-30}$ esu $\times 10^{-30}$ esu $\times 10^{-30}$ esu
	<i>Dipole</i> $\mu\beta$ $\beta_{HRS}$ $\beta_{zzz}$ $\beta_{avg}$	12.3874 3189.7923 189.6275 389.2179 453.3399	Debye $\times 10^{-48}$ esu $\times 10^{-30}$ esu $\times 10^{-30}$ esu $\times 10^{-30}$ esu
	<i>Dipole</i> $\mu\beta$ $\beta_{HRS}$ $\beta_{zzz}$ $\beta_{avg}$	12.3873 1133.1658 67.1893 138.5588 160.7741	Debye $\times 10^{-48}$ esu $\times 10^{-30}$ esu $\times 10^{-30}$ esu $\times 10^{-30}$ esu
	<i>Dipole</i> $\mu\beta$ $\beta_{HRS}$ $\beta_{zzz}$ $\beta_{avg}$	15.5632 4095.9052 194.3602 392.3326 465.5648	Debye $\times 10^{-48}$ esu $\times 10^{-30}$ esu $\times 10^{-30}$ esu $\times 10^{-30}$ esu



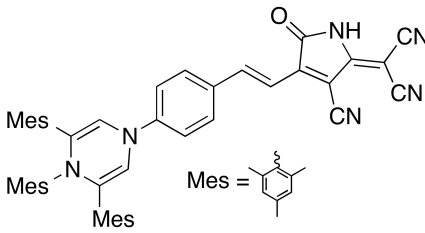
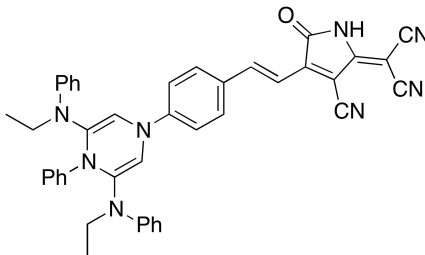
R-11

<i>cam-b3lyp</i> (vacuo)	<i>Dipole</i>	15.4985	Debye
	$\mu\beta$	4522.4932	$\times 10^{-48}$ esu
	$\beta_{HRS}$	209.7742	$\times 10^{-30}$ esu
	$\beta_{zzz}$	455.9916	$\times 10^{-30}$ esu
	$\beta_{avg}$	504.1204	$\times 10^{-30}$ esu
<i>cam-b3lyp</i> (chloroform)	<i>Dipole</i>	15.4986	Debye
	$\mu\beta$	12808.5774	$\times 10^{-48}$ esu
	$\beta_{HRS}$	592.9647	$\times 10^{-30}$ esu
	$\beta_{zzz}$	1290.5905	$\times 10^{-30}$ esu
	$\beta_{avg}$	1426.7398	$\times 10^{-30}$ esu
$\Psi_{062x}$	<i>Dipole</i>	15.4986	Debye
	$\mu\beta$	4827.0833	$\times 10^{-48}$ esu
	$\beta_{HRS}$	223.5663	$\times 10^{-30}$ esu
	$\beta_{zzz}$	486.4064	$\times 10^{-30}$ esu
	$\beta_{avg}$	537.8048	$\times 10^{-30}$ esu
$\Psi_{062x}$ (chloroform)	<i>Dipole</i>	18.4958	Debye
	$\mu\beta$	16437.5213	$\times 10^{-48}$ esu
	$\beta_{HRS}$	641.6877	$\times 10^{-30}$ esu
	$\beta_{zzz}$	1364.7111	$\times 10^{-30}$ esu
	$\beta_{avg}$	1545.6923	$\times 10^{-30}$ esu

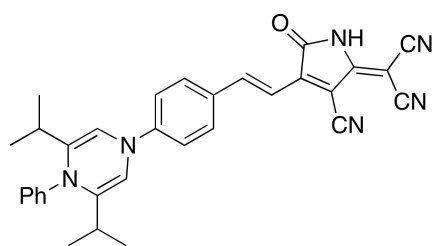


R-12

<i>cam-b3lyp</i> (vacuo)	<i>Dipole</i>	18.3053	Debye
	$\mu\beta$	6119.1748	$\times 10^{-48}$ esu
	$\beta_{HRS}$	236.2610	$\times 10^{-30}$ esu
	$\beta_{zzz}$	537.7179	$\times 10^{-30}$ esu
	$\beta_{avg}$	568.7266	$\times 10^{-30}$ esu
<i>cam-b3lyp</i> (chloroform)	<i>Dipole</i>	18.3080	Debye
	$\mu\beta$	19748.9742	$\times 10^{-48}$ esu
	$\beta_{HRS}$	761.6093	$\times 10^{-30}$ esu
	$\beta_{zzz}$	1733.4704	$\times 10^{-30}$ esu
	$\beta_{avg}$	1834.7562	$\times 10^{-30}$ esu
$\Psi_{062x}$	<i>Dipole</i>	18.3085	Debye
	$\mu\beta$	6443.2749	$\times 10^{-48}$ esu
	$\beta_{HRS}$	248.4683	$\times 10^{-30}$ esu
	$\beta_{zzz}$	565.9227	$\times 10^{-30}$ esu
	$\beta_{avg}$	598.4885	$\times 10^{-30}$ esu
$\Psi_{062x}$ (chloroform)	<i>Dipole</i>	22.4662	Debye
	$\mu\beta$	25677.0217	$\times 10^{-48}$ esu
	$\beta_{HRS}$	809.8543	$\times 10^{-30}$ esu
	$\beta_{zzz}$	1818.1091	$\times 10^{-30}$ esu
	$\beta_{avg}$	1952.4805	$\times 10^{-30}$ esu

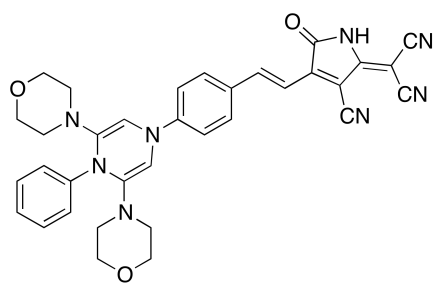
 <p style="text-align: center;">R-13</p>	<i>Dipole</i> $\mu\beta$ $\beta_{HRS}$ $\beta_{zzz}$ $\beta_{avg}$	17.9403 5691.2394 224.8610 504.5859 542.1023	Debye $\times 10^{-48}$ esu $\times 10^{-30}$ esu $\times 10^{-30}$ esu $\times 10^{-30}$ esu
	<i>Dipole</i> $\mu\beta$ $\beta_{HRS}$ $\beta_{zzz}$ $\beta_{avg}$	17.9407 16880.9637 667.0342 1497.3281 1607.6660	Debye $\times 10^{-48}$ esu $\times 10^{-30}$ esu $\times 10^{-30}$ esu $\times 10^{-30}$ esu
	$\Psi_{\beta\beta\beta}^{xyz}$ $\mu\beta$ $\beta_{HRS}$ $\beta_{zzz}$ $\beta_{avg}$	17.9412 6017.2695 237.4706 533.3869 572.8573	Debye $\times 10^{-48}$ esu $\times 10^{-30}$ esu $\times 10^{-30}$ esu $\times 10^{-30}$ esu
	<i>Dipole</i> $\mu\beta$ $\beta_{HRS}$ $\beta_{zzz}$ $\beta_{avg}$	21.7567 21734.7238 711.4121 1570.6955 1715.9790	Debye $\times 10^{-48}$ esu $\times 10^{-30}$ esu $\times 10^{-30}$ esu $\times 10^{-30}$ esu
 <p style="text-align: center;">R-14</p>	<i>Dipole</i> $\mu\beta$ $\beta_{HRS}$ $\beta_{zzz}$ $\beta_{avg}$	16.6550 4422.0558 190.8316 412.7220 459.3242	Debye $\times 10^{-48}$ esu $\times 10^{-30}$ esu $\times 10^{-30}$ esu $\times 10^{-30}$ esu
	<i>Dipole</i> $\mu\beta$ $\beta_{HRS}$ $\beta_{zzz}$ $\beta_{avg}$	16.6536 13233.7085 570.3421 1236.6253 1373.4585	Debye $\times 10^{-48}$ esu $\times 10^{-30}$ esu $\times 10^{-30}$ esu $\times 10^{-30}$ esu
	$\Psi_{\beta\beta\beta}^{xyz}$ $\mu\beta$ $\beta_{HRS}$ $\beta_{zzz}$ $\beta_{avg}$	16.6535 4704.8398 202.7666 438.6376 488.6022	Debye $\times 10^{-48}$ esu $\times 10^{-30}$ esu $\times 10^{-30}$ esu $\times 10^{-30}$ esu
	<i>Dipole</i> $\mu\beta$ $\beta_{HRS}$ $\beta_{zzz}$ $\beta_{avg}$	20.2917 17176.1783 612.2175 1291.4032 1476.1326	Debye $\times 10^{-48}$ esu $\times 10^{-30}$ esu $\times 10^{-30}$ esu $\times 10^{-30}$ esu





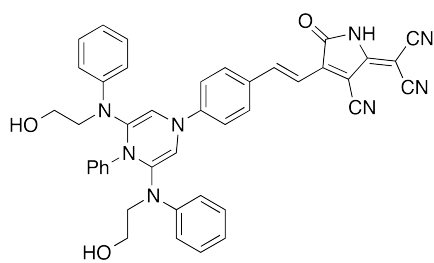
R-15

<i>cam-b3lyp</i> (vacuo)	<i>Dipole</i>	16.9839	Debye
	$\mu\beta$	4518.6342	$\times 10^{-48}$ esu
	$\beta_{HRS}$	189.5959	$\times 10^{-30}$ esu
	$\beta_{zzz}$	422.2746	$\times 10^{-30}$ esu
	$\beta_{avg}$	455.9520	$\times 10^{-30}$ esu
<i>cam-b3lyp</i> (chloroform)	<i>Dipole</i>	16.9828	Debye
	$\mu\beta$	14811.2568	$\times 10^{-48}$ esu
	$\beta_{HRS}$	621.0373	$\times 10^{-30}$ esu
	$\beta_{zzz}$	1382.1417	$\times 10^{-30}$ esu
	$\beta_{avg}$	1494.6633	$\times 10^{-30}$ esu
$\Psi_{062x}$	<i>Dipole</i>	16.9822	Debye
	$\mu\beta$	4755.4282	$\times 10^{-48}$ esu
	$\beta_{HRS}$	199.2776	$\times 10^{-30}$ esu
	$\beta_{zzz}$	444.3471	$\times 10^{-30}$ esu
	$\beta_{avg}$	479.6146	$\times 10^{-30}$ esu
$\Psi_{062x}$ (chloroform)	<i>Dipole</i>	21.0825	Debye
	$\mu\beta$	19449.5241	$\times 10^{-48}$ esu
	$\beta_{HRS}$	658.6764	$\times 10^{-30}$ esu
	$\beta_{zzz}$	1449.4565	$\times 10^{-30}$ esu
	$\beta_{avg}$	1586.6356	$\times 10^{-30}$ esu



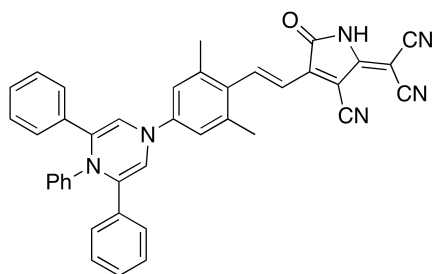
R-16

<i>cam-b3lyp</i> (vacuo)	<i>Dipole</i>	15.5362	Debye
	$\mu\beta$	3741.0775	$\times 10^{-48}$ esu
	$\beta_{HRS}$	172.8472	$\times 10^{-30}$ esu
	$\beta_{zzz}$	376.3596	$\times 10^{-30}$ esu
	$\beta_{avg}$	415.8540	$\times 10^{-30}$ esu
<i>cam-b3lyp</i> (chloroform)	<i>Dipole</i>	15.5362	Debye
	$\mu\beta$	11517.1302	$\times 10^{-48}$ esu
	$\beta_{HRS}$	532.0296	$\times 10^{-30}$ esu
	$\beta_{zzz}$	1156.0334	$\times 10^{-30}$ esu
	$\beta_{avg}$	1280.7352	$\times 10^{-30}$ esu
$\Psi_{062x}$	<i>Dipole</i>	15.5374	Debye
	$\mu\beta$	3973.2572	$\times 10^{-48}$ esu
	$\beta_{HRS}$	183.2433	$\times 10^{-30}$ esu
	$\beta_{zzz}$	399.4510	$\times 10^{-30}$ esu
	$\beta_{avg}$	441.3502	$\times 10^{-30}$ esu
$\Psi_{062x}$ (chloroform)	<i>Dipole</i>	19.2078	Debye
	$\mu\beta$	15194.3503	$\times 10^{-48}$ esu
	$\beta_{HRS}$	569.3597	$\times 10^{-30}$ esu
	$\beta_{zzz}$	1221.3020	$\times 10^{-30}$ esu
	$\beta_{avg}$	1372.2099	$\times 10^{-30}$ esu



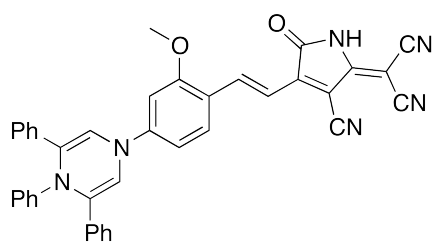
R-17

<i>cam-b3lyp</i> (vacuo)	<i>Dipole</i>	17.7093	Debye
	$\mu\beta$	4806.5000	$\times 10^{-48}$ esu
	$\beta_{HRS}$	194.1344	$\times 10^{-30}$ esu
	$\beta_{zzz}$	422.4721	$\times 10^{-30}$ esu
	$\beta_{avg}$	468.5523	$\times 10^{-30}$ esu
<i>cam-b3lyp</i> (chloroform)	<i>Dipole</i>	17.7078	Debye
	$\mu\beta$	14673.8659	$\times 10^{-48}$ esu
	$\beta_{HRS}$	593.4954	$\times 10^{-30}$ esu
	$\beta_{zzz}$	1285.7295	$\times 10^{-30}$ esu
	$\beta_{avg}$	1432.3838	$\times 10^{-30}$ esu
$\Psi_{062x}$	<i>Dipole</i>	17.7071	Debye
	$\mu\beta$	5088.6294	$\times 10^{-48}$ esu
	$\beta_{HRS}$	205.1621	$\times 10^{-30}$ esu
	$\beta_{zzz}$	447.1513	$\times 10^{-30}$ esu
	$\beta_{avg}$	495.7220	$\times 10^{-30}$ esu
$\Psi_{062x}$ (chloroform)	<i>Dipole</i>	21.4581	Debye
	$\mu\beta$	18956.2836	$\times 10^{-48}$ esu
	$\beta_{HRS}$	633.6284	$\times 10^{-30}$ esu
	$\beta_{zzz}$	1360.6898	$\times 10^{-30}$ esu
	$\beta_{avg}$	1531.1295	$\times 10^{-30}$ esu



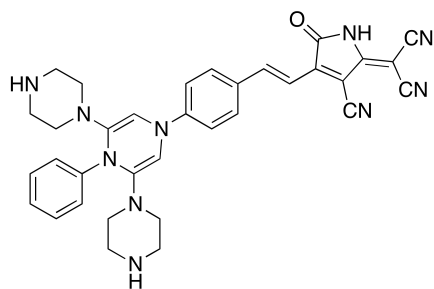
R-18

<i>cam-b3lyp</i> (vacuo)	<i>Dipole</i>	15.3338	Debye
	$\mu\beta$	4212.9127	$\times 10^{-48}$ esu
	$\beta_{HRS}$	197.4243	$\times 10^{-30}$ esu
	$\beta_{zzz}$	431.2675	$\times 10^{-30}$ esu
	$\beta_{avg}$	473.9754	$\times 10^{-30}$ esu
<i>cam-b3lyp</i> (chloroform)	<i>Dipole</i>	15.3310	Debye
	$\mu\beta$	12053.2215	$\times 10^{-48}$ esu
	$\beta_{HRS}$	563.8237	$\times 10^{-30}$ esu
	$\beta_{zzz}$	1229.9070	$\times 10^{-30}$ esu
	$\beta_{avg}$	1356.2622	$\times 10^{-30}$ esu
$\Psi_{062x}$	<i>Dipole</i>	15.3309	Debye
	$\mu\beta$	4519.9938	$\times 10^{-48}$ esu
	$\beta_{HRS}$	211.4419	$\times 10^{-30}$ esu
	$\beta_{zzz}$	462.6491	$\times 10^{-30}$ esu
	$\beta_{avg}$	508.2247	$\times 10^{-30}$ esu
$\Psi_{062x}$ (chloroform)	<i>Dipole</i>	18.5368	Debye
	$\mu\beta$	15866.2023	$\times 10^{-48}$ esu
	$\beta_{HRS}$	616.0084	$\times 10^{-30}$ esu
	$\beta_{zzz}$	1323.7231	$\times 10^{-30}$ esu
	$\beta_{avg}$	1483.5525	$\times 10^{-30}$ esu



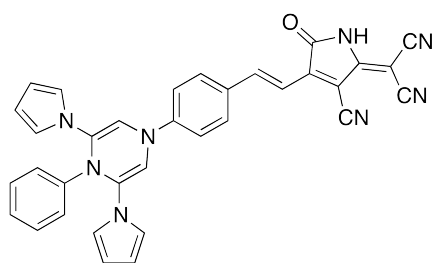
R-19

<i>cam-b3lyp</i> vacuo	<i>Dipole</i>	16.3890	Debye
	$\mu\beta$	3914.6742	$\times 10^{-48}$ esu
	$\beta_{HRS}$	167.9590	$\times 10^{-30}$ esu
	$\beta_{zzz}$	393.3211	$\times 10^{-30}$ esu
	$\beta_{avg}$	402.8927	$\times 10^{-30}$ esu
<i>cam-b3lyp</i> (chloroform)	<i>Dipole</i>	16.3874	Debye
	$\mu\beta$	11304.6430	$\times 10^{-48}$ esu
	$\beta_{HRS}$	483.8743	$\times 10^{-30}$ esu
	$\beta_{zzz}$	1131.9711	$\times 10^{-30}$ esu
	$\beta_{avg}$	1163.2573	$\times 10^{-30}$ esu
$\Psi_{000}^{00x}$	<i>Dipole</i>	16.3873	Debye
	$\mu\beta$	4208.9016	$\times 10^{-48}$ esu
	$\beta_{HRS}$	180.2682	$\times 10^{-30}$ esu
	$\beta_{zzz}$	422.5640	$\times 10^{-30}$ esu
	$\beta_{avg}$	432.9368	$\times 10^{-30}$ esu
<i>m062x</i> (chloroform)	<i>Dipole</i>	19.8225	Debye
	$\mu\beta$	14862.0752	$\times 10^{-48}$ esu
	$\beta_{HRS}$	527.0806	$\times 10^{-30}$ esu
	$\beta_{zzz}$	1218.8429	$\times 10^{-30}$ esu
	$\beta_{avg}$	1268.7257	$\times 10^{-30}$ esu



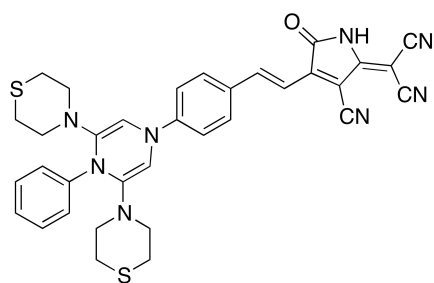
R-20

<i>cam-b3lyp</i> vacuo	<i>Dipole</i>	16.2689	Debye
	$\mu\beta$	4092.6929	$\times 10^{-48}$ esu
	$\beta_{HRS}$	180.7721	$\times 10^{-30}$ esu
	$\beta_{zzz}$	393.2095	$\times 10^{-30}$ esu
	$\beta_{avg}$	434.7689	$\times 10^{-30}$ esu
<i>cam-b3lyp</i> (chloroform)	<i>Dipole</i>	16.2694	Debye
	$\mu\beta$	12875.6615	$\times 10^{-48}$ esu
	$\beta_{HRS}$	567.0848	$\times 10^{-30}$ esu
	$\beta_{zzz}$	1238.2843	$\times 10^{-30}$ esu
	$\beta_{avg}$	1365.1840	$\times 10^{-30}$ esu
$\Psi_{000}^{00x}$	<i>Dipole</i>	16.2690	Debye
	$\mu\beta$	4344.2126	$\times 10^{-48}$ esu
	$\beta_{HRS}$	191.5066	$\times 10^{-30}$ esu
	$\beta_{zzz}$	417.1465	$\times 10^{-30}$ esu
	$\beta_{avg}$	461.1198	$\times 10^{-30}$ esu
<i>m062x</i> (chloroform)	<i>Dipole</i>	20.1121	Debye
	$\mu\beta$	16908.4780	$\times 10^{-48}$ esu
	$\beta_{HRS}$	605.9457	$\times 10^{-30}$ esu
	$\beta_{zzz}$	1294.5693	$\times 10^{-30}$ esu
	$\beta_{avg}$	1460.4300	$\times 10^{-30}$ esu



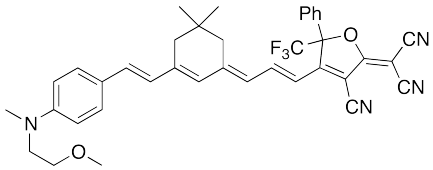
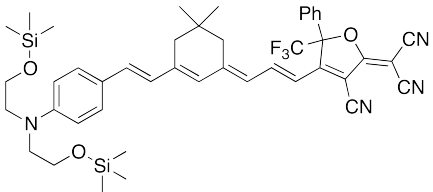
R-21

<i>cam-b3lyp</i> (vacuo)	<i>Dipole</i>	12.3824	Debye
	$\mu\beta$	2584.4197	$\times 10^{-48}$ esu
	$\beta_{HRS}$	151.5305	$\times 10^{-30}$ esu
	$\beta_{zzz}$	317.4414	$\times 10^{-30}$ esu
	$\beta_{avg}$	364.9301	$\times 10^{-30}$ esu
<i>cam-b3lyp</i> (chloroform)	<i>Dipole</i>	12.3843	Debye
	$\mu\beta$	6771.1235	$\times 10^{-48}$ esu
	$\beta_{HRS}$	396.7647	$\times 10^{-30}$ esu
	$\beta_{zzz}$	832.1122	$\times 10^{-30}$ esu
	$\beta_{avg}$	955.4404	$\times 10^{-30}$ esu
$\psi_{00}^{00}$	<i>Dipole</i>	12.3845	Debye
	$\mu\beta$	2792.0050	$\times 10^{-48}$ esu
	$\beta_{HRS}$	163.3239	$\times 10^{-30}$ esu
	$\beta_{zzz}$	342.8712	$\times 10^{-30}$ esu
	$\beta_{avg}$	393.8115	$\times 10^{-30}$ esu
$\mu_{00}^{00}$ (chloroform)	<i>Dipole</i>	14.8193	Debye
	$\mu\beta$	8727.5787	$\times 10^{-48}$ esu
	$\beta_{HRS}$	432.5306	$\times 10^{-30}$ esu
	$\beta_{zzz}$	870.8392	$\times 10^{-30}$ esu
	$\beta_{avg}$	1042.9469	$\times 10^{-30}$ esu



R-22

<i>cam-b3lyp</i> (vacuo)	<i>Dipole</i>	15.5066	Debye
	$\mu\beta$	3922.4599	$\times 10^{-48}$ esu
	$\beta_{HRS}$	181.9540	$\times 10^{-30}$ esu
	$\beta_{zzz}$	393.3464	$\times 10^{-30}$ esu
	$\beta_{avg}$	437.7091	$\times 10^{-30}$ esu
<i>cam-b3lyp</i> (chloroform)	<i>Dipole</i>	15.5076	Debye
	$\mu\beta$	12219.1790	$\times 10^{-48}$ esu
	$\beta_{HRS}$	566.7147	$\times 10^{-30}$ esu
	$\beta_{zzz}$	1221.5666	$\times 10^{-30}$ esu
	$\beta_{avg}$	1364.5342	$\times 10^{-30}$ esu
$\psi_{00}^{00}$	<i>Dipole</i>	15.5080	Debye
	$\mu\beta$	4155.8226	$\times 10^{-48}$ esu
	$\beta_{HRS}$	192.3978	$\times 10^{-30}$ esu
	$\beta_{zzz}$	416.6126	$\times 10^{-30}$ esu
	$\beta_{avg}$	463.3609	$\times 10^{-30}$ esu
$\mu_{00}^{00}$ (chloroform)	<i>Dipole</i>	19.2766	Debye
	$\mu\beta$	16127.6917	$\times 10^{-48}$ esu
	$\beta_{HRS}$	603.2186	$\times 10^{-30}$ esu
	$\beta_{zzz}$	1285.6409	$\times 10^{-30}$ esu
	$\beta_{avg}$	1454.0761	$\times 10^{-30}$ esu

 <p style="text-align: center;">YLD-124M</p>	<i>Dipole</i> $\mu\beta$ $\beta_{HRS}$ $\beta_{zzz}$ $\beta_{avg}$	20.7774 4843.7888 177.2178 324.1447 426.3199	Debye $\times 10^{-48}$ esu $\times 10^{-30}$ esu $\times 10^{-30}$ esu $\times 10^{-30}$ esu
	<i>Dipole</i> $\mu\beta$ $\beta_{HRS}$ $\beta_{zzz}$ $\beta_{avg}$	20.7763 13552.7647 490.9072 924.0015 1181.2377	Debye $\times 10^{-48}$ esu $\times 10^{-30}$ esu $\times 10^{-30}$ esu $\times 10^{-30}$ esu
	<i>Dipole</i> $\mu\beta$ $\beta_{HRS}$ $\beta_{zzz}$ $\beta_{avg}$	20.7759 5319.0401 193.8792 356.4684 467.2286	Debye $\times 10^{-48}$ esu $\times 10^{-30}$ esu $\times 10^{-30}$ esu $\times 10^{-30}$ esu
	<i>Dipole</i> $\mu\beta$ $\beta_{HRS}$ $\beta_{zzz}$ $\beta_{avg}$	25.9908 18897.8854 546.2065 1026.4985 1316.8991	Debye $\times 10^{-48}$ esu $\times 10^{-30}$ esu $\times 10^{-30}$ esu $\times 10^{-30}$ esu
 <p style="text-align: center;">YLD-124TMS</p>	<i>Dipole</i> $\mu\beta$ $\beta_{HRS}$ $\beta_{zzz}$ $\beta_{avg}$	21.5677 6136.0044 209.7172 421.2932 504.3321	Debye $\times 10^{-48}$ esu $\times 10^{-30}$ esu $\times 10^{-30}$ esu $\times 10^{-30}$ esu
	<i>Dipole</i> $\mu\beta$ $\beta_{HRS}$ $\beta_{zzz}$ $\beta_{avg}$	21.5678 15858.0574 537.2482 1106.7487 1292.4591	Debye $\times 10^{-48}$ esu $\times 10^{-30}$ esu $\times 10^{-30}$ esu $\times 10^{-30}$ esu
	<i>Dipole</i> $\mu\beta$ $\beta_{HRS}$ $\beta_{zzz}$ $\beta_{avg}$	21.5684 6715.2422 228.8289 461.0190 551.2016	Debye $\times 10^{-48}$ esu $\times 10^{-30}$ esu $\times 10^{-30}$ esu $\times 10^{-30}$ esu
	<i>Dipole</i> $\mu\beta$ $\beta_{HRS}$ $\beta_{zzz}$ $\beta_{avg}$	26.3806 21439.0137 594.5852 1211.3032 1433.1786	Debye $\times 10^{-48}$ esu $\times 10^{-30}$ esu $\times 10^{-30}$ esu $\times 10^{-30}$ esu

## Appendix B

## PYTHON CODE FOR GDR.PY

```

1 #gdr.py rev. 1.0.3
2 #Nathaniel Phillips–Sylvain, 2014
3 #The below code was originally written for MATLAB by Dr. Bruce Eichinger. It
4 #has been converted to Python using the numpy library. The only requirements
5 #to use it are Python and numpy. Type the following to use it in your code:
6 #from gdr import GDR
7 #
8 #and then to call it, use
9 #GDR([x,y,z],[xxx,xyx,xyy,yyy,xxz,xyz,yyz,xzz,yzz,zzz])
10 #The function returns the dipole moment(D), muBeta, BetaHRS, BetaVec
11 #and BetaTot
12 #BetaVec is the same as BetaZZZ
13 #
14 #This function converts Gaussian data into beta hrs and beta zzz so as to
15 #be compatible with DMol method. The Gaussian dipole data is in x,y,z
16 #components, and the beta data is
17 # bxxx bxyx bxyy byyy bxxz bxyz byyz bxzz byzz bzzz
18 #The straightforward way to handle this is to convert to ijk notation and
19 #apply the algorithm used with DMol calculations.
20
21 from __future__ import division
22 import numpy as np
23
24 def GDR(mu,b):
25
26     b = np.asarray(b)
27     mutemp = np.asarray(mu)
28     M = np.linalg.norm(mutemp)
29
30 # This takes a 1x3 vector and finds the matrix that rotates
31 # the vector to the z axis. The function returns the rotation matrix
32 # and the new vector (as a check). Note that the vector is represented
33 # as a row, and the way that the matrix is constructed one needs to take the
34 # transpose to get the new vector. To construct the rotation, note that mu
35 # = |mu|xunit vector, so that one row of the rotation matrix is the unit
36 # vector. The other two rows are constructed using Gram–Schmidt
37 # orthogonalization, making certain that the rows are unit vectors.
38
39     u = mutemp / M
40     t = np.sqrt(1 - u[0]**2)
41

```

```

42 Rt = np.matrix([[ 0,      u[2]/t,      -u[1]/t],
43                  [ t,      -u[0]*u[1]/t,  -u[0]*u[2]/t],
44                  [ u[0],   u[1],        u[2]]
45                  ])
46 R = Rt.getT()
47 munu = mutemp * R
48 b = -b / 2
49
50 # The preceding line was modified 9/7/05 to change from Taylor's series
51 # convention to
52 # perturbation series convention. This also changes the sign to correct for
53 # the wrong sign convention used by Gaussian.
54 #
55 # b1=b111, b2 =b112=b211=b121, b3=b122=b212=b221, b4=b222,
56 # b5=b113=b131=b311, b6=b123=b321=b132=b312=b213=b231, b7=b223=b232=b322,
57 # b8=b133=b313=b331, b9 = b233=b323=b332, b10 = b333
58
59 Beta=np.zeros((3,3,3))
60
61 Beta[0,0,0]=b[0]
62
63 Beta[1,0,0]=b[1]
64 Beta[0,0,1]=Beta[1,0,0]
65 Beta[0,1,0]=Beta[1,0,0]
66
67 Beta[0,1,1]=b[2]
68 Beta[1,1,0]=Beta[0,1,1]
69 Beta[1,0,1]=Beta[0,1,1]
70
71 Beta[1,1,1]=b[3]
72
73 Beta[2,0,0]=b[4]
74 Beta[0,0,2]=Beta[2,0,0]
75 Beta[0,2,0]=Beta[2,0,0]
76
77 Beta[1,0,2]=b[5]
78 Beta[0,1,2]=Beta[1,0,2]
79 Beta[0,2,1]=Beta[1,0,2]
80 Beta[1,2,0]=Beta[1,0,2]
81 Beta[2,0,1]=Beta[1,0,2]
82 Beta[2,1,0]=Beta[1,0,2]
83
84 Beta[2,1,1]=b[6]
85 Beta[1,1,2]=Beta[2,1,1]
86 Beta[1,2,1]=Beta[2,1,1]
87
88 Beta[0,2,2]=b[7]
89 Beta[2,2,0]=Beta[0,2,2]
90 Beta[2,0,2]=Beta[0,2,2]

```

```

91  Beta[1,2,2]=b[8]
92  Beta[2,2,1]=Beta[1,2,2]
93  Beta[2,1,2]=Beta[1,2,2]
94
95  Beta[2,2,2]=b[9]
96
97  beta1=R.T * Beta[:, :, 0] * R
98  beta2=R.T * Beta[:, :, 1] * R
99  beta3=R.T * Beta[:, :, 2] * R
100  Betat=np.zeros((3,3,3))
101  Betat[:, :, 0]=beta1
102  Betat[:, :, 1]=beta2
103  Betat[:, :, 2]=beta3
104  BetaT=np.transpose(Betat,(2,0,1))
105  B=np.zeros((3,3,3))
106  t=np.zeros((3,3,3))
107  for n in range(3):
108      t[:, :, n]=R.T * BetaT[:, :, n]
109  B=np.transpose(t,(1,2,0))
110  Bpp=0.6 * np.trace(B[:, :, 2])
111  muBeta=M * 2.5418 * Bpp * 0.863916 * 10 ** -50
112  diag=0
113  sum_=0
114  for k in range(3):
115      diag=diag + B[k,k,k] ** 2
116  for k in range(3):
117      for m in range(3):
118          sum_=sum_ + (16 * B[k,k,k] * B[k,m,m] + 38 * B[k,k,m] ** 2) / 105
119  b2= 12 * diag / 35 + sum_ + 16 * (B[0,0,1] * B[1,2,2] + B[1,1,2] * B
[2,0,0] + B[2,2,0] * B[0,1,1]) / 105 + (20 / 35) * B[0,1,2] ** 2
120  bx=B[0,0,0] + B[0,1,1] + B[0,2,2]
121  by=B[1,1,1] + B[1,0,0] + B[1,2,2]
122  bz=B[2,2,2] + B[2,0,0] + B[2,1,1]
123  b1=np.sqrt(b2)
124  mu = mumu
125  mu_Debyes = mumu * 2.5418
126  Beta_HRS=b1 * 0.863916 * 10**-32
127  Beta_zzz=B[2,2,2] * 0.863916 * 10**-32
128  Beta_avg=np.sqrt(bx ** 2 + by ** 2 + bz ** 2) * 0.863916 * 10**-32
129
130  return dict("dipole" = mu_Debyes[0,2], "mubeta" = muBeta, "betaHRS" =
Beta_HRS, "betaZZZ" = Beta_zzz, "betaAVG" = Beta_avg)

```



## VITA

Anything that's human is mentionable, and anything that is mentionable can be more manageable. When we can talk about our feelings, they become less overwhelming, less upsetting, and less scary. The people we trust with that important talk can help us know that we are not alone.

– Fred Rogers